

© Copyright 2016

Wei Qin

Ecophysiology of marine ammonia-oxidizing archaea

Wei Qin

A dissertation

submitted in partial fulfillment of the

requirements for the degree of

Doctor of Philosophy

University of Washington

2016

Reading Committee:

David A. Stahl, Chair

Anitra E. Ingalls

Robert M. Morris

Program Authorized to Offer Degree:

Department of Civil and Environmental Engineering

University of Washington

Abstract

Ecophysiology of marine ammonia-oxidizing archaea

Wei Qin

Chair of the Supervisory Committee:
Professor David A. Stahl
Department of Civil and Environmental Engineering

Ammonia oxidizing archaea (AOA) are one of the most abundant prokaryotes in the ocean and span diverse oceanic provinces. In addition to having a dominant role in marine nitrification, they are implicated as a major source of atmospherically active gases methane and nitrogen oxides. However, the scarcity of cultured isolates for laboratory study has hindered developing an understanding of specific metabolic traits and physicochemical factors controlling their activities and distribution. In this thesis, I report the isolation and characterization of three new marine AOA (strains HCA1, HCE1, and PS0) and show distinct adaptations to pH, salinity, temperature, light, and reactive oxygen species relative to the model AOA *Nitrosopumilus maritimus* strain SCM1. Increases in nitrous oxide (N₂O) production in response to decreasing oxygen (O₂) tensions was quantified and found consistent with an AOA contribution to the

accumulation of N_2O in suboxic regions of oxygen minimum zones. Normal growth of strain SCM1 was shown to be coupled with balanced production and consumption of nitric oxide (NO). A central role of NO in archaeal ammonia oxidation was confirmed by specific inhibition using an NO-scavenger (2-phenyl-4,4,5,5-tetramethylimidazole-1-oxyl-3-oxide). The determination of high cellular quotas of cobalamin now implicates the AOA as major contributors to cobalamin in seawater. Gene expression studies showed that the entire cobalamin biosynthesis pathway is regulated by the level of nitrosative stress, suggesting that an interplay between NO production and cobalamin synthesis is central to the ecophysiology of marine AOA. Apart from having a major influence on the nitrogen cycle, their glycerol dibiphytanyl glycerol tetraether (GDGT) membrane lipids are widely used to reconstruct past sea surface temperatures by means of TEX_{86} paleothermometer. However, the TEX_{86} proxy must now be reevaluated in consideration of the observation that O_2 concentration greatly influences GDGT composition, leading to significant increases in TEX_{86} -derived temperatures with increasing O_2 limitation.

TABLE OF CONTENTS

	Page
List of Figures	iii
List of Tables	vii
Chapter 1. Introduction	1
Chapter 2. Marine ammonia-oxidizing archaeal isolates display obligate mixotrophy and wide ecotypic variation	16
Chapter 3. <i>Nitrosopumilus maritimus</i> gen. nov., sp. nov., <i>Nitrosopumilus cobalaminogenes</i> gen. nov., sp. nov., <i>Nitrosopumilus oxyclinae</i> gen. nov., sp. nov., and <i>Nitrosopumilus ureaphilus</i> gen. nov., sp. nov., four marine ammonia-oxidizing archaea of the phylum <i>Thaumarchaeota</i>	53
Chapter 4. Influence of oxygen availability on the activities of ammonia-oxidizing archaea	102
Chapter 5. The production of nitric oxide by marine ammonia-oxidizing archaea and inhibition of archaeal ammonia oxidation by a nitric oxide scavenger	124
Chapter 6. Influence of ammonia and copper availabilities on the molecular physiology of the marine ammonia-oxidizing archaeon <i>Nitrosopumilus maritimus</i>	164
Chapter 7. Confounding effects of oxygen and temperature on the TEX ₈₆ signature of marine thaumarchaeota	221
Chapter 8. Summary and Perspectives.....	263
Chapter 9. Other Scientific Contributions	269

9.1	Order <i>Nitropumilales</i> , Family <i>Nitrosopumilaceae</i> , Genus <i>Nitrosopumilus</i>	269
9.2	Order <i>Nitrosocaldales</i> , Family <i>Nitrosocaldaceae</i> , Genus <i>Nitrosocaldus</i>	271
9.3	Two distinct pools of B ₁₂ analogs reveal community interdependencies in the ocean	273
9.4	Ammonia oxidation kinetics and temperature sensitivity of a natural marine community dominated by Archaea.....	275
9.5	Variable influence of light and temperature upon ammonia oxidation activity in marine <i>Thaumarchaeota</i>	277

LIST OF FIGURES

Figure Number	Page
Figure 2.1. Growth and morphology of strains HCA1 and PS0.	43
Figure 2.2. Phylogenetic relationships among <i>amoA</i> gene sequences of strains HCA1, PS0, and SCM1	44
Figure 2.3. Maximum likelihood phylogenetic tree based on 16S rRNA gene sequences.	45
Figure 2.4. Temperature dependence of the growth of SCM1, HCA1, and PS0.....	46
Figure 2.5. Influence of pH and salinity on growth.....	47
Figure 2.6. Photoinhibition and recovery of ammonia oxidation of the three AOA strains.	48
Figure 2.7. Nitrite production and growth curves of strains HCA1, PS0, and SCM1 with 100 μ M α -ketoglutaric acid	49
Figure 2.8. The specific growth yields of cultures of three AOA isolates with 100 μ M α -ketoglutaric acid.	50
Figure 2.9. Growth of PS0 in artificial seawater medium containing urea.....	51
Figure 3.1. Correlation of the growth of strain HCE1 with the stoichiometric ammonia oxidation to nitrite.....	86
Figure 3.2. Influence of temperature on growth.	87
Figure 3.3. The effect of pH and salinity on the growth of strain HCE1.....	88
Figure 3.4. Nitrite production by marine AOA isolates at different initial ammonia concentrations.	89
Figure 3.5. Effect of organic compounds on the specific growth rate of strain SCM1. ..	90
Figure 3.6. The specific growth rates of strains HCA1, HCE1, and PS0 with supplementation of small organic acids	91
Figure 3.7. Correlation of the growth of strain SCM1 and total cobalamin synthesis. ...	92
Figure 3.8. Transmission electron micrographs of negative stained strain HCE1 cells. .	93
Figure 3.9. S-layer structure of strain SCM1.	94

Figure 3.10. Maximum-likelihood tree based on the 16S rRNA sequences showing the phylogenetic relationships of the order <i>Nitrosopumilales</i> , the family <i>Nitrosopumilaceae</i> , and the genus <i>Nitrosopumilus</i>	95
Figure 3.11. Maximum-likelihood phylogenetic tree based on <i>amoA</i> gene sequences showing the phylogenetic relationships of <i>Nitrosopumilus</i> genus, <i>Nitrosopumilaceae</i> family, and <i>Nitrosopumilales</i> order.	96
Figure 4.1. Oxygen-dependent growth kinetics of marine AOA.....	116
Figure 4.2. Growth curve of strain HCA1 with α -ketoglutarate or H ₂ O ₂ scavengers....	117
Figure 4.3. The specific growth rates and specific growth yields of strain PS0 cultures supplemented with H ₂ O ₂ scavengers, α -keto acids, or a common algal exudate. ..	118
Figure 4.4. Short-term and long-term effects of different concentrations of H ₂ O ₂ on the ammonia oxidation activity of exponential phase SCM1 cells.	119
Figure 4.5. Growth curve of strain HCA1 with α -ketoglutarate or H ₂ O ₂ scavengers. .	120
Figure 4.6. Nitrite-normalized N ₂ O yields of strain SCM1 with α -ketoglutarate relative to controls without α -ketoglutarate.	121
Figure 5.1. Metabolism of NO in SCM1.	153
Figure 5.2. Growth of SCM1 as a function of initial ammonia and nitrite concentrations.	154
Figure 5.3. Inhibition of ammonia oxidation in SCM1 by acetylene.	155
Figure 5.4. Effect of different concentrations of DEDTC on the growth of mid-exponential phase SCM1 cells.	156
Figure 5.5. Response of marine AOA isolates, and natural communities and AOB strains to the nitrogen free radical scavenger PTIO and ATU.....	157
Figure 5.6. Influence of PTIO and PTI on ammonia oxidation activity of mid-exponential phase SCM1 cells.	158
Figure 5.7. Influence of ammonia starvation on the response of <i>N. europaea</i> and <i>N. briensis</i> to PTIO addition.....	159
Figure 5.8. Influence of ATU and nitrapyrin on ammonia oxidation activity of SCM1.	160
Figure 5.9. Hydrography, inorganic nitrogen nutrients, ammonia oxidation rates and AOA and β -AOB <i>amoA</i> gene copy numbers in Hood Canal, WA, on June 2010..	161

Figure 5.10. Hydrography, inorganic nitrogen nutrients, total prokaryotic cell counts, and AOA and β -AOB <i>amoA</i> gene copy numbers in Ocean Station Papa, North Pacific Ocean, on August 2013.....	162
Figure 5.11. The influence of PTIO and ATU on the sample $\delta^{15}\text{N}$ measurement.....	163
Figure 6.1. Proteome of <i>N. maritimus</i>	210
Figure 6.2. Unsupervised hierarchical clustering of <i>N. maritimus</i> cultures grown with different ammonia and copper availabilities.....	211
Figure 6.3. Comparative transcriptome responses of <i>N. maritimus</i> cultures to ammonia starvation vs. recovery and Cu limitation vs. Cu toxicity.....	212
Figure 6.4. Transcriptional changes for the proposed ammonia oxidation, electron transfer and ammonia assimilation pathways in response to ammonia starvation, recovery, Cu limitation, and Cu excess conditions.	213
Figure 6.5. Transcript copies of <i>amoA</i> , <i>B</i> and <i>C</i> per cell during late exponential growth and stationary phase of <i>Nitrosopumilus maritimus</i> and <i>Nitrosomonas europaea</i>	214
Figure 6.6. Spontaneous oxygen uptake rate of <i>N. maritimus</i> cells during late exponential growth and before and after ammonia spike following time periods of ammonia-starvation.....	215
Figure 6.7. Transcriptional changes for the thaumarchaeotal 3-HP/4-HB carbon fixation pathway in response to ammonia starvation, recovery, Cu limitation, and Cu excess conditions.	216
Figure 6.8. Phylogenetic trees of gene encoding acetoacetyl-CoA beta-ketothiolase.....	218
Figure 6.9. Transcriptional changes for the thaumarchaeotal cobalamin synthesis pathway in response to ammonia starvation, recovery, Cu limitation, and Cu excess conditions.	219
Figure 6.10. Chromatograms showing the distribution of AdoCbl, MeCbl, and NO_2Cbl in <i>N. maritimus</i> cells grown under different copper treatments.....	220
Figure 7.1. Structures of the GDGT core lipids of marine AOA.....	247
Figure 7.2. Reconstructed TEX_{86} -derived temperatures of four marine AOA isolates incubated at 25°C	248

Figure 7.3. Effects of temperature on the ammonia oxidation activities of strains SCM1, HCA1 and HCE1.....	249
Figure 7.4. Correlations of TEX ₈₆ values with growth temperatures of strains SCM1, HCA1 and HCE1.	250
Figure 7.5. Relative abundances of GDGTs in total cellular lipids of marine AOA strains SCM1, HCA1 and HCE1 at different temperatures.	251
Figure 7.6. Correlation of TEX ₈₆ -derived temperature with growth temperature of strains SCM1, HCA1 and HCE1.	253
Figure 7.7. Correlations of ring index values with growth temperatures of strains SCM1, HCA1 and HCE1.....	254
Figure 7.8. Effects of O ₂ concentration on the ammonia oxidation activities of strains SCM1 and PS0.....	255
Figure 7.9. HPLC/MS base peak chromatogram showing the distribution of GDGT species of marine AOA.	256
Figure 7.10. Relative abundances of GDGTs in total cellular lipids of marine AOA strains SCM1 and PS0 with different O ₂ concentrations.	257
Figure 7.11. Effects of O ₂ concentration on the reconstructed TEX ₈₆ temperatures of strains SCM1 and PS0	258

LIST OF TABLES

Table Number	Page
Table 2.1. Growth kinetics of ammonia oxidation for three marine AOA isolates.	52
Table 2.2. Activation energy and Q_{10} values of ammonia oxidation for three marine AOA strains and other bacterial nitrifiers.	52
Table 2.3. Cell yields and growth rates in marine AOA pure cultures with 100 μ M α -ketoglutaric acid over controls without organic substrate.	52
Table 3.1. Main characteristics of marine <i>Thaumarchaeota</i> strains SCM1, HCA1, HCE1 and PS0	97
Table 4.1. Growth and N ₂ O production of strains SCM1 and PS0 at different O ₂ concentrations.	122
Table 7.1. Cell densities, lipid contents and TEX ₈₆ values of different marine AOA strains grown at selected temperatures.....	259
Table 7.2. Relative abundances of GDGTs in total cellular lipids and ring index values of marine AOA isolates grown at selected temperatures.....	260
Table 7.3. Cell densities, O ₂ utilization and TEX ₈₆ values of marine AOA strains grown at selected initial headspace O ₂ concentrations	261
Table 7.4. Relative abundances of GDGTs in total cellular lipids and ring index values of strains SCM1 and PS0 grown at selected initial headspace O ₂ concentrations	262

ACKNOWLEDGEMENTS

I would especially like to acknowledge and thank my advisor, Prof. David A. Stahl, who continually dedicates himself to science. He has been an excellent role model for me as a strong-willed and successful scientist. I would like to appreciate his warm mentorship and continuous encouragement throughout the long years of my master and doctoral studies, field work, and lab research. I have always been amazed by how lucky I was to have an opportunity to join Stahl lab and work on projects studying the most wonderful and important microbe ammonia-oxidizing archaea. I also sincerely thank my committee, Prof. Anitra E. Ingalls, Prof. Robert M. Morris, Prof. H. David Stensel, and Prof. Christine Queitsch for their time and support. Prof. Anitra E. Ingalls has particularly been of terrific help in sharing with me various resources and putting my ideas into practice.

I would also like to extend my special thanks for Dr. Willm Martens-Habbena for getting me started in science, nurturing my interest in microbiology, and answering the countless questions about science and life. In particular, I would like to express my gratitude to my supportive and creative lab family – Kelley Meinhardt, Frederick von Netzer, Nejc Stopnisek, Nick Elliott, Anthony Bertagnolli, David Vuono, Jason Flower, and Birte Meyer. In addition, I would like to thank my undergraduate assistant Julia Kobelt for her great lab work.

I also really appreciate to have opportunities to work with the most outstanding oceanographers on dimensions project. Thanks also go to project PIs Ginger Armbrust, Al Devol, and Jim Moffett for their guidance and valuable suggestions. Special recognition is also extended to Shady Amin for mentoring me and sharing ideas unconditionally; Katherine Heal, “the queen of cobalamin” for extensive discussions on cobalamin analysis; Laura Carlson for supporting on lipid analysis; Rachel Lundeen for providing expertise on proteomics analysis; and Rachel Horak for providing her extensive field work expertise. I really enjoy and appreciate the great collaborative working atmosphere of dimensions group. You are great blessings as co-workers!

I also want to extend my greatest and deepest appreciations to my parents for their unconditional love and support. I would also like to thank the endless prayers and support from my church family. Lastly, but most of all, I would like to thank my wife Belinda for sharing her love, support, understanding, and trust with me. No one could ask for a better lifelong companion who most intensely continues to inspire me how to be the person I am trying to become. It is an understatement to say that this dissertation would not be what it is without all the people mentioned above.

DEDICATION

For Dad, Mom, and Belinda.

Chapter 1.

Introduction

Discovery of ammonia-oxidizing archaea

For decades, *Archaea* were defined as obligate extremophiles and restricted to high-temperature, extremely acidic, hypersaline, or strictly anoxic habitats (Woese et al., 1978). However, this perception was overturned with the discovery of mesophilic marine Group I (MGI) and Group II *Archaea* from temperate and oxygenated ocean waters (DeLong, 1992; Fuhrman et al., 1992). Detailed molecular surveys indicated that MGI are among the most ubiquitous and abundant marine prokaryotes, approaching 40% of total bacterioplankton in the meso- and bathypelagic zones (Karner et al., 2001), and constituting a considerable fraction of the microbial biomass in the ocean (Schattenhofer et al., 2009). Marine metagenomic studies first hinted at the metabolic potential of MGI, as a copper-containing membrane-bound monooxygenase (Cu-MMO) gene was found on a MGI-associated scaffold (Venter et al., 2004). Although Cu-MMOs consist of a diverse family of enzymes having broad substrate range, this gene was provisionally annotated as coding for an ammonia monooxygenase (AMO), based on ~25% amino acid identity with bacterial AMO (Venter et al., 2004), although also sharing significant identity (~50%) with the bacterial particulate methane monooxygenase (Sayavedra-Soto et al., 2011; Tavormina et al., 2011). Therefore, demonstration of a capacity for archaeal ammonia oxidation awaited the isolation of the first chemolithoautotrophic marine ammonia-oxidizing archaeon (AOA) “*Candidatus Nitrosopumilus maritimus*” SCM1, which established the definitive link between the MGI AMO-encoding genes and nitrification (Könneke et al., 2005).

Since the isolation of the first representative strain SCM1, the same general cultivation strategy has been widely applied to culture additional members of archaeal ammonia oxidizers from a variety of habitats, including marine, soil, freshwater, wastewater, and hot springs (Stahl and de la Torre, 2012a). Available AOA cultures grow at temperatures as high as 74°C (“*Candidatus Nitrosocaldus yellowstonii*” HL72) (de la Torre et al., 2008), pH as low as 4.0 (“*Candidatus Nitrosotalea*” sp. Nd2) (Lehtovirta-Morley et al., 2014), salinities between 55 and 96‰ (SCM1) (Elling et al., 2015; Widderich et al., 2015), oxygen (O₂) concentrations of 1 μM or lower (“*Candidatus Nitrosopumilus*” sp. PS0) (Qin et al., 2015d), and ammonia concentrations up to 100 mM (“*Candidatus Nitrosocosmicus franklandus*” C13) (Lehtovirta-Morley et al., 2016b). It has been shown that even phylogenetically closely related AOA strains display distinct physiological characteristics, supporting fine niche partitioning and ecological differentiation (Lehtovirta-Morley et al., 2014; Qin et al., 2014; Bayer et al., 2015). The ongoing metagenomics studies further extend our limited knowledge of genetic diversity of the globally distributed AOA (Bartossek et al., 2012; Stewart et al., 2012; Bertagnolli et al., 2015; Doxey et al., 2015). Comparative genomics and metagenomics have revealed that all AOA form a novel and deep-branching phylum, the *Thaumarchaeota*, within the *Archaea* (Brochier-Armanet et al., 2008; Spang et al., 2010).

Physiological and Genomic characterization of marine AOA

N. maritimus is the first cultivated representative of ammonia-oxidizing archaea (Könneke et al., 2005). *N. maritimus* is among the smallest free-living microorganisms, with a diameter of 0.17–0.22 μm and a length of 0.50–0.90 μm. Exponentially growing cells of *N. maritimus* with a cell

volume of $\sim 0.023 \mu\text{m}^3$ contain approximately 16–20 fg dry weight per cell, leading to a conspicuously high biovolume-to-biomass conversion factor of 0.70–0.87 fg dry weight per μm^3 (Martens-Habbena et al., 2009b). Actively growing cells contain 2.08 ± 0.12 fg of total lipids per cell, which reaches approximately 10% of cellular dry weight (Qin et al., 2015d). Its small genome (1,645,259 base pairs) accounts for 8–10% of dry cell weight (Walker et al., 2010). Cells reproduce by binary fission. Unique features of the *N. maritimus* cell cycle distinguish this species from other archaea, having a very long pre-replication phase (G_1 phase), a remarkably extensive replication stage (S phase), and a very short post-replication stage (G_2 phase, mitosis, and cell division) (Pelve et al., 2011). Although its genome possesses genes of both FtsZ-based and CdvABC-based cell division systems, *N. maritimus* employs the Cdv mechanism primarily for cell division (Pelve et al., 2011).

Using strain SCM1 as a model organism, detailed studies of ammonia oxidation kinetics and the biochemical characterizations of the carbon dioxide (CO_2) fixation pathway identified adaptive features associated with growth under extreme ammonia limitation (Martens-Habbena et al., 2009b; Könneke et al., 2014). Strain SCM1 has a remarkably low half saturation constant (K_m) for ammonia oxidation of 133 nM total ammonia ($\text{NH}_3 + \text{NH}_4^+$) and an exceptionally high ammonia affinity of $68,700 \text{ l g}^{-1} \text{ cells h}^{-1}$, which is among the highest substrate affinities yet reported for any microorganisms (Martens-Habbena et al., 2009b). High-affinity for ammonia is coupled with the most energy-efficient aerobic pathway for carbon fixation yet characterized, which together are thought to contribute to the remarkable ecological success of oligotrophic marine AOA (Martens-Habbena et al., 2009b; Könneke et al., 2014).

Archaeal ammonia oxidizers associate with the distinct and deeply-branching phylum *Thaumarchaeota*, which is divided into four major phylogenetic sub-lineages, group I.1 a, group I.1 a-associated, group I.1 b, and ThAOA (Thermophilic AOA) (Brochier-Armanet et al., 2008; Spang et al., 2010). Members of marine AOA are almost exclusively affiliated with the group I.1 a *Thaumarchaeota* (Biller et al., 2012). Despite the enormous metabolic and functional diversity, all sequenced AOA representatives share common genomic features such as a copper-based enzymatic system for ammonia oxidation and electron transfer, a variant of the autotrophic 3-hydroxypropionate/4-hydroxybutyrate (HP/HB) cycle for carbon fixation, and a complete cobalamin (vitamin B₁₂) synthesis pathway (Walker et al., 2010; Spang et al., 2012; Lebedeva et al., 2013; Santoro et al., 2015; Heal et al., 2016). In addition, all investigated AOA strains synthesize the same type of membrane lipids, the glycerol dibiphytanyl glycerol tetraether (GDGT) lipids with crenarchaeol as the characteristic component (de la Torre et al., 2008; Pitcher et al., 2011; Damsté et al., 2012; Elling et al., 2015; Qin et al., 2015d), the apolar lipid methoxy archaeol (Elling et al., 2014), and the same suite of membrane-bound respiratory menaquinones with 6 isoprenoid units (Elling et al., 2016).

Although the overall stoichiometry of ammonia oxidation to nitrite by *N. maritimus* is identical with that of ammonia-oxidizing bacteria (AOB), the underlying biochemical pathways appear to be vastly different. No canonical inventory for the iron-based electron transfer system of AOB has been identified in genomes of *N. maritimus* and all other sequenced ammonia-oxidizing *Thaumarchaeota*; rather, AOA utilize primarily the copper-centered enzymatic systems for ammonia oxidation and electron transfer, including the putative AMO (ammonia monooxygenase), putative copper-NirK (nitrite reductase), blue copper-containing plastocyanin-

like electron carriers, and a membrane-bound putative quinone reductase with blue copper domains (Walker et al., 2010). The presence of a remarkably high number of copper-containing metalloenzymes in *N. maritimus* also suggests a high copper requirement for growth. The copper-limiting threshold for growth is $10^{-12.7}$ mol L⁻¹ free cupric ion. This threshold is higher than determined for some denitrifying bacteria and the plastocyanin-containing oceanic diatom *Thalassiosira oceanica* (Amin et al., 2013). Another apparent divergence in the biochemistry of ammonia oxidation by AOA and AOB is the lack of an identifiable homologue of the bacterial hydroxylamine dehydrogenase (HAO)-encoding genes in any thaumarchaeotal genomes, even though *N. maritimus* produces NH₂OH as an intermediate in its ammonia oxidation pathway (Vajjala et al., 2013). These observations suggest the presence of a novel enzyme, or novel enzyme system, for conversion of NH₂OH to NO₂⁻ in AOA.

Ecological significance of marine AOA

Since the discovery of ammonia oxidation within the domain *Archaea*, considerable efforts have been made to elucidate details about the actual significance of archaeal ammonia oxidation for the global cycling of nitrogen, particularly in regard to their significance to nitrification related nitrous oxide (N₂O) emission (Francis et al., 2005; Könneke et al., 2005; Leininger et al., 2006; Mincer et al., 2007; Agogué et al., 2008a; Santoro et al., 2010; Santoro et al., 2011; Löscher et al., 2012; Jung et al., 2014b; Stieglmeier et al., 2014a). Previous extensive archaeal *amoA* (the gene coding for the α -subunit of the AMO) gene surveys demonstrated the widespread presence of the putative *amoA* genes in divergent MGI, suggestive of their significant role in marine nitrification (Francis et al., 2005). However, given the extremely low ammonia concentrations in the ocean and the thermodynamically low energy yield of ammonia oxidation ($\Delta G^{\circ} = -271$ kJ

$\text{mol}^{-1} \text{NH}_4^+$) (Wood, 1986), it remained uncertain whether all members of MGI obligatorily depend on ammonia as the sole energy source for growth. For example, Agogué *et al.* speculated that most deep-sea MGI are incapable of autotrophic ammonia oxidation and are likely heterotrophs using organic matter for growth based on a marked decrease in the ratio of *amoA* : MGI 16S rRNA genes with depth (Agogué *et al.*, 2008a). This vertical gradient of decreasing ratio was however later shown to be mainly caused by primer bias (Sintes *et al.*, 2013).

Marine AOA appear to be active within the oxygenated and productive lower euphotic zone, potentially competing with phytoplankton for the reduced forms of nitrogen and largely contributing to endogenously generated nitrite (and subsequently nitrate) to sustain primary production in marine surface waters (Martens-Habbena *et al.*, 2009b; Beman *et al.*, 2012a; Horak *et al.*, 2013; Newell *et al.*, 2013; Smith *et al.*, 2014). In lower euphotic zone and deeper, the putative archaeal *amoA* gene copy numbers generally surpass those of their bacterial counterparts by more than 1,000-fold. The significant correlation between putative archaeal *amoA* gene copy numbers, transcriptional activity, and nitrification rates further implicates marine AOA as significant contributors to in situ nitrification (Francis *et al.*, 2005; Horak *et al.*, 2013; Newell *et al.*, 2013). In addition to predominating in oxygenated oceanic regions, tracer, metatranscriptomic, and metaproteomic studies indicate that marine AOA are abundant in low- O_2 environments, such as the suboxic zones of OMZs and surficial sediments (Francis *et al.*, 2005; Sahan and Muyzer, 2008; Lam *et al.*, 2009; Kalvelage *et al.*, 2011; Beman *et al.*, 2012b; Stewart *et al.*, 2012; Hawley *et al.*, 2014). Notably, Stewart *et al.* 2012 reported that transcripts encoding the thaumarchaeotal ammonium transporter (*Amt*) constituted more than 10% of all

reads in samples collected from the OMZ upper boundary of the Eastern Tropical South Pacific (~10 $\mu\text{M O}_2$), consistent with a high affinity for O_2 (Stewart et al., 2012). Indeed, a recent study of the O_2 uptake kinetics of ammonia oxidation in OMZ waters revealed extremely low K_m values of $333 \pm 130 \text{ nM O}_2$ (Bristow et al., 2016). Therefore, archaeal ammonia oxidation is closely coupled with nitrogen loss processes of anaerobic ammonia oxidation (anammox) and denitrification in the OMZs by providing nitrite to anammox bacteria and denitrifiers (Yan et al., 2012b).

Environmental variables affecting the distribution and activity of marine AOA

Although the AOA are now of generally recognized centrality in marine nitrification, relatively little is known about the environmental variables influencing their distribution and activities in the open ocean. Inferences of environmental variables influencing environmental distribution and activity have mostly been drawn from ecophysiological characterization of the few available pure cultures of marine AOA (Martens-Habbena et al., 2009b; Amin et al., 2013; Qin et al., 2014; Bayer et al., 2016), pointing to the possible significance of Cu availability and high affinities for ammonia and oxygen (Martens-Habbena et al., 2009b; Amin et al., 2013; Qin et al., 2015d). Notably, inferences from culture are generally consistent with direct measurements of marine environments in which AOA dominate, where ammonia oxidation has been associated with exceptionally low K_m values for ammonia (as low as 22.8 nM total ammonia plus ammonium) and oxygen (as low as 203 nM) (Bristow et al., 2016; Peng et al., 2016). The high substrate affinities of marine AOA reflect their remarkable adaptation to growth under conditions of constantly low energy flux, suggested to provide competitive advantage relative to AOB, and is consistent with the high activity and abundance of marine AOA observed in ammonium-

limited and unproductive marine environments, as represented by oligotrophic gyre and deep oceans (Mincer et al., 2007; Sintes et al., 2013), and low oxygen regions, such as the hypoxic boundaries of oxygen minimum zones (Peng et al., 2016).

These data together suggest that low ammonia availability and competition with phytoplankton for regenerated ammonia in the upper water column should not be limiting factors for the AOA, implicating photosensitivity as a possibly more relevant controlling variable. Indeed, marine AOA abundance and ammonia oxidation rates showed generally consistent negative relationship with ambient light intensity in diverse geographical regions (Mincer et al., 2007; Beman et al., 2012a; Horak et al., 2013; Newell et al., 2013; Peng et al., 2016). However, a recent study by Smith et al. (2014) reported that light did not have an inhibitory effect on ammonia oxidation in California coastal waters. The “Water Column A” (WCA) genotypes of the marine AOA in their study sites appeared to be light-tolerant and were able to maintain similar or even higher ammonia oxidation rates at high irradiance intensities compared to dark controls (Smith et al., 2014). In addition, recently published studies of light sensitivity of AOA in culture have shown significant variability among phylogenetically closely related marine AOA strains (Qin et al., 2014). Therefore, light remains a poorly constrained variable controlling nitrate regeneration within the photic zone.

In addition, as for much of microorganism, temperature is a master regulator of the growth and metabolic activity of cultivated marine AOA. Different marine AOA isolates displayed different temperature optima and they are generally adapted to the *in situ* temperatures of their original habitats, suggesting that temperature is likely an important determinant of the population

structure and diversity of AOA in marine environments (Qin et al., 2014). Our current understanding of temperature regulation on archaeal ammonia oxidation activity is based on very few studies in restricted coastal areas (Horak et al., 2013). However, much of its significance remains unknown in pelagic oceans. Other physiochemical parameters, such as pH and salinity, show relatively small variation in open oceans and therefore are not considered as major determinants in controlling the distribution and activity of AOA in these environments.

Membrane lipid composition of marine AOA and application of thaumarchaeal lipids as paleotemperature proxy

The cell membrane of marine AOA is comprised of a monolayer cell membrane, consisting of crenarchaeol as the major glycerol dibiphytanyl glycerol tetraether (GDGT) lipid with zero to five cycloalkyl rings. The incorporation of a cyclohexyl moiety into crenarchaeol, a unique structural feature of thaumarchaeotal lipids, has been used as a molecular marker for marine AOA (Pearson and Ingalls, 2013). Although environmental analyses have been used to infer that Marine Group II *Euryarchaeota* contain crenarchaeol, this has yet to be confirmed by analysis of cultured cells (Lincoln et al., 2014a, b; Schouten et al., 2014). The introduction of cyclohexane rings into tetraether lipids has been found to reduce membrane permeability to small ions (Koyanagi et al., 2016). Relative to the bacterial membrane bi-layer, the membrane-spanning lipids of AOA are less permeable to ions and protons (van de Vossenberg et al., 1998; Valentine, 2007). Lower permeability is suggested to reduce maintenance energy costs, an important adaptive feature of extreme oligophiles such as the AOA. Thus, growth temperature-dependent modulation of membrane composition is likely associated with maintenance of appropriate permeability, as well as other membrane functions (van de Vossenberg et al., 1998). The

influence of temperature on membrane composition has been the major focus of studies of the environmental distribution of archaeal membrane lipids in the present and for interpreting lipids preserved in the sedimentary record (Pearson and Ingalls, 2013). In particular, the correlation between sea surface temperature (SST) and the cyclopentane ring distribution of GDGTs in a sample set of globally distributed core top sediments is the basis for a widely applied paleotemperature proxy, TEX_{86} (TetraEther index of lipids with 86 carbon atoms). The TEX_{86} proxy has been used to reconstruct surface ocean temperature as far back as the Middle Jurassic (Schouten et al., 2002; Jenkyns et al., 2012). However, the extent to which temperature is the causative agent behind the correlation has not fully been examined. Moreover, it is not evident how a group of organisms that live at depths below the upper-photoc zone and are the dominant prokaryote of the abyss can record SST via a physiological response. TEX_{86} reconstructions of the distant past, when oceanic conditions could be quite different from today, present the greatest challenge to interpretation. For example, inferred Cretaceous SSTs are higher than physically plausible for the ocean (Schouten et al., 2003). Thus, considerable efforts have been made to develop and apply new TEX_{86} equations suitable for high temperature environments (TEX_{86}^H), low temperature environments (TEX_{86}^L), local systems (TEX_{86}'), the marine water column, and mesocosms (Wuchter et al., 2004; Wuchter et al., 2005; Sluijs et al., 2006; Kim et al., 2010; Shevenell et al., 2011). However, the influence of environmental factors other than temperature on GDGT distribution and TEX_{86} value remains uncertain.

References

- Agogu , H., Brink, M., Dinasquet, J., and Herndl, G.J. (2008a) Major gradients in putatively nitrifying and non-nitrifying Archaea in the deep North Atlantic. *Nature* **456**: 788-791.
- Amin, S.A., Moffett, J.W., Martens-Habbena, W., Jacquot, J.E., Han, Y., Devol, A. et al. (2013) Copper requirements of the ammonia-oxidizing archaeon *Nitrosopumilus maritimus* SCM1 and implications for nitrification in the marine environment. *Limnol Oceanogr* **58**: 2037-2045.
- Bartossek, R., Spang, A., Weidler, G., Lanzen, A., and Schleper, C. (2012) Metagenomic analysis of ammonia-oxidizing archaea affiliated with the soil group. *Front Microbiol* **3**.
- Bayer, B., Vojvoda, J., Offre, P., Alves, R.J., Elisabeth, N.H., Garcia, J.A. et al. (2015) Physiological and genomic characterization of two novel marine thaumarchaeal strains indicates niche differentiation. *Isme J*.
- Bayer, B., Vojvoda, J., Offre, P., Alves, R.J.E., Elisabeth, N.H., Garcia, J.A.L. et al. (2016) Physiological and genomic characterization of two novel marine thaumarchaeal strains indicates niche differentiation. *Isme J* **10**: 1051-1063.
- Beman, J.M., Popp, B.N., and Alford, S.E. (2012a) Quantification of ammonia oxidation rates and ammonia-oxidizing archaea and bacteria at high resolution in the Gulf of California and eastern tropical North Pacific Ocean. *Limnol Oceanogr* **57**: 711-726.
- Beman, J.M., Bertics, V.J., Braunschweiler, T., and Wilson, J.M. (2012b) Quantification of ammonia oxidation rates and the distribution of ammonia-oxidizing Archaea and Bacteria in marine sediment depth profiles from Catalina Island, California. *Front Microbiol* **3**.
- Bertagnolli, A.D., Meinhardt, K.A., Pannu, M., Brown, S., Strand, S., Fransen, S.C., and Stahl, D.A. (2015) Influence of edaphic and management factors on the diversity and abundance of ammonia-oxidizing thaumarchaeota and bacteria in soils of bioenergy crop cultivars. *Env Microbiol Rep* **7**: 312-320.
- Biller, S.J., Mosier, A.C., Wells, G.F., and Francis, C.A. (2012) Global biodiversity of aquatic ammonia-oxidizing archaea is partitioned by habitat. *Front Microbiol* **3**.
- Bristow, L.A., Dalsgaard, T., Tiano, L., Mills, D.B., Bertagnolli, A.D., Wright, J.J. et al. (2016) Ammonium and nitrite oxidation at nanomolar oxygen concentrations in oxygen minimum zone waters. *Proceedings of the National Academy of Sciences* **113**: 10601-10606.
- Brochier-Armanet, C., Boussau, B., Gribaldo, S., and Forterre, P. (2008) Mesophilic crenarchaeota: proposal for a third archaeal phylum, the Thaumarchaeota. *Nat Rev Microbiol* **6**: 245-252.
- Damst , J.S.S., Rijpstra, W.I.C., Hopmans, E.C., Jung, M.Y., Kim, J.G., Rhee, S.K. et al. (2012) Intact polar and core glycerol dibiphytanyl glycerol tetraether lipids of group I.1a and I.1b *Thaumarchaeota* in soil. *Appl Environ Microb* **78**: 6866-6874.
- de la Torre, J.R., Walker, C.B., Ingalls, A.E., K nneke, M., and Stahl, D.A. (2008) Cultivation of a thermophilic ammonia oxidizing archaeon synthesizing crenarchaeol. *Environ Microbiol* **10**: 810-818.
- Delong, E.F. (1992) Archaea in Coastal Marine Environments. *Proceedings of the National Academy of Sciences of the United States of America* **89**: 5685-5689.
- Doxey, A.C., Kurtz, D.A., Lynch, M.D.J., Sauder, L.A., and Neufeld, J.D. (2015) Aquatic metagenomes implicate Thaumarchaeota in global cobalamin production. *Isme J* **9**: 461-471.
- Elling, F.J., K nneke, M., Mu mann, M., Greve, A., and Hinrichs, K.U. (2015) Influence of temperature, pH, and salinity on membrane lipid composition and TEX₈₆ of marine planktonic thaumarchaeal isolates. *Geochim Cosmochim Acta* **171**: 238-255.
- Elling, F.J., K nneke, M., Lipp, J.S., Becker, K.W., Gagen, E.J., and Hinrichs, K.U. (2014) Effects of growth phase on the membrane lipid composition of the thaumarchaeon

- Nitrosopumilus maritimus* and their implications for archaeal lipid distributions in the marine environment. *Geochim Cosmochim Acta* **141**: 579-597.
- Elling, F.J., Becker, K.W., Könneke, M., Schroder, J.M., Kellermann, M.Y., Thomm, M., and Hinrichs, K.U. (2016) Respiratory quinones in Archaea: phylogenetic distribution and application as biomarkers in the marine environment. *Environ Microbiol* **18**: 692-707.
- Francis, C.A., Roberts, K.J., Beman, J.M., Santoro, A.E., and Oakley, B.B. (2005) Ubiquity and diversity of ammonia-oxidizing archaea in water columns and sediments of the ocean. *P Natl Acad Sci USA* **102**: 14683-14688.
- Fuhrman, J.A., Mccallum, K., and Davis, A.A. (1992) Novel Major Archaeobacterial Group from Marine Plankton. *Nature* **356**: 148-149.
- Hawley, A.K., Brewer, H.M., Norbeck, A.D., Pasa-Tolic, L., and Hallam, S.J. (2014) Metaproteomics reveals differential modes of metabolic coupling among ubiquitous oxygen minimum zone microbes. *P Natl Acad Sci USA* **111**: 11395-11400.
- Heal, K.R., Qin, W., Ribalet, F., Bertagnolli, A.D., Coyote-Maestas, W., Hmelo, L.R. et al. (2016) Two distinct pools of B₁₂ analogs reveal community interdependencies in the ocean. *P Natl Acad Sci USA*.
- Horak, R.E.A., Qin, W., Schauer, A.J., Armbrust, E.V., Ingalls, A.E., Moffett, J.W. et al. (2013) Ammonia oxidation kinetics and temperature sensitivity of a natural marine community dominated by Archaea. *Isme J* **7**: 2023-2033.
- Jenkyns, H.C., Schouten-Huibers, L., Schouten, S., and Damsté, J.S.S. (2012) Warm Middle Jurassic-Early Cretaceous high-latitude sea-surface temperatures from the Southern Ocean. *Clim Past* **8**: 215-226.
- Jung, M.Y., Well, R., Min, D., Giesemann, A., Park, S.J., Kim, J.G. et al. (2014b) Isotopic signatures of N₂O produced by ammonia-oxidizing archaea from soils. *ISME J* **8**: 1115-1125.
- Kalvelage, T., Jensen, M.M., Contreras, S., Revsbech, N.P., Lam, P., Günter, M. et al. (2011) Oxygen sensitivity of anammox and coupled N-cycle processes in oxygen minimum zones. *PLoS ONE* **6**.
- Karner, M.B., DeLong, E.F., and Karl, D.M. (2001) Archaeal dominance in the mesopelagic zone of the Pacific Ocean. *Nature* **409**: 507-510.
- Kim, J.H., van der Meer, J., Schouten, S., Helmke, P., Willmott, V., Sangiorgi, F. et al. (2010) New indices and calibrations derived from the distribution of crenarchaeal isoprenoid tetraether lipids: Implications for past sea surface temperature reconstructions. *Geochim Cosmochim Acta* **74**: 4639-4654.
- Könneke, M., Bernhard, A.E., de la Torre, J.R., Walker, C.B., Waterbury, J.B., and Stahl, D.A. (2005) Isolation of an autotrophic ammonia-oxidizing marine archaeon. *Nature* **437**: 543-546.
- Könneke, M., Schubert, D.M., Brown, P.C., Hugler, M., Standfest, S., Schwander, T. et al. (2014) Ammonia-oxidizing archaea use the most energy-efficient aerobic pathway for CO₂ fixation. *P Natl Acad Sci USA* **111**: 8239-8244.
- Koyanagi, T., Leriche, G., Onofrei, D., Holland, G.P., Mayer, M., and Yang, J. (2016) Cyclohexane Rings Reduce Membrane Permeability to Small Ions in Archaea-Inspired Tetraether Lipids. *Angew Chem Int Ed Engl* **55**: 1890-1893.
- Lam, P., Lavik, G., Jensen, M.M., van de Vossenberg, J., Schmid, M., Woebken, D. et al. (2009) Revising the nitrogen cycle in the Peruvian oxygen minimum zone. *Proc Natl Acad Sci USA* **106**: 4752-4757.
- Lebedeva, E.V., Hatzenpichler, R., Pelletier, E., Schuster, N., Hauzmayer, S., Bulaev, A. et al. (2013) Enrichment and Genome Sequence of the Group I. 1a Ammonia-Oxidizing Archaeon

- "Ca. Nitrosotenuis uzonensis" Representing a Clade Globally Distributed in Thermal Habitats. *Plos One* **8**.
- Lehtovirta-Morley, L.E., Ge, C.R., Ross, J., Yao, H.Y., Nicol, G.W., and Prosser, J.I. (2014) Characterisation of terrestrial acidophilic archaeal ammonia oxidisers and their inhibition and stimulation by organic compounds. *Fems Microbiol Ecol* **89**: 542-552.
- Lehtovirta-Morley, L.E., Ross, J., Hink, L., Weber, E.B., Gubry-Rangin, C., Thion, C. et al. (2016b) Isolation of '*Candidatus Nitrosocosmicus franklandus*', a novel ureolytic soil archaeal ammonia oxidiser with tolerance to high ammonia concentration. *FEMS microbiology ecology*.
- Leininger, S., Urich, T., Schloter, M., Schwark, L., Qi, J., Nicol, G.W. et al. (2006) Archaea predominate among ammonia-oxidizing prokaryotes in soils. *Nature* **442**: 806-809.
- Lincoln, S.A., Wai, B., Eppley, J.M., Church, M.J., Summons, R.E., and DeLong, E.F. (2014a) Planktonic Euryarchaeota are a significant source of archaeal tetraether lipids in the ocean. *Proc Natl Acad Sci USA* **111**: 9858-9863.
- Lincoln, S.A., Wai, B., Eppley, J.M., Church, M.J., Summons, R.E., and DeLong, E.F. (2014b) Reply to Schouten et al.: Marine Group II planktonic Euryarchaeota are significant contributors to tetraether lipids in the ocean. *P Natl Acad Sci USA* **111**: E4286-E4286.
- Löscher, C.R., Kock, A., Könneke, M., LaRoche, J., Bange, H.W., and Schmitz, R.A. (2012) Production of oceanic nitrous oxide by ammonia-oxidizing archaea. *Biogeosciences* **9**: 2419-2429.
- Martens-Habbena, W., Berube, P.M., Urakawa, H., de la Torre, J.R., and Stahl, D.A. (2009b) Ammonia oxidation kinetics determine niche separation of nitrifying Archaea and Bacteria. *Nature* **461**: 976-U234.
- Mincer, T.J., Church, M.J., Taylor, L.T., Preston, C., Karl, D.M., and DeLong, E.F. (2007) Quantitative distribution of presumptive archaeal and bacterial nitrifiers in Monterey Bay and the North Pacific Subtropical Gyre. *Environ Microbiol* **9**: 1162-1175.
- Newell, S.E., Fawcett, S.E., and Ward, B.B. (2013) Depth distribution of ammonia oxidation rates and ammonia-oxidizer community composition in the Sargasso Sea. *Limnol Oceanogr* **58**: 1491-1500.
- Pearson, A., and Ingalls, A.E. (2013) Assessing the use of archaeal lipids as marine environmental proxies. *Annu Rev Earth Planet Sci* **41**: 359-384.
- Pelve, E.A., Lindsas, A.C., Martens-Habbena, W., de la Torre, J.R., Stahl, D.A., and Bernander, R. (2011) Cdv-based cell division and cell cycle organization in the thaumarchaeon *Nitrosopumilus maritimus*. *Mol Microbiol* **82**: 555-566.
- Peng, X.F., Fuchsman, C.A., Jayakumar, A., Warner, M.J., Devol, A.H., and Ward, B.B. (2016) Revisiting nitrification in the Eastern Tropical South Pacific: A focus on controls. *J Geophys Res Oceans* **121**: 1667-1684.
- Pitcher, A., Hopmans, E.C., Mosier, A.C., Park, S.J., Rhee, S.K., Francis, C.A. et al. (2011) Core and Intact Polar Glycerol Dibiphytanyl Glycerol Tetraether Lipids of Ammonia-Oxidizing Archaea Enriched from Marine and Estuarine Sediments. *Appl Environ Microb* **77**: 3468-3477.
- Qin, W., Carlson, L.T., Armbrust, E.V., Devol, A.H., Moffett, J.W., Stahl, D.A., and Ingalls, A.E. (2015d) Confounding effects of oxygen and temperature on the TEX₈₆ signature of marine Thaumarchaeota. *P Natl Acad Sci USA* **112**: 10979-10984.
- Qin, W., Amin, S.A., Martens-Habbena, W., Walker, C.B., Urakawa, H., Devol, A.H. et al. (2014) Marine ammonia-oxidizing archaeal isolates display obligate mixotrophy and wide ecotypic variation. *P Natl Acad Sci USA* **111**: 12504-12509.

- Sahan, E., and Muyzer, G. (2008) Diversity and spatio-temporal distribution of ammonia-oxidizing Archaea and Bacteria in sediments of the Westerschelde estuary. *FEMS Microbiol Ecol* **64**: 175-186.
- Santoro, A.E., Casciotti, K.L., and Francis, C.A. (2010) Activity, abundance and diversity of nitrifying archaea and bacteria in the central California Current. *Environ Microbiol* **12**: 1989-2006.
- Santoro, A.E., Buchwald, C., McIlvin, M.R., and Casciotti, K.L. (2011) Isotopic Signature of N₂O Produced by Marine Ammonia-Oxidizing Archaea. *Science* **333**: 1282-1285.
- Santoro, A.E., Dupont, C.L., Richter, R.A., Craig, M.T., Carini, P., McIlvin, M.R. et al. (2015) Genomic and proteomic characterization of "Candidatus Nitrosopelagicus brevis": An ammonia-oxidizing archaeon from the open ocean. *P Natl Acad Sci USA* **112**: 1173-1178.
- Sayavedra-Soto, L.A., Hamamura, N., Liu, C.W., Kimbrel, J.A., Chang, J.H., and Arp, D.J. (2011) The membrane-associated monooxygenase in the butane-oxidizing Gram-positive bacterium *Nocardioides* sp. strain CF8 is a novel member of the AMO/PMO family. *Env Microbiol Rep* **3**: 390-396.
- Schattenhofer, M., Fuchs, B.M., Amann, R., Zubkov, M.V., Tarran, G.A., and Pernthaler, J. (2009) Latitudinal distribution of prokaryotic picoplankton populations in the Atlantic Ocean. *Environ Microbiol* **11**: 2078-2093.
- Schouten, S., Hopmans, E.C., Schefuß, E., and Damsté, J.S.S. (2002) Distributional variations in marine crenarchaeotal membrane lipids: a new tool for reconstructing ancient sea water temperatures? *Earth Planet Sci Lett* **204**: 265-274.
- Schouten, S., Villanueva, L., Hopmans, E.C., van der Meer, M.T.J., and Damsté, J.S.S. (2014) Are Marine Group II Euryarchaeota significant contributors to tetraether lipids in the ocean? *P Natl Acad Sci USA* **111**: E4285-E4285.
- Schouten, S., Hopmans, E.C., Forster, A., van Breugel, Y., Kuypers, M.M.M., and Damsté, J.S.S. (2003) Extremely high sea-surface temperatures at low latitudes during the middle Cretaceous as revealed by archaeal membrane lipids. *Geology* **31**: 1069-1072.
- Shevenell, A.E., Ingalls, A.E., Domack, E.W., and Kelly, C. (2011) Holocene Southern Ocean surface temperature variability west of the Antarctic Peninsula. *Nature* **470**: 250-254.
- Sintes, E., Bergauer, K., De Corte, D., Yokokawa, T., and Herndl, G.J. (2013) Archaeal *amoA* gene diversity points to distinct biogeography of ammonia-oxidizing Crenarchaeota in the ocean. *Environ Microbiol* **15**: 1647-1658.
- Sluijs, A., Schouten, S., Pagani, M., Woltering, M., Brinkhuis, H., Damsté, J.S.S. et al. (2006) Subtropical arctic ocean temperatures during the Palaeocene/Eocene thermal maximum. *Nature* **441**: 610-613.
- Smith, J.M., Chavez, F.P., and Francis, C.A. (2014) Ammonium uptake by phytoplankton regulates nitrification in the sunlit ocean. *PLoS ONE* **9**.
- Spang, A., Hatzenpichler, R., Brochier-Armanet, C., Rattei, T., Tischler, P., Spieck, E. et al. (2010) Distinct gene set in two different lineages of ammonia-oxidizing archaea supports the phylum Thaumarchaeota. *Trends Microbiol* **18**: 331-340.
- Spang, A., Poehlein, A., Offre, P., Zumbragel, S., Haider, S., Rychlik, N. et al. (2012) The genome of the ammonia-oxidizing *Candidatus Nitrososphaera gargensis*: insights into metabolic versatility and environmental adaptations. *Environ Microbiol* **14**: 3122-3145.
- Stahl, D.A., and de la Torre, J.R. (2012a) Physiology and Diversity of Ammonia-Oxidizing Archaea. *Annu Rev Microbiol* **66**: 83-101.

- Stewart, F.J., Ulloa, O., and DeLong, E.F. (2012) Microbial metatranscriptomics in a permanent marine oxygen minimum zone. *Environ Microbiol* **14**: 23-40.
- Stieglmeier, M., Mooshammer, M., Kitzler, B., Wanek, W., Zechmeister-Boltenstern, S., Richter, A., and Schleper, C. (2014a) Aerobic nitrous oxide production through N-nitrosating hybrid formation in ammonia-oxidizing archaea. *Isme J* **8**: 1135-1146.
- Tavormina, P.L., Orphan, V.J., Kalyuzhnaya, M.G., Jetten, M.S.M., and Klotz, M.G. (2011) A novel family of functional operons encoding methane/ammonia monooxygenase-related proteins in gammaproteobacterial methanotrophs. *Env Microbiol Rep* **3**: 91-100.
- Vajrala, N., Martens-Habbena, W., Sayavedra-Soto, L.A., Schauer, A., Bottomley, P.J., Stahl, D.A., and Arp, D.J. (2013) Hydroxylamine as an intermediate in ammonia oxidation by globally abundant marine archaea. *P Natl Acad Sci USA* **110**: 1006-1011.
- Valentine, D.L. (2007) Adaptations to energy stress dictate the ecology and evolution of the Archaea. *Nature Rev Microbiol* **5**: 316-323.
- van de Vossenberg, J.L.C.M., Driessen, A.J.M., and Konings, W.N. (1998) The essence of being extremophilic: the role of the unique archaeal membrane lipids. *Extremophiles* **2**: 163-170.
- Venter, J.C., Remington, K., Heidelberg, J.F., Halpern, A.L., Rusch, D., Eisen, J.A. et al. (2004) Environmental genome shotgun sequencing of the Sargasso Sea. *Science* **304**: 66-74.
- Walker, C.B., de la Torre, J.R., Klotz, M.G., Urakawa, H., Pinel, N., Arp, D.J. et al. (2010) Nitrosopumilus maritimus genome reveals unique mechanisms for nitrification and autotrophy in globally distributed marine crenarchaea. *P Natl Acad Sci USA* **107**: 8818-8823.
- Widderich, N., Czech, L., Elling, F.J., Könneke, M., Stoveken, N., Pittelkow, M. et al. (2015) Strangers in the archaeal world: osmstress-responsive biosynthesis of ectoine and hydroxyectoine by the marine thaumarchaeon *Nitrosopumilus maritimus*. *Environ Microbiol*.
- Woese, C.R., Magrum, L.J., and Fox, G.E. (1978) Archaeobacteria. *J Mol Evol* **11**: 245-252.
- Wood, P.M. (1986) Nitrification as a bacterial energy source. In *Nitrification*. Prosser, J.I. (ed). Oxford, United Kingdom: IRL Press, pp. 39-62.
- Wuchter, C., Schouten, S., Coolen, M.J.L., and Damsté, J.S.S. (2004) Temperature-dependent variation in the distribution of tetraether membrane lipids of marine Crenarchaeota: Implications for TEX₈₆ paleothermometry. *Paleoceanography* **19**.
- Wuchter, C., Schouten, S., Wakeham, S.G., and Damsté, J.S.S. (2005) Temporal and spatial variation in tetraether membrane lipids of marine Crenarchaeota in particulate organic matter: Implications for TEX₈₆ paleothermometry. *Paleoceanography* **20**.
- Yan, J., Haaijer, S.C.M., den Camp, H.J.M.O., van Niftrik, L., Stahl, D.A., Konneke, M. et al. (2012b) Mimicking the oxygen minimum zones: stimulating interaction of aerobic archaeal and anaerobic bacterial ammonia oxidizers in a laboratory-scale model system. *Environ Microbiol* **14**: 3146-3158.

Chapter 2.

Marine ammonia-oxidizing archaeal isolates display obligate mixotrophy and wide ecotypic variation

Wei Qin^a, Shady A. Amin^b, Willm Martens-Habbena^a, Christopher B. Walker^a,
Hidetoshi Urakawa^c, Allan H. Devol^b, Anitra E. Ingalls^b, James W. Moffett^d,
E. Virginia Armbrust^b, and David A. Stahl^{a,1}

Published in *Proceedings of the National Academy of Sciences of the United States of America*

2014

vol. 111, no. 34, 12504–12509, doi: 10.1073/pnas.1324115111

^aDepartment of Civil and Environmental Engineering, University of Washington, Seattle, WA 98195; ^bSchool of Oceanography, University of Washington, Seattle, WA 98195; ^cDepartment of Marine and Ecological Sciences, Florida Gulf Coast University, Fort Myers, FL 33965; ^dDepartment of Biological Sciences, University of Southern California, Los Angeles, CA 90089

¹Corresponding author E-mail: dastahl@u.washington.edu.

Abstract

Ammonia-oxidizing archaea (AOA) are now implicated in exerting significant control over the form and availability of reactive nitrogen species in marine environments. Detailed studies of specific metabolic traits and physicochemical factors controlling their activities and distribution have not been well constrained in part due to the scarcity of isolated AOA strains. Here we report the isolation of two new coastal marine AOA, strains PS0 and HCA1. Comparison of the new strains to *Nitrosopumilus maritimus* strain SCM1, the only marine AOA in pure culture thus far, demonstrated distinct adaptations to pH, salinity, organic carbon, temperature, and light. Strain PS0 sustained nearly 80% of ammonia oxidation activity at a pH as low as 5.9, indicating that coastal strains may be less sensitive to the ongoing reduction in ocean pH. Notably, the two novel isolates are obligate mixotrophs that rely on uptake and assimilation of organic carbon compounds, suggesting a direct coupling between chemolithotrophy and organic matter assimilation in marine food webs. All three isolates showed only minor photoinhibition at $15 \mu\text{E m}^{-2} \text{s}^{-1}$ and rapid recovery of ammonia oxidation in the dark, consistent with an AOA contribution to the primary nitrite maximum and the plausibility of a diurnal cycle of archaeal ammonia oxidation activity in the euphotic zone. Together, these findings highlight an unexpected adaptive capacity within closely related Marine Group I AOA and provide new understanding of the physiological basis of the remarkable ecological success reflected by their generally high abundance in marine environments.

Significance Statement

Ammonia-oxidizing archaea (AOA) influence the form and availability of nitrogen in marine environments, are a major contributor to N_2O release and plausible indirect source of methane in

the upper ocean. Thus, their sensitivity to ocean acidification and other physicochemical changes associated with climate change has global significance. We here report on the physiological response of novel AOA isolates to key environmental variables. Although reported as highly sensitive to reduction in ocean pH, we now show that some coastal marine AOA can remain active with increasing acidification of the oceans. All AOA isolates assimilate fixed carbon and two are obligate mixotrophs, suggesting this globally significant assemblage serves a significant function in coupling chemolithotrophy with organic matter assimilation in marine food webs.

Introduction

The discovery of ammonia-oxidizing archaea (AOA), sometimes constituting up to nearly 40% of marine microbial plankton, challenged the traditional view of microbial controls of nitrogen speciation in the ocean (Karner et al., 2001; Francis et al., 2005; Agogue et al., 2008a; Prosser and Nicol, 2008; Sintez et al., 2013). The AOA are now generally recognized as the major drivers of nitrification in marine environments (Prosser and Nicol, 2008; Santoro et al., 2010; Beman et al., 2012a; Horak et al., 2013). Their activities are of importance to trophic interactions that influence primary production and export of carbon to the deep ocean, they are a known source of atmospheric greenhouse gases (nitrous oxide and indirectly methane), and their high demand for copper may also alter food web dynamics (Karl et al., 2008; Walker et al., 2010; Santoro et al., 2011; Löscher et al., 2012; Metcalf et al., 2012; Amin et al., 2013).

Although enrichments of novel AOA strains belonging to Groups I.1a and I.1b from a variety of marine and terrestrial environments have been reported (de la Torre et al., 2008; Hatzenpichler et

al., 2008; Lehtovirta-Morley et al., 2011; Santoro and Casciotti, 2011; Tourna et al., 2011; French et al., 2012; Kim et al., 2012a; Mosier et al., 2012a), no additional pure cultures of marine representatives have been described since the isolation of *Nitrosopumilus maritimus* strain SCM1 (henceforth referred to as SCM1) (Könneke et al., 2005). Yet many complex biological traits of significance to marine biogeochemistry and marine food webs cannot be unambiguously established using metagenomic, metatranscriptomic studies and enrichment cultures. Initial understanding of the physiological basis for high AOA abundance in the marine water column came from the demonstration that SCM1 is an extreme oligotroph, having one of the highest affinities (low K_s) for ammonia (here defined as combined ammonia/ammonium) yet observed in pure culture (Martens-Habbena et al., 2009a). The discovery of a novel pathway for methylphosphonate synthesis, a plausible source of methane in the upper ocean, in the AOA and other abundant marine plankton (including *Pelagibacter* and *Prochlorococcus*) was made possible by genomic and biochemical characterization of SCM1 (Karl et al., 2008; Metcalf et al., 2012). More recent physiological studies examining the copper requirements of SCM1 provided a framework to evaluate the significance of copper in controlling the environmental distribution and activity of marine AOA (Amin et al., 2013).

The capture of a greater representation of AOA environmental diversity in pure culture should therefore serve to expand understanding of traits influencing their activity patterns in coastal and open marine systems. For example, a capacity to use fixed carbon and urea as alternative carbon and energy sources, respectively, has been suggested by tracer, metagenomic, and metatranscriptomic studies (Ouverney and Fuhrman, 2001; Herndl et al., 2005; Ingalls et al., 2006; Teira et al., 2006; Hansman et al., 2009; Konstantinidis et al., 2009; Hollibaugh et al.,

2011; Yakimov et al., 2011; Alonso-Saez et al., 2012). The contribution of AOA to endogenously generated nitrate in marine surface waters, of fundamental relevance to the source of nitrogen sustaining primary production in the photic zone, was suggested by relating nitrification activity and the archaeal *amoA* (the gene coding for the α -subunit of the ammonia monooxygenase) distribution patterns (Caffrey et al., 2007; Beman et al., 2008; Church et al., 2010; Beman et al., 2012a; Horak et al., 2013). A reported sensitivity of marine populations to small reductions in pH, important to understanding the possible impact of ongoing ocean acidification on the marine nitrogen cycle, was inferred from a pH perturbation study (Beman et al., 2011). Thus, as was shown for studies of SCM1, the availability of additional AOA isolates will both inform inferences made in the field as well as provide a physiological basis to direct future field research.

We now report the isolation of two novel coastal marine AOA strains from the Puget Sound estuary system in Washington State, significantly expanding the ecotypic diversity of marine *Thaumarchaeota* available in pure culture. Despite relatively close phylogenetic relationships, the three marine isolates comprise physiologically distinct ecotypes of AOA, varying in their capacity to use different carbon and energy sources, and in their tolerance to changes in pH, salinity, and light. These distinctive differences are directly relevant to their possible contribution to nitrification in different marine environments – including lower salinity coastal regions, the photic zone of the upper water column, and the increasing acidification of ocean waters associated with climate change.

Results

Enrichment and isolation of marine AOA. Enrichment cultures were initiated from Puget Sound main basin near surface (47.55 N, 122.28 W) and 50 m water from the Puget Sound Regional Synthesis Model (PRISM) Station P10 (47.91 N, 122.62 W) in Hood Canal. Our previous molecular surveys showed these coastal waters to be dominated by AOA, relative to ammonia-oxidizing bacteria (AOB) (Huguet et al., 2010b; Urakawa et al., 2010; Horak et al., 2013). Predominance of AOA was consistent with generally sub-micromolar concentrations of ammonia at these stations, sufficient to support AOA such as SCM1 but not known AOB (Martens-Habbena et al., 2009a). Enrichment conditions were designed to simulate the low substrate availability of these marine systems. The growth medium was supplemented with 2 μM NH_4Cl and cultures were incubated at 15 °C (see *SI Materials and Methods*).

Once the enrichments showed stable activity, they were transferred to artificial seawater medium supplemented with 2 μM NH_4Cl and 100 μM α -ketoglutaric acid. Earlier studies of strain SCM1 had shown that only a few central metabolites, including α -ketoglutaric acid, stimulated growth (see *SI Materials and Methods*). Highly enriched AOA cultures were obtained following approximately 2 years of consecutive transfer of 10% (vol/vol) late exponential phase subcultures into the same medium. Comparable growth kinetics were observed at ammonia concentrations between 2 and 500 μM ammonia, but concentrations above 1 mM significantly impaired growth. Thus, 500 μM ammonia was subsequently used to isolate the two new AOA strains from enrichment culture. Pure cultures were ultimately obtained by filtration of the enrichment cultures through a 0.22 μm Millex-GP syringe filter, and diluting the filtrate to extinction (see *SI Materials and Methods*). The two new oligotrophic AOA strains were designated HCA1 (Hood Canal station P10) and PS0 (Puget Sound main basin).

Exponential growth of both isolates in synthetic seawater medium containing 500 μM ammonia and 100 μM α -ketoglutaric acid was supported by the near stoichiometric oxidation of ammonia to nitrite (Fig. 2.1A, B). No growth was observed in medium containing α -ketoglutaric acid and no ammonia, supplemented with nitrite or nitrate as possible nitrogen sources. The maximum specific growth rates for strains HCA1 and PS0 were 0.55 d^{-1} and 0.23 d^{-1} , respectively. The growth rate of HCA1 was comparable to SCM1 (0.65 d^{-1}) and the one described thermophilic AOA, “*Candidatus Nitrosocaldus yellowstonii*” (0.8 d^{-1}) (Könneke et al., 2005; de la Torre et al., 2008). The lower growth rate of PS0 was similar to the previously described pelagic AOA enrichments, CN25 and CN75 (0.17 d^{-1}) and to the estimated *in situ* growth rates of AOA in winter polar waters (0.21 d^{-1}) (Santoro and Casciotti, 2011; Alonso-Saez et al., 2012). Since both strains were of similar shape and size to SCM1 (Fig. 2.1C, D; see description below), calculations of maximum ammonia oxidation activity were based on the reported cellular biomass of SCM1, using a factor of $10.2 \text{ fg protein cell}^{-1}$ (Martens-Habbena et al., 2009a). The values for HCA1 ($24.5 \mu\text{mol NH}_4^+ \text{ mg protein}^{-1} \text{ h}^{-1}$) and PS0 ($12.2 \mu\text{mol NH}_4^+ \text{ mg protein}^{-1} \text{ h}^{-1}$) (Table 2.1) were both lower than SCM1 ($51.9 \mu\text{mol NH}_4^+ \text{ mg protein}^{-1} \text{ h}^{-1}$) and characterized AOB ($30\text{-}80 \mu\text{mol NH}_4^+ \text{ mg protein}^{-1} \text{ h}^{-1}$) (Ward, 1987; Prosser, 1989), but within the range estimated for *in situ* cell-specific rates of a natural marine community ($0.2\text{-}15 \text{ fmol NH}_4^+ \text{ cell}^{-1} \text{ d}^{-1}$) (Santoro et al., 2010).

Morphology and phylogeny. The morphologies of strains HCA1 and PS0, as characterized by transmission electron microscopy (Fig. 2.1C, D), are very similar to SCM1 (Könneke et al., 2005). Both are small rods, with a diameter of 0.15 to 0.26 μm and a length of 0.65 to 1.59 μm .

Unlike “*Candidatus Nitrosoarchaeum limnia*” (Mosier et al., 2012a), no flagella were observed. Cells reproducing by typical binary fission were also observed in images of mid-exponential phase cultures.

We earlier reported on the high similarity and synteny of the SCM1 genome to the metagenome of globally distributed Marine Group I Archaea (Walker et al., 2010). A close phylogenetic relationship between strain SCM1 and the two new isolates was here established by 16S rRNA and *amoA* gene sequencing. All are affiliated with *Thaumarchaeota* Group I.1a, together forming a monophyletic clade sharing >95% *amoA* and >99% 16S rRNA gene sequence identity (Fig. 2.2 and Fig. 2.3). The *amoA* genes are more than 11% divergent from environmental sequences previously termed marine water column clusters “A” and “B”, and more than 16% divergent from the symbiotic archaeon “*Candidatus Cenarchaeum symbiosum*” (Francis et al., 2005; Hallam et al., 2006). “*Candidatus Nitrosoarchaeum limnia*”, previously described in an enrichment from a low-salinity estuarine system in California, differed from the new isolates by greater than 4% and 7% sequence divergence of the 16S rRNA and *amoA* genes, respectively (Blainey et al., 2011). All share less than 90% and 80% identity with the 16S rRNA and *amoA* genes, respectively, of the cultured soil representatives “*Candidatus Nitrosotalea devanaterre*” and *Nitrososphaera viennensis* (Lehtovirta-Morley et al., 2011; Tourna et al., 2011).

Relationships between growth rate, temperature, salinity, and pH. The temperature dependent growth kinetics of the new isolates differed significantly from strain SCM1. The highest growth rates for strains HCA1 and PS0 were observed at 25 °C and 26 °C, respectively, in contrast to a maximum at 32 °C for strain SCM1 (Fig. 2.4A-C). No growth (nitrite production)

could be detected for SCM1 at 10 °C, whereas the two new isolates continued to grow at 10 °C. An Arrhenius analysis revealed a good linear relationship between the natural logarithm of the ammonia oxidation rate and the inverse of the absolute temperature (Fig. 2.4D). The inferred activation energy (78.25 kJ mol⁻¹) and Q_{10} value (2.89) of SCM1 were somewhat greater than strain HCA1 (E_a =67.67 kJ mol⁻¹, Q_{10} =2.62) and strain PS0 (E_a =64.20 kJ mol⁻¹, Q_{10} =2.49). These values are comparable to those estimated for representatives of estuarine nitrifying bacteria (E_a =67.4-82.5 kJ mol⁻¹, Q_{10} =2.7-3.3) (Helder and Devries, 1983) (Table 2.2).

Growth of strains SCM1 and HCA1 was restricted to pH values between 6.8 and 8.1, with the highest ammonia oxidation rates observed at pH 7.3 (Fig. 2.5A). In contrast, strain PS0 grew well at significantly lower pH values, having a maximum growth rate at pH 6.8 and maintaining nearly 80% of its maximum growth rate at pH values as low as 5.9. At pH values closer to that of open ocean surface waters (~ 8.1), the growth of PS0 was depressed relative to the other two isolates. Thus, strain PS0 appears well adapted to the lower pH waters of the Puget Sound main basin from where it was isolated, having a pH range of 7.71 to 8.05 near the surface and of 7.70 to 7.83 at depths greater than 100m (Feely et al., 2010). No ammonia oxidation was observed at pH 8.7 for any of the strains, which is consistent with observations of other neutrophilic AOA (Jung et al., 2011b; Tourna et al., 2011; Kim et al., 2012a).

Salinity is also a significant environmental variable, particularly in coastal regions influenced by varying inputs of terrestrial freshwater. The Hood Canal fjord is influenced by seasonally varying riverine and surface runoff sources of freshwater, and by the intrusion of low pH and high salinity water from seasonal coastal upwelling of deep ocean water (Moore et al., 2010).

All strains grew best at mid-salinity (25 to 32‰), but differed markedly in response to low and high salinity conditions (Fig. 2.5B). Strain SCM1 grew well at high salinities (35 to 40‰), was significantly inhibited at 20‰, and ceased to grow at 15‰. Strains HCA1 and PS0 were less inhibited at 20‰ and still remained active at 15‰. However, unlike SCM1, both of these strains were significantly inhibited at 40‰. Since 40‰ is much higher than the normal oceanic environment, these differences likely reflect strain specific adaptations to the varying salinities intrinsic to this coastal system.

Photoinhibition. The influence of light on growth kinetics was examined by controlled exposure of the isolates to polychromatic light from a cool, white fluorescent lamp. Growth rate was measured at different intensities of illumination and under three different illumination regimes: continuous dark, continuous illumination, and a 14h dark/10h light cycle. Differential growth during light and dark periods of the imposed diurnal cycle was also examined. All isolates were differentially inhibited. Strain SCM1 was significantly less photosensitive (Fig. 2.6A) than the other two isolates when exposed to a diurnal light cycle, showing no apparent inhibition (relative to cultures incubated in the dark) at low light fluxes (15 and $40 \mu\text{E m}^{-2} \text{s}^{-1}$) and retaining about 20% of its maximum growth rate at the highest light intensity examined ($180 \mu\text{E m}^{-2} \text{s}^{-1}$). However, under continuous illumination this strain was completely inhibited at $120 \mu\text{E m}^{-2} \text{s}^{-1}$ (Fig. 2.6B). Although exhibiting somewhat greater light sensitivity, the response of HCA1 was similar to SCM1, showing reduced specific growth rates of 11% and 22% at 15 and $40 \mu\text{E m}^{-2} \text{s}^{-1}$, respectively, and complete inhibition at $180 \mu\text{E m}^{-2} \text{s}^{-1}$ (Fig. 2.6A). Strain PS0 was the most light sensitive of the three AOA isolates, being partially inhibited at low light fluxes (19% and 39%

inhibition at 15 and 40 $\mu\text{E m}^{-2} \text{s}^{-1}$, respectively), 80% inhibited at 60 $\mu\text{E m}^{-2} \text{s}^{-1}$, and completely inhibited at 80 $\mu\text{E m}^{-2} \text{s}^{-1}$.

The greater inhibition observed with continuous illumination relative to an imposed dark/light cycle suggested that a recovery of activity was possible during the dark period. Dark recovery of strain HCA1 was shown by an increased growth rate during the dark period (Fig. 2.6C). To further evaluate dark recovery of completely light-inhibited cultures, strain SCM1 cultures were first incubated under continuous illumination at 60 $\mu\text{E m}^{-2} \text{s}^{-1}$ until growth ceased (~ 100 hours) and then transferred to the dark. These cultures began to recover within 24 hours and completely converted all ammonia to nitrite, but at a significantly reduced growth rate compared to dark-incubated controls (Fig. 2.6D). Thus, although the data confirmed sensitivity of AOA to light, they also suggest that significant ammonia oxidation is possible in the upper water column.

Assimilation of organic carbon. Isolation of HCA1 and PS0 required the addition of a low concentration of α -ketoglutaric acid to the inorganic basal medium. Both strains oxidized approximately half of the added ammonia to nitrite following initial transfer from α -ketoglutaric acid supplemented into organic carbon-free media (1% inoculum), and failed to grow following a second transfer into organic carbon-free media (Fig. 2.7A, B). The oxidation of half of the ammonia following the first transfer likely reflected either use of endogenous cellular reserves or the carryover of a low amount of α -ketoglutaric acid in the inoculum. As previously reported, strain SCM1 was capable of chemolithoautotrophic growth, oxidizing all added ammonia in the absence of an organic carbon supplement. However, SCM1 growth rate and cell yield were greater in cultures supplemented with α -ketoglutaric acid (Fig. 2.7C and Table 2.3). Since cell

yield per mole of ammonia oxidized was greater for all strains in organic carbon supplemented media (from 93.4 to 112.6×10^{12} cells mol⁻¹ NH₄⁺ for SCM1, no growth to 80.8×10^{12} cells mol⁻¹ NH₄⁺ for HCA1, and no growth to 70.4×10^{12} cells mol⁻¹ NH₄⁺ for PS0) (Fig. 2.8), these results suggested that mixotrophic growth may be the preferred lifestyle of marine AOA.

Growth of strain PS0 on urea. The genetic potential for using urea to fuel nitrification has been reported for the marine group I *Thaumarchaeota* (Konstantinidis et al., 2009; Alonso-Saez et al., 2012). However, direct physiological support has to date been lacking. We therefore examined the capacity of each strain to grow in an ammonia free medium supplemented with approximately 100 μM urea. As predicted from the SCM1 genome sequence, previously reported to lack genes annotated for urea transport and degradation, no growth or nitrite production was observed for SCM1 cultures following more than 3 months of incubation. Likewise, no growth of strain HCA1 was observed in the urea medium. In contrast, strain PS0 grew by near stoichiometric conversion of urea (~90 μM) to nitrite (~180 μM) in 17 days (Fig. 2.9) at a specific growth rate (0.18 d⁻¹) comparable to its growth on ammonia (0.23 d⁻¹).

Discussion

Since the successful isolation of the first ammonia-oxidizing archaeon (SCM1) from a seawater aquarium (Könneke et al., 2005) using low ammonia concentrations for selective enrichment, the same general approach has been widely used to enrich additional AOA from soil, fresh water, marine and geothermal habitats (de la Torre et al., 2008; Hatzenpichler et al., 2008; Jung et al., 2011b; Lehtovirta-Morley et al., 2011; Santoro and Casciotti, 2011; Tourna et al., 2011; French et al., 2012; Kim et al., 2012a; Mosier et al., 2012a). However, despite significant efforts to

obtain new isolates from enrichment cultures, other than SCM1 only *Nitrososphaera viennensis* strain EN76 from garden soil has been reported in pure culture (Tourna et al., 2011). In contrast to chemolithoautotrophic growth of SCM1, *N. viennensis* and the new marine isolates require organic carbon, a requirement that may account for the virtual absence of publications describing additional isolates. Presumably the coexisting bacteria provide essential nutrients, and without appropriate nutrient supplementation the AOA cannot be maintained (Tourna et al., 2011; French et al., 2012; Kim et al., 2012a). For example, the isolation of the soil AOA *N. viennensis* required the addition of pyruvate (Tourna et al., 2011). However, pyruvate addition has not been sufficient for the isolation of AOA from other enrichment cultures (French et al., 2012), suggesting that different ecotypes vary in their carbon assimilation capabilities. Here we isolated two *N. maritimus*-related strains from coastal water using α -ketoglutaric acid as an organic nutrient source, demonstrating the significance of another organic compound to the growth of an AOA lineage in marine environments.

The three strains (SCM1, HCA1 and PS0) described here are relatively closely related members of a marine AOA lineage that differ markedly in basic physiological features. Although strain SCM1 was isolated from a tropical marine aquarium, it shares high genomic similarity with marine metagenomic sequences and has an apparent half-saturation constant (K_s) for ammonia oxidation (133 nM) comparable to K_s values determined directly in open ocean waters (65-112 nM) (Könneke et al., 2005; Martens-Habbena et al., 2009a; Walker et al., 2010; Horak et al., 2013; Newell et al., 2013). The optimum growth temperature near 30-33 °C, and a preference for salinities (32-40 ‰) higher than the newly described coastal isolates, also suggests that strain SCM1 was originally native to tropical ocean waters.

All isolates vary significantly in sensitivity to light and pH. These features relate directly to abiotic factors controlling their environmental distribution and response to the ongoing reduction in ocean pH (Zeebe, 2012). The sensitivity of marine AOA to ocean acidification has been inferred from a limited number of short-term studies of experimentally acidified ocean water (Huesemann et al., 2002; Beman et al., 2011; Kitidis et al., 2011). For example, a recent study by Beman et al. (Beman et al., 2011) reported significant inhibition of ammonia oxidation (8-38% reduction in rates) following relatively small pH reductions of both coastal and open ocean waters in which AOA were the dominant ammonia-oxidizing population. This effect was associated with the reported requirement for the use of ammonia (NH_3), not ammonium (NH_4^+), as a substrate for ammonia-oxidizing bacteria such as the marine AOB *Nitrosococcus oceani* (Ward, 1987). The concentration of this form is significantly reduced by small reductions in pH. However, as yet there is no evidence that AOA have the same substrate requirement as AOB. In fact, the description of “*Candidatus Nitrosotalea devanaterrea*”, an acidophilic terrestrial AOA growing optimally at pH values near 4, suggests that the NH_4^+ ion is more likely the substrate for this organism (Lehtovirta-Morley et al., 2011). Our observation that marine AOA strain PS0 grows well at pH 5.9 suggests that at least some AOA populations have the capacity to adapt to ongoing reductions in ocean pH. If the ammonium ion is the preferred substrate, ocean acidification may actually promote the growth of AOA, influencing oceanic production of N_2O now associated primarily with their activities (Santoro et al., 2011; Löscher et al., 2012).

Light has long been implicated as a major factor controlling the activity and distribution of both ammonia oxidizers and nitrite oxidizers in the water column. The inhibitory effect of light on

cultured AOB has been known for decades and attributed to photooxidative damage of the copper-containing ammonia monooxygenase (Hooper and Terry, 1974; Shears and Wood, 1985; Hyman and Arp, 1992). Archaeal photosensitivity was recently reported for marine, soil and fresh water AOA strains, including SCM1 (French et al., 2012; Merbt et al., 2012). At a light intensity similar to the base of the euphotic zone ($15 \mu\text{E m}^{-2} \text{s}^{-1}$), Merbt et al. (2012) reported the growth of SCM1 was almost completely inhibited with no evidence of dark recovery during an imposed diurnal cycle (Merbt et al., 2012). In contrast, we found only a marginal inhibitory effect of a comparable diurnal light regime on strain SCM1 (2.5% at $15 \mu\text{E m}^{-2} \text{s}^{-1}$) and a similarly low inhibition of novel strains HCA1 and PS0 to this light regime. Even under continuous illumination, the growth rate of SCM1 was reduced by only 11.8% at this light flux. At higher intensities (40 and $60 \mu\text{E m}^{-2} \text{s}^{-1}$) these isolates were capable of rapid dark recovery from photoinhibition, suggesting that ammonia oxidation in upper regions of the euphotic zone could follow a diurnal cycle (Hollibaugh et al., 2014b; Pedneault et al., 2014). Although we have no explanation for the disparity between this and the previous study, these data provide physiological explanation for the high abundance and activity of AOA near the bottom of the euphotic zone as inferred by relating *amoA* gene and transcript abundance to *in situ* ammonia oxidation rate measurements (Beman et al., 2008; Santoro et al., 2010; Beman et al., 2012a; Horak et al., 2013).

The requirement of the new isolates for organic carbon amplifies growing appreciation of the importance of mixotrophy in marine food webs and provided direct physiological support for previous isotopic studies suggesting both organic and inorganic carbon sources were assimilated by marine *Thaumarchaeota* (Herndl et al., 2005; Ingalls et al., 2006; Agogué et al., 2008a;

Hansman et al., 2009). There are obvious energetic advantages to the use of organic carbon to supplement or alleviate carbon fixation. In addition, organic material might serve as an alternative source of reductant, other than electrons derived solely from ammonia, for the ammonia monooxygenase. Our demonstration that isolate PS0 is capable of using urea as an alternative energy source also provided the first direct physiological confirmation of an activity implicated by marine genomic data sets (Konstantinidis et al., 2009; Yakimov et al., 2011; Alonso-Saez et al., 2012). If the AOA have an affinity for urea comparable to their remarkably low K_s for ammonia, they may also effectively compete with phytoplankton for this reduced form of nitrogen, a question that can now be addressed using this new isolate.

The new physiological data begin to define ecotype variation within the AOA and to disentangle environmental variables influencing the abundance and activity of populations now thought to play a fundamental role in the shaping of the marine nitrogen cycle. For example, the requirement of the new isolates for organic carbon suggests that substrates other than ammonia could limit the distribution of some environmental populations. Characterized ammonia-oxidizing bacteria are unable to grow at pH values significantly below 7 (Suzuki et al., 1974; Ward, 1987; Allison and Prosser, 1993). This has fostered speculation that the AOA may suffer similar inhibition at acidic pH. However, our demonstration of significant variation in pH adaptation among closely related AOA suggests that ongoing ocean acidification is more likely to change the distribution of competing AOA lineages and, as a consequence, alter the marine nitrogen cycle in unexpected ways. Finally, since these studies encompassed only a small and genetically closely circumscribed set of AOA, relative to the much greater genetic diversity

revealed by ongoing metagenomic surveys, they point to a rich and mostly unexplored physiological diversity of the marine AOA.

Materials and Methods

Enrichment and Isolation of marine AOA. Low added ammonia (2 μ M) was used to selectively enrich and isolate AOA from seawater samples collected from the Puget Sound estuary in Washington State (*SI Materials and Methods*). Pure cultures were obtained by filtration of the enrichment cultures through a syringe filter, and diluting the filtrate to extinction. For details, see *SI Materials and Methods*.

Growth experiments. All materials and methods for physiology experiments are described in detail in supplementary information.

Transmission Electron Microscopy. Preparation of the novel AOA isolates for examination by transmission electron microscopy is described in supplementary information.

Sequencing and Phylogenetic Analysis. Sequences of AOA 16S rRNA and *amoA* genes were obtained using an ABI 3730xl sequencer. Phylogenetic trees were generated using MEGA5 as described in *SI Materials and Methods*.

SI Materials and Methods

Enrichment of marine AOA. Seawater samples for enrichment of AOA were collected from Puget Sound surface sediment on a beach in August 2006 and from 50m water depth at the Puget

Sound Regional Synthesis Model (PRISM) Station P10 (47.91 N, 122.62 W) in Hood Canal, Washington State, USA in October 2008. It was previously reported that AOA, rather than AOB, are mainly responsible for nitrification in these regions (Huguet et al., 2010b; Urakawa et al., 2010; Horak et al., 2013). The water samples were stored in on-deck incubators maintained at seawater surface temperature in the dark and transferred to the laboratory the same day. Strain PS0 was enriched in artificial seawater supplemented with 500 μM NH_4Cl and selected by filtration (0.45 μm pore size) during each successive transfer into fresh media supplemented with streptomycin. Following previous reports of a high specific affinity for ammonia of strain SCM1 and its possible competition for ammonia with heterotrophic marine picoplankton, enrichment conditions were designed to select for oligotrophic ammonia oxidizers solely based on high affinity for ammonia. Initially, 20 enrichments were established in 15ml glass tubes by supplementing 10 ml water sample with 2 μM NH_4Cl . Samples were incubated at 15 °C and monitored for ammonium consumption in 2-3 day intervals. Over a period of three months, stable ammonia oxidation activity could be established in 18 out of 20 enrichments by repeatedly supplementing with 2 μM NH_4Cl .

The influence of organic substrates on growth and activity of the first isolated marine AOA, *Nitrosopumilus maritimus* strain SCM1 was investigated prior to the enrichment of new AOA strains. The growth response of strain SCM1 was surveyed using single additions of 59 different potential organic substrates. Strain SCM1 showed a clear increase in specific growth rate only when supplemented with TCA cycle intermediates, including α -ketoglutarate, pyruvate and oxaloacetate (8.3% increase with pyruvate and 21.4% increase with oxaloacetate, respectively). Most organic substrates had no effect or inhibited growth of this strain. Thus, α -ketoglutaric acid

was selected as a potential organic nutrient source for the subsequent enrichment of the novel AOA strains. Following reproducible growth in the filtered seawater media, subcultures were transferred to both artificial seawater medium supplemented with 100 μM α -ketoglutaric acid and organic carbon-free medium. Eventually, out of 20 AOA enrichments initiated, only 2 enrichments with added α -ketoglutaric acid achieved stable growth. No growth was observed in organic carbon-free medium. The stable enrichment strain HCA1 was then maintained in artificial seawater medium supplemented with 2 μM NH_4Cl and 100 μM α -ketoglutaric acid. Synthetic seawater was autoclaved (Könneke et al., 2005), cooled to room temperature, and the following components added from sterile stock solutions: 3.0 ml 1 M sodium bicarbonate, 5.0 ml 0.4 g l^{-1} KH_2PO_4 , 1ml 7.5 mM FeNaEDTA, 1ml non-chelated trace element mixture (Martens-Habbena et al., 2009a), and 2 μl 1M NH_4Cl . None of enrichments could be maintained in synthetic medium without α -ketoglutaric acid. Two highly enriched cultures were obtained after more than two years of low ammonium selection (2 μM NH_4Cl).

Isolation of marine AOA. Growth rates of cultures supplemented with 50 μM , 200 μM and 500 μM instead of only 2 μM NH_4Cl were comparable. However, the growth of the novel AOA strains was inhibited at ammonium concentrations higher than 1mM. Hence, the higher concentrations of ammonium without inhibitory effects were used to further isolate marine AOA in bicarbonate-buffered synthetic marine Crenarchaeota medium. The cultures were additionally supplemented with 100 μM α -ketoglutaric acid and 40 mg l^{-1} streptomycin and incubated at 20 $^\circ\text{C}$ in the dark without shaking. Pure cultures were obtained by filtering exponential phase enrichment cultures through 0.22 μm Millex-GP syringe filters, followed by repeated end-point dilution in streptomycin and α -ketoglutaric acid supplemented medium. The absence of bacterial

contaminants was checked by PCR, showing no amplification with general primers for the bacterial 16S rRNA gene (Lane, 1991) or with those specific for the *amoA* gene of ammonia-oxidizing bacteria (Rotthauwe et al., 1997; Purkhold et al., 2000). The purity of AOA cultures was routinely monitored by microscopic inspection and by absence of bacterial growth in marine broth medium (5 g peptone and 1 g yeast extract, 250 ml Milli-Q water, and 750 ml autoclaved seawater).

Growth experiments. Strains PS0 and HCA1 were transferred from bicarbonate-buffered medium (see above) to HEPES-buffered synthetic crenarchaeota medium (Martens-Habbena et al., 2009a) supplemented with 500 μM NH_4Cl and 100 μM α -ketoglutaric acid. Since no difference in growth rate was observed for the HEPES- and bicarbonate-buffered media, unless otherwise indicated, the growth response of each strain to varying temperature, salinity, pH, and light was determined in triplicate 100 or 500 ml cultures using the HEPES-buffered medium. The pH of the medium was adjusted to a range between 5.9 and 8.7 using a pH meter (Orion model 420, Thermo Scientific, Waltham, MA, USA) for initial titration with either 12.1 M HCl or 5 M KOH, followed by verification of pH values in the range of 7 to 9 using the indicator dye *m*-cresol purple before inoculation (Dickson, 2007). No, or only a negligible, decrease in pH could be detected between the beginning and end of each growth experiment. To assess the influence of salinity on growth, a stock solution of artificial seawater at 40‰ was prepared containing NaCl (32.5 g l^{-1}), $\text{MgSO}_4 \cdot 7\text{H}_2\text{O}$ (6.25 g l^{-1}), $\text{MgCl}_2 \cdot 6\text{H}_2\text{O}$ (6.25 g l^{-1}), $\text{CaCl}_2 \cdot 2\text{H}_2\text{O}$ (1.875 g l^{-1}) and KBr (0.125 g l^{-1}), and portions of it taken and diluted with Milli-Q water to 15 to 35‰. To investigate the inhibitory effect of light, cultures were grown in glass bottles that were either kept in the dark or exposed to cool white fluorescent lamps (Phillips F17T8/TL741,

17W) with wavelength output ranging from 410-720 nm (Tong et al., 2008). Light intensities measured inside and outside the growth bottle with a Biospherical Instruments QSL-2100 radiometer (San Diego, CA) showed less than 10% attenuation of light by the glass. For growth experiments examining the utilization of urea as an energy source, the background ammonium concentration in the urea medium was less than 1 μM and thus did not represent a major source of energy.

Activation energy and Q_{10} . Activation energies were calculated based on the slopes of linear regression lines of Arrhenius plots. Q_{10} values between the minimum growth temperature and temperature optimum were obtained using:

$$Q_{10} = \exp \left[\frac{E_a \cdot 10}{RT(T + 10)} \right]$$

Here E_a is the activation energy (J mol^{-1}), R is the molecular gas constant ($8.314 \text{ J K}^{-1} \text{ mol}^{-1}$), and T is the absolute temperature (K).

Growth Parameters Measurements. Ammonia concentration was measured by the o-phthalaldehyde fluorescence method (Holmes et al., 1999) and a fluorescence microplate reader (Infinite F500, TECAN, USA) (standard concentration range: 0-1000 μM , n=5 concentrations, $R^2 > 0.997$). The concentration of nitrite and urea were determined spectrophotometrically using the Griess reagent (Stickland, 1972) (standard concentration range: 0-1000 μM , n=6 concentrations, $R^2 > 0.999$) and diacetyl monoxime (Grasshoff, 1999a) (standard concentration range: 0-500 μM , n=6 concentrations, $R^2 > 0.999$), respectively. Total cell counts were determined using moviol-SybrGreen I staining protocol (Lunau et al., 2005). Briefly, the

mounting medium was freshly prepared by adding 3 μ l of SybrGreen I stock solution (Invitrogen, Carlsbad, USA) and 2 μ l of 1 M ascorbic acid solution into 200 μ l of the moviol solution (moviol 4-88, Fluka, Switzerland). Cells were filtered on a 0.02- μ m Anopore membrane filter (Whatman, Germany), and then stained with 20 μ l of mixed microscopic mounting medium. Cell numbers were determined using a Zeiss Axioskop 2 MOT epifluorescence microscope to count 20 random fields of view for each sample with 10 to 100 cells per field.

Transmission Electron Microscopy. Cells of strains HCA1 and PS0 were fixed overnight with half-strength Karnovsky's fixative (Karnovsk.Mj, 1965), transferred to a 200-mesh formvar-coated copper grid for 30 min, and then washed successively in a small volume of fresh 0.1 M cacodylate buffer and ultrapure water. Staining of cells was performed by swirling the grid in a drop of 1% uranyl acetate. Liquid was drained off with filter paper and the grid dried overnight in a desiccator. Each preparation was examined with a JEOL JEM-1400 transmission electron microscope at an accelerating voltage of 120 KV and magnification of 10,000 and 20,000X (Electron Microscopy Core Facility, Fred Hutchinson Cancer Research Center, Seattle, WA).

Sequencing and Phylogenetic Analysis of 16S rRNA and *amoA* Genes. Cells were collected by vacuum filtration on 0.22- μ m Sterivex-GP filters (Millipore Corporation, MA, USA). DNA extracts were obtained by using modified phenol-chloroform method (Urakawa et al., 2010). The AOA 16S rRNA and *amoA* genes were PCR amplified using archaeal-specific primers Arch21F/Arch958R (DeLong, 1992) and CrenAmoAModF/CrenAmoAModR (Mincer et al., 2007), respectively, with the protocols described in the original papers (DeLong, 1992; Mincer et

al., 2007). Amplified products were purified with MinElute PCR Purification kit (Qiagen, Maryland, USA) and cloned using a TOPO TA PCR Cloning kit (Invitrogen). Sequences were obtained using an ABI 3730xl sequencer (Applied Biosystems System operated by the High-Throughput Genomics Center, Seattle, WA). The 16S rRNA and *amoA* genes sequences of strains HCA1 and PS0 were deposited in GenBank under accession numbers KF957663, KF957664, KF957665, and KF957666. The DNA sequences of 16S rRNA and *amoA* genes were aligned with CLUSTAL W program and the phylogenetic relationships were analyzed by maximum-likelihood method with Kimura 2-parameter correction using MEGA5. Bootstrap support was based on 1000 iterations for each analysis.

Acknowledgements

We thank B. Schneider and the FHCRC EM staff for performing transmission electron microscopy, and the Captain and crew of the R/V Clifford A. Barnes for their assistance with sample collection. We thank the technical assistance of Sun-Li Beatteay. This work was funded by the United States National Science Foundation grants MCB-0604448 and Dimensions of Biodiversity Program OCE-1046017.

References

- Agogu e, H., Brink, M., Dinasquet, J., and Herndl, G.J. (2008a) Major gradients in putatively nitrifying and non-nitrifying Archaea in the deep North Atlantic. *Nature* **456**: 788-791.
- Allison, S.M., and Prosser, J.I. (1993) Ammonia oxidation at low pH by attached populations of nitrifying bacteria. *Soil Biol Biochem* **25**: 935-941.
- Alonso-Saez, L., Waller, A.S., Mende, D.R., Bakker, K., Farnelid, H., Yager, P.L. et al. (2012) Role for urea in nitrification by polar marine Archaea. *Proc Natl Acad Sci USA* **109**: 17989-17994.
- Amin, S.A., Moffett, J.W., Martens-Habbena, W., Jacquot, J.E., Han, Y., Devol, A. et al. (2013) Copper requirements of the ammonia-oxidizing archaeon *Nitrosopumilus maritimus* SCM1 and implications for nitrification in the marine environment. *Limnol Oceanogr* **58**: 2037-2045.

- Beman, J.M., Popp, B.N., and Francis, C.A. (2008) Molecular and biogeochemical evidence for ammonia oxidation by marine *Crenarchaeota* in the Gulf of California *ISME J* **2**: 429-441.
- Beman, J.M., Popp, B.N., and Alford, S.E. (2012a) Quantification of ammonia oxidation rates and ammonia-oxidizing archaea and bacteria at high resolution in the Gulf of California and eastern tropical North Pacific Ocean. *Limnol Oceanogr* **57**: 711-726.
- Beman, J.M., Chow, C.E., King, A.L., Feng, Y.Y., Fuhrman, J.A., Andersson, A. et al. (2011) Global declines in oceanic nitrification rates as a consequence of ocean acidification. *Proc Natl Acad Sci USA* **108**: 208-213.
- Blainey, P.C., Mosier, A.C., Potanina, A., Francis, C.A., and Quake, S.R. (2011) Genome of a low-salinity ammonia-oxidizing archaeon determined by single-cell and metagenomic analysis. *PLoS ONE* **6**: e16626.
- Caffrey, J.M., Bano, N., Kalanetra, K., and Hollibaugh, J.T. (2007) Ammonia oxidation and ammonia-oxidizing bacteria and archaea from estuaries with differing histories of hypoxia. *ISME J* **1**: 660-662.
- Church, M.J., Wai, B., Karl, D.M., and DeLong, E.F. (2010) Abundances of crenarchaeal *amoA* genes and transcripts in the Pacific Ocean. *Environ Microbiol* **12**: 679-688.
- de la Torre, J.R., Walker, C.B., Ingalls, A.E., Könneke, M., and Stahl, D.A. (2008) Cultivation of a thermophilic ammonia oxidizing archaeon synthesizing crenarchaeol. *Environ Microbiol* **10**: 810-818.
- Delong, E.F. (1992) Archaea in Coastal Marine Environments. *Proceedings of the National Academy of Sciences of the United States of America* **89**: 5685-5689.
- Dickson, A.G., Sabine CL and Christian JR (2007) *Guide to best practices for ocean CO₂ measurements*.: PICES Special Publication.
- Feely, R.A., Alin, S.R., Newton, J., Sabine, C.L., Warner, M., Devol, A. et al. (2010) The combined effects of ocean acidification, mixing, and respiration on pH and carbonate saturation in an urbanized estuary. *Est Coast Shelf Sci* **88**: 442-449.
- Francis, C.A., Roberts, K.J., Beman, J.M., Santoro, A.E., and Oakley, B.B. (2005) Ubiquity and diversity of ammonia-oxidizing archaea in water columns and sediments of the ocean. *P Natl Acad Sci USA* **102**: 14683-14688.
- French, E., Kozłowski, J.A., Mukherjee, M., Bullerjahn, G., and Bollmann, A. (2012) Ecophysiological characterization of ammonia-oxidizing archaea and bacteria from freshwater. *Appl Environ Microbiol* **78**: 5773-5780.
- Grasshoff, K., Kremling K, Erhard M. (1999a) *Methods of seawater analysis*. New York: Wiley-VCH.
- Hallam, S.J., Konstantinidis, K.T., Putnam, N., Schleper, C., Watanabe, Y., Sugahara, J. et al. (2006) Genomic analysis of the uncultivated marine crenarchaeote *Cenarchaeum symbiosum*. *Proc Natl Acad Sci USA* **103**: 18296-18301.
- Hansman, R.L., Griffin, S., Watson, J.T., Druffel, E.R.M., Ingalls, A.E., Pearson, A., and Aluwihare, L.I. (2009) The radiocarbon signature of microorganisms in the mesopelagic ocean. *Proc Natl Acad Sci USA* **106**: 6513-6518.
- Hatzenpichler, R., Lebedeva, E.V., Spieck, E., Stoecker, K., Richter, A., Daims, H., and Wagner, M. (2008) A moderately thermophilic ammonia-oxidizing crenarchaeote from a hot spring. *P Natl Acad Sci USA* **105**: 2134-2139.
- Helder, W., and Devries, R.T.P. (1983) Estuarine nitrite maxima and nitrifying bacteria (Ems-Dollard estuary). *Neth J Sea Res* **17**: 1-18.

- Herndl, G.J., Reinthaler, T., Teira, E., van Aken, H., Veth, C., Pernthaler, A., and Pernthaler, J. (2005) Contribution of Archaea to total prokaryotic production in the deep Atlantic Ocean. *Appl Environ Microbiol* **71**: 2303-2309.
- Hollibaugh, J.T., Gifford, S., Sharma, S., Bano, N., and Moran, M.A. (2011) Metatranscriptomic analysis of ammonia-oxidizing organisms in an estuarine bacterioplankton assemblage. *Isme J* **5**: 866-878.
- Hollibaugh, J.T., Gifford, S.M., Moran, M.A., Ross, M.J., Sharma, S., and Tolar, B.B. (2014b) Seasonal variation in the metatranscriptomes of a Thaumarchaeota population from SE USA coastal waters. *Isme J* **8**: 685-698.
- Holmes, R.M., Aminot, A., Kerouel, R., Hooker, B.A., and Peterson, B.J. (1999) A simple and precise method for measuring ammonium in marine and freshwater ecosystems. *Can J Fish Aquat Sci* **56**: 1801-1808.
- Hooper, A.B., and Terry, K.R. (1974) Photoinactivation of ammonia oxidation in *Nitrosomonas*. *J Bacteriol* **119**: 899-906.
- Horak, R.E.A., Qin, W., Schauer, A.J., Armbrust, E.V., Ingalls, A.E., Moffett, J.W. et al. (2013) Ammonia oxidation kinetics and temperature sensitivity of a natural marine community dominated by Archaea. *Isme J* **7**: 2023-2033.
- Huesemann, M.H., Skillman, A.D., and Creelius, E.A. (2002) The inhibition of marine nitrification by ocean disposal of carbon dioxide. *Mar Poll Bull* **44**: 142-148.
- Huguet, C., Martens-Habben, W., Urakawa, H., Stahl, D.A., and Ingalls, A.E. (2010b) Comparison of extraction methods for quantitative analysis of core and intact polar glycerol dialkyl glycerol tetraethers (GDGTs) in environmental samples. *Limnol Oceanogr-Meth* **8**: 127-145.
- Hyman, M.R., and Arp, D.J. (1992) $^{14}\text{C}_2\text{H}_2$ -labeling and $^{14}\text{CO}_2$ -labeling studies of the *de novo* synthesis of polypeptides by *Nitrosomonas-europaea* during recovery from acetylene and light inactivation of ammonia monooxygenase. *J Biol Chem* **267**: 1534-1545.
- Ingalls, A.E., Shah, S.R., Hansman, R.L., Aluwihare, L.I., Santos, G.M., Druffel, E.R.M., and Pearson, A. (2006) Quantifying archaeal community autotrophy in the mesopelagic ocean using natural radiocarbon. *Proc Natl Acad Sci USA* **103**: 6442-6447.
- Jung, M.Y., Park, S.J., Min, D., Kim, J.S., Rijpstra, W.I.C., Damste, J.S.S. et al. (2011b) Enrichment and characterization of an autotrophic ammonia-oxidizing archaeon of mesophilic crenarchaeal group I.1a from an agricultural soil. *Appl Environ Microbiol* **77**: 8635-8647.
- Karl, D.M., Beversdorf, L., Bjorkman, K.M., Church, M.J., Martinez, A., and DeLong, E.F. (2008) Aerobic production of methane in the sea. *Nature Geosci* **1**: 473-478.
- Karner, M.B., DeLong, E.F., and Karl, D.M. (2001) Archaeal dominance in the mesopelagic zone of the Pacific Ocean. *Nature* **409**: 507-510.
- Karnovsk.Mj (1965) A formaldehyde-glutaraldehyde fixative of high osmolality for use in electron microscopy. *J Cell Biol* **27**: 137A.
- Kim, J.G., Jung, M.Y., Park, S.J., Rijpstra, W.I.C., Damste, J.S.S., Madsen, E.L. et al. (2012a) Cultivation of a highly enriched ammonia-oxidizing archaeon of thaumarchaeotal group I.1b from an agricultural soil. *Environ Microbiol* **14**: 1528-1543.
- Kitidis, V., Laverock, B., McNeill, L.C., Beesley, A., Cummings, D., Tait, K. et al. (2011) Impact of ocean acidification on benthic and water column ammonia oxidation. *Geophys Res Lett* **38**.
- Könneke, M., Bernhard, A.E., de la Torre, J.R., Walker, C.B., Waterbury, J.B., and Stahl, D.A. (2005) Isolation of an autotrophic ammonia-oxidizing marine archaeon. *Nature* **437**: 543-546.

- Konstantinidis, K.T., Braff, J., Karl, D.M., and DeLong, E.F. (2009) Comparative metagenomic analysis of a microbial community residing at a depth of 4,000 meters at station ALOHA in the North Pacific subtropical gyre. *Appl Environ Microbiol* **75**: 5345-5355.
- Lane, D.J. (1991) 16S/23S rRNA sequencing. In *Nucleic acid techniques in bacterial systematics*. Stackebrandt, E., and M. Goodfellow (ed). Chichester, United Kingdom: John Wiley & Sons, pp. 115-175.
- Lehtovirta-Morley, L.E., Stoecker, K., Vilcinskas, A., Prosser, J.I., and Nicol, G.W. (2011) Cultivation of an obligate acidophilic ammonia oxidizer from a nitrifying acid soil. *Proc Natl Acad Sci USA* **108**: 15892-15897.
- Löscher, C.R., Kock, A., Könneke, M., LaRoche, J., Bange, H.W., and Schmitz, R.A. (2012) Production of oceanic nitrous oxide by ammonia-oxidizing archaea. *Biogeosciences* **9**: 2419-2429.
- Lunau, M., Lemke, A., Walther, K., Martens-Habbena, W., and Simon, M. (2005) An improved method for counting bacteria from sediments and turbid environments by epifluorescence microscopy. *Environ Microbiol* **7**: 961-968.
- Martens-Habbena, W., Berube, P.M., Urakawa, H., de la Torre, J.R., and Stahl, D.A. (2009a) Ammonia oxidation kinetics determine niche separation of nitrifying Archaea and Bacteria. *Nature* **461**: 976-979.
- Merbt, S.N., Stahl, D.A., Casamayor, E.O., Marti, E., Nicol, G.W., and Prosser, J.I. (2012) Differential photoinhibition of bacterial and archaeal ammonia oxidation. *FEMS Microbiol Lett* **327**: 41-46.
- Metcalf, W.W., Griffin, B.M., Cicchillo, R.M., Gao, J.T., Janga, S.C., Cooke, H.A. et al. (2012) Synthesis of Methylphosphonic Acid by Marine Microbes: A Source for Methane in the Aerobic Ocean. *Science* **337**: 1104-1107.
- Mincer, T.J., Church, M.J., Taylor, L.T., Preston, C., Karl, D.M., and DeLong, E.F. (2007) Quantitative distribution of presumptive archaeal and bacterial nitrifiers in Monterey Bay and the North Pacific Subtropical Gyre. *Environ Microbiol* **9**: 1162-1175.
- Moore, S.K., Mantua, N.J., Newton, J.A., Kawase, M., Warner, M.J., and Kellogg, J.P. (2010) A descriptive analysis of temporal and spatial patterns of variability in Puget Sound oceanographic properties. *Est Coast Shelf Sci* **87**: 174-174.
- Mosier, A.C., Lund, M.B., and Francis, C.A. (2012a) Ecophysiology of an ammonia-oxidizing archaeon adapted to low-salinity habitats. *Microb Ecol* **64**: 955-963.
- Newell, S.E., Fawcett, S.E., and Ward, B.B. (2013) Depth distribution of ammonia oxidation rates and ammonia-oxidizer community composition in the Sargasso Sea. *Limnol Oceanogr* **58**: 1491-1500.
- Ouverney, C.C., and Fuhrman, J.A. (2001) Marine planktonic archaea take up amino acids. *Appl Environ Microbiol* **66**: 4829-4833.
- Pedneault, E., Galand, P.E., Polvin, M., Tremblay, J.E., and Lovejoy, C. (2014) Archaeal *amoA* and *ureC* genes and their transcriptional activity in the Arctic Ocean. *Sci Rep* **4**.
- Prosser, J.I. (1989) Autotrophic nitrification in bacteria. *Adv Microb Physiol* **30**: 125-181.
- Prosser, J.I., and Nicol, G.W. (2008) Relative contributions of archaea and bacteria to aerobic ammonia oxidation in the environment. *Environ Microbiol* **10**: 2931-2941.
- Purkhold, U., Pommerening-Roser, A., Juretschko, S., Schmid, M.C., Koops, H.P., and Wagner, M. (2000) Phylogeny of all recognized species of ammonia oxidizers based on comparative 16S rRNA and *amoA* sequence analysis: Implications for molecular diversity surveys. *Appl Environ Microbiol* **66**: 5368-5382.

- Rotthauwe, J.H., Witzel, K.P., and Liesack, W. (1997) The ammonia monooxygenase structural gene *amoA* as a functional marker: Molecular fine-scale analysis of natural ammonia-oxidizing populations. *Appl Environ Microbiol* **63**: 4704-4712.
- Santoro, A.E., and Casciotti, K.L. (2011) Enrichment and characterization of ammonia-oxidizing archaea from the open ocean: phylogeny, physiology and stable isotope fractionation. *Isme J* **5**: 1796-1808.
- Santoro, A.E., Casciotti, K.L., and Francis, C.A. (2010) Activity, abundance and diversity of nitrifying archaea and bacteria in the central California Current. *Environ Microbiol* **12**: 1989-2006.
- Santoro, A.E., Buchwald, C., McIlvin, M.R., and Casciotti, K.L. (2011) Isotopic Signature of N₂O Produced by Marine Ammonia-Oxidizing Archaea. *Science* **333**: 1282-1285.
- Shears, J.H., and Wood, P.M. (1985) Spectroscopic evidence for a photosensitive oxygenated state of ammonia mono-oxygenase. *Biochem J* **226**: 499-507.
- Sintes, E., Bergauer, K., De Corte, D., Yokokawa, T., and Herndl, G.J. (2013) Archaeal *amoA* gene diversity points to distinct biogeography of ammonia-oxidizing Crenarchaeota in the ocean. *Environ Microbiol* **15**: 1647-1658.
- Stickland, J.D.H., and T. R. Parsons (1972) *A practical handbook of seawater analysis*. Ottawa: Bull Fish Res Bd Canada.
- Suzuki, I., Dular, U., and Kwok, S.C. (1974) Ammonia or ammonium ion as substrate for oxidation by *Nitrosomonas-europaea* cells and extracts. *J Bacteriol* **120**: 556-558.
- Teira, E., van Aken, H., Veth, C., and Herndl, G.J. (2006) Archaeal uptake of enantiomeric amino acids in the meso- and bathypelagic waters of the North Atlantic. *Limnol Oceanogr* **51**: 60-69.
- Tong, H.Y., Leasure, C.D., Hou, X.W., Yuen, G., Briggs, W., and He, Z.H. (2008) Role of root UV-B sensing in *Arabidopsis* early seedling development. *Proc Natl Acad Sci USA* **105**: 21039-21044.
- Tourna, M., Stieglmeier, M., Spang, A., Könneke, M., Schintlmeister, A., Urich, T. et al. (2011) *Nitrososphaera viennensis*, an ammonia oxidizing archaeon from soil. *Proc Natl Acad Sci USA* **108**: 8420-8425.
- Urakawa, H., Martens-Habbena, W., and Stahl, D.A. (2010) High abundance of ammonia-oxidizing archaea in coastal waters, determined using a modified DNA extraction method. *Appl Environ Microbiol* **76**: 2129-2135.
- Walker, C.B., de la Torre, J.R., Klotz, M.G., Urakawa, H., Pinel, N., Arp, D.J. et al. (2010) *Nitrosopumilus maritimus* genome reveals unique mechanisms for nitrification and autotrophy in globally distributed marine crenarchaea. *P Natl Acad Sci USA* **107**: 8818-8823.
- Ward, B.B. (1987) Kinetic-studies on ammonia and methane oxidation by *Nitrosococcus-oceanus*. *Arch Microbiol* **147**: 126-133.
- Yakimov, M.M., La Cono, V., Smedile, F., DeLuca, T.H., Juarez, S., Ciordia, S. et al. (2011) Contribution of crenarchaeal autotrophic ammonia oxidizers to the dark primary production in Tyrrhenian deep waters (Central Mediterranean Sea). *ISME J* **5**: 945-961.
- Zeebe, R.E. (2012) History of seawater carbonate chemistry, atmospheric CO₂, and ocean acidification. *Annu Rev Earth Planet Sci* **40**: 141-165.

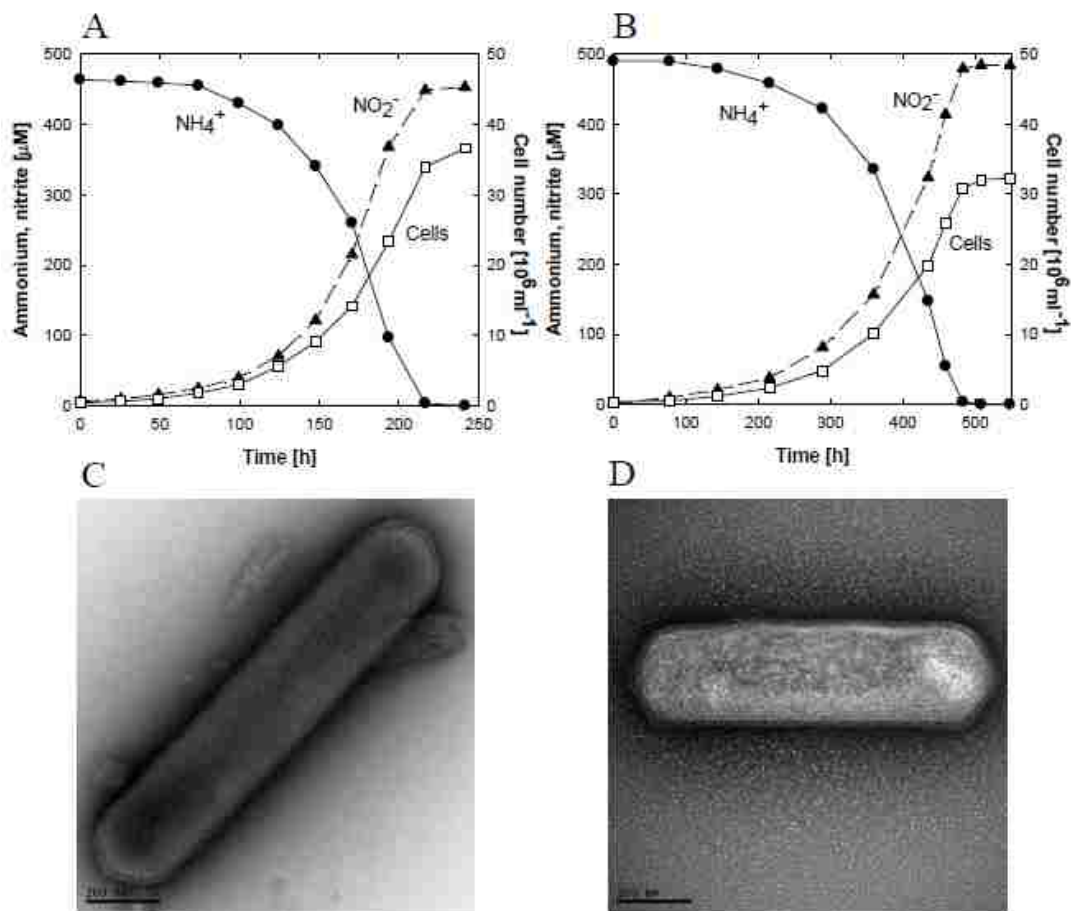


Figure 2.1. Growth and morphology of strains HCA1 and PS0.

Correlation between ammonia oxidation and growth of HCA1 (A) and PS0 (B) in an artificial seawater medium containing 500 μM NH_4^+ and 100 μM α -ketoglutaric acid. Transmission electron micrographs of negative-stained cells of HCA1 (C) and PS0 (D). Scale bars equal 200 nm.

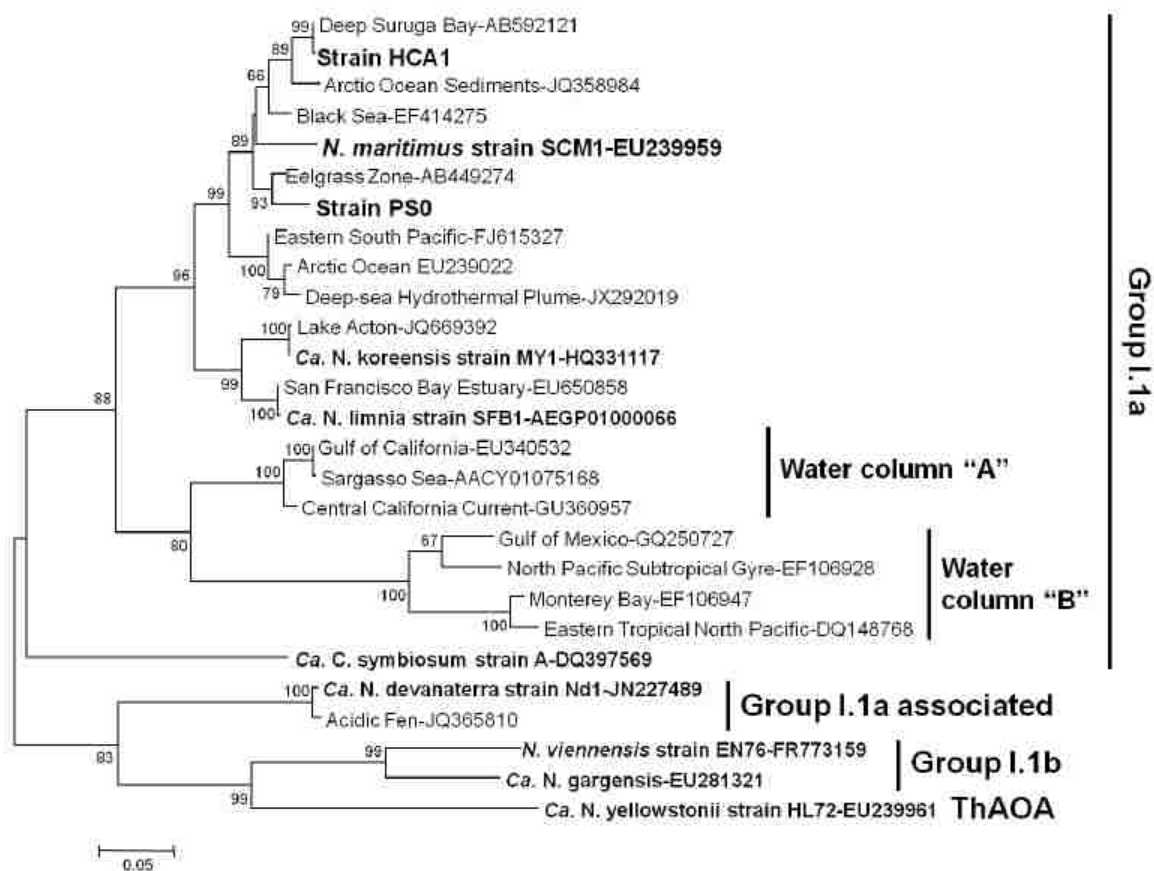


Figure 2.2. Phylogenetic relationships among *amoA* gene sequences of strains HCA1, PS0, and SCM1 and described AOA representatives, as well as relevant environmental clone sequences.

The tree was constructed using the maximum-likelihood method with Kimura 2-parameter correction. Confidence values were based on 1000 bootstrap replications. Scale bar represents 0.05 nucleotide changes per position.

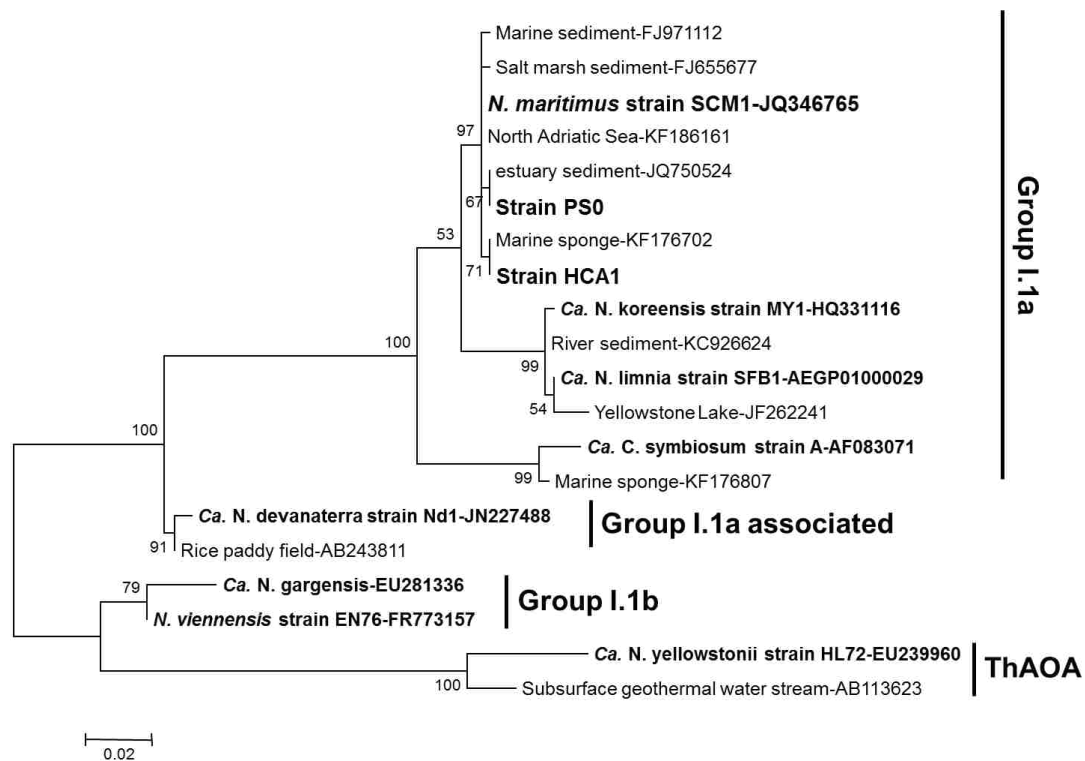


Figure 2.3. Maximum likelihood phylogenetic tree based on 16S rRNA gene sequences. Confidence values were based on 1000 bootstrap replications. The scale bar represents an estimated sequence divergence of 2%.

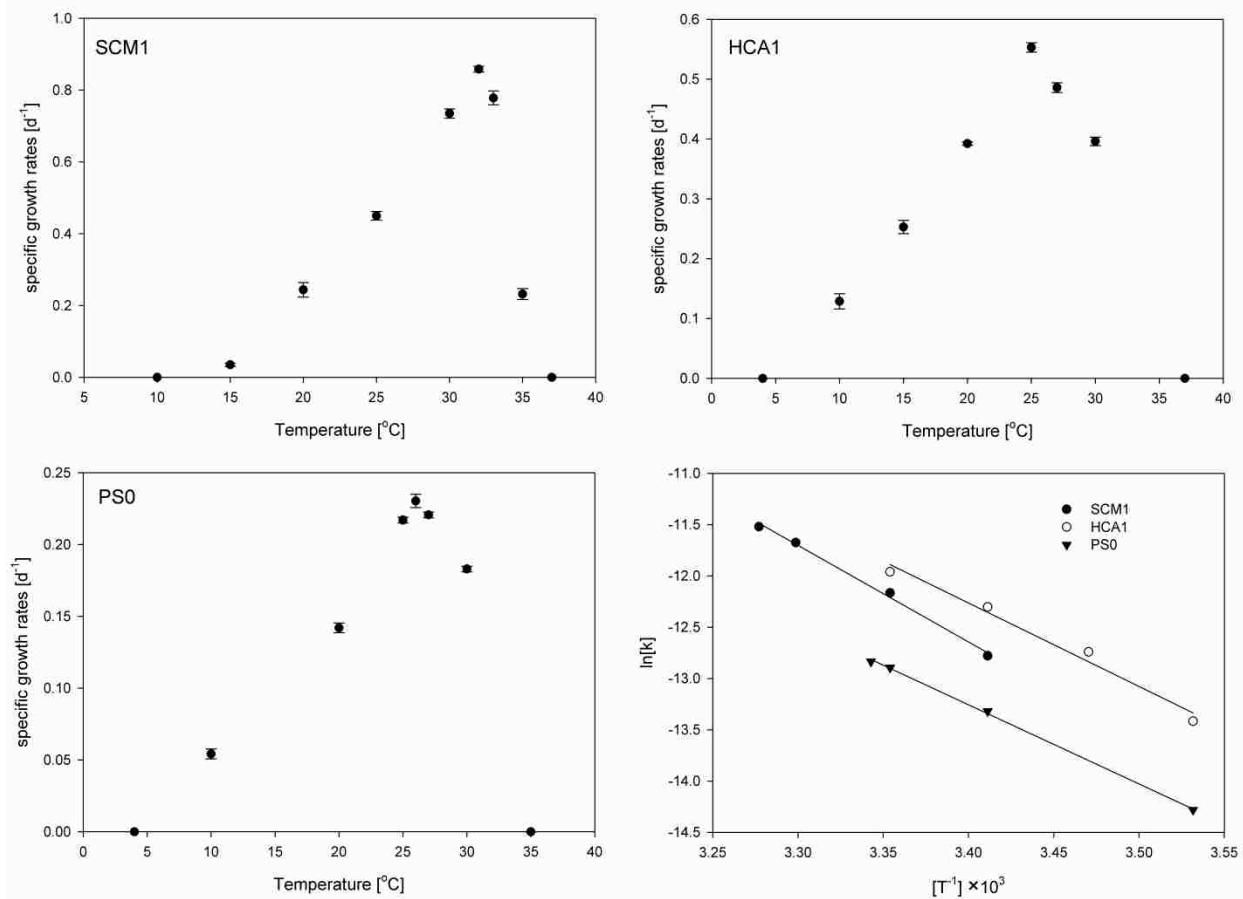


Figure 2.4. Temperature dependence of the growth of SCM1 (A), HCA1 (B), and PS0 (C). (D) Arrhenius analysis showing correlation coefficients of 0.99, 0.98, and 0.99 for strains SCM1, HCA1, and PS0 respectively. Data are presented as the mean of triplicate cultures.

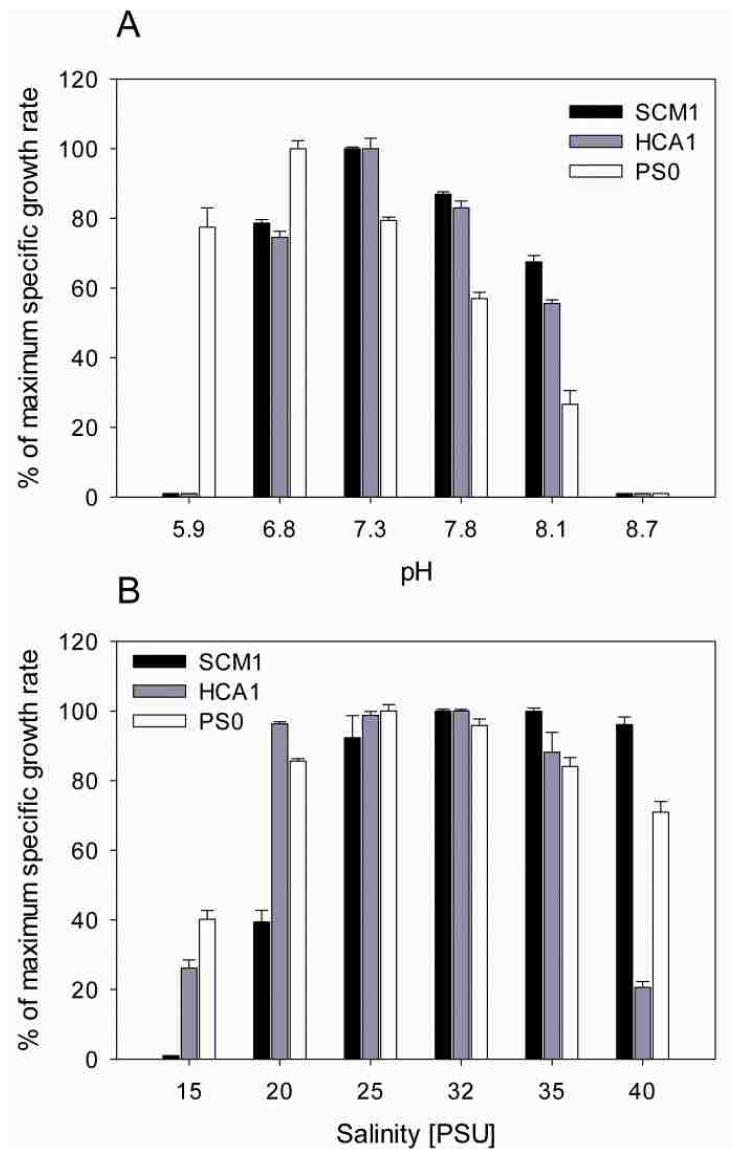


Figure 2.5. Influence of pH (A) and salinity (B) on growth.

Values represent % of specific growth rates of cultures grown under different pH and salinity values relative to those at pH and salinity optima. Error bars represent the standard deviation of triplicate cultures.

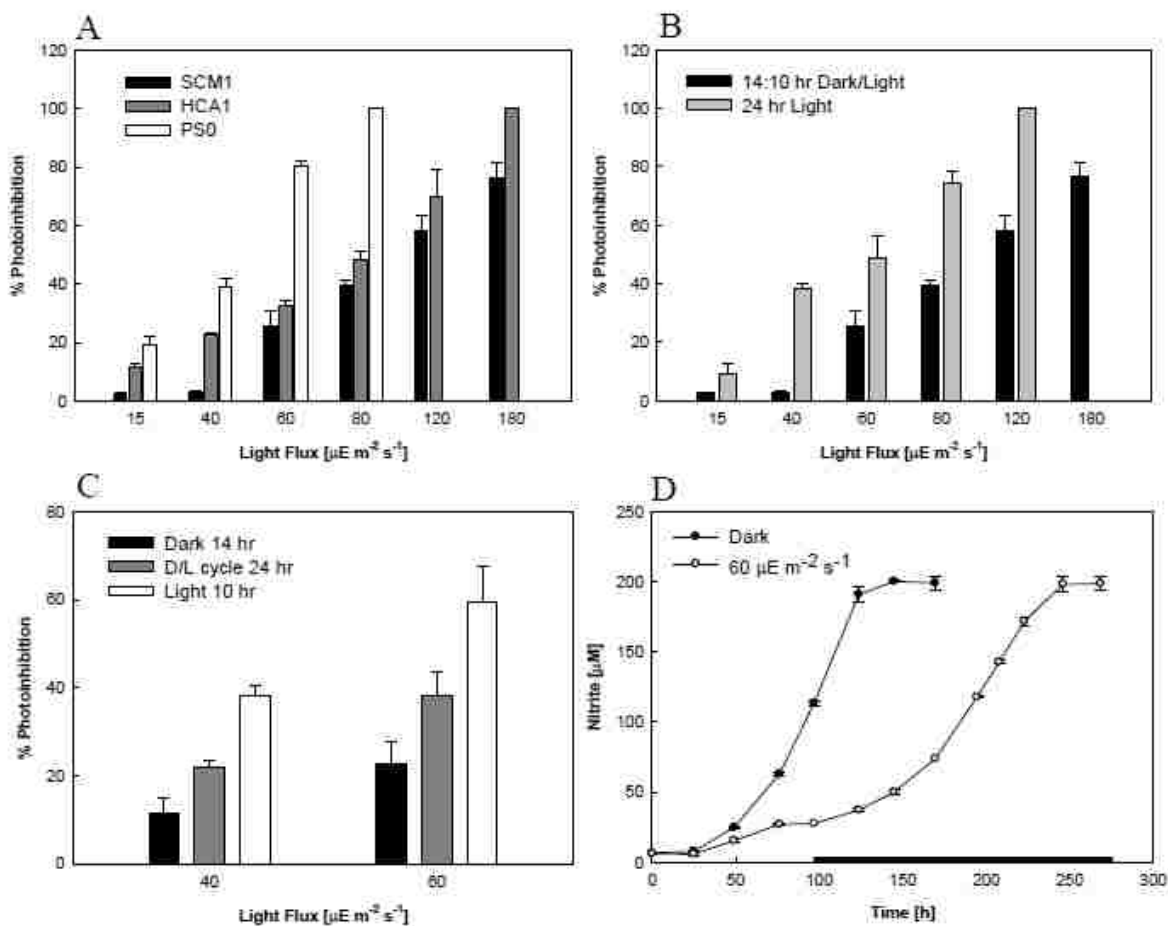


Figure 2.6. Photoinhibition and recovery of ammonia oxidation of the three AOA strains.

Values represent % inhibition of cultures grown under continuous illumination or dark/light cycles relative to cultures grown in the dark. (A) The inhibitory effects of light on all three isolates under a 14:10 hour dark/light cycle at different intensities from 15 to 180 $\mu\text{E m}^{-2} \text{s}^{-1}$. (B) Photoinhibition of strain SCM1 under continuous light (15 to 120 $\mu\text{E m}^{-2} \text{s}^{-1}$) and dark/light cycles (15 to 180 $\mu\text{E m}^{-2} \text{s}^{-1}$). (C) The reduction in specific growth rate of strain HCA1 with cycling between periods of 14 hour dark and 10 hour light at 40 and 60 $\mu\text{E m}^{-2} \text{s}^{-1}$. (D) The recovery of light-inhibited SCM1 cultures (open circles) following transfer to the dark after 100 hours of continuous illumination (60 $\mu\text{E m}^{-2} \text{s}^{-1}$) compared to continuous growth in the dark (dark circles). Error bars represent the standard deviation of triplicate incubations.

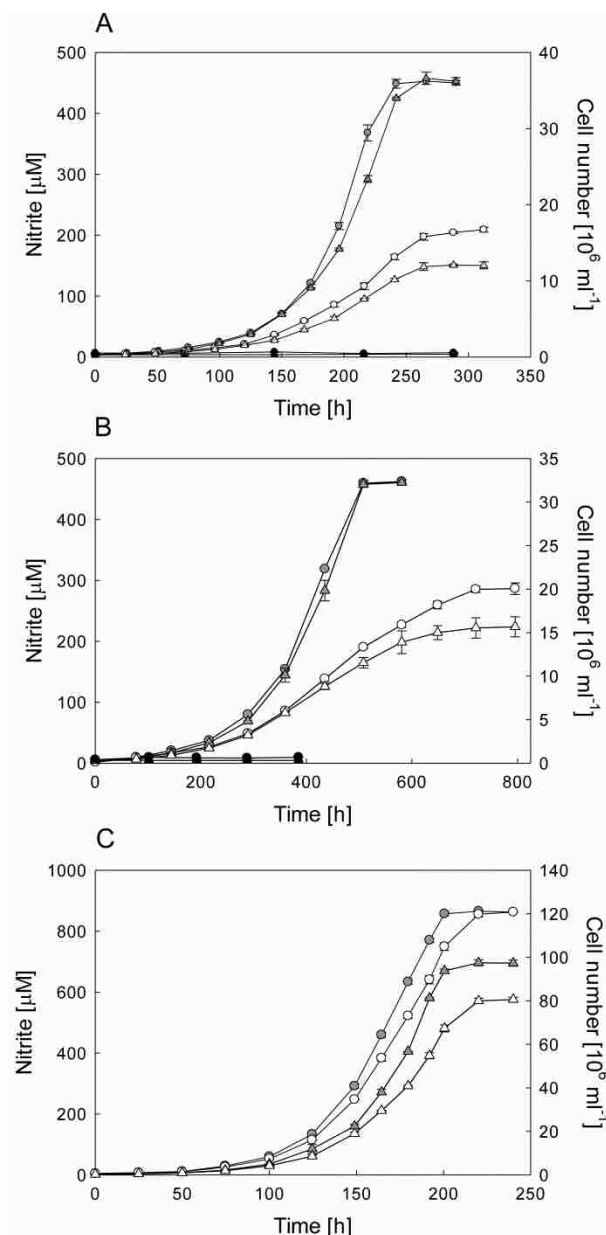


Figure 2.7. Nitrite production (circles) and growth curves (triangles) of strains HCA1 (A), PS0 (B), and SCM1 (C) with 100 μM α -ketoglutaric acid (gray) relative to controls without organic carbon supplements.

(first transfer: white; second transfer: black). No second transfer is included in panel C, since SCM1 has the demonstrated capacity to sustain growth under strictly autotrophic conditions (Könneke et al., 2005; Martens-Habbena et al., 2009a). Error bars represent the standard deviation of triplicate cultures (Please note that in the most cases the error bars are too small to be visible in the figure).

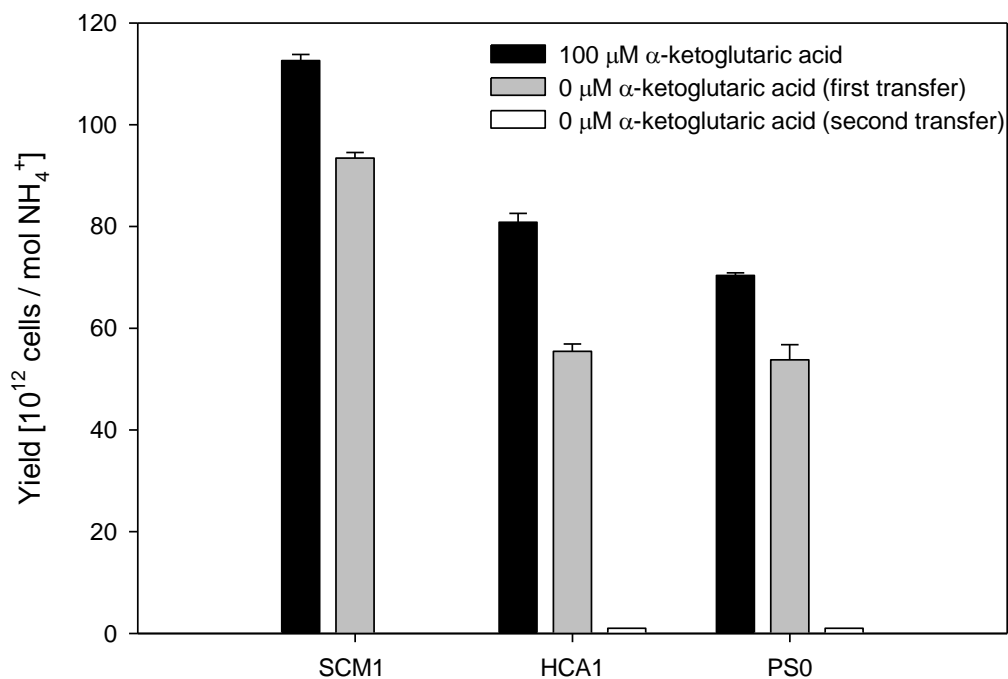


Figure 2.8. The specific growth yields of cultures of three AOA isolates with 100 μM α -ketoglutaric acid (black) relative to controls without α -ketoglutaric acid (first transfer: gray; second transfer: white).

The specific growth yields were calculated from cell numbers. Error bars represent the standard deviation of data from triplicate cultures.

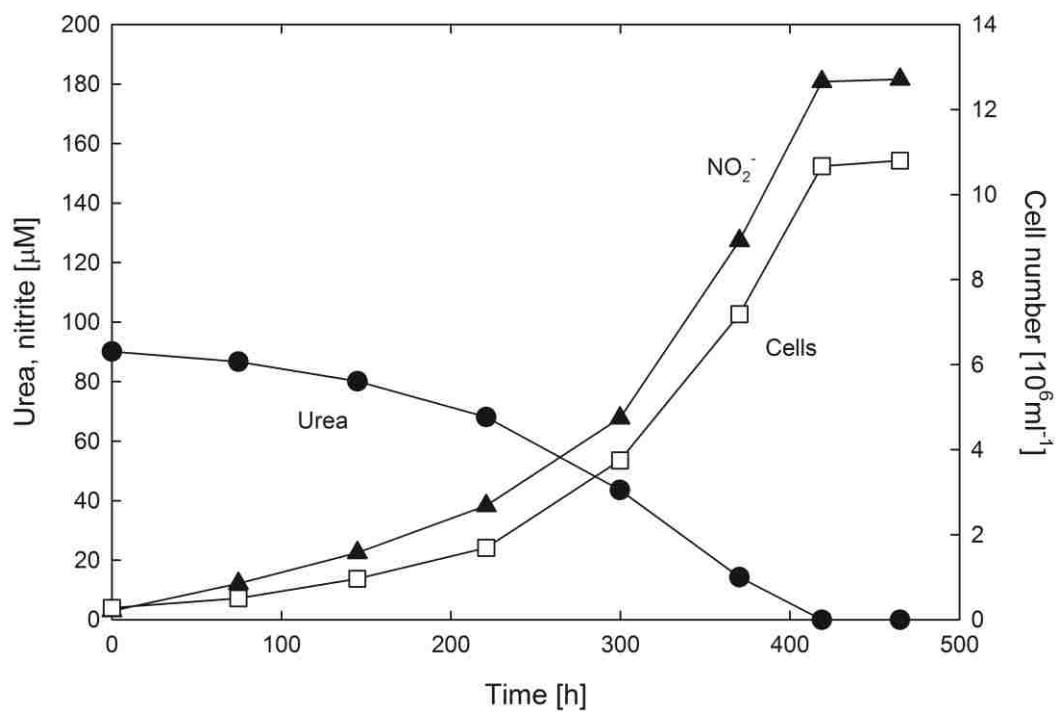


Figure 2.9. Growth of PS0 in artificial seawater medium containing 90 μM urea, showing near stoichiometric conversion of urea to nitrite.

Data points are the mean values of triplicate cultures.

Table 2.1. Growth kinetics of ammonia oxidation for three marine AOA isolates.

Strain	Maximum specific rates per cell [fmol NO ₂ ⁻ cell ⁻¹ d ⁻¹]	Maximum specific activities based on biomass [μmol NH ₄ ⁺ mg protein ⁻¹ h ⁻¹]
SCM1	12.7	51.9
HCA1	6.0	24.5
PS0	2.9	12.2

Table 2.2. Activation energy and Q_{10} values of ammonia oxidation for three marine AOA strains and other bacterial nitrifiers.

Strain	Temperature range (°C)	Activation energy [kJ mol ⁻¹]	Q_{10}
SCM1	20 to 32	78.25	2.89
HCA1	10 to 25	67.67	2.62
PS0	10 to 26	64.20	2.49
Estuarine <i>Nitrosomonas sp.</i>	10 to 20	82.5	3.3
Estuarine <i>Nitrobacter sp.</i>	10 to 20	67.4	2.7

Table 2.3. Cell yields and growth rates in marine AOA pure cultures with 100μM α-ketoglutaric acid over controls without organic substrate.

Strain	α-ketoglutaric acid [μM]	Maximum Cells density [10 ⁷ cells ml ⁻¹]	Specific growth rate [d ⁻¹]
SCM1	100	9.7	0.78
	0	8.1	0.76
HCA1	100	3.7	0.55
	0 (first transfer)	1.2	0.43
	0 (second transfer)	0.0	0.00
PS0	100	3.2	0.23
	0 (first transfer)	1.5	0.19
	0 (second transfer)	0.0	0.00

Chapter 3.

Nitrosopumilus maritimus* gen. nov., sp. nov., *Nitrosopumilus cobalaminogenes* gen. nov., sp. nov., *Nitrosopumilus oxycliniae* gen. nov., sp. nov., and *Nitrosopumilus ureaphilus* gen. nov., sp. nov., four marine ammonia-oxidizing archaea of the phylum *Thaumarchaeota

Wei Qin^a, Katherine R. Heal^b, Rasika Ramdasi^c, Julia N. Kobelt^d, Willm Martens-Habbena^{a, e}, Anthony D. Bertagnolli^{a, f}, Shady A. Amin^g, Christopher B. Walker^a, Hidetoshi Urakawa^h, Martin Könnekeⁱ, Allan H. Devol^b, James W. Moffett^j, E. Virginia Armbrust^b, Grant J. Jensen^c, Anitra E. Ingalls^b, David A. Stahl^{a, 1}

Submitted to *International Journal of Systematic and Evolutionary Microbiology*
(Under review).

^aDepartment of Civil and Environmental Engineering, University of Washington, Seattle, WA, USA; ^bSchool of Oceanography, University of Washington, Seattle, WA, USA; ^cDepartment of Biology, California Institute of Technology, Pasadena, CA, USA; ^dDepartment of Biology, University of Washington, Seattle, WA, USA; ^eDepartment of Microbiology and Cell Science & Fort Lauderdale Research and Education Center, Institute of Food and Agricultural Sciences, University of Florida, FL, USA; ^fSchool of Biological Sciences, Georgia Institute of Technology, Atlanta, GA, USA; ^gDepartment of Chemistry, New York University Abu Dhabi, Abu Dhabi, UAE; ^hDepartment of Marine and Ecological Sciences, Florida Gulf Coast University, Fort Myers, FL, USA; ⁱOrganic Geochemistry Group, MARUM–Center for Marine Environmental Sciences, University of Bremen, Bremen, Germany; ^jDepartments of Biological Sciences and Earth Sciences and Civil and Environmental Engineering, University of Southern California, Los Angeles, CA, USA.

¹Corresponding author E-mail: dastahl@u.washington.edu.

Abstract

Four mesophilic, neutrophilic, and aerobic marine ammonia-oxidizing archaea, designated strains SCM1, HCA1, HCE1, and PS0, were isolated from a tropical marine fish tank, dimly lit deep coastal waters, the lower euphotic zone of coastal waters, and near-surface sediment in the Puget Sound estuary, respectively. Cells are straight or slightly curved small rods, 0.15–0.26 μm in diameter and 0.50–1.59 μm in length. Motility was not observed, although strain PS0 possess genes associated with archaeal flagella and chemotaxis, suggesting it may be motile under some conditions. Cell membranes consist of glycerol dibiphytanyl glycerol tetraether (GDGT) lipids, with crenarchaeol as the major component. Strain SCM1 displays a single surface layer (S-layer) with p6 symmetry, distinct from the p3-S-layer reported for the soil ammonia-oxidizing archaeon *Nitrososphaera viennensis* EN76. Respiratory quinones consist of fully saturated and monounsaturated menaquinones with 6 isoprenoid units in the side chain. Cells obtain energy from ammonia oxidation and use carbon dioxide as carbon source; addition of an α -keto acid (α -ketoglutaric acid) was necessary to sustain growth of strains HCA1, HCE1, and PS0. Strain PS0 uses urea as a source of energy for growth. All strains synthesize vitamin B₁ (thiamine), B₂ (riboflavin), B₆ (pyridoxine), and B₁₂ (cobalamin). Optimal growth occurs between 25 and 32°C, between pH 6.8 and 7.3, and between 25‰ and 37‰ salinity. All strains have a low mol% G+C content of 33.0–34.2. Strains are related by 98% or greater 16S rRNA gene sequence identity, sharing ~85% 16S rRNA gene sequence identity with *Nitrososphaera viennensis* EN76. All four isolates are well separated by phenotypic and genotypic

characteristics and are here assigned to distinct species within the genus *Nitrosopumilus* gen. nov. Isolates SCM1, HCA1, HCE1, and PS0 are type strains of the species *Nitrosopumilus maritimus* gen. nov., sp. nov., *Nitrosopumilus cobalaminogenes* gen. nov., sp. nov., *Nitrosopumilus oxyclinae* gen. nov., sp. nov., and *Nitrosopumilus ureaphilus* gen. nov., sp. nov., respectively. In addition, we propose the family *Nitrosopumilaceae* fam. nov. and the order *Nitrosopumilales* ord. nov. within the class *Nitrososphaeria*.

Introduction

For decades, *Archaea* were defined as obligate extremophiles and restricted to high-temperature, extremely acidic, hypersaline, or strictly anoxic habitats (Woese et al., 1978). However, this perception was overturned with the discovery of mesophilic marine Group I (MGI) and Group II *Archaea* from temperate and oxygenated ocean waters (DeLong, 1992; Fuhrman et al., 1992). Detailed molecular surveys indicated that MGI are among the most ubiquitous and abundant marine prokaryotes, approaching 40% of total bacterioplankton in the meso- and bathypelagic zones (Karner et al., 2001), and constituting a considerable fraction of the microbial biomass in the ocean (Schattenhofer et al., 2009). Marine metagenomic studies first hinted at the metabolic potential of MGI, as a copper-containing membrane-bound monooxygenase (Cu-MMO) gene was found on a MGI-associated scaffold (Venter et al., 2004). Although Cu-MMOs consist of a diverse family of enzymes having broad substrate range, this gene was provisionally annotated as coding for an ammonia monooxygenase (AMO), based on ~25% amino acid identity with bacterial AMO (Venter et al., 2004), although also sharing significant identity (~50%) with the bacterial particulate methane monooxygenase (Sayavedra-Soto et al., 2011; Tavormina et al., 2011). Therefore, demonstration of a capacity for archaeal ammonia oxidation awaited the

isolation of the first chemolithoautotrophic marine ammonia-oxidizing archaeon (AOA) “*Candidatus Nitrosopumilus maritimus*” SCM1, which established the definitive link between the MGI AMO-encoding genes and nitrification (Könneke et al., 2005). Subsequent extensive archaeal *amoA* (the gene coding for the α -subunit of the AMO) gene surveys demonstrated the widespread presence of the putative *amoA* genes in divergent MGI, suggestive of their significant role in marine nitrification (Francis et al., 2005). However, given the extremely low ammonia concentrations in the ocean and the thermodynamically low energy yield of ammonia oxidation ($\Delta G^{\circ} = -271 \text{ kJ mol}^{-1} \text{ NH}_4^+$) (Wood, 1986), it remained uncertain whether all members of MGI obligatorily depend on ammonia as the sole energy source for growth. For example, Agogué *et al.* speculated that most deep-sea MGI are incapable of autotrophic ammonia oxidation and are likely heterotrophs using organic matter for growth based on a marked decrease in the ratio of *amoA* : MGI 16S rRNA genes with depth (Agogué et al., 2008c). This vertical gradient of decreasing ratio was however later shown to be mainly caused by primer bias (Sintes et al., 2013). Using strain SCM1 as a model organism, detailed studies of ammonia oxidation kinetics and the biochemical characterizations of the carbon dioxide (CO_2) fixation pathway identified adaptive features associated with growth under extreme ammonia limitation (Martens-Habbena et al., 2009b; Könneke et al., 2014). Strain SCM1 has a remarkably low half saturation constant (K_m) for ammonia oxidation of 133 nM total ammonia ($\text{NH}_3 + \text{NH}_4^+$) and an exceptionally high ammonia affinity of $68,700 \text{ l g}^{-1} \text{ cells h}^{-1}$, which is among the highest substrate affinities yet reported for any microorganisms (Martens-Habbena et al., 2009b). High-affinity for ammonia is coupled with the most energy-efficient aerobic pathway for carbon fixation yet characterized, which together are thought to contribute to the remarkable ecological success of oligotrophic marine AOA (Martens-Habbena et al., 2009b;

Könneke et al., 2014). It is now widely accepted that they are major contributors of marine nitrification (Horak et al., 2013; Newell et al., 2013; Peng et al., 2015), and appear to be almost completely responsible for ammonia oxidation in oligotrophic oceans (Martens-Habbena et al., 2015).

Since the isolation of the first representative strain SCM1, the same general cultivation strategy has been widely applied to culture additional members of archaeal ammonia oxidizers from a variety of habitats, including marine, soil, freshwater, wastewater, and hot springs (Stahl and de la Torre, 2012a). Available AOA cultures grow at temperatures as high as 74°C (“*Candidatus Nitrosocaldus yellowstonii*” HL72) (de la Torre et al., 2008), pH as low as 4.0 (“*Candidatus Nitrosotalea*” sp. Nd2) (Lehtovirta-Morley et al., 2014), salinities between 55 and 96‰ (SCM1) (Elling et al., 2015; Widderich et al., 2015), oxygen (O₂) concentrations of 1 μM or lower (“*Candidatus Nitrosopumilus*” sp. PS0) (Qin et al., 2015d), and ammonia concentrations up to 100 mM (“*Candidatus Nitrosocosmicus franklandus*” C13) (Lehtovirta-Morley et al., 2016b). It has been shown that even phylogenetically closely related AOA strains display distinct physiological characteristics, supporting fine niche partitioning and ecological differentiation (Lehtovirta-Morley et al., 2014; Qin et al., 2014; Bayer et al., 2015). Despite the enormous metabolic and functional diversity, all sequenced AOA representatives share common genomic features such as a copper-based enzymatic system for ammonia oxidation and electron transfer, a variant of the autotrophic 3-hydroxypropionate/4-hydroxybutyrate (HP/HB) cycle for carbon fixation, and a complete cobalamin (vitamin B₁₂) synthesis pathway (Walker et al., 2010; Spang et al., 2012; Lebedeva et al., 2013; Santoro et al., 2015; Heal et al., 2016). In addition, all investigated AOA strains synthesize the same type of membrane lipids, the glycerol dibiphytanyl

glycerol tetraether (GDGT) lipids with crenarchaeol as the characteristic component (de la Torre et al., 2008; Pitcher et al., 2011; Damsté et al., 2012; Elling et al., 2015; Qin et al., 2015d), the apolar lipid methoxy archaeol (Elling et al., 2014), and the same suite of membrane-bound respiratory menaquinones with 6 isoprenoid units (Elling et al., 2016).

Archaeal ammonia oxidizers associate with the distinct and deeply-branching phylum *Thaumarchaeota*, which is divided into four major phylogenetic sub-lineages, group I.1 a, group I.1 a-associated, group I.1 b, and ThAOA (Thermophilic AOA) (Brochier-Armanet et al., 2008; Spang et al., 2010). Members of marine AOA are almost exclusively affiliated with the group I.1 a *Thaumarchaeota* (Biller et al., 2012). Classification of AOA available in pure culture or enrichment embraces this general phylogenetic structure in consideration of additional ecological, physiological, and biochemical data (Pester et al., 2011; Hatzenpichler, 2012; Stahl and de la Torre, 2012a). However, few strains have been validly described. Here we report the formal taxonomic description of four closely related marine isolates: a novel marine thaumarchaeote from the primary nitrite maximum layer in Puget Sound coastal waters (strain HCE1) and the previously reported thaumarchaeal isolates SCM1, HCA1, and PS0. We extend the original descriptions of these three AOA isolates (Qin et al., 2014), presenting additional characterizations of the cell envelope structure and vitamin synthesis. Based on these data we formally propose the species *Nitrosopumilus maritimus* sp. nov., which is assigned as the type species of the genus *Nitrosopumilus* gen. nov. Furthermore, the physiological and genomic characteristics indicate that strains HCA1, HCE1, and PS0 represent three novel species of this genus, for which the names *Nitrosopumilus cobalaminogenes* sp. nov., *Nitrosopumilus oxycliniae* sp. nov., and *Nitrosopumilus ureaphilus* sp. nov. are proposed, respectively. We also propose

the genus *Nitrosopumilus* (Qin et al., 2015c) as the type genus of the family *Nitrosopumilaceae* fam. nov. (Qin et al., 2015b) and the order *Nitrosopumilales* ord. nov. (Qin et al., 2015a) within the class *Nitrososphaeria* (Stieglmeier et al., 2014b).

Results and Discussion

Physiology

Growth of four strains of marine AOA was accompanied by stoichiometric conversion of ammonia to nitrite (Fig. 3.1) (Martens-Habbena et al., 2009b; Qin et al., 2014). The maximum cell-specific ammonia oxidation rate for strain PS0 ($2.9 \text{ fmol cell}^{-1} \text{d}^{-1}$) was lower than the other three strains ($5.8\text{--}12.7 \text{ fmol cell}^{-1} \text{d}^{-1}$) (Table 3.1), but comparable to a described open ocean AOA, “*Candidatus Nitrosopelagicus brevis*” CN25 ($\sim 2 \text{ fmol cell}^{-1} \text{d}^{-1}$) (Santoro and Casciotti, 2011). These values were generally within the range of the estimated per cell ammonia oxidation rate for field surveys in the Eastern Tropical North Pacific Ocean ($0.1\text{--}4.1 \text{ fmol cell}^{-1} \text{d}^{-1}$) and off the California coast ($0.2\text{--}15 \text{ fmol cell}^{-1} \text{d}^{-1}$) (Santoro et al., 2010; Peng et al., 2015). Their physiologies differed significantly with respect to the distinct adaptations to temperature, pH, salinity, light, organic acids, and tolerance to elevated concentrations of ammonia and nitrite. The temperature optima of strains HCA1, HCE1, and PS0 were between 25 and 26°C , whereas strain SCM1 grew optimally at the higher temperature of 32°C (Fig. 3.2 and Table 3.1). Notably, HCE1 was psychrotolerant and able to grow (based on cell counts and nitrite production), albeit very slowly, at temperature as low as 4°C (generation time of ~ 65 d); while slow growth of strain SCM1 only occurred at 15°C (generation time of ~ 20 d), and no growth was observed at 10°C (Fig. 3.2). All four strains of marine AOA preferred circum-neutral pH, with the highest growth rates at pH $6.8\text{--}7.3$ (Table 3.1). Unlike the other three strains, HCE1

ceased to grow at pH 8.1, a value within the average pH range of surface oceans (Fig. 3.3a). Remarkably, strain PS0 is well adapted to low-pH, sustaining approximately 80% of its maximum growth rate at pH 5.9 (Qin et al., 2014). All strains have an obligate salt requirement, and grow best at 25–37‰ salinity (Table 3.1). Although three coastal AOA strains (HCA1, HCE1, and PS0) were capable of growth at oceanic salinities, they grew well at lower salinities commonly seen in coastal waters. In particular, strain HCE1 grew over a wide salinity range (10–40‰) (Fig. 3.3b), possibly indicating adaptation to seasonal fluctuations in coastal salinity. Strain SCM1 was tolerant of salinities between 55 and 96‰, but was unable to grow at 15‰ salinity (Qin et al., 2014; Elling et al., 2015; Widderich et al., 2015). Strain SCM1 was earlier reported to have genes necessary for the synthesis of ectoine-type compatible osmolytes (Walker et al., 2010; Urakawa et al., 2011) and, accordingly, the synthesis of both ectoine and hydroxyectoine was subsequently confirmed (Widderich et al., 2015). Homologous sequences were also reported in the draft genomes of halotolerant *Nitrosopumilus* species from the brine-seawater interface (Ngugi et al., 2015), further suggesting a role of ectoines in the salt adaptation of *Nitrosopumilus* sub-lineages. Intriguingly, these genes were not identified in the genomes of *Nitrosopumilus* species enriched from low-salinity estuary and coastal environments (e.g., in “*Candidatus Nitrosopumilus salaria*” BD31, “*Candidatus Nitrosopumilus piranensis*” D3C, and “*Candidatus Nitrosopumilus adriaticus*” NF5) (Mosier et al., 2012b; Bayer et al., 2015), highlighting genotypic differentiation within the *Nitrosopumilus* genus associated with their niche diversification.

All strains displayed substantially different sensitivities to high ammonium concentrations (Fig. 3.4 and Table 3.1). Notably, strain HCE1 was significantly more sensitive to ammonium than

other described members of *Thaumarchaeota*, being almost completely inhibited at 1 mM initial ammonium concentration (Fig. 3.4a); no growth was observed at 2 and 3 mM ammonium. As previously reported (Martens-Habbena et al., 2015), strain SCM1 tolerates up to 10 mM ammonium, although a substantial increase in the length of lag phase was observed at this concentration (Fig. 3.4b). Strain HCA1 exhibited somewhat greater ammonium sensitivity than SCM1, showing no apparent inhibition at 1 mM ammonium, partial inhibition at 2–5 mM, and nearly complete inhibition at 10 mM (Fig. 3.4c). Strain PS0 was the most ammonium-tolerant of the four AOA strains, showing comparable growth rates (as measured by nitrite production) in the presence of 0.2–10 mM initial ammonium concentrations and remaining active at 20 mM (Fig. 3.4d). Growth was completely suppressed only at 50 mM. Additionally, at higher initial ammonium concentrations, the accumulation of nitrite and/or toxic intermediates also impaired growth, potentially leading to the incomplete conversion of ammonium to nitrite (Fig. 3.4). In addition to ammonia, strain PS0 and one of its close relatives “*Candidatus Nitrosopumilus piranensis*” D3C use urea as energy source (Table 3.1) (Qin et al., 2014; Bayer et al., 2015). The presence of a complete *ure* gene cluster consisting of urease, urease accessory proteins, and urea transporters in the draft genome of PS0 is consistent with a capacity for urea utilization (W. Qin and D. Stahl, unpublished). By contrast, strains HCA1, HCE1, and SCM1 do not encode for urease and were incapable of growth on urea (Table 3.1).

Although strain SCM1 was able to grow chemolithoautotrophically by ammonia oxidation and CO₂ fixation via a modified 3-hydroxypropionate/4-hydroxybutyrate (HP/HB) pathway (Könneke et al., 2014), an increase in growth rate and cell yield has been observed when supplemented with small amounts of (100 μM) simple organic molecules (pyruvate,

oxaloacetate, and α -ketoglutarate) (Qin et al., 2014) (Fig. 3.5). However, apart from these three tricarboxylic acid cycle intermediates, none of the tested 61 different organic substrates, including small organic acids, alcohols, sugars, amines, amino acids, vitamins, energy compounds, and complex organic compounds had a positive effect on the growth of SCM1 (Fig. 3.5). Similar to strains HCA1 and PS0, the pure culture of HCE1 was established and maintained in organic carbon supplemented medium, rather than in organic carbon-free medium. Comparable growth rates of the three strains were obtained in medium supplemented with pyruvate or oxaloacetate in lieu of the previously reported α -ketoglutarate (Fig. 3.6). The primary role of these α -keto acids in supporting the growth of HCA1, HCE1, and PS0 is likely via peroxide detoxification (Kim et al., 2016). In contrast, no growth was observed for the three strains in organic carbon-free medium or in medium supplemented with glycolate (Fig. 3.6).

As predicted from genomic potential, all strains produced B-vitamins thiamin (B_1), riboflavin (B_2), and pyridoxine (B_6) (Table 3.1). A common feature of the available thaumarchaeotal genomes and metagenomes is the presence of cobalamin (vitamin B_{12}) biosynthetic genes. In agreement with this conserved genetic capacity, the production of adenosylcobalamin (Ado-Cbl), methylcobalamin (Me-Cbl), and hydroxocobalamin (OH-Cbl) was confirmed for all four strains (Table 3.1). Specifically, Ado-Cbl, an active form of B_{12} , is the cofactor of methylmalonyl-CoA mutase, a key enzyme involved in thaumarchaeotal CO_2 fixation pathway (Walker et al., 2010; Doxey et al., 2015). Total intracellular Ado-Cbl concentration increased with the exponential growth of SCM1, and was the dominant form of B_{12} in actively growing cultures, revealing the tight correlation between Ado-Cbl biosynthesis and activity of *Thaumarchaeota* (Fig. 3.7). Notably, all strains of marine AOA had conspicuously high $B_{12} : C$

cell quotas, ranging from 2800 to 11600 nmol B₁₂ per mol C (Table 3.1). Although our calculations were based on the upper limit of B₁₂ production of marine AOA cells under optimal growth conditions without cobalt limitation, these values generally exceed those of characterized heterotrophic bacteria (0.6-6800 nmol B₁₂ mol⁻¹ C, measured by bioassay) (Taylor and Sullivan, 2008). The high cellular quotas and common capacity for B₁₂ synthesis among AOA now implicate this abundant group of marine microorganisms in the provision of B₁₂ to vitamin-dependent populations in oceanic systems (Doxey et al., 2015; Heal et al., 2016).

Strains SCM1 and PS0 both are adapted to life under O₂ limitation, sustaining high ammonia oxidation activity at low O₂ concentrations found in suboxic regions of oxygen minimum zones (<10 μM O₂) (Qin et al., 2015d). The K_m value for O₂ uptake of strain SCM1 was previously reported to be 3.91 μM (Martens-Habbena et al., 2009b). Notably, these strains continued to actively oxidize ammonia and divide below 1 μM O₂ (Qin et al., 2015d). Increasing amounts of nitrous oxide (N₂O) under reduced O₂ tensions have been reported for strain SCM1 (Löscher et al., 2012). The similar impact of O₂ availability on N₂O yield was also observed with “*Candidatus Nitrosoarchaeum koreensis*” MY1 and “*Candidatus Nitrosoarchaeum limnia*” SFB1 (Jung et al., 2011a; Mosier et al., 2012a). However, in more recent studies, Stieglmeier et al. (2014) and Kozłowski et al. (2016) found no significant difference in the N₂O yield of pure cultures of SCM1 and *Nitrososphaera viennensis* EN76 with varying O₂ concentrations, and further attributed N₂O production to the abiotic reaction catalyzed by reduced iron in the medium (Stieglmeier et al., 2014a; Kozłowski et al., 2016a). Besides the production of atmospherically active trace gas N₂O, nitric oxide (NO) was also released from SCM1 culture during active ammonia oxidation (Martens-Habbena et al., 2015). Prior demonstration of inhibition of SCM1

and *Nitrososphaera viennensis* EN76 ammonia oxidation by addition of the NO scavenger 2-phenyl-4,4,5,5-tetramethylimidazoline-1-oxyl-3-oxide (PTIO) implicated this nitrogen free radical as a participant in a novel pathway for ammonia oxidation (Martens-Habbena et al., 2015; Kozłowski et al., 2016a). In contrast, the AOB are relatively insensitive to PTIO (Martens-Habbena et al., 2015; Kozłowski et al., 2016a). AOA and AOB also differed in the sensitivity to linear aliphatic 1-alkynes (C₆ to C₉). For instance, low concentrations of octyne (C₈; <10 μM) completely inhibited the two AOB *Nitrosomonas europaea* and *Nitrospira multififormis*, but had little effect on SCM1, *Nitrososphaera viennensis* EN76, and “*Candidatus Nitrososphaera gargensis*” Ga9.2 (Taylor et al., 2013; Taylor et al., 2015). Similarly, strains SCM1 and HCA1 showed high resistance to allylthiourea and nitrapyrin, which have been commonly used to inhibit ammonia oxidation by AOB (Martens-Habbena et al., 2015). In contrast, other common nitrification inhibitors, such as acetylene and diethyl dithiocarbamate, had strong inhibitory effects on both strain SCM1 and its bacterial counterparts (Martens-Habbena et al., 2015).

Morphology

All four strains are morphologically indistinguishable, sharing very similar shape and size (Fig. 3.8a) (Qin et al., 2014). They are slender, straight or slightly curved rods, typically 0.15–0.26 μm in diameter and 0.50–1.59 μm in length. Cells divide by binary fission (Pelve et al., 2011; Qin et al., 2014). Given a long replication phase (S phase) (Pelve et al., 2011), significantly elongated cells were occasionally observed in actively growing cultures (Fig. 3.8b). Cells occurred singly. Motility was not observed for any strains. Genes associated with chemotaxis and archaeal flagella were identified in the draft genome of strain PS0, suggestive of potential

motility, but flagella were not observed using electron microscopy (EM) for cells grown under the described conditions.

The highly ordered surface layer (S-layer) is a major structural feature of the cell, covering the entire cell surface (Albers and Meyer, 2011). S-layers are common to both *Archaea* and *Bacteria*, and thought to primarily contribute to structural rigidity and general protection (Albers and Meyer, 2011). The regular S-layer lattices exhibit oblique (p1 or p2), square (p4), or hexagonal (p3 or p6) symmetry, and are assembled into the highly ordered two-dimensional arrays by an entropically driven process (Albers and Meyer, 2011). Electron CryoTomography (ECT) was used to visualize the structural details of S-layer of SCM1 cells. Differing from the traditional EM techniques, ECT images the S-layer in its near-native state by avoiding deformations caused by staining, drying on grids, or metal shadowing (Pilhofer et al., 2010). In “side” view, the SCM1 S-layer appears to have a comb-like structure (Fig. 3.9a). Imaging of the surface (“Top” view) revealed a honeycomb-like lattice of regularly spaced hexagonal units (Fig. 3.9b). To achieve higher resolution, approximately 200 S-layer subunits were extracted from one tomogram and used to generate a “molecular” resolution (~ 4 nm) structure of the S-layer lattice. The averaged subtomogram clearly showed that each S-layer structural unit consists of six protein subunits surrounding a central pore, revealing a hexagonal p6 symmetry of the S-layer lattice (Fig. 3.9c). The distance between two neighboring vertices of the hexagons is ~8 nm and the center-to-center distance between two hexagonal S-layer subunits is ~22 nm, within the range of typical values for S-layer (2.5-35 nm) (Sleytr and Sára, 1997). The six-fold symmetry was further confirmed by the Fourier transform (Fig. 3.9d). Recently, the S-layer lattice with similar dimension constant (~21 nm) but different symmetry (p3) was reported for a

group I.1 b thaumarchaeote, *Nitrososphaera viennensis* EN76 (Stieglmeier et al., 2014b). p6-S-layers are distributed over a wide range of phylogenetic branches in the domain *Archaea*, whereas p3-symmetry types have only been described for the order *Sulfolobales* besides *N. viennensis* (Albers and Meyer, 2011). The S-layer symmetry and lattice constant are often unique characteristics shared by members of the closely related taxons. As additional thaumarchaeotal S-layer structural information emerges, it will be of interest to assess whether a clear phylogenetic boundary exists between species with p6-S-layer and those with p3-S-layer within the phylum *Thaumarchaeota*.

Strain SCM1 possessed a cytoplasmic membrane bounded by an S-layer that delimits a quasi-periplasmic space (Fig. 3.9a). The monolayer cell membrane of strain SCM1 is comprised of GDGT core lipids bound to glyco- or phosphor- polar head groups (Elling et al., 2014). The core lipids consisted mainly of GDGTs with 0–4 cyclopentane rings (GDGT-0–4) and crenarchaeol, the characteristic GDGT of *Thaumarchaeota*, containing a cyclohexane ring and 4 cyclopentane rings (Elling et al., 2014; Qin et al., 2015d). Only minor amounts of crenarchaeol regioisomer (Cren') occurred in four strains of marine AOA as well as other investigated group I.1 a *Thaumarchaeota* (Pitcher et al., 2011; Elling et al., 2015; Qin et al., 2015d), whereas its much higher proportions have been observed in group I.1 b *Thaumarchaeota* (Pitcher et al., 2010; Damsté et al., 2012). Hydroxylated GDGTs were observed exclusively in group I.1 a and the associated group, but not in group I.1 b *Thaumarchaeota* (Damsté et al., 2012; Lehtovirta-Morley et al., 2016a). In addition, although GDGTs with a trihexose headgroup occurred in soil *Thaumarchaeota* “*Candidatus Nitrosotalea devanaterre*” Nd1 and *Nitrososphaera viennensis* EN76 (Damsté et al., 2012; Lehtovirta-Morley et al., 2016a), they have not been detected in any

marine *Thaumarchaeota* analyzed so far. These marked differences together suggest that the core and intact polar GDGTs compositions in *Thaumarchaeota* likely reflect both phylogenetic distributions and ecological niche differentiation. The membrane lipid composition of *Nitrosopumilus* species was recently shown to be influenced by O₂ concentration, showing an apparent increase of GDGT-2 at the expense of GDGT-0 and GDGT-1 at lower O₂ tensions (Qin et al., 2015d). The core and intact polar GDGTs of strain SCM1 also changed with growth phase (Elling et al., 2014). Subsequent work on lipid compositional changes in response to ammonia oxidation rate supported the suggestion by Elling et al. (2014) that energy and reducing power limitation leads to shifts in core GDGT composition, hypothesizing that GDGT cyclization is related to energy flow through the cell (Hurley et al., 2016). In contrast, changes in salinity and pH had no significant impact on membrane lipid composition (Elling et al., 2015).

Phylogeny

Although the four strains of marine AOA displayed distinct physiological characteristics and metabolic capacities, they shared close phylogenetic relationships, united by ~98% 16S rRNA and ~94% *amoA* gene sequence identity. Phylogenetic analysis of 16S rRNA and *amoA* genes placed these strains within a highly supported monophyletic clade tightly associated with other marine group I.1 a *Thaumarchaeota* and distinct from the low-salinity and fresh water AOA lineages (Fig. 3.10 and Fig. 3.11). They shared less than 94% and 85% identity with the 16S rRNA and *amoA* genes, respectively, with other deeply-branching groups of group I.1 a *Thaumarchaeota*, including “*Candidatus Nitrosopelagicus brevis*” CN25, “*Candidatus Cenarchaeum symbiosum*” A, “*Candidatus Nitrosotenuis uzonensis*” N4, and “*Candidatus Nitrosotenuis chungbukensis*” MY2. Similarly, sequences of their 16S rRNA and *amoA* genes

were more than 11% and 21% divergent, respectively, from those of other major sub-lineages of *Thaumarchaeota* including group I.1 a-associated, group I.1 b, and ThAOA. Consistent with most mesophilic marine and lacustrine *Thaumarchaeota*, all four marine AOA strains have a low mol% G+C content of 33.0–34.2 (Table 3.1), which are ~3% lower than that determined for the soil acidophilic strain “*Candidatus Nitrosotalea devanaterre*” Nd1 (group I.1 a-associated), ~8% lower than that of a moderately thermophilic strain “*Candidatus Nitrosotenuis uzonensis*” N4 (group I.1 a), and > 14% lower than group I.1 b strains “*Candidatus Nitrososphaera gargensis*” Ga9.2 (48.3%), “*Candidatus Nitrososphaera evergladensis*” SR1 (50.1%) and *Nitrososphaera viennensis* EN76 (52.7%). Despite high similarities of G+C content and the sequences of two phylogenetically informative genes, their whole genomes shared less than 84% average nucleotide identity (ANI) (W. Qin and D. Stahl, unpublished). These values are far below the threshold range (95–96%) now generally accepted for species definition (Kim et al., 2014). Therefore, in addition to *Nitrosopumilus maritimus* SCM1, we propose that strains HCA1, HCE1, and PS0 be assigned to three novel species as *Nitrosopumilus cobalaminogenes*, *Nitrosopumilus oxycliniae*, and *Nitrosopumilus ureaphilus*, respectively.

Description of *Nitrosopumilus* gen. nov.

Nitrosopumilus (Ni.tro.so.pu.mi.lus. M.L. adj. *nitrosus* nitrous; L. masc. adj. *pumilus* dwarf; M.L. masc. n. *Nitrosopumilus* a dwarf producing nitrite).

Cells are straight or slightly curved rods 0.49–2.00 μm in length and 0.15–0.27 μm in width.

Occurring singly. Nonmotile or motile by polar to subpolar flagella (Bayer et al., 2015). Cell envelope consists of a hexagonally arrayed single S-layer and a monolayer cytoplasmic membrane containing GDGT lipids with 0 to 5 cycloalkyl moieties. The major GDGT

membrane lipid, crenarchaeol, contains four cyclopentyl moieties and one cyclohexyl moiety. The respiratory quinones are saturated and monounsaturated menaquinones with 6 isoprenoid units (Elling et al., 2016). Aerobic. Chemolithoautotrophic growth by ammonia oxidation to nitrite using CO₂ as carbon source, although some organic acids may be needed for growth. Many, but not all, species also use urea as a source of energy for growth. Their apparent half-saturation constants (K_m) for O₂ uptake and ammonia oxidation are 1.17–3.91 μM and 0.13–0.61 μM total ammonia (NH₃ + NH₄⁺), respectively (Martens-Habbena et al., 2009b; Park et al., 2010). Cells tolerate up to 20 mM ammonium. Mesophilic, optimal growth temperature between 25 and 32°C. Neutrophilic, pH optimum between 6.8 and 7.3. Slight to moderate halophilic, salinity optimum between 25 and 37‰. Cells are sensitive to light. Members are capable of vitamin B₁, B₂, B₆, and B₁₂ synthesis. Occur free-living in a wide range of marine systems, including surface oceans, hadal oceans, saltwater aquaria, brackish waters, marine and estuarine sediments, salt marshes, and brine-seawater interfaces. Phylogenetic analyses of 16S rRNA and *amoA* sequences indicate that species of the genus *Nitrosopumilus* form a highly supported monophyletic lineage within the group I.1 a *Thaumarchaeota*. Their closest relatives affiliate with the provisional genus “*Nitrosoarchaeum*” (represented by “*Candidatus Nitrosoarchaeum koreensis*” MY1, “*Candidatus Nitrosoarchaeum limnia*” BG20 and SFB1) commonly found in low-salinity and freshwater environments (Jung et al., 2011a; Mosier et al., 2012a). The DNA G+C content is 33.0–34.2 mol %. The type species is *Nitrosopumilus maritimus*.

Description of *Nitrosopumilus maritimus* sp. nov.

Nitrosopumilus maritimus (ma.ri'ti.mus. L. masc. adj. *maritimus* belonging to the sea; describing its habitat).

Displays the following properties in addition to those given in the genus description. Slender rods with a length of 0.50–0.90 μm and a diameter of 0.17–0.22 μm . Motility is not observed. The cell envelope consists of an S-layer with p6 symmetry covering a monolayer cytoplasmic membrane. The apparent K_m values of O_2 uptake and ammonia oxidation are $3.91 \pm 0.57 \mu\text{M}$ and $0.133 \pm 0.038 \mu\text{M}$, respectively. Cells grow better at low O_2 concentrations of 5–10% headspace O_2 than 21% O_2 . Cells tolerate ammonia and nitrite concentrations of up to 10 mM and 2 mM, respectively. Urease negative. Growth occurs between 15 and 35°C, with an optimum of 32°C. The pH range for growth is between 6.8 and 8.1, with the optimum at pH 7.3. The salinity range for growth is between 16 and 96‰, with the optimum at 32–37‰ salinity. The minimum generation time is around 19 h. Cells are photosensitive and completely inhibited by continuous illumination at the light intensity of $120 \mu\text{E m}^{-2} \text{s}^{-1}$ (Qin et al., 2014). Both ectoine and hydroxyectoine are synthesized in cells in response to osmotic shock (Widderich et al., 2015). Cells are capable of B_{12} synthesis with the B_{12} :C cell quotas of 2800–3500 nmol B_{12} per mol cellular carbon.

The type strain is SCM1^T(= NCIMB 15022^T), isolated from a tropical marine fish tank at the Seattle Aquarium in Seattle, Washington, USA. The G+C content of the genomic DNA of the type strain is 34.2 mol%.

Description of *Nitrosopumilus cobalaminogenes* sp. nov.

Nitrosopumilus cobalaminogenes (co.ba.la.mi.no'ge.nes. N.L. neut. n. *cobaltum* cobalt; N.L. neut. n. *ammoniacum* ammonia/amine; Gr. v. *gennao* to make, to produce; N.L. adj.

cobalaminogenes cobalamin producing, referring to the high cobalamin cell quotas of the type strain).

Displays the following properties in addition to those described above for the genus. Cells are straight small rods 0.65–1.27 μm in length and 0.15–0.26 μm in width. Non-motile. Urease negative. Optimum growth occurs with 0.2–1 mM ammonium and ammonium tolerance is up to 10 mM at pH 7.5. Optimal growth temperature: 25°C; range, 10–30°C. Optimal pH: 7.3; range, 6.8–8.1. Optimal salinity: 32‰; range, 15–40‰ salinity. The minimum doubling time is around 30 h. Cells are sensitive to light and completely inhibited by cycles of 14-h dark/10-h light at the light intensity of 180 $\mu\text{E m}^{-2} \text{s}^{-1}$ (Qin et al., 2014). B₁₂ is synthesized at a high carbon specific cell quota level, ranging from 9300 to 11600 nmol B₁₂ per mol cellular carbon.

The type strain is HCA1, obtained from a depth of 50 m seawater at the Puget Sound Regional Synthesis Model Station P10 (47.91 N, 122.62 W) in Hood Canal, Washington, USA. The G+C content of the genomic DNA of the type strain is 33.0 mol%.

Description of *Nitrosopumilus oxyclinae* sp. nov.

Nitrosopumilus oxyclinae (o.xy'cli.nae. Gr. adj. *oxys* sharp/acid; Gr. v. *clinein* decline; *oxyclinae* referring to the oxycline from where the type strain was isolated).

Slender rods, 0.17–0.26 $\mu\text{m} \times$ 0.69–0.93 μm . Non-motile. Urease negative. Cells are sensitive to high concentrations of ammonium with an ammonium tolerance of up to 1 mM at pH 7.5.

Psychrotolerant, growing between 4 and 30°C, with optimum growth at 25°C. Growth occurs at pH 6.4–7.8 (optimum pH 7.3) and at 10–40‰ salinity (optimum 25‰). The minimum doubling time is around 33 h. Cells are capable of B₁₂ synthesis with the B₁₂:C cell quotas of 4200–5300

nmol B₁₂ per mol cellular carbon. Other general characteristics are the same as those described for the genus.

The type strain is HCE1, isolated from a depth of 17 m seawater (nitrite maximum) within the oxycline of the Puget Sound Regional Synthesis Model Station P12 (47.42 N, 123.11 W) in Hood Canal, Washington, USA. The G+C content of the genomic DNA of the type strain is 33.1 mol%.

Description of *Nitrosopumilus ureaphilus* sp. nov.

Nitrosopumilus ureaphilus (u.re.a.phil.us. Gr. n. *urum* urine; Gr. adj. *philos* loving; M.L. masc. adj. *ureaphilus* loving urea).

Straight, or slightly curved rods, 0.22–0.26 μm × 0.76–1.59 μm. Non-motile, although the presence of genes for an archaeal flagellum and chemotaxis indicate cells may be motile under some conditions. Urea can serve as a source of energy for growth. The maximum ammonium tolerance is 20 mM at pH 7.5. Cells grow best at ambient O₂ concentration (21% O₂), but still sustain high ammonia oxidation activity at O₂ concentrations lower than 10 μM and continue to actively oxidize ammonia and divide at sub-micromolar O₂. Growth occurs between 10–30°C (optimum 26°C) and at 15–40‰ salinity (optimum 25–32‰). The optimal pH is 6.8, but cells grow well at a pH as low as 5.9. The minimum doubling time is around 54 h. Cells are light sensitive and completely inhibited by cycles of 14-h dark/10-h light at the light intensity of 80 μE m⁻² s⁻¹ (Qin et al., 2014). They produce B₁₂ with the carbon specific quotas of B₁₂ ranging from 4700 to 5900 nmol B₁₂ per mol cellular carbon. Otherwise, the description is the same as that for the genus.

The type strain is PS0, originated from a near-shore surface sediment (47.59 N, 122.40 W) in Puget Sound near Seattle, Washington, USA. The G+C content of the genomic DNA of the type strain is 33.4 mol%.

Description of *Nitrosopumilaceae* fam. nov.

Nitrosopumilaceae (Ni.tro.so.pu.mi.la'ce.ae. M.L. masc. n. *Nitrosopumilus* type genus of the family; *-aceae* ending to denote a family; M.L. fem. pl. n. *Nitrosopumilaceae* the family of the genus *Nitrosopumilus*).

Mesophilic, neutrophilic, motile or nonmotile, free-living or symbiotic, straight or slightly curved rods. Obligatorily aerobic ammonia-oxidizing archaea; some members also use urea as substrate. Autotrophic, fixing CO₂ by a modified HP/HB cycle, although some organic material may be needed to support growth. Found in a variety of habitats, including marine, freshwater, wastewater, and soil. Members of this family comprise a distinct branch within the group I.1 a *Thaumarchaeota* based on both 16S rRNA and *amoA* sequences analyses. In contrast to the provisional family “*Nitrosotenuaceae*” (represented by “*Candidatus Nitrosotenuis uzonensis*” N4, “*Candidatus Nitrosotenuis chungbukensis*” MY2, and “*Candidatus Nitrosotenuis cloacae*” SAT1) (Lebedeva et al., 2013; Jung et al., 2014a; Li et al., 2016a), their growth does not occur under moderately thermophilic condition. So far, the family comprises the genus *Nitrosopumilus*, “*Candidatus Nitrosoarchaeum*”, “*Candidatus Nitrosopelagicus*” (represented by “*Candidatus Nitrosopelagicus brevis*” CN25) (Santoro et al., 2015), and “*Candidatus Cenarchaeum*” (represented by “*Candidatus Cenarchaeum symbiosum*” A) (Preston et al., 1996). The type genus is *Nitrosopumilus*. See also description of the genus for features.

Description of *Nitrosopumilales* ord. nov.

Nitrosopumilales (Ni.tro.so.pu.mi.la'les. M.L. masc. n. *Nitrosopumilus* type genus of the order; -ales ending to denote an order; M.L. fem. pl. n. *Nitrosopumilales* the order of the genus *Nitrosopumilus*).

Slender rods or irregular cocci. Obligate aerobes. Chemolithoautotrophs, using ammonia as energy source and CO₂ as carbon source, although some organic material may be needed for growth. Membrane lipids contain acyclic and cyclized GDGTs with up to 5 cycloalkyl rings. Crenarchaeol is a major core GDGT, while its regioisomer (Cren') is detected in minor abundances. Hydroxylated GDGTs are exclusively observed for *Thaumarchaeota* affiliated to this order. Cells contain saturated and monounsaturated menaquinones with 6 isoprenoid units in the side chain. Mesophilic to moderately thermophilic. Neutrophilic. Free-living or symbiotic. All investigated genomes of the members of this order possess cobalamin biosynthesis genes, suggesting that the production of B₁₂ might be common within the *Nitrosopumilales* order. The order *Nitrosopumilales* refers to the group I.1 a *Thaumarchaeota*, which is phylogenetically distinct from the orders “*Candidatus Nitrosotaleales*” (refers to group I.1 a-associated; represented by “*Candidatus Nitrosotalea devanaterria*” Nd1) (Lehtovirta-Morley et al., 2011), *Nitrososphaerales* (refers to the group I.1 b) (Stieglmeier et al., 2014b) and “*Candidatus Nitrosocaldales*” (refers to the ThAOA group; represented by “*Candidatus Nitrosocaldus yellowstonii*” HL72) (de la Torre et al., 2008) within the class *Nitrososphaeria*. Occur worldwide in marine, terrestrial, and geothermal habitats. This order contains the families *Nitrosopumilaceae* and “*Candidatus Nitrosotenuaceae*”. The type genus is *Nitrosopumilus*.

Methods

Sample Source and Culture Maintenance. Strain SCM1 was isolated from a tropical marine fish tank at the Seattle Aquarium in Seattle, Washington, USA (Könneke et al., 2005). Strains HCA1 was recovered from a depth of 50 m water at the Puget Sound Regional Synthesis Model (PRISM; <http://www.prism.washington.edu>) station P10 and strain HCE1 at a depth of 17 m water (nitrite max) at the PRISM station P12, both in Hood Canal, Washington, USA (Qin et al., 2014; Qin et al., 2015d). Strain PS0 was obtained from a nearshore marine surface sediment in Seattle, Washington, USA (47.59 N, 122.40 W) (Qin et al., 2014). The enrichment and isolation strategies were described previously by Könneke *et al.* (2005) and Qin *et al.* (2014). Briefly, strains SCM1 and PS0 were enriched in bicarbonate-buffered Synthetic Crenarchaeota Medium (SCM) (Könneke et al., 2005; Martens-Habbena et al., 2009b; Qin et al., 2014) supplemented with 1mM and 500 μ M NH_4Cl , respectively, while a lower amount of NH_4Cl (2 μ M) was used to selectively enrich strains HCA1 and HCE1. Growth was monitored by ammonium consumption, nitrite production and microscopic cell counts (Könneke et al., 2005; Qin et al., 2014). Pure cultures were obtained via a combination of multiple isolation strategies, such as end-point dilution, antibiotic addition (40 mg l^{-1} streptomycin), filtration (0.22- and 0.45- μ m pore-size), and organic acids supplementation (100 μ M α -ketoglutaric acid). Axenic strain SCM1 was maintained in HEPES-buffered SCM containing (l^{-1}) 26 g NaCl, 5 g $\text{MgSO}_4 \cdot 7\text{H}_2\text{O}$, 5 g $\text{MgCl}_2 \cdot 6\text{H}_2\text{O}$, 1.5 g $\text{CaCl}_2 \cdot 2\text{H}_2\text{O}$, 0.1 g KBr, 10 ml HEPES buffer (1 M HEPES and 0.6 M NaOH), 2 ml NaHCO_3 (1 M), 5 ml KH_2PO_4 (0.4 g l^{-1}), 1 ml FeNaEDTA solution (7.5 M), 1 ml trace element solution, and 1 ml NH_4Cl (1 M) (Martens-Habbena et al., 2009b). Strains HCA1, HCE1, and PS0 were maintained in bicarbonate-buffered SCM containing 3 mM NaHCO_3 supplemented with 200 μ M NH_4Cl , and 100 μ M α -ketoglutaric acid (Qin et al., 2014). The

isolates were cultured in 2 l flasks containing ~400 ml medium in the dark without shaking at 20°C (HCA1, HCE1, and PS0) or at 30°C (SCM1).

Physiological Characterization. We previously determined the growth response of strains SCM1, HCA1, and PS0 to varying temperature, pH, salinity, light, and O₂ concentration (Qin et al., 2014; Qin et al., 2015d). Similarly, in order to investigate the influence of key environmental variables on the growth of strain HCE1, late exponential or early stationary phase cultures were inoculated (1%, v/v transfer) into 100ml HEPES-buffered SCM supplemented with 200 μM NH₄Cl and 100 μM α-ketoglutarate and incubated at temperatures ranging from 4 to 37°C, at pH values ranging from 6.4 to 8.1, and at salinities ranging from 10 to 40‰. To assess the tolerance of all strains to high concentrations of ammonia, cells from exponentially growing cultures were transferred to HEPES-buffered SCM with initial ammonia concentrations ranging from 200 μM to 50 mM NH₄Cl.

The effect of organic substrates on the growth of strain SCM1 was surveyed by inoculating exponential phase culture (1% transfer) into 100 ml SCM individually supplemented with 64 different organic compounds (micromolar range). Three tricarboxylic acid cycle intermediates pyruvate, oxaloacetate, and α-ketoglutarate, which showed positive effects on the growth of SCM1, were selected as potential organic supplements for growth of strains HCA1, HCE1, and PS0. These pure cultures were maintained in SCM supplemented with 100 μM α-ketoglutaric acid before investigating the effect of different organic substrates on their growth. Therefore, two consecutive transfers (1%, v/v) into organic-free medium were completed to minimize the carryover of α-ketoglutarate in the inoculum before addition of the other organic supplements.

Growth in 100 ml SCM supplemented with 100 μ M pyruvate, oxaloacetate, α -ketoglutarate, as well as glycolate, a common algal exudate was compared to controls lacking organic carbon supplement. Growth was regularly monitored for two consecutive transfers (1%, v/v) in each medium. If not otherwise indicated, all growth experiments were carried out in triplicates in the dark without shaking.

Vitamins synthesis. To measure vitamin production from four AOA strains, cultures were grown at optimal growth temperatures in 100–150 ml HEPES-buffered SCM without vitamin additions. Growth was monitored by nitrite production and microscopic cell counts as previously described by Qin *et al.* (2014). Strain SCM1 was harvested at five time points on 0.22- μ m Nylon membrane filters (Millipore Co., MA, USA), corresponding to the time of inoculation, mid-lag, early exponential, mid-exponential, and late exponential phases of growth. The other three strains were harvested in the late exponential phase on 0.22- μ m Durapore membrane filters (Millipore Co., MA, USA). Cells were harvested in the dark to minimize vitamin photodegradation and stored at -20°C prior to analysis. Cells were disrupted by bead beating in a solution of methanol:acetonitrile:water with formic acid (40:40:20 with 0.1% formic acid) (Rabinowitz and Kimball, 2007) followed by analysis using liquid-chromatography mass spectrometry (LC-MS) (Heal *et al.*, 2014b), with modifications as previously described (Heal *et al.*, 2016). Vitamin B₁, B₂, and B₁₂ were measured as previously described (Heal *et al.*, 2014b; Heal *et al.*, 2016) and an active form of B₆ (pyridoxal phosphate) was monitored using a parent mass of 248.04 and daughter masses of 94.15 and 150.15 with collision energies of 28 and 16 V, respectively. For each vitamin compound, we relied on at least two mass transitions matching the retention time of a standard to identify the compound.

Microscopy. Exponentially growing HCE1 cells were prepared for transmission electron microscopy (TEM) examination as previously described by Qin *et al.* (2014). TEM images were recorded with a JEOL JEM-1400 transmission electron microscope operated at 120 kV and magnification of 15,000 and 20,000 \times (Electron Microscopy Core Facility, Fred Hutchinson Cancer Research Center, Seattle, WA). Electron CryoTomography (ECT) was used to visualize the structural details of the S-layer of strain SCM1. Exponential phase cells of strain SCM1 were concentrated by filtration and suspended in PBS containing BSA-treated colloidal gold fiducial markers (10 nm) (Iancu *et al.*, 2006; Mastronarde, 2006). From this solution, 3 μ l was applied to R2/2 copper Quantifoil EM grids (Quantifoil Micro Tools, Germany). Using a vitrobot Mark III (FEI) maintained at 80% humidity and 30 $^{\circ}$ C of temperature, the excess liquid was blotted and the grids were plunged frozen in a liquid ethane-propane mixture. The cryopreserved grids were imaged using FEI PolaraTM G2 (FEI Company, Hillsboro, OR) 300 kV field emission gun transmission electron microscope. The tomograms (22,000 \times magnification) were collected and analyzed using UCSF Tomo software (University of California, San Francisco) and IMOD software package.

Phylogenetic Analysis. The 16S rRNA (1248 nucleic acid positions) and *amoA* (576 nucleic acid positions) sequences of currently available cultivated AOA representatives were first aligned using CLUSTALW and manually inspected (Thompson *et al.*, 1994). The maximum-likelihood method with Kimura 2-parameter correction and 500 bootstrap replicates was used to construct 16S rRNA and *amoA* gene phylogenetic trees using MEGA software version 7.0.14 (Kumar *et al.*, 2016). The 16S rRNA and *amoA* sequences of strain SCM1 was deposited

previously in GenBank database (accession number CP000866). The full 16S rRNA and *amoA* sequences of strains HCA1, HCE1 and PS0 reported in this study are deposited under accession numbers KX950754 to KX950759.

Cell cryopreservation and resuscitation. Prior to cryopreservation, all strains were grown in standard growth medium at their optimal temperatures to late exponential phase. One-half milliliter of exponential growing culture was transferred into a 1 ml cryotube (Thermo Fisher Scientific, Rochester, NY, USA) containing 0.5 ml of 20% glycerol (Sigma-Aldrich, St. Louis, MO). Vials were gently mixed, incubated at 20°C for 15 mins, and then preserved at –80°C. The cryopreserved cells were resuscitated after 6 months. Frozen stocks were thawed on ice in the dark, and immediately transferred to sterile centrifuge tubes, followed by centrifugation for 45 mins at 10,000 × g at 10°C. The supernatant with glycerol was removed to reduce toxicity and the cell pellet was gently resuspended with 1ml standard growth medium. Subsequently, cultures were transferred into 6 ml of fresh medium and incubated at the temperature optimum of each strain.

Acknowledgements

We thank B. Schneider and the FHCRC EM staff for performing transmission electron microscopy, and the Captain and crew of the R/V Clifford A. Barnes for their assistance with sample collection. We thank Adam Gee, Emily Chang, Jessie Zhou, Dr. Robert Morris, and Vega Shah for technical assistance and Andrea Teichgräber and Kelley Meinhardt for helpful discussions. This work was funded by the United States National Science Foundation grants

MCB-0604448 (to D.A.S.) and Dimensions of Biodiversity Program OCE-1046017 (to D.A.S., A.E.I., E.V.A., A.H.D., J.W.M.).

References

- Agogu , H., Brink, M., Dinasquet, J., and Herndl, G.J. (2008c) Major gradients in putatively nitrifying and non-nitrifying Archaea in the deep North Atlantic. *Nature* **456**: 788-U772.
- Albers, S.V., and Meyer, B.H. (2011) The archaeal cell envelope. *Nat Rev Microbiol* **9**: 414-426.
- Bayer, B., Vojvoda, J., Offre, P., Alves, R.J., Elisabeth, N.H., Garcia, J.A. et al. (2015) Physiological and genomic characterization of two novel marine thaumarchaeal strains indicates niche differentiation. *Isme J*.
- Biller, S.J., Mosier, A.C., Wells, G.F., and Francis, C.A. (2012) Global biodiversity of aquatic ammonia-oxidizing archaea is partitioned by habitat. *Front Microbiol* **3**.
- Brochier-Armanet, C., Boussau, B., Gribaldo, S., and Forterre, P. (2008) Mesophilic crenarchaeota: proposal for a third archaeal phylum, the Thaumarchaeota. *Nat Rev Microbiol* **6**: 245-252.
- Damst , J.S.S., Rijpstra, W.I.C., Hopmans, E.C., Jung, M.Y., Kim, J.G., Rhee, S.K. et al. (2012) Intact polar and core glycerol dibiphytanyl glycerol tetraether lipids of group I.1a and I.1b *Thaumarchaeota* in soil. *Appl Environ Microb* **78**: 6866-6874.
- de la Torre, J.R., Walker, C.B., Ingalls, A.E., K nneke, M., and Stahl, D.A. (2008) Cultivation of a thermophilic ammonia oxidizing archaeon synthesizing crenarchaeol. *Environ Microbiol* **10**: 810-818.
- Delong, E.F. (1992) Archaea in Coastal Marine Environments. *Proceedings of the National Academy of Sciences of the United States of America* **89**: 5685-5689.
- Doxey, A.C., Kurtz, D.A., Lynch, M.D.J., Sauder, L.A., and Neufeld, J.D. (2015) Aquatic metagenomes implicate Thaumarchaeota in global cobalamin production. *Isme J* **9**: 461-471.
- Elling, F.J., K nneke, M., Mu mann, M., Greve, A., and Hinrichs, K.U. (2015) Influence of temperature, pH, and salinity on membrane lipid composition and TEX₈₆ of marine planktonic thaumarchaeal isolates. *Geochim Cosmochim Acta* **171**: 238-255.
- Elling, F.J., K nneke, M., Lipp, J.S., Becker, K.W., Gagen, E.J., and Hinrichs, K.U. (2014) Effects of growth phase on the membrane lipid composition of the thaumarchaeon *Nitrosopumilus maritimus* and their implications for archaeal lipid distributions in the marine environment. *Geochim Cosmochim Acta* **141**: 579-597.
- Elling, F.J., Becker, K.W., K nneke, M., Schroder, J.M., Kellermann, M.Y., Thomm, M., and Hinrichs, K.U. (2016) Respiratory quinones in Archaea: phylogenetic distribution and application as biomarkers in the marine environment. *Environ Microbiol* **18**: 692-707.
- Francis, C.A., Roberts, K.J., Beman, J.M., Santoro, A.E., and Oakley, B.B. (2005) Ubiquity and diversity of ammonia-oxidizing archaea in water columns and sediments of the ocean. *P Natl Acad Sci USA* **102**: 14683-14688.
- Fuhrman, J.A., Mccallum, K., and Davis, A.A. (1992) Novel Major Archaeobacterial Group from Marine Plankton. *Nature* **356**: 148-149.
- Hatzenpichler, R. (2012) Diversity, Physiology, and Niche Differentiation of Ammonia-Oxidizing Archaea. *Appl Environ Microb* **78**: 7501-7510.

- Heal, K.R., Carlson, L.T., Devol, A.H., Armbrust, E.V., Moffett, J.W., Stahl, D.A., and Ingalls, A.E. (2014b) Determination of four forms of vitamin B₁₂ and other B vitamins in seawater by liquid chromatography/tandem mass spectrometry. *Rapid communications in mass spectrometry* : *RCM* **28**: 2398-2404.
- Heal, K.R., Qin, W., Ribalet, F., Bertagnolli, A.D., Coyote-Maestas, W., Hmelo, L.R. et al. (2016) Two distinct pools of B₁₂ analogs reveal community interdependencies in the ocean. *P Natl Acad Sci USA*.
- Horak, R.E.A., Qin, W., Schauer, A.J., Armbrust, E.V., Ingalls, A.E., Moffett, J.W. et al. (2013) Ammonia oxidation kinetics and temperature sensitivity of a natural marine community dominated by Archaea. *Isme J* **7**: 2023-2033.
- Hurley, S.J., Elling, F.J., Könneke, M., Buchwald, C., Wankel, S.D., Santoro, A.E. et al. (2016) Influence of ammonia oxidation rate on thaumarchaeal lipid composition and the TEX₈₆ temperature proxy. *P Natl Acad Sci USA* **113**: 7762-7767.
- Iancu, C.V., Tivol, W.F., Schooler, J.B., Dias, D.P., Henderson, G.P., Murphy, G.E. et al. (2006) Electron cryotomography sample preparation using the Vitrobot. *Nat Protoc* **1**: 2813-2819.
- Jung, M.Y., Park, S.J., Kim, S.J., Kim, J.G., Damsté, J.S.S., Jeon, C.O., and Rhee, S.K. (2014a) A mesophilic, autotrophic, ammonia-oxidizing archaeon of thaumarchaeal group I.1a cultivated from a deep oligotrophic soil horizon. *Appl Environ Microb* **80**: 3645-3655.
- Jung, M.Y., Park, S.J., Min, D., Kim, J.S., Rijpstra, W.I.C., Damsté, J.S.S. et al. (2011a) Enrichment and characterization of an autotrophic ammonia-oxidizing archaeon of mesophilic crenarchaeal group I.1a from an agricultural soil. *Appl Environ Microb* **77**: 8635-8647.
- Karner, M.B., DeLong, E.F., and Karl, D.M. (2001) Archaeal dominance in the mesopelagic zone of the Pacific Ocean. *Nature* **409**: 507-510.
- Kim, J.G., Park, S.J., Damsté, J.S.S., Schouten, S., Rijpstra, W.I.C., Jung, M.Y. et al. (2016) Hydrogen peroxide detoxification is a key mechanism for growth of ammonia-oxidizing archaea. *P Natl Acad Sci USA* **113**: 7888-7893.
- Kim, M., Oh, H.S., Park, S.C., and Chun, J. (2014) Towards a taxonomic coherence between average nucleotide identity and 16S rRNA gene sequence similarity for species demarcation of prokaryotes. *Int J Syst Evol Micr* **64**: 346-351.
- Könneke, M., Bernhard, A.E., de la Torre, J.R., Walker, C.B., Waterbury, J.B., and Stahl, D.A. (2005) Isolation of an autotrophic ammonia-oxidizing marine archaeon. *Nature* **437**: 543-546.
- Könneke, M., Schubert, D.M., Brown, P.C., Hugler, M., Standfest, S., Schwander, T. et al. (2014) Ammonia-oxidizing archaea use the most energy-efficient aerobic pathway for CO₂ fixation. *P Natl Acad Sci USA* **111**: 8239-8244.
- Kozłowski, J.A., Stieglmeier, M., Schleper, C., Klotz, M.G., and Stein, L.Y. (2016a) Pathways and key intermediates required for obligate aerobic ammonia-dependent chemolithotrophy in bacteria and Thaumarchaeota. *Isme J*.
- Kumar, S., Stecher, G., and Tamura, K. (2016) MEGA7: Molecular Evolutionary Genetics Analysis version 7.0 for bigger datasets. *Molecular biology and evolution*.
- Lebedeva, E.V., Hatzenpichler, R., Pelletier, E., Schuster, N., Hauzmayer, S., Bulaev, A. et al. (2013) Enrichment and Genome Sequence of the Group I. 1a Ammonia-Oxidizing Archaeon "Ca. Nitrosotenuis uzonensis" Representing a Clade Globally Distributed in Thermal Habitats. *Plos One* **8**.
- Lehtovirta-Morley, L.E., Stoecker, K., Vilcinskis, A., Prosser, J.I., and Nicol, G.W. (2011) Cultivation of an obligate acidophilic ammonia oxidizer from a nitrifying acid soil. *Proc Natl Acad Sci USA* **108**: 15892-15897.

- Lehtovirta-Morley, L.E., Ge, C.R., Ross, J., Yao, H.Y., Nicol, G.W., and Prosser, J.I. (2014) Characterisation of terrestrial acidophilic archaeal ammonia oxidisers and their inhibition and stimulation by organic compounds. *Fems Microbiol Ecol* **89**: 542-552.
- Lehtovirta-Morley, L.E., Sayavedra-Soto, L.A., Gallois, N., Schouten, S., Stein, L.Y., Prosser, J.I., and Nicol, G.W. (2016a) Identifying potential mechanisms enabling acidophily in the ammonia-oxidising archaeon '*Candidatus Nitrosotalea devanattera*'. *Appl Environ Microbiol*.
- Lehtovirta-Morley, L.E., Ross, J., Hink, L., Weber, E.B., Gubry-Rangin, C., Thion, C. et al. (2016b) Isolation of '*Candidatus Nitrosocosmicus franklandus*', a novel ureolytic soil archaeal ammonia oxidiser with tolerance to high ammonia concentration. *FEMS microbiology ecology*.
- Li, Y., Ding, K., Wen, X., Zhang, B., Shen, B., and Yang, Y. (2016a) A novel ammonia-oxidizing archaeon from wastewater treatment plant: Its enrichment, physiological and genomic characteristics. *Sci Rep* **6**: 23747.
- Löscher, C.R., Kock, A., Könneke, M., LaRoche, J., Bange, H.W., and Schmitz, R.A. (2012) Production of oceanic nitrous oxide by ammonia-oxidizing archaea. *Biogeosciences* **9**: 2419-2429.
- Martens-Habbena, W., Berube, P.M., Urakawa, H., de la Torre, J.R., and Stahl, D.A. (2009b) Ammonia oxidation kinetics determine niche separation of nitrifying Archaea and Bacteria. *Nature* **461**: 976-U234.
- Martens-Habbena, W., Qin, W., Horak, R.E.A., Urakawa, H., Schauer, A.J., Moffett, J.W. et al. (2015) The production of nitric oxide by marine ammonia-oxidizing archaea and inhibition of archaeal ammonia oxidation by a nitric oxide scavenger. *Environ Microbiol* **17**: 2261-2274.
- Mastrorarde, D.N. (2006) Fiducial Marker and Hybrid Alignment Methods for Single- and Double-axis Tomography. In *Electron Tomography: Methods for Three-Dimensional Visualization of Structures in the Cell*. Frank, J. (ed). New York, NY: Springer New York, pp. 163-185.
- Mosier, A.C., Lund, M.B., and Francis, C.A. (2012a) Ecophysiology of an ammonia-oxidizing archaeon adapted to low-salinity habitats. *Microb Ecol* **64**: 955-963.
- Mosier, A.C., Allen, E.E., Kim, M., Ferriera, S., and Francis, C.A. (2012b) Genome Sequence of "*Candidatus Nitrosopumilus salaria*" BD31, an Ammonia-Oxidizing Archaeon from the San Francisco Bay Estuary. *J Bacteriol* **194**: 2121-2122.
- Newell, S.E., Fawcett, S.E., and Ward, B.B. (2013) Depth distribution of ammonia oxidation rates and ammonia-oxidizer community composition in the Sargasso Sea. *Limnol Oceanogr* **58**: 1491-1500.
- Ngugi, D.K., Blom, J., Alam, I., Rashid, M., Ba-Alawi, W., Zhang, G.S. et al. (2015) Comparative genomics reveals adaptations of a halotolerant thaumarchaeon in the interfaces of brine pools in the Red Sea. *Isme J* **9**: 396-411.
- Park, B.J., Park, S.J., Yoon, D.N., Schouten, S., Damsté, J.S.S., and Rhee, S.K. (2010) Cultivation of autotrophic ammonia-oxidizing archaea from marine sediments in coculture with sulfur-oxidizing bacteria. *Appl Environ Microb* **76**: 7575-7587.
- Pelve, E.A., Lindas, A.C., Martens-Habbena, W., de la Torre, J.R., Stahl, D.A., and Bernander, R. (2011) Cdv-based cell division and cell cycle organization in the thaumarchaeon *Nitrosopumilus maritimus*. *Mol Microbiol* **82**: 555-566.
- Peng, X.F., Fuchsman, C.A., Jayakumar, A., Oleynik, S., Martens-Habbena, W., Devol, A.H., and Ward, B.B. (2015) Ammonia and nitrite oxidation in the Eastern Tropical North Pacific. *Global Biogeochem Cy* **29**: 2034-2049.

- Pester, M., Schleper, C., and Wagner, M. (2011) The Thaumarchaeota: an emerging view of their phylogeny and ecophysiology. *Curr Opin Microbiol* **14**: 300-306.
- Pilhofer, M., Ladinsky, M.S., McDowall, A.W., and Jensen, G.J. (2010) Bacterial TEM: new insights from cryo-microscopy. *Method Cell Biol* **96**: 21-45.
- Pitcher, A., Hopmans, E.C., Mosier, A.C., Park, S.J., Rhee, S.K., Francis, C.A. et al. (2011) Core and Intact Polar Glycerol Dibiphytanyl Glycerol Tetraether Lipids of Ammonia-Oxidizing Archaea Enriched from Marine and Estuarine Sediments. *Appl Environ Microb* **77**: 3468-3477.
- Pitcher, A., Rychlik, N., Hopmans, E.C., Spieck, E., Rijpstra, W.I.C., Ossebaar, J. et al. (2010) Crenarchaeol dominates the membrane lipids of *Candidatus Nitrososphaera gargensis*, a thermophilic Group I. 1b Archaeon. *Isme J* **4**: 542-552.
- Preston, C.M., Wu, K.Y., Molinski, T.F., and DeLong, E.F. (1996) A psychrophilic crenarchaeon inhabits a marine sponge: *Cenarchaeum symbiosum* gen nov, sp. nov. *P Natl Acad Sci USA* **93**: 6241-6246.
- Qin, W., Martens-Habbena, W., Kobelt, J.N., and Stahl, D.A. (2015a) *Candidatus Nitrosopumilales*. In *Bergey's Manual of Systematics of Archaea and Bacteria*: John Wiley & Sons, Ltd.
- Qin, W., Martens-Habbena, W., Kobelt, J.N., and Stahl, D.A. (2015b) *Candidatus Nitrosopumilaceae*. In *Bergey's Manual of Systematics of Archaea and Bacteria*: John Wiley & Sons, Ltd.
- Qin, W., Martens-Habbena, W., Kobelt, J.N., and Stahl, D.A. (2015c) *Candidatus Nitrosopumilus*. In *Bergey's Manual of Systematics of Archaea and Bacteria*: John Wiley & Sons, Ltd.
- Qin, W., Carlson, L.T., Armbrust, E.V., Devol, A.H., Moffett, J.W., Stahl, D.A., and Ingalls, A.E. (2015d) Confounding effects of oxygen and temperature on the TEX₈₆ signature of marine Thaumarchaeota. *P Natl Acad Sci USA* **112**: 10979-10984.
- Qin, W., Amin, S.A., Martens-Habbena, W., Walker, C.B., Urakawa, H., Devol, A.H. et al. (2014) Marine ammonia-oxidizing archaeal isolates display obligate mixotrophy and wide ecotypic variation. *P Natl Acad Sci USA* **111**: 12504-12509.
- Rabinowitz, J.D., and Kimball, E. (2007) Acidic acetonitrile for cellular metabolome extraction from *Escherichia coli*. *Anal Chem* **79**: 6167-6173.
- Santoro, A.E., and Casciotti, K.L. (2011) Enrichment and characterization of ammonia-oxidizing archaea from the open ocean: phylogeny, physiology and stable isotope fractionation. *Isme J* **5**: 1796-1808.
- Santoro, A.E., Casciotti, K.L., and Francis, C.A. (2010) Activity, abundance and diversity of nitrifying archaea and bacteria in the central California Current. *Environ Microbiol* **12**: 1989-2006.
- Santoro, A.E., Dupont, C.L., Richter, R.A., Craig, M.T., Carini, P., McIlvin, M.R. et al. (2015) Genomic and proteomic characterization of "*Candidatus Nitrosopelagicus brevis*": An ammonia-oxidizing archaeon from the open ocean. *P Natl Acad Sci USA* **112**: 1173-1178.
- Sayavedra-Soto, L.A., Hamamura, N., Liu, C.W., Kimbrel, J.A., Chang, J.H., and Arp, D.J. (2011) The membrane-associated monooxygenase in the butane-oxidizing Gram-positive bacterium *Nocardioides* sp. strain CF8 is a novel member of the AMO/PMO family. *Env Microbiol Rep* **3**: 390-396.
- Schattenhofer, M., Fuchs, B.M., Amann, R., Zubkov, M.V., Tarran, G.A., and Pernthaler, J. (2009) Latitudinal distribution of prokaryotic picoplankton populations in the Atlantic Ocean. *Environ Microbiol* **11**: 2078-2093.

- Sintes, E., Bergauer, K., De Corte, D., Yokokawa, T., and Herndl, G.J. (2013) Archaeal *amoA* gene diversity points to distinct biogeography of ammonia-oxidizing Crenarchaeota in the ocean. *Environ Microbiol* **15**: 1647-1658.
- Sleytr, U.B., and Sára, M. (1997) Bacterial and archaeal S-layer proteins: Structure-function relationships and their biotechnological applications. *Trends Biotechnol* **15**: 20-26.
- Spang, A., Hatzenpichler, R., Brochier-Armanet, C., Rattei, T., Tischler, P., Spieck, E. et al. (2010) Distinct gene set in two different lineages of ammonia-oxidizing archaea supports the phylum Thaumarchaeota. *Trends Microbiol* **18**: 331-340.
- Spang, A., Poehlein, A., Offre, P., Zumbragel, S., Haider, S., Rychlik, N. et al. (2012) The genome of the ammonia-oxidizing Candidatus Nitrososphaera gargensis: insights into metabolic versatility and environmental adaptations. *Environ Microbiol* **14**: 3122-3145.
- Stahl, D.A., and de la Torre, J.R. (2012a) Physiology and Diversity of Ammonia-Oxidizing Archaea. *Annu Rev Microbiol* **66**: 83-101.
- Stieglmeier, M., Mooshammer, M., Kitzler, B., Wanek, W., Zechmeister-Boltenstern, S., Richter, A., and Schleper, C. (2014a) Aerobic nitrous oxide production through N-nitrosating hybrid formation in ammonia-oxidizing archaea. *Isme J* **8**: 1135-1146.
- Stieglmeier, M., Klingl, A., Alves, R.J.E., Rittmann, S.K.M.R., Melcher, M., Leisch, N., and Schleper, C. (2014b) Nitrososphaera viennensis gen. nov., sp nov., an aerobic and mesophilic, ammonia-oxidizing archaeon from soil and a member of the archaeal phylum Thaumarchaeota. *Int J Syst Evol Micr* **64**: 2738-2752.
- Tavormina, P.L., Orphan, V.J., Kalyuzhnaya, M.G., Jetten, M.S.M., and Klotz, M.G. (2011) A novel family of functional operons encoding methane/ammonia monooxygenase-related proteins in gammaproteobacterial methanotrophs. *Env Microbiol Rep* **3**: 91-100.
- Taylor, A.E., Vajrala, N., Giguere, A.T., Gitelman, A.I., Arp, D.J., Myrold, D.D. et al. (2013) Use of aliphatic n-alkynes to discriminate soil nitrification activities of ammonia-oxidizing thaumarchaea and bacteria. *Appl Environ Microbiol* **79**: 6544-6551.
- Taylor, A.E., Taylor, K., Tennigkeit, B., Palatinszky, M., Stieglmeier, M., Myrold, D.D. et al. (2015) Inhibitory effects of C₂ to C₁₀ 1-alkynes on ammonia oxidation in two *Nitrososphaera* species. *Appl Environ Microbiol* **81**: 1942-1948.
- Taylor, G.T., and Sullivan, C.W. (2008) Vitamin B₁₂ and cobalt cycling among diatoms and bacteria in Antarctic sea ice microbial communities. *Limnol Oceanogr* **53**: 1862-1877.
- Thompson, J.D., Higgins, D.G., and Gibson, T.J. (1994) Clustal-W - Improving the Sensitivity of Progressive Multiple Sequence Alignment through Sequence Weighting, Position-Specific Gap Penalties and Weight Matrix Choice. *Nucleic Acids Res* **22**: 4673-4680.
- Urakawa, H., Martens-Habbena, W., and Stahl, D.A. (2011) Physiology and genomics of ammonia-oxidizing archaea. In *Nitrification*. BB Ward, M.K., DJ Arp (ed). Washington, DC: ASM Press, pp. 117-155.
- Venter, J.C., Remington, K., Heidelberg, J.F., Halpern, A.L., Rusch, D., Eisen, J.A. et al. (2004) Environmental genome shotgun sequencing of the Sargasso Sea. *Science* **304**: 66-74.
- Walker, C.B., de la Torre, J.R., Klotz, M.G., Urakawa, H., Pinel, N., Arp, D.J. et al. (2010) Nitrosopumilus maritimus genome reveals unique mechanisms for nitrification and autotrophy in globally distributed marine crenarchaea. *P Natl Acad Sci USA* **107**: 8818-8823.
- Widderich, N., Czech, L., Elling, F.J., Könneke, M., Stoveken, N., Pittelkow, M. et al. (2015) Strangers in the archaeal world: osmostress-responsive biosynthesis of ectoine and hydroxyectoine by the marine thaumarchaeon *Nitrosopumilus maritimus*. *Environ Microbiol.*
- Woese, C.R., Magrum, L.J., and Fox, G.E. (1978) Archaeobacteria. *J Mol Evol* **11**: 245-252.

Wood, P.M. (1986) Nitrification as a bacterial energy source. In *Nitrification*. Prosser, J.I. (ed). Oxford, United Kingdom: IRL Press, pp. 39-62.

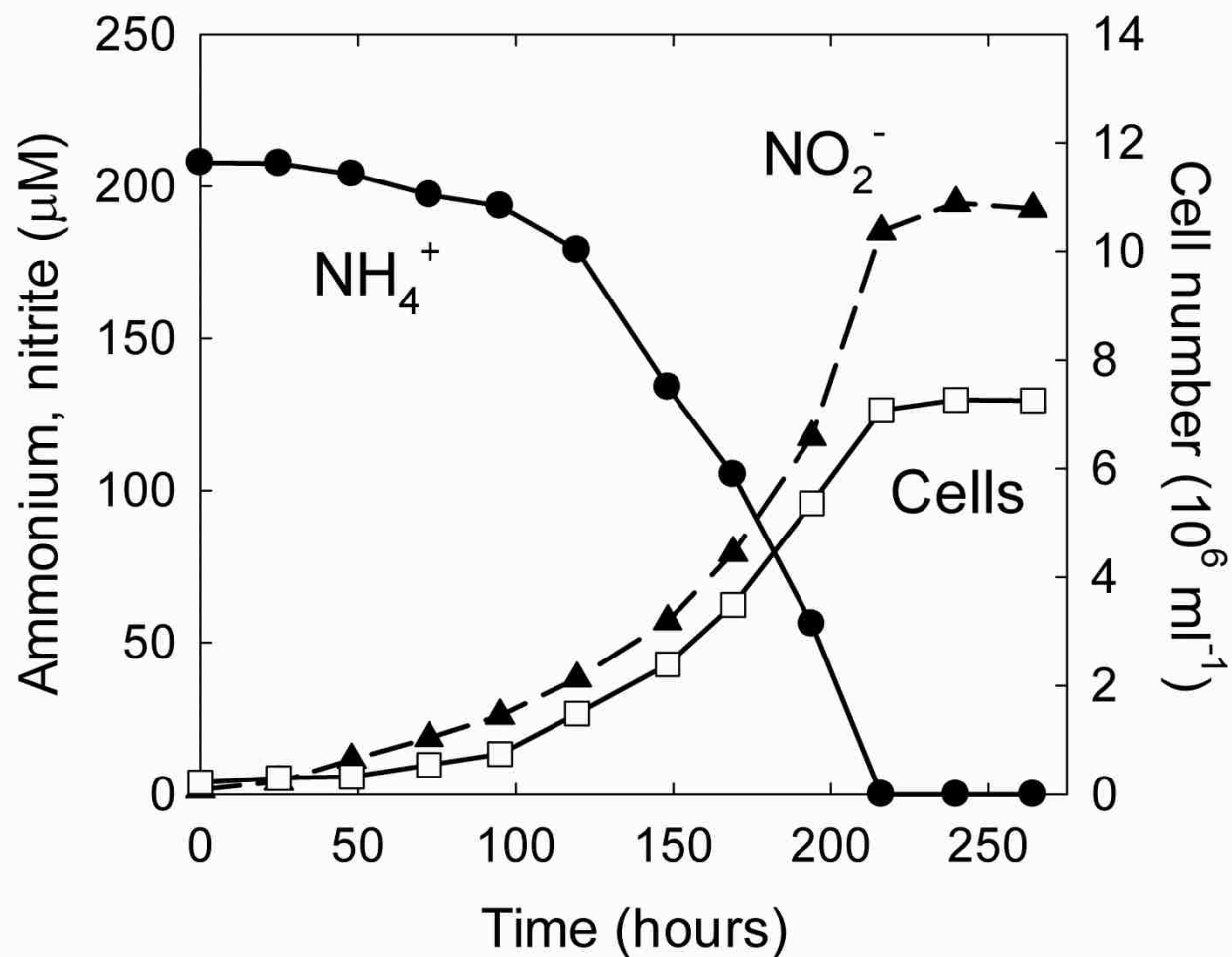


Figure 3.1. Correlation of the growth of strain HCE1 with the stoichiometric ammonia oxidation to nitrite.

Each data point represents the mean of triplicate cultures.

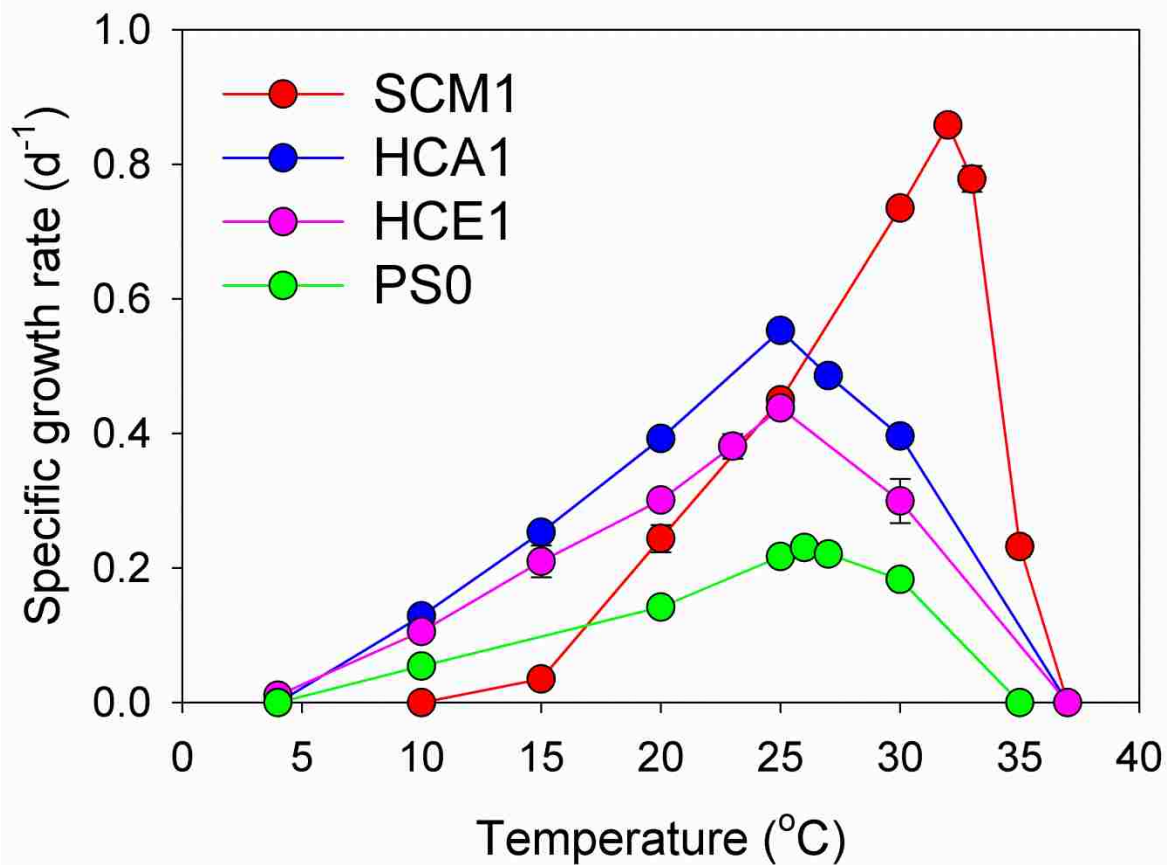


Figure 3.2. Influence of temperature on growth.

Error bars represent the SD of triplicate cultures. Error bars smaller than symbols are not shown.

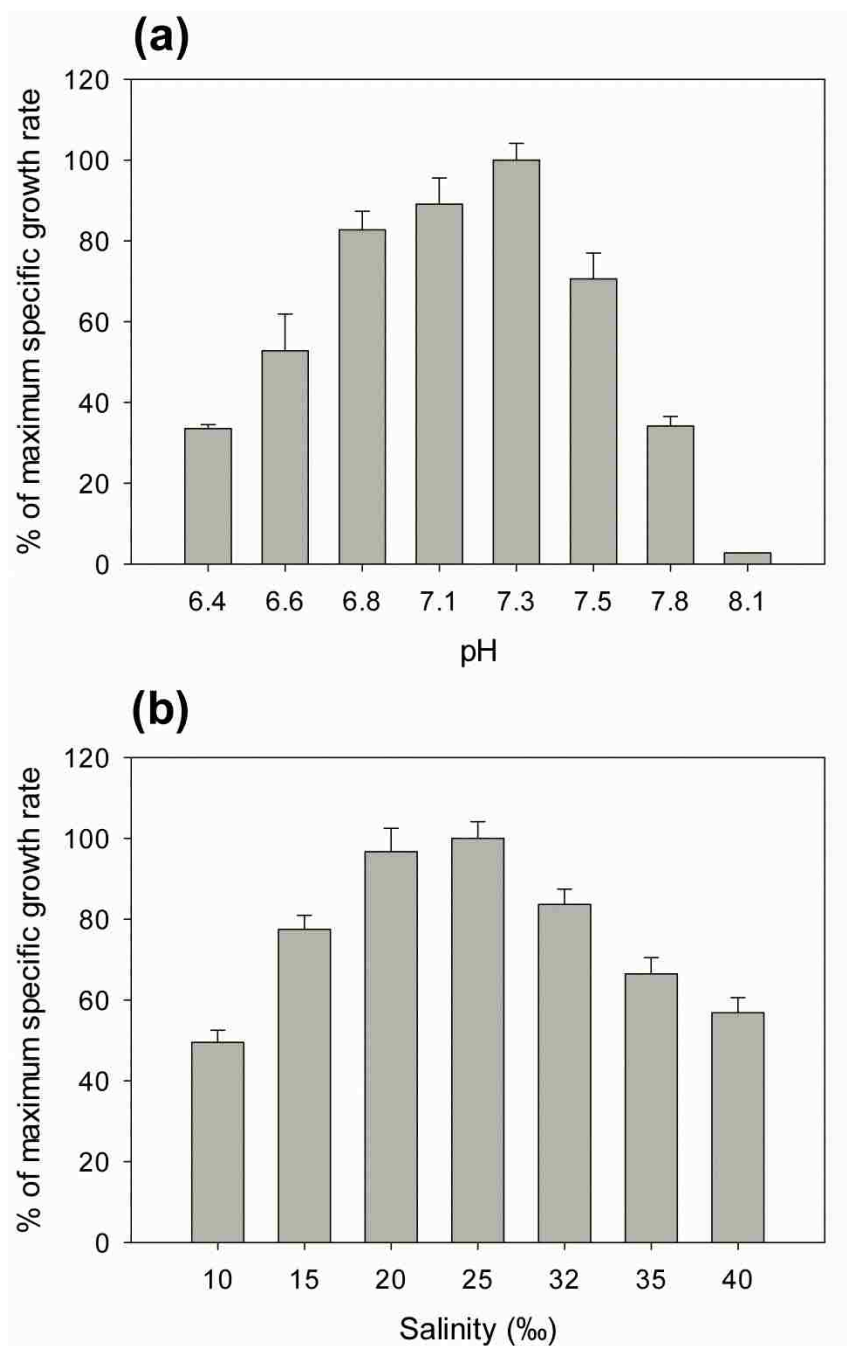


Figure 3.3. The effect of pH (a) and salinity (b) on the specific growth rate of strain HCE1 expressed as a percentage compared with those at pH and salinity optima, respectively.

Error bars represent the SD of the mean of triplicate cultures.

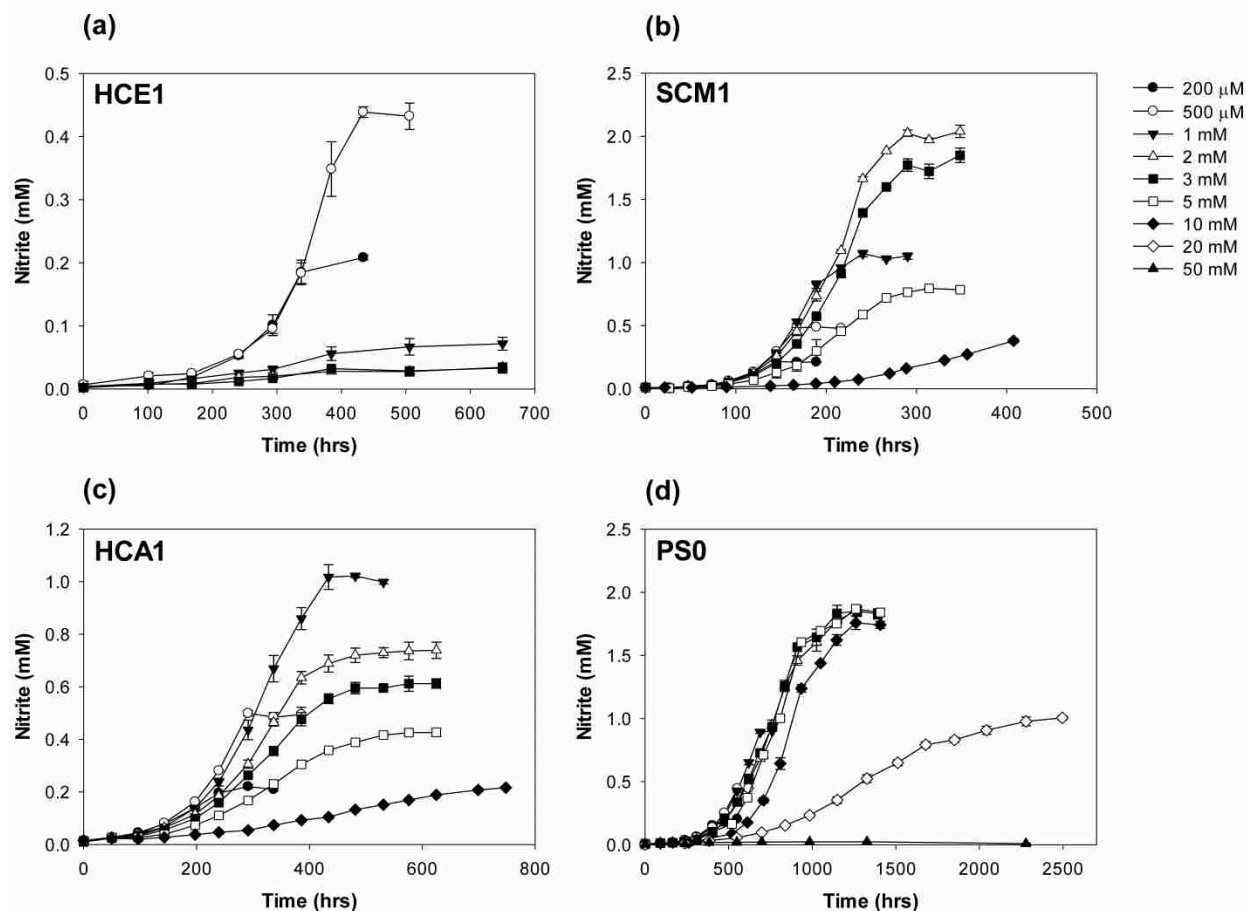


Figure 3.4. Nitrite production by strains HCE1 (a), SCM1 (b), HCA1 (c), and PS0 (d) at different initial ammonia concentrations.

Error bars represent the SD of the mean of triplicate incubations. Error bars smaller than symbols are not shown.

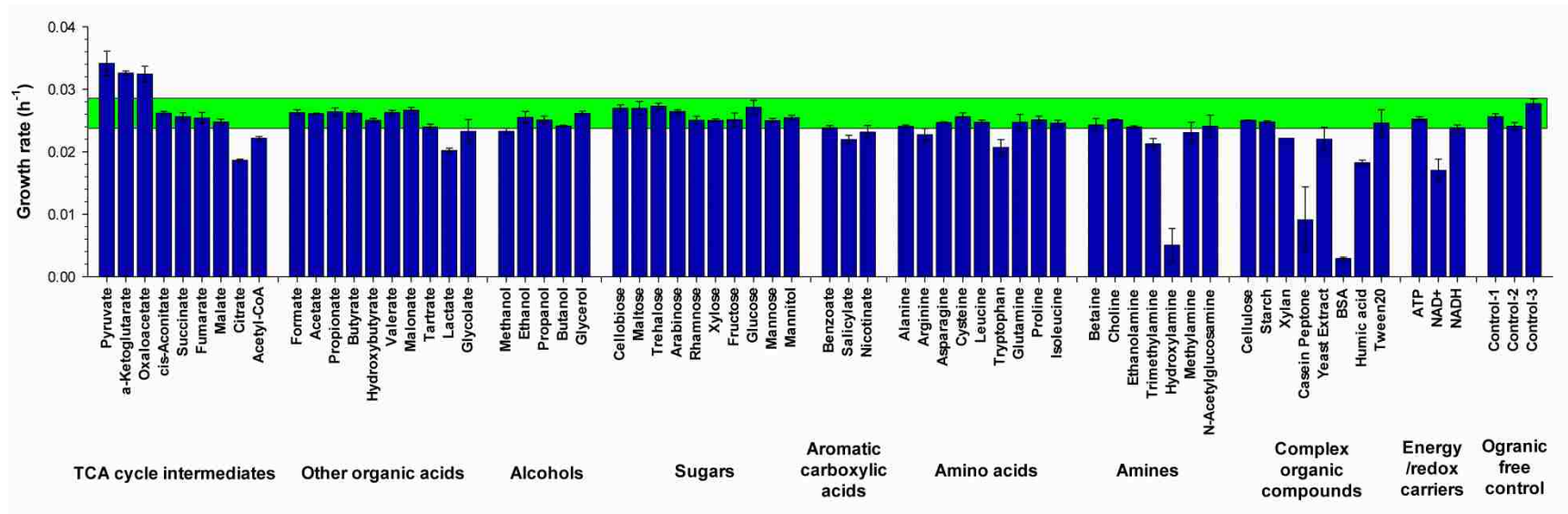


Figure 3.5. Effect of organic compounds on the specific growth rate of strain SCM1.

All organic compounds were tested in the concentration of 100 μ M, with the exception of complex organic compounds in different concentrations (starch: 0.01%, w/v; cellulose, xylan, humic acid, casein peptone, and BSA: 0.005%, w/v; yeast extract: 0.0005%, w/v; polysorbate 20: 0.0001%, w/v). The green shaded area represents the specific growth rate range of controls without organic carbon supplements.

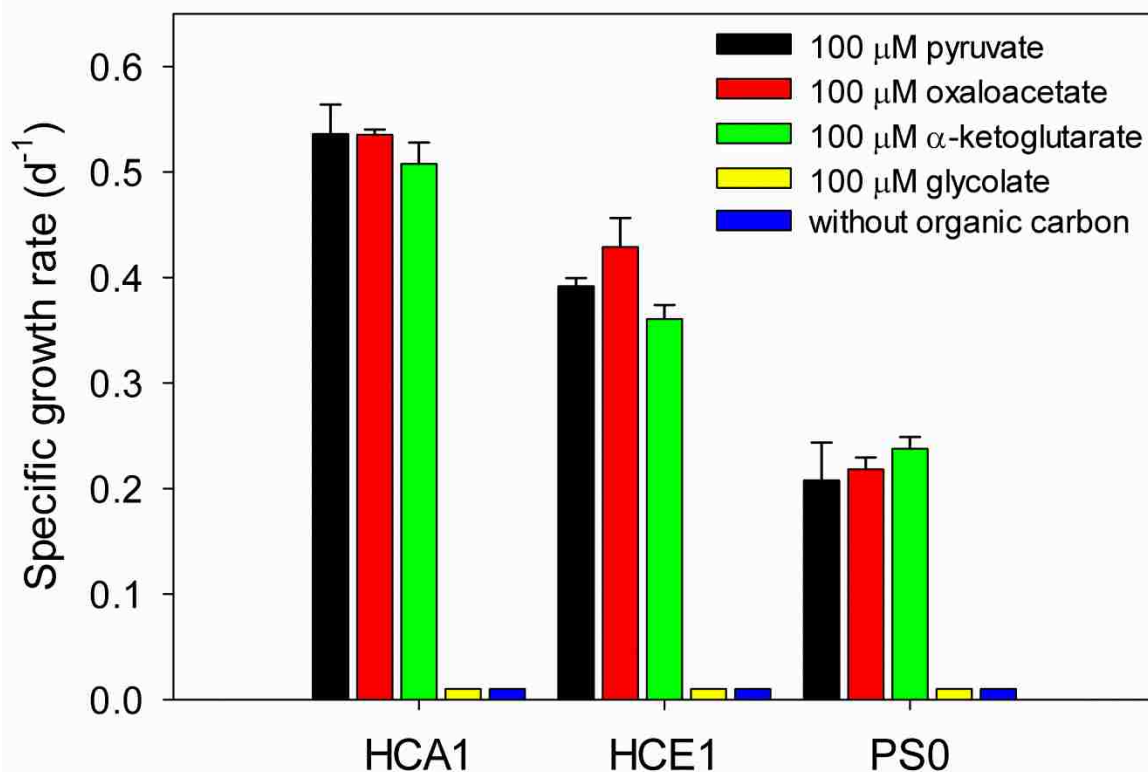


Figure 3.6. The specific growth rates of strains HCA1, HCE1, and PS0 with supplementation of 100 μM pyruvate (black), 100 μM oxaloacetate (red), 100 μM α-ketoglutarate (green), and 100 μM glycolate relative to controls without organic carbon supplements.

Error bars represent the SD of data from triplicate cultures.

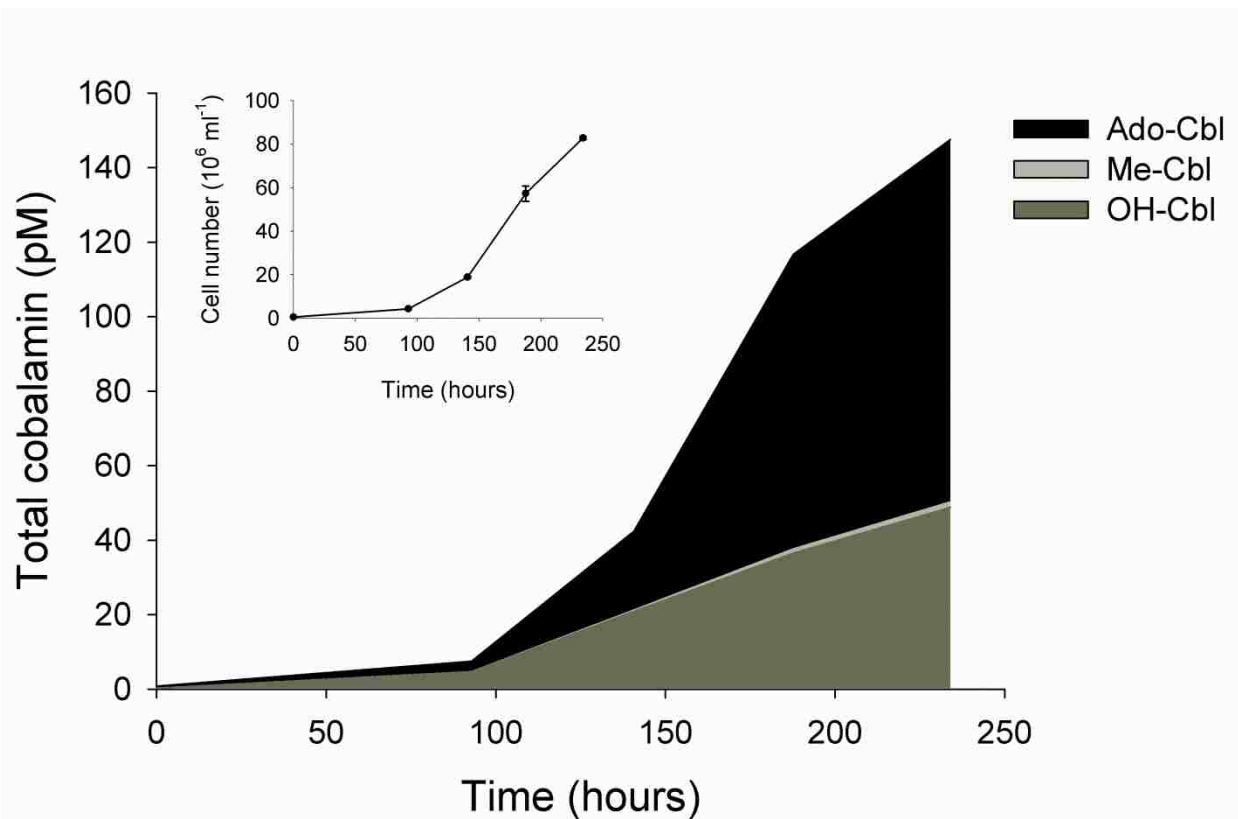
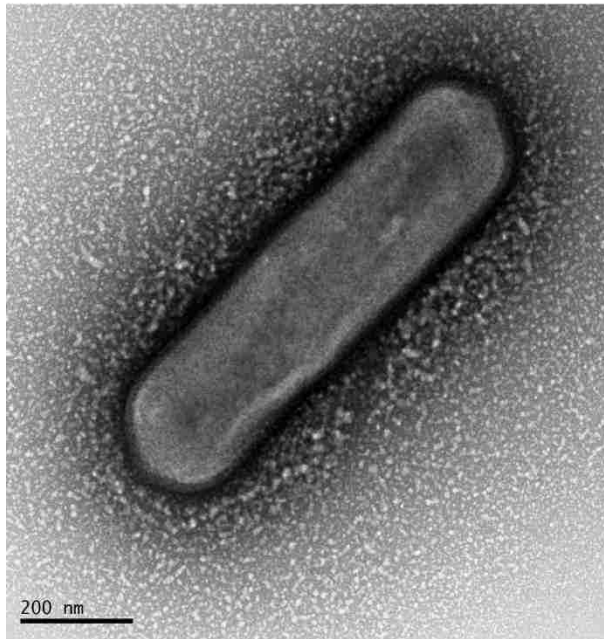


Figure 3.7. Correlation of the growth of strain SCM1 (inset panel) and total cobalamin synthesis.

The individual contributions of Ado-Cbl, Me-Cbl, and OH-Cbl to total cobalamin production are shown by different shaded regions. Error bars represent the SD of triplicates. Error bars smaller than symbols are not shown.

(a)



(b)

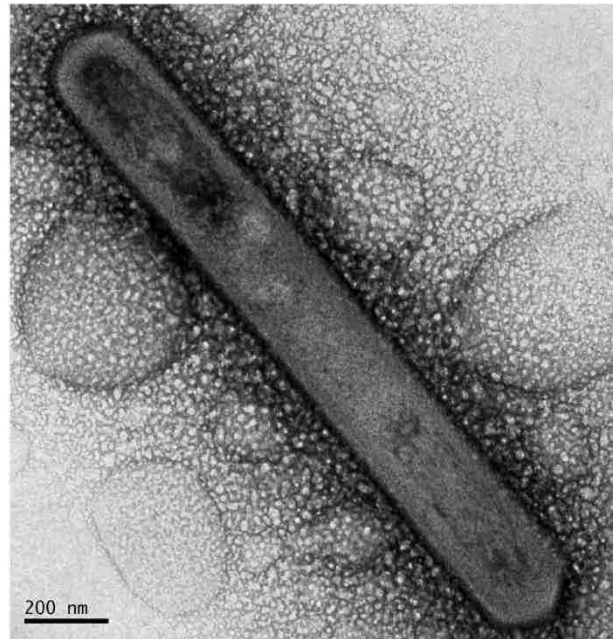


Figure 3.8. Transmission electron micrographs of negative stained strain HCE1 cells in normal shape (a) and elongated shape (b) (Scale bar: 200 nm).

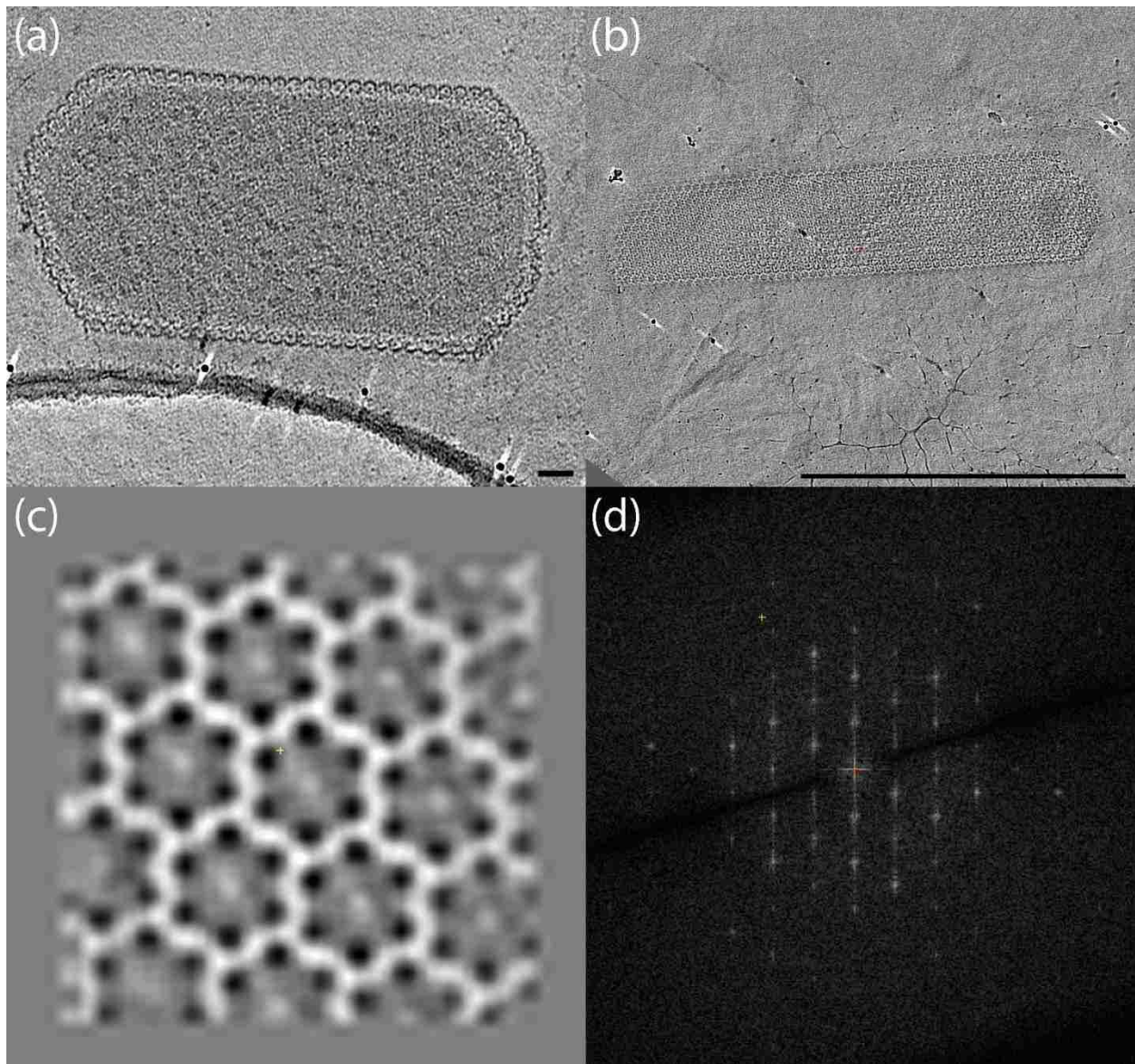


Figure 3.9. S-layer structure of strain SCM1.

(a) Side view of S-layer showing comb-like pattern. (Scale bar: 50 nm) (b) Surface view of S-layer showing honeycomb-like pattern. (Scale bar: 1 μ m) (c) Subtomogram averages of S-layer showing hexagonal subunits in p6-symmetry. (d) Fourier transform of the subtomogram.

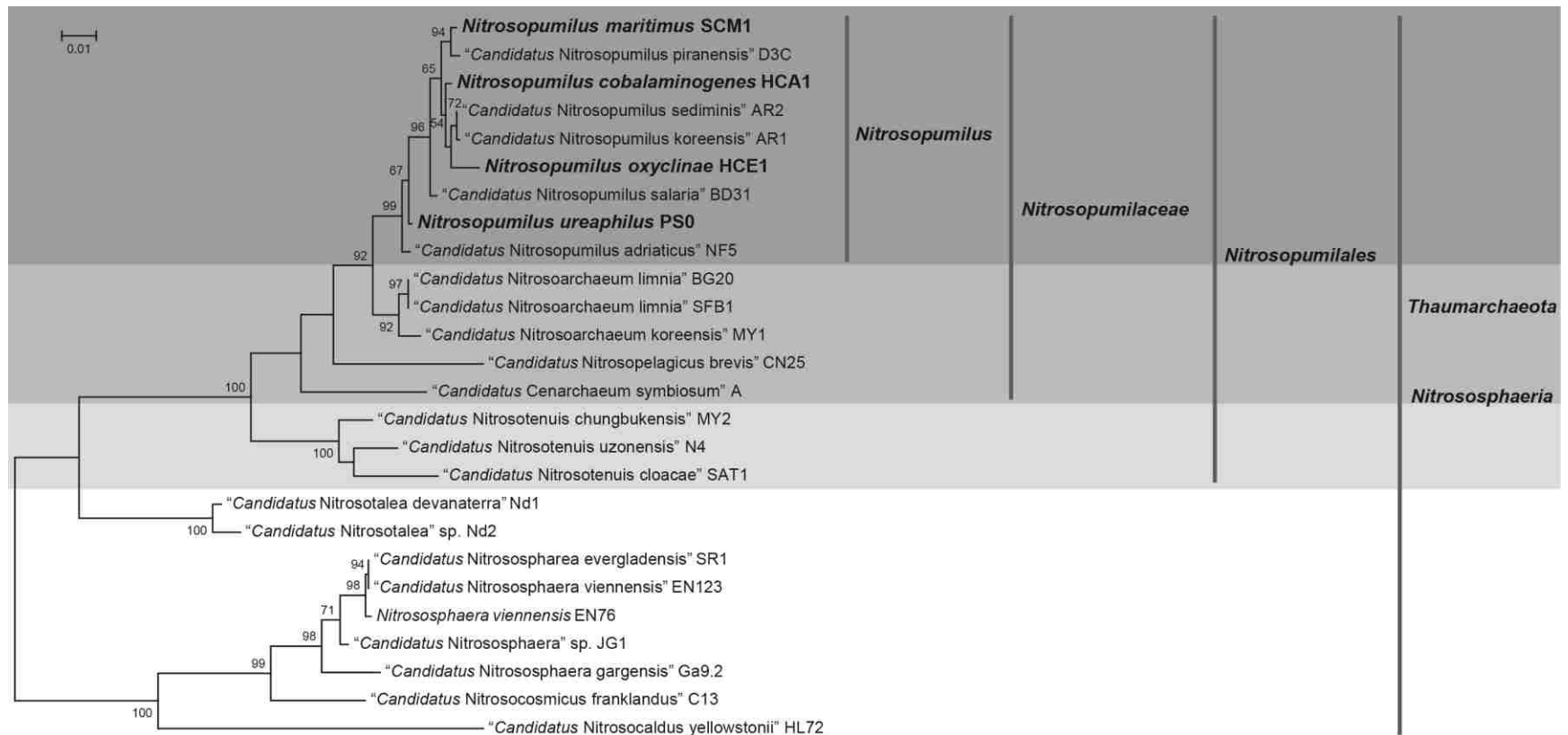


Figure 3.10. Maximum-likelihood tree based on the 16S rRNA sequences showing the phylogenetic relationships of the order *Nitrosopumilales*, the family *Nitrosopumilaceae*, and the genus *Nitrosopumilus*.

Confidence values are on the basis of 500 bootstrap replications. The scale bar represents 1% estimated sequence divergence.



Figure 3.11. Maximum-likelihood phylogenetic tree based on *amoA* gene sequences showing the phylogenetic relationships of *Nitrosopumilus* genus, *Nitrosopumilaceae* family, and *Nitrosopumilales* order.

Confidence values are based on 500 bootstrap replications. Scar bar represents 0.05 fixed mutation per nucleotide position.

Table 3.1. Main characteristics of marine *Thaumarchaeota* strains SCM1, HCA1, HCE1 and PS0^a

Characteristic	SCM1	HCA1	HCE1	PS0
Growth temperature (°C)				
Range	15–35	10–30	4–30	10–30
Optimum	32	25	25	26
Growth pH				
Range	6.8–8.1	6.8–8.1	6.4–7.8	5.9–8.1 ^b
Optimum	7.3	7.3	7.3	6.8
Salinity (‰)				
Range	16–55	15–40	10–40	15–40
Optimum	32–37	32	25–32	25
Maximum cell-specific ammonia oxidation rates (fmol cell ⁻¹ d ⁻¹)	12.7	6.0	5.8	2.9
Ammonium tolerance (mM)	10	10	1	20
Use of urea	–	–	–	+
B-vitamin synthesis				
B ₁ (thiamine)	+	+	+	+
B ₂ (riboflavin)	+	+	+	+
B ₆ (pyridoxin)	+	+	+	+
Ado-B ₁₂ (adenosylcobalamin)	+	+	+	+
Me-B ₁₂ (methylcobalamin)	+	+	+	+
OH-B ₁₂ (hydroxocobalamin)	+	+	+	+
B ₁₂ cell quotas (nmol B ₁₂ per mol carbon) ^c	2800–3500	9300–11600	4200–5300	4700–5900
DNA G+C content (mol%)	34.2	33.0	33.1	33.4

^aSymbols: +, positive; –, negative.

^bStrain PS0 maintained ~80% of the maximum ammonia oxidation activity at pH 5.9 and the effects of lower pH on its growth were not tested in this study.

^cThe data of B₁₂ cell quotas are adapted from Heal et al. (2016).

Supplementary information

Complete 16S rRNA and *amoA* gene sequences of marine AOA species *Nitrosopumilus cobalaminogenes* HCA1, *Nitrosopumilus oxyclinae* HCE1, and *Nitrosopumilus ureaphilus* PS0.

>16S_rRNA_Nitrosopumilus cobalaminogenes strain HCA1 [organism=Archaea Archaea; Thaumarchaeota; Nitrosopumilales; Nitrosopumilaceae] (accession number: KX950757)
 AATCCGGTTGATCCTGCCGGACCTGACTGCTATCGGATTGATACTAAGCCATGCGAG
 TCATTGTAGCAATACAAGGCAGACGGCTCAGTAACGCGTAGTCAACCTAACCTATG
 GACGGGAATAACCTCGGGAACTGAGAATAATGCCCGATAGAACACTATACCTGGA
 ATGGTTTGTGTTCCAAATGATTTATCGCCGTAGGATGGGACTGCGGCCTATCAGTTT
 GTTGGTGAGGTAATGGCCACCAAGACTATTACAGGTACGGGCTCTGAGAGGAGTA
 GCCCGGAGATGGGTACTGAGACACGGACCCAGGCCCTATGGGGCGCAGCAGGCGA
 GAAAACCTTTGCAATGTGCGAAAGCACGACAAGGTTAATCCGAGTGGTTTGTGCTAA
 ACGAACCTTTTGTGCGTCTAGAAACACCGATGAATAAGGGGTGGGCAAGTTCTGGT
 GTCAGCCGCCGCGGTAAAACCAGCACCTCAAGTGGTCAGGATGATTATTGGGCCTA
 AAGCATCCGTAGCCGGCTCTGTAAGTTTTCGGTTAAATCTGTACGCTCAACGTACAG
 GCTGCCGGGAATACTGCAGAGCTAGGGAGTGGGAGAGGTAGACGGTACTCGGTAGG
 AAGGGGTAAAATCCTTTGATCTATTGATGACCACCTGTGGCGAAGGCGGTCTACCAG
 AACACGTCCGACGGTGAGGGATGAAAGCTGGGGGAGCAAACCGGATTAGATACCCG
 GGTAGTCCCAGCTGTAAACTATGCAAACCTCAGTGATGCATTGGCTTGTGGCCAATGC
 AGTGCTGCAGGGAAGCCGTTAAGTTTGCCGCCTGGGAAGTACGTACGCAAGTATGA
 AACTTAAAGGAATTGGCGGGGGAGCACCAAGGGGTGAAGCCTGCGGTTCAATTG
 GAGTCAACGCCAGAAATCTTACCCGGAGAGACAGCAGAATGAAGGTCAAGCTGAAG
 ACTTTACCAGACAAGCTGAGAGGTGGTGCATGGCCGTCGCCAGCTCGTGCCGTGAG
 ATGTCCTGTTAAGTCAGGTAACGAGCGAGATCCCTGCCTCTAGTTGCCACCATTACT
 CTCAGGAGTAGTGGGGCGAATTAGCGGGACCGCCGCAGTTAATGCGGAGGAAGGAA
 GGGGCCACGGCAGGTCAGTATGCCCCGAAACTCTGGGGCCACACGCGGGCTGCAAT
 GGTAACGACAATGGGTTTCAAATCCGAAAGGATGAGGTAATCCTCAAACGTTACCA
 CAGTTATGACTGAGGGCTGCAACTCGCCCTCACGAATATGGAATCCCTAGTAACTGC
 GTGTCATTATCGCGCGGTGAATACGTCCCTGCTCCTTGCACACACCGCCCGTCGTTTC
 ATTGAAGTGAGCTCTTAGCGAGGTGACGTCTGATTGGCGTTATCGAACTTGGGGTTC
 GTGACAAGGGAAAAGTCGTAACAAGGTGACCGTAGGGGAACCTGCGGTTCGGATCAC
 CTCCT

>16S_rRNA_Nitrosopumilus oxyclinae strain HCE1 Archaea Archaea; Thaumarchaeota;
 Nitrosopumilales; Nitrosopumilaceae (accession number: KX950758)
 AATCCGGTTGATCCTGCCGGACCTGACTGCTATCGGATTGATACTAAGCCATGCGAG
 TCATTGTAGCAATACAAGGCATACGGCTCAGTAACGCGTAGTCAACCTAACCTATGG
 ACGAGAATAACCTCGGGAACTGAGAATAATGCTCGATAGAACACTATATCTGGAA
 TGGTTTGTGTTCCAAATGATTTATCGCCGTAGGATGGGACTGCGGCCTATCAGTTTGT
 TGGTGAGGTAATGGCCACCAAGACTATTACAGGTACGGGCTCTGAGAGGAGTAGC
 CCGGAGATGGGTACTGAGACACGGACCCAGGCCCTATGGGGCGCAGCAGGCGAGA
 AAACCTTTGCAATGTGCGAAAGCACGACAAGGTTAATCCGAGTGATTTGTGCTAAAC
 GAATCTTTTGTAGTCTAGAAACACTAACGAATAAGGGGTGGGCAAGTTCTGGTGT
 CAGCCGCCGCGGTAAAACCAGCACCTCAAGTGGTCAGGATGATTATTGGGCCTAAA

GCATCCGTAGCCGGCTCTGTAAGTTTTCGGTTAAATCTGTACGCTTAACGTACAGGC
 TGCCGGGAATACTGCAGAGCTAGGGAGTGGGAGAGGTAGACGGTACTCGGTAGGAA
 GGGGTAAAATCCTTTGATCTATTGATGACCACCTGTGGCGAAGGCGGTCTACCAGAA
 CACGTCCGACGGTGAGGGATGAAAGCTGGGGGAGCAAACCGGATTAGATACCCGGG
 TAGTCCCAGCTGTAAACTATGCAAACCTCAGTGATGCATTGACTTGTGGTCAATGCAG
 TGCTGCAGGGAAGCCGTTAAGTTTGCCGCCTGGGAAGTACGTACGCAAGTATGAAA
 CTAAAGGAATTGGCGGGGGAGCACCACAAGGGGTGAAGCCTGCGGTTCAATTGGA
 GTCAACGCCAGAAATCTTACCCGGAGAGACAGCAGAATGAAGGTCAAGCTGAAGAC
 TTTACCAGACAAGCTGAGAGGTGGTGCATGGCCGTCGCCAGCTCGTGCCGTGAGAT
 GTCCTGTTAAGTCAGGTAACGAGCGAGATCCCTGCCTCTAGTTGCCACCATTACTCT
 CAGGAGTAGTGGGGCGAATTAGCGGGACCGCCGCAGTTAATGCGGAGGAAGGAAG
 GGGCCACGGCAGGTCAGTATGCCCCGAAACTCTGGGGCCACACGCGGGGCTGCAATG
 GTAACGACAATGGGTTTCAAATCCGAAAGGATGAGGTAATCCTCAAACGTTACCAC
 AGTTATGACTGAGGGCTGCAACTCGCCCTCACGAATATGGAATCCCTAGTAAATGCG
 TGTCATTATCGCGCGTTGAATACGTCCCTGCTCCTTGCACACACCGCCCGTCGTTTCA
 TTGAAGTGAGCTCTTAGCGAGGTGACGTCTGATTGGCGTTATCGAACTTGGGGTTTCG
 TGACAAGGGAAAAGTCGTAACAAGGTGACCGTAGGGGAACCTGCGGTCGGATCACC
 TCCT

>16S_rRNA_Nitrosopumilus ureaphilus strain PS0 Archaea Archaea; Thaumarchaeota;
 Nitrosopumilales; Nitrosopumilaceae (accession number: KX950759)

AATCCGGTTGATCCTGCCGGACCTGACTGCTATCGGATTGATACTAAGCCATGCGAG
 TCATTGTAGCAATACAAGGCAGACGGCTCAGTAACGCGTAGTCAACCTACCCTATGG
 ACGGGAATAACCTCGGGAAACTGAGAATAATGCCCCGATAGAACATTATGCCTGGAA
 TGGTTTATGTTTCAAATGATTTATCGCCGTAGGATGGGACTGCGGCCTATCAGTTTGT
 TGGTGAGGTAATGGCCCACCAAGACTATTACAGGTACGGGCTCTGAGAGGAGTAGC
 CCGGAGATGGGTACTGAGACACGGACCCAGGCCCTATGGGGCGCAGCAGGCGAGA
 AAACCTTTGCAATGTGCGAAAGCACGACAAGGTTAATCCGAGTGGTTTCTGCTAAAG
 GAACCTTTTGTGAGTCCCTAGAAACACTGATGAATAAGGGGTGGGCAAGTTCTGGTGT
 CAGCCGCCGCGGTAAAACCAGCACCTCAAGTGGTCAGGATGATTATTGGGCCTAAA
 GCATCCGTAGCCGGCTCTATAAGTTTTCGGTTAAATCTGTACGCTCAACGTACAGGC
 TGCCGGGAATACTGCAGAGCTAGGGAGTGGGAGAGGTAGACGGTACTCGGTAGGAA
 GGGGTAAAATCCTTTGATCTATTGATGACCACCTGTGGCGAAGGCGGTCTACCAGAA
 CACGTCCGACGGTGAGGGATGAAAGCTGGGGGAGCAAACCGGATTAGATACCCGGG
 TAGTCCCAGCTGTAAACTATGCAAACCTCAGTGATGCATTGGCTTGTGGCCAATGCAG
 TGCTGCAGGGAAGCCGTTAAGTTTGCCGCCTGGGAAGTACGTACGCAAGTATGAAA
 CTAAAGGAATTGGCGGGGGAGCACCACAAGGGGTGAAGCCTGCGGTTCAATTGGA
 GTCAACGCCAGAAATCTTACCCGGAGAGACAGCAGAATGAAGGTCAAGCTGAAGAC
 TTTACCAGACAAGCTGAGAGGTGGTGCATGGCCGTCGCCAGCTCGTGCCGTGAGAT
 GTCCTGTTAAGTCAGGTAACGAGCGAGATCCCTGCCTCTAGTTGCCACCATTACTCT
 CAGGAGTAGTGGGGCGAATTAGCGGGACCGCCGCAGTTAATGCGGAGGAAGGAAG
 GGGCCACGGCAGGTCAGTATGCCCCGAAACTCTGGGGCCACACGCGGGGCTGCAATG
 GTAATGACAATGGGTTTCAAATCCGAAAGGAGGAGGTAATCCCCAACATTACCAC
 AGTTATGACTGAGGGCTGCAACTCGCCCTCACGAATATGGAATCCCTAGTAACTGCG
 TGTCATTATCGCGCGGTGAATACGTCCCTGCTCCTTGCACACACCGCCCGTCGTTTCA
 TTGAAGTGAGCTTTTAGCGAGGTGACGTCTGATTGGCGTTATCGAACTTGAAGTTTCG

TGACAAGGGAAAAGTCGTAACAAGGTGACCGTAGGGGAACCTGCGGTCGGATCACC
TCCT

>amoA_Nitrosopumilus cobalaminogenes strain HCA1 [organism=Archaea Archaea;
Thaumarchaeota; Nitrosopumilales; Nitrosopumilaceae] (accession number: KX950754)
ATGGTCTGGTTAAGACGATGTACACACTACTTATTCATAGTAGTGTGCAGTTAAC
TCAACACTGTAAACAATTAATGCAGGAGACTACATCTTCTACACTGACTGGGCTTGG
ACTTCGTACACGGTATTCTCAATATCGCAAACGTTGATGCTAATTGTAGGTGCTACA
TACTATCTTACATTTACAGGCGTTCCAGGCACAGCAACGTACTACGCTCTAATTATG
ACGGTATACACATGGGTAGCAAAAGGCGCATGGTTCGCACTTGGTTATCCATATGAC
TTCATTGTAACCTCAGTTTGGCTACCTTCAGCAATGCTGTTGGACTTGGTTTACTGGG
CAACAAAGAAGAACAAGCACAGCTTGATACTGTTTCGGCGGCGTACTAGTAGGAATG
TCATTACCATTGTTCAACATGGTAAACCTGATAACAGTAGCAGACCCACTAGAAACG
GCATTCAAATATCCAAGACCAACATTGCCACCATATATGACACCAATCGAACCGCA
AGTAGGTAAATTCTATAACAGCCCAGTTGCTCTCGGTGCAGGTGCAGGTGCAGTATT
GGCATGTACATTTGCAGCTTTAGGTTGTAAATTGAACACTTGGACATACAGATGGAT
GGCCGCTTGGTCAAAGTGGGACTAA

>amoA_Nitrosopumilus oxycliniae strain HCE1 Archaea Archaea; Thaumarchaeota;
Nitrosopumilales; Nitrosopumilaceae (accession number: KX950755)
ATGGTCTGGTTAAGACGATGTACACACTACTTATTCATAGTAGTGTGCAGTTAAC
TCAACACTGTAAACAATTAATGCAGGAGACTACATCTTCTACACTGACTGGGCTTGG
ACTTCGTACACGGTATTTCAATATCGCAAACGTTGATGCTTATTGTAGGTGCTACAT
ACTATCTTACATTTACAGGCGTTCCAGGCACAGCAACGTACTACGCTCTAATTATGA
CAGTATACACATGGATTGCAAAAGGTGCATGGTTTGCCTCGGATATCCATATGACT
TCATTGTAACCTCAGTTTGGCTACCTTCAGCAATGCTGTTGGATTTGGTTTACTGGGC
AACAAAGAAGAACAAGCACTCCTTGATACTGTTTGGCGGCGTACTGGTAGGAATGT
CATTACCATTGTTCAACATGGTAAACCTGATAACAGTAGCAGACCCACTAGAAACG
GCATTCAAATATCCAAGACCAACATTGCCACCATATATGACACCAATCGAACCGCA
AGTCGGCAAATTCTATAACAGCCCAGTTGCTCTCGGTGCAGGTGCAGGTGCAGTATT
GGCATGTACATTTGCAGCTTTAGGTTGTAAATTGAACACTTGGACATACAGATGGAT
GGCCGCTTGGTCAAAGTGGGACTAA

>amoA_Nitrosopumilus ureaphilus strain PS0 Archaea Archaea; Thaumarchaeota;
Nitrosopumilales; Nitrosopumilaceae (accession number: KX950756)
ATGGTCTGGTTAAGACGATGTACACACTACTTATTCATAGTAGTGTGCAGTTAAC
TCAACACTGTAAACAATTAATGCAGGAGACTACATCTTCTACACTGACTGGGCTTGG
ACTTCGTACACGGTATTTCAATATCGCAAACGTTGATGCTAATTGTGGGTGCAACA
TATTACCTAACATTTACAGGCGTTCCAGGCACAGCAACGTACTACGCTCTAATTATG
ACAGTATACACATGGGTAGCAAAAGCCGCATGGTTTTTCGCTAGGATATCCATATGAC
TTCATTGTAGTTCCAGTTTGGTTACCATCAGCAATGCTGTTGGACTTGGTATACTGGG
CAACAAAGAAGAACAAGCACTCCTTGATACTGTTTGGCGGCGTACTGGTAGGAATG
TCATTACCATTATTCAATATGGTAAACCTGATAACAGTTGCAGACCCACTAGAAACG
GCATTCAAATATCCAAGACCAACATTGCCACCATATGACACCAATAGAACCTCA
AGTTGGAAAGTTCTATAACAGCCCAGTTGGCTTTAGGTTGCAGGTGCGGGTGCAGTATT

GGCATGTACTTTTGCAGCATTAGGTTGCAAACCTGAACACTTGGACATACAGATGGAT
GGCCGCTTGGTCAAAGTGGGACTAA

Chapter 4.

Influence of oxygen availability on the activities of ammonia-oxidizing archaea

Wei Qin^a, Kelley A. Meinhardt^a, James W. Moffett^b, Allan H. Devol^c, E. Virginia Armbrust^c,
Anitra E. Ingalls^c, and David A. Stahl^{a,1}

Submitted to *Environmental Microbiology Reports*
(Minor revision)

^aDepartment of Civil and Environmental Engineering, University of Washington, Seattle, WA 98195; ^bDepartments of Biological Sciences and Earth Sciences and Civil and Environmental Engineering, University of Southern California, Los Angeles, CA, 90089; ^cSchool of Oceanography, University of Washington, Seattle, WA 98195

¹Corresponding author E-mail: dastahl@u.washington.edu.

Abstract

Recent studies point to the importance of oxygen (O_2) in controlling the distribution and activity of marine ammonia-oxidizing archaea (AOA), one of the most abundant prokaryotes in the ocean. The AOA are associated with regions of low O_2 tension in oceanic oxygen minimum zones (OMZs), and O_2 availability is suggested to influence their production of the ozone-depleting greenhouse gas nitrous oxide (N_2O). We show that marine AOA available in pure culture sustain high ammonia oxidation activity at low μM O_2 concentrations characteristic of suboxic regions of OMZs ($<10 \mu M O_2$) and that atmospheric concentrations of O_2 may inhibit the growth of some environmental populations. We quantify the increasing N_2O production by marine AOA with decreasing O_2 tensions, consistent with the plausibility of an AOA contribution to the accumulation of N_2O at the oxic-anoxic redox boundaries of OMZs. Variable sensitivity to peroxide also suggests that endogenous or exogenous reactive oxygen species are of importance in determining the environmental distribution of some populations.

Introduction

Nitrous oxide (N_2O) is a significant greenhouse gas with a global warming potential 297 times higher than that of carbon dioxide (IPCC, 2007) and is predicted to be the dominant ozone-depleting substance throughout the 21st century (Ravishankara et al., 2009). Contributing to both stratospheric ozone destruction and global warming, its atmospheric concentration has risen steadily at a rate of $\sim 0.25\%$ per year over past decades, and this trend is predicted to continue (Wuebbles, 2009). Marine biological N_2O emissions account for nearly one-third of the total N_2O natural inputs, and significant sources are the hypoxic boundaries of oxygen minimum zones (OMZs) (Yoshinari, 1976; Cohen and Gordon, 1978; Nevison et al., 2003). The marine

ammonia-oxidizing archaea (AOA) (assigned to the archaeal phylum *Thaumarchaeota*) are one of the most active and abundant of planktonic populations in OMZ hypoxic boundary regions (Ulloa et al., 2012; Bristow et al., 2016; Peng et al., 2016). Comprising up to 40% of marine microbiota, these archaea are generally recognized to exert primary control of oceanic nitrification (Martens-Habbena et al., 2009b; Horak et al., 2013; Newell et al., 2013; Martens-Habbena et al., 2015), appear adapted to high and low oxygen (O₂) marine environments, and are associated with the greater part of oceanic N₂O emissions (Santoro et al., 2011; Löscher et al., 2012; Peng et al., 2016).

Available environmental and culture-based data point to a high affinity of the AOA for O₂ (Martens-Habbena et al., 2009b; Park et al., 2010; Qin et al., 2015d; Bristow et al., 2016; Peng et al., 2016). Those in culture exhibit variable sensitivity to reactive oxygen species (ROS) generated under standard laboratory conditions of atmospheric O₂ (Kim et al., 2016). Although O₂ is also recognized as a factor influencing N₂O production by AOA in culture, and thus may also be of environmental significance (Jung et al., 2011a; Löscher et al., 2012; Mosier et al., 2012a), laboratory studies have been inconsistent. Löscher and associates (2012) reported significant elevation of N₂O production by the marine AOA isolate *Nitrosopumilus maritimus* SCM1 with decreasing O₂ concentrations (Löscher et al., 2012). In contrast, Stieglmeier et al. (2014) reported little variation in N₂O production with varying O₂ concentration for both *N. maritimus* and the terrestrial isolate *Nitrososphaera viennensis* EN76 (Stieglmeier et al., 2014a). In consideration of those data, the objectives of this study were twofold: to quantify O₂ affinity for two available marine isolates (strains SCM1 and PS0) in relationship to N₂O production and to evaluate significance of ROS in governing growth kinetics at the higher O₂ concentrations

typical of laboratory studies. To achieve this, we monitored the growth and N₂O production of strains SCM1 and PS0 across a wide range of O₂ levels (0.1% – 21% O₂). Our results demonstrate a high adaptive capacity of marine AOA for growth under both high and low O₂ concentrations and a significant influence of reduced O₂ concentrations on N₂O production.

Results and Discussion

Effect of O₂ concentration on the growth of marine AOA. To determine the influence of O₂-deficient conditions on AOA growth rates and yields, we monitored the growth of marine AOA isolates SCM1 and PS0 at various headspace O₂ concentrations, between 0.1% (~1 μM dissolved O₂) and 21% O₂ (197–209 μM dissolved O₂). The initial cell densities of SCM1 ($2.8 \times 10^5 \pm 7.8 \times 10^3$ cells ml⁻¹) and PS0 ($2.7 \times 10^5 \pm 2.7 \times 10^4$ cells ml⁻¹) cultures were comparable to AOA cell abundance observed in the ocean (~10⁵ cell ml⁻¹) (Table 1). The ammonia (10 μmol) was completely oxidized to nitrite in cultures with 0.5% to 21% initial headspace O₂ (29.8–1252.7 μmol O₂), achieving comparable cell densities for SCM1 (6.3×10^6 to 7.9×10^6 cells ml⁻¹) and PS0 (6.7×10^6 to 7.0×10^6 cells ml⁻¹) at these concentrations (Table 1). In contrast, there was insufficient O₂ at the 0.1% (6.0 μmol) and 0.2% (11.9 μmol) additions to oxidize all ammonia (Table 1). These cultures consumed all available O₂ in near stoichiometric relation to nitrite production (~5.1 and ~8.2 μmol nitrite for 0.1% and 0.2% O₂, respectively; 1.34 ± 0.16 mole of O₂/mole of NO₂⁻, n=6) (Table 1). The final cell densities of SCM1 cultures at 0.1% O₂ and PS0 cultures at 0.2% O₂ were 4.0×10^6 cells ml⁻¹ and 6.7×10^6 cells ml⁻¹, respectively (Table 1). Growth with increasing O₂ limitation followed Monod-type kinetics (Fig. 4.1). The maximum specific growth rate of PS0 was observed at ambient conditions (21% O₂). In contrast, strain SCM1 had significantly higher growth rates at lower O₂ concentrations (5% and 10% O₂) as compared with those at 21% O₂ ($p < 0.05$, n=5). The best-fit K_s values for growth of SCM1 and

PS0 were $3.41 \mu\text{M O}_2$ (s.d. 0.013, n=5) and $1.18 \mu\text{M O}_2$ (s.d. 0.015, n=3), respectively (Fig. 4.1). Considering these values are based on assumed equilibration between headspace and dissolved O_2 concentrations, the estimated K_s value of SCM1 is comparable but somewhat lower than that previously determined using microrespirometry (K_m for O_2 uptake of $3.91 \mu\text{M}$) (Martens-Habbena et al., 2009b). The K_s of PS0 was similar to the value reported ($2.01 \mu\text{M}$) for a marine sedimentary AOA enrichment, strain AR1 (Park et al., 2010). Neither isolate grew in the absence of O_2 (no ammonia consumption or nitrite production).

Inhibition by reactive oxygen species. In consideration of the recent report by Kim et al. (2016) of a role of hydrogen peroxide (H_2O_2) scavengers in sustaining the growth of AOA in culture, we reevaluated our previous interpretation that α -ketoglutarate supported growth of marine AOA isolates by providing an essential source of carbon (Qin et al., 2014). Our results confirm those of Kim et al. 2016: less than 1% of added pyruvate labeled in the C2 position was incorporated into the cellular material of strain SCM1 ($0.35 \pm 0.08\%$, n=7) (for details, see Supporting Information), and the growth requirement of strains HCA1 and PS0 for α -keto acids could be alleviated by the addition of H_2O_2 scavengers (10 units ml^{-1} catalase or $100 \mu\text{M}$ dimethylthiourea) to the growth medium (Fig. 4.2 and 4.3). However, strain HCA1 incubated in organic carbon and peroxide scavenger-free medium had some capacity to recover growth following extended laboratory incubation (Fig. 4.2). In addition, strain SCM1 was able to oxidize all added ammonia in the absence of organic carbon and peroxide scavenger supplements (Qin et al., 2014). Its ammonia oxidation activity was insensitive to environmental levels of H_2O_2 (in submicromolar range) (Fig. 4.4) (Herut et al., 1998; Yuan and Shiller, 2004, 2005). While short-term inhibition was found at $5 \mu\text{M H}_2\text{O}_2$, SCM1 cultures began to recover within 24

hours and were able to convert all ammonia to nitrite (Fig. 4.4). Ammonia oxidation by SCM1 was completely inhibited only at 10 μM and higher concentrations of H_2O_2 (Fig. 4.4 and 4.5). Thus, these findings suggest that, as yet, there is insufficient information to assess the possible environmental significance of ROS in controlling the distribution and activity of AOA.

Effect of O_2 concentration on N_2O production by marine AOA. N_2O production measured in pure cultures of strains SCM1 and PS0 was inversely correlated with O_2 concentration (Table 1). The N_2O yield normalized to nitrite production ($\text{N}_2\text{O}/\text{NO}_2^-$) of SCM1 increased from 0.011% to 0.074% with decreasing O_2 from 21% to 0.1% (Table 1). Likewise, the highest N_2O yield for PS0 was observed at 0.2% O_2 (0.059%) and the lowest yield at 21% O_2 (0.010%) (Table 1). The per-cell N_2O production at the lowest O_2 treatments was 9.6 $\text{amol N}_2\text{O cell}^{-1}$ for SCM1 (0.1% O_2) and 7.3 $\text{amol N}_2\text{O cell}^{-1}$ for PS0 (0.2% O_2), about 7 and 5 times the production at 21% O_2 for SCM1 (1.3 $\text{amol N}_2\text{O cell}^{-1}$) and PS0 (1.5 $\text{amol N}_2\text{O cell}^{-1}$), respectively (Table 1). At ambient O_2 concentrations ($\sim 21\%$ O_2), N_2O yields ($\text{N}_2\text{O}/\text{NO}_2^-$) for strains SCM1 and PS0 were of the same order of magnitude as previously reported for representatives of Group I.1 a and I.1 b AOA (Santoro et al., 2011; Kim et al., 2012b; Löscher et al., 2012; Jung et al., 2014b; Stieglmeier et al., 2014a), but more than two orders of magnitude lower than the yield measured for a terrestrial acidophilic AOA affiliated to I.1 a-associated group, strain CS (4.28%) (Jung et al., 2014b). No significant difference was observed in the N_2O yield from SCM1 cultures grown with 100 μM α -ketoglutarate compared with that of cultures without organic carbon supplements (Fig. 4.6).

These physiological properties are consistent with the results of several environmental studies.

The Marine Group I archaea have been shown to be abundant and active within the oxygenated

and productive lower euphotic zone, potentially competing with phytoplankton for reduced forms of nitrogen and largely contributing to endogenously-generated nitrite (and subsequently nitrate) to sustain primary production in marine surface waters (Yool et al., 2007; Martens-Habbenha et al., 2009b; Beman et al., 2012a; Horak et al., 2013; Newell et al., 2013; Smith et al., 2014). In addition to predominating in oxygenated oceanic regions, tracer, metatranscriptomic, and metaproteomic studies indicate that marine AOA are abundant in low-O₂ environments, such as the suboxic zones of OMZs and surficial sediments (Francis et al., 2005; Sahan and Muyzer, 2008; Lam et al., 2009; Kalvelage et al., 2011; Beman et al., 2012b; Stewart et al., 2012; Hawley et al., 2014). Notably, Stewart et al. 2012 reported that transcripts encoding the thaumarchaeotal ammonium transporter (Amt) constituted more than 10% of all reads in samples collected from the OMZ upper boundary of the Eastern Tropical South Pacific (~10 μM O₂), consistent with a high affinity for O₂ (Stewart et al., 2012). Indeed, a recent study of the O₂ uptake kinetics of ammonia oxidation in OMZ waters revealed extremely low K_m values of 333 ± 130 nM O₂ (Bristow et al., 2016). The low K_s value for O₂ of strain PS0 (~1 μM or lower) clearly demonstrates the capacity of AOA to perform ammonia oxidation at extremely low O₂ concentrations. Additionally, strain SCM1 grew best under reduced O₂ concentrations of 5% and 10% in the headspace (compared to 21% O₂), suggesting a preference for low-O₂ environments.

Previously reported relationships between N₂O production and O₂ concentrations for strain SCM1 have been inconsistent (Löscher et al., 2012; Stieglmeier et al., 2014a). Löscher et al. (2012) reported an increase in the N₂O yield of SCM1 as initial O₂ concentration decreased from 287 μM (atmospheric condition) to 112 μM (~10% headspace O₂) (Löscher et al., 2012). A

similar relationship between decreasing O₂ and increasing N₂O was also observed for other members of the Group I.1a AOA enriched from agricultural soil and low-salinity estuary sediment (Jung et al., 2011a; Mosier et al., 2012a). On the other hand, a more recent study by Stieglmeier et al. (2014) reported 5-fold higher yield of N₂O (0.050%) by strain SCM1 at atmospheric conditions than those measured here (0.009%) and no dependence on O₂ concentrations between 218 μM and 20 μM (comparable to the 21% to 2% headspace O₂ concentrations evaluated in this study) (Stieglmeier et al., 2014a). The reported increased production of N₂O at atmospheric conditions cannot be attributed to the inclusion of 100 μM oxaloacetate in their growth medium, since in the present study we were unable to observe any change in N₂O yield with inclusion of the same concentration of α-keto acids. Although we have no explanation for the disparity, the present study supports the potential for archaeal ammonia oxidation to be a significant source of N₂O in the suboxic regions of the OMZs and is consistent with molecular data showing the high abundance of AOA transcripts and proteins in low-O₂ marine environments (Kalvelage et al., 2011; Stewart et al., 2012; Hawley et al., 2014; Peng et al., 2016). This is also supported by a previous study using a transient time distribution approach to estimate the global subsurface production of oceanic N₂O, attributing 93% of production to nitrification (Freing et al., 2012).

Hydroxylamine dehydrogenase (HAO) and nitric oxide reductase (NOR) play key roles in N₂O formation by AOB (Hooper and Terry, 1979; Stein, 2011b; Kozłowski et al., 2014). No homologs of these two enzymes have been identified in the complete genome sequences of any *Thaumarchaeota* (Hallam et al., 2006; Walker et al., 2010; Kim et al., 2011; Spang et al., 2012). Recently, an ¹⁵N tracer experiment with *N. viennensis* showed a nearly equal contribution of N

atoms from ammonia and nitrite to N_2O production, suggesting a different mechanism of N_2O formation by AOA through an abiotic N-nitrosation reaction between electrophilic nitric oxide and nucleophilic hydroxylamine (NH_2OH) (Stieglmeier et al., 2014a). Both have been detected during ammonia oxidation by SCM1 (Vajrala et al., 2013; Martens-Habbena et al., 2015). It is likely that as O_2 becomes limiting, the accumulation of pathway intermediates such as these promote the formation of N_2O . Another mechanism for N_2O formation of significance to terrestrial acidophilic AOA is the formation of the nitrosonium cation (NO^+) from nitrous acid ($HONO$). Formation of NO^+ is favored at low pH and could contribute to abiotic hybrid N_2O formation via electrophilic N-nitrosation of NH_2OH (Spott et al., 2011). This may be an important source of N_2O in some terrestrial systems (Martikainen and Deboer, 1993; Mørkved et al., 2007) and could account for the reported two orders of magnitude higher of N_2O yield (N_2O/NO_2^-) from an acidophilic AOA strain (Jung et al., 2014a) compared to the AOA isolates characterized in this study .

In summary, our experiments clearly showed that low O_2 levels ($<10 \mu M O_2$) in suboxic regions of OMZs would be sufficient to support the growth of strains SCM1 and PS0. These data better quantify the relationship between N_2O production and O_2 concentration and should help constrain estimates of the contribution by AOA to oceanic N_2O production. Our studies also confirm a sensitivity of some AOA isolates to ROS and indicate the need for further studies to better constrain the environmental significance of this sensitivity. However, as yet, the characterization of AOA in culture has not informed environmental data indicating that a significant fraction of cellular carbon is derived from organic carbon (Ingalls et al., 2006). Finally, these data also suggest that the predicted increases in ocean deoxygenation associated

with climate change may intensify N₂O production from archaeal ammonia oxidation and that low-O₂-adapted marine AOA ecotypes will likely become of increasing global importance (Freing et al., 2012; Capone and Hutchins, 2013).

SI Materials and Methods

¹⁴C labeling experiment. The incorporation of pyruvate by *N. maritimus* SCM1 was investigated by measuring the ¹⁴C content in the biomass and medium fractions of cultures grown with [2-¹⁴C]-labeled pyruvate. In seven replicates, 5 ml of Synthetic Crenarchaeota Medium was inoculated with late exponential-phase SCM1 culture and 100 μM pyruvate (containing 5% pyruvic acid, sodium salt [2-¹⁴C] (specific activity 9.12 μCi μmol⁻¹, PerkinElmer, Waltham, MA)). Triplicate unlabeled, inoculated (growth) and labeled, uninoculated (¹⁴C addition) controls were also included. After incubating 7 d in the dark at 30°C, a small volume of each culture was removed for a nitrite assay. The remainder was filtered through a 0.22 μm GTTP Isopore polycarbonate filter (EMD Millipore, Darmstadt, Germany) to collect cell biomass. Filters were washed with 5 mL MilliQ water. The filters and 50–200 μl of filtrate medium were added to separate glass scintillation vials with 10 ml Ultima Gold scintillation liquid (PerkinElmer) and agitated to mix. Label incorporation was determined using a PerkinElmer Tri-Carb 2800TR liquid scintillation counter with QuantSmart v2.03 software. After ¹⁴C background and counting efficiency determination (95.8%), samples were counted for 2 min with a 0.5 min pre-count delay and automatic tSIE quench correction. The total cell carbon content was estimated based on the cell counts and a factor of 9.2 fg of organic carbon per SCM1 cell (Papoutsakis, 1984; Martens-Habbena et al., 2009b; Urakawa, 2011).

Acknowledgements

We thank Julia Kobelt and Manmeet Pannu for technical assistance. This study was funded by National Science Foundation Grants MCB-0604448 and Dimensions of Biodiversity Program OCE-1046017. The authors declare that they have no conflict interests.

References

- Beman, J.M., Popp, B.N., and Alford, S.E. (2012a) Quantification of ammonia oxidation rates and ammonia-oxidizing archaea and bacteria at high resolution in the Gulf of California and eastern tropical North Pacific Ocean. *Limnol Oceanogr* **57**: 711-726.
- Beman, J.M., Bertics, V.J., Braunschweiler, T., and Wilson, J.M. (2012b) Quantification of ammonia oxidation rates and the distribution of ammonia-oxidizing Archaea and Bacteria in marine sediment depth profiles from Catalina Island, California. *Front Microbiol* **3**.
- Bristow, L.A., Dalsgaard, T., Tiano, L., Mills, D.B., Bertagnolli, A.D., Wright, J.J. et al. (2016) Ammonium and nitrite oxidation at nanomolar oxygen concentrations in oxygen minimum zone waters. *Proceedings of the National Academy of Sciences* **113**: 10601-10606.
- Capone, D.G., and Hutchins, D.A. (2013) Microbial biogeochemistry of coastal upwelling regimes in a changing ocean. *Nat Geosci* **6**: 711-717.
- Cohen, Y., and Gordon, L.I. (1978) Nitrous oxide in the oxygen minimum of the eastern tropical North Pacific: evidence for its consumption during denitrification and possible mechanisms for its production. *Deep-Sea Res* **25**: 509-524.
- Francis, C.A., Roberts, K.J., Beman, J.M., Santoro, A.E., and Oakley, B.B. (2005) Ubiquity and diversity of ammonia-oxidizing archaea in water columns and sediments of the ocean. *P Natl Acad Sci USA* **102**: 14683-14688.
- Freing, A., Wallace, D.W.R., and Bange, H.W. (2012) Global oceanic production of nitrous oxide. *Phil Trans R Soc B-Biological Sciences* **367**: 1245-1255.
- Hallam, S.J., Konstantinidis, K.T., Putnam, N., Schleper, C., Watanabe, Y., Sugahara, J. et al. (2006) Genomic analysis of the uncultivated marine crenarchaeote *Cenarchaeum symbiosum*. *Proc Natl Acad Sci USA* **103**: 18296-18301.
- Hawley, A.K., Brewer, H.M., Norbeck, A.D., Pasa-Tolic, L., and Hallam, S.J. (2014) Metaproteomics reveals differential modes of metabolic coupling among ubiquitous oxygen minimum zone microbes. *P Natl Acad Sci USA* **111**: 11395-11400.
- Herut, B., Shoham-Frider, E., Kress, N., Fiedler, U., and Angel, D.L. (1998) Hydrogen peroxide production rates in clean and polluted coastal marine waters of the Mediterranean, Red and Baltic Seas. *Marine Poll Bull* **36**: 994-1003.
- Hooper, A.B., and Terry, K.R. (1979) Hydroxylamine oxidoreductase of *Nitrosomonas* production of nitric-oxide from hydroxylamine. *Biochim Biophys Acta* **571**: 12-20.
- Horak, R.E.A., Qin, W., Schauer, A.J., Armbrust, E.V., Ingalls, A.E., Moffett, J.W. et al. (2013) Ammonia oxidation kinetics and temperature sensitivity of a natural marine community dominated by Archaea. *Isme J* **7**: 2023-2033.

- Ingalls, A.E., Shah, S.R., Hansman, R.L., Aluwihare, L.I., Santos, G.M., Druffel, E.R.M., and Pearson, A. (2006) Quantifying archaeal community autotrophy in the mesopelagic ocean using natural radiocarbon. *Proc Natl Acad Sci USA* **103**: 6442-6447.
- IPCC (2007) Contribution of Working Group I to the Fourth Assessment Report of the Intergovernmental Panel on Climate Change. In *Climate change 2007: the physical science basis*. Cambridge: Cambridge University Press.
- Jung, M.Y., Park, S.J., Kim, S.J., Kim, J.G., Damsté, J.S.S., Jeon, C.O., and Rhee, S.K. (2014a) A mesophilic, autotrophic, ammonia-oxidizing archaeon of thaumarchaeal group I.1a cultivated from a deep oligotrophic soil horizon. *Appl Environ Microb* **80**: 3645-3655.
- Jung, M.Y., Well, R., Min, D., Giesemann, A., Park, S.J., Kim, J.G. et al. (2014b) Isotopic signatures of N₂O produced by ammonia-oxidizing archaea from soils. *ISME J* **8**: 1115-1125.
- Jung, M.Y., Park, S.J., Min, D., Kim, J.S., Rijpstra, W.I.C., Damsté, J.S.S. et al. (2011a) Enrichment and characterization of an autotrophic ammonia-oxidizing archaeon of mesophilic crenarchaeal group I.1a from an agricultural soil. *Appl Environ Microb* **77**: 8635-8647.
- Kalvelage, T., Jensen, M.M., Contreras, S., Revsbech, N.P., Lam, P., Günter, M. et al. (2011) Oxygen sensitivity of anammox and coupled N-cycle processes in oxygen minimum zones. *PLoS ONE* **6**.
- Kim, B.K., Jung, M.Y., Yu, D.S., Park, S.J., Oh, T.K., Rhee, S.K., and Kim, J.F. (2011) Genome Sequence of an Ammonia-Oxidizing Soil Archaeon, "*Candidatus Nitrosoarchaeum koreensis*" MY1. *J Bacteriol* **193**: 5539-5540.
- Kim, J.G., Jung, M.Y., Park, S.J., Rijpstra, W.I.C., Damsté, J.S.S., Madsen, E.L. et al. (2012b) Cultivation of a highly enriched ammonia-oxidizing archaeon of thaumarchaeotal group I.1b from an agricultural soil. *Environ Microbiol* **14**: 1528-1543.
- Kim, J.G., Park, S.J., Damsté, J.S.S., Schouten, S., Rijpstra, W.I.C., Jung, M.Y. et al. (2016) Hydrogen peroxide detoxification is a key mechanism for growth of ammonia-oxidizing archaea. *P Natl Acad Sci USA* **113**: 7888-7893.
- Kozłowski, J.A., Price, J., and Stein, L.Y. (2014) Revision of N₂O-producing pathways in the ammonia-oxidizing bacterium *Nitrosomonas europaea* ATCC 19718. *Appl Environ Microbiol* **80**: 4930-4935.
- Lam, P., Lavik, G., Jensen, M.M., van de Vossenberg, J., Schmid, M., Woebken, D. et al. (2009) Revising the nitrogen cycle in the Peruvian oxygen minimum zone. *Proc Natl Acad Sci USA* **106**: 4752-4757.
- Löscher, C.R., Kock, A., Könneke, M., LaRoche, J., Bange, H.W., and Schmitz, R.A. (2012) Production of oceanic nitrous oxide by ammonia-oxidizing archaea. *Biogeosciences* **9**: 2419-2429.
- Martens-Habbena, W., Berube, P.M., Urakawa, H., de la Torre, J.R., and Stahl, D.A. (2009b) Ammonia oxidation kinetics determine niche separation of nitrifying Archaea and Bacteria. *Nature* **461**: 976-U234.
- Martens-Habbena, W., Qin, W., Horak, R.E.A., Urakawa, H., Schauer, A.J., Moffett, J.W. et al. (2015) The production of nitric oxide by marine ammonia-oxidizing archaea and inhibition of archaeal ammonia oxidation by a nitric oxide scavenger. *Environ Microbiol* **17**: 2261-2274.
- Martikainen, P.J., and Deboer, W. (1993) Nitrous-Oxide Production and Nitrification in Acidic Soil from a Dutch Coniferous Forest. *Soil Biol Biochem* **25**: 343-347.
- Mørkved, P.T., Dörsch, P., and Bakken, L.R. (2007) The N₂O product ratio of nitrification and its dependence on long-term changes in soil pH. *Soil Biol Biochem* **39**: 2048-2057.

- Mosier, A.C., Lund, M.B., and Francis, C.A. (2012a) Ecophysiology of an ammonia-oxidizing archaeon adapted to low-salinity habitats. *Microb Ecol* **64**: 955-963.
- Nevison, C., Butler, J.H., and Elkins, J.W. (2003) Global distribution of N₂O and the delta N₂O-AOU yield in the subsurface ocean. *Glob Biogeochem Cycles* **17**.
- Newell, S.E., Fawcett, S.E., and Ward, B.B. (2013) Depth distribution of ammonia oxidation rates and ammonia-oxidizer community composition in the Sargasso Sea. *Limnol Oceanogr* **58**: 1491-1500.
- Papoutsakis, E.T. (1984) Equations and Calculations for Fermentations of Butyric-Acid Bacteria. *Biotechnol Bioeng* **26**: 174-187.
- Park, B.J., Park, S.J., Yoon, D.N., Schouten, S., Damsté, J.S.S., and Rhee, S.K. (2010) Cultivation of autotrophic ammonia-oxidizing archaea from marine sediments in coculture with sulfur-oxidizing bacteria. *Appl Environ Microb* **76**: 7575-7587.
- Peng, X.F., Fuchsman, C.A., Jayakumar, A., Warner, M.J., Devol, A.H., and Ward, B.B. (2016) Revisiting nitrification in the Eastern Tropical South Pacific: A focus on controls. *J Geophys Res Oceans* **121**: 1667-1684.
- Qin, W., Carlson, L.T., Armbrust, E.V., Devol, A.H., Moffett, J.W., Stahl, D.A., and Ingalls, A.E. (2015d) Confounding effects of oxygen and temperature on the TEX₈₆ signature of marine Thaumarchaeota. *P Natl Acad Sci USA* **112**: 10979-10984.
- Qin, W., Amin, S.A., Martens-Habben, W., Walker, C.B., Urakawa, H., Devol, A.H. et al. (2014) Marine ammonia-oxidizing archaeal isolates display obligate mixotrophy and wide ecotypic variation. *P Natl Acad Sci USA* **111**: 12504-12509.
- Ravishankara, A.R., Daniel, J.S., and Portmann, R.W. (2009) Nitrous oxide (N₂O): The dominant ozone-depleting substance emitted in the 21st century. *Science* **326**: 123-125.
- Sahan, E., and Muyzer, G. (2008) Diversity and spatio-temporal distribution of ammonia-oxidizing Archaea and Bacteria in sediments of the Westerschelde estuary. *FEMS Microbiol Ecol* **64**: 175-186.
- Santoro, A.E., Buchwald, C., McIlvin, M.R., and Casciotti, K.L. (2011) Isotopic Signature of N₂O Produced by Marine Ammonia-Oxidizing Archaea. *Science* **333**: 1282-1285.
- Smith, J.M., Chavez, F.P., and Francis, C.A. (2014) Ammonium uptake by phytoplankton regulates nitrification in the sunlit ocean. *PLoS ONE* **9**.
- Spang, A., Poehlein, A., Offre, P., Zumbiegel, S., Haider, S., Rychlik, N. et al. (2012) The genome of the ammonia-oxidizing Candidatus Nitrososphaera gargensis: insights into metabolic versatility and environmental adaptations. *Environ Microbiol* **14**: 3122-3145.
- Spott, O., Russow, R., and Stange, C.F. (2011) Formation of hybrid N₂O and hybrid N₂ due to codenitrification: First review of a barely considered process of microbially mediated N-nitrosation. *Soil Biol Biochem* **43**: 1995-2011.
- Stein, L.Y. (2011b) Surveying N₂O-producing pathways in bacteria. *Methods Enzymol: Research on Nitrification and Related Processes, Vol 486, Part A* **486**: 131-152.
- Stewart, F.J., Ulloa, O., and DeLong, E.F. (2012) Microbial metatranscriptomics in a permanent marine oxygen minimum zone. *Environ Microbiol* **14**: 23-40.
- Stieglmeier, M., Mooshammer, M., Kitzler, B., Wanek, W., Zechmeister-Boltenstern, S., Richter, A., and Schleper, C. (2014a) Aerobic nitrous oxide production through N-nitrosating hybrid formation in ammonia-oxidizing archaea. *Isme J* **8**: 1135-1146.
- Ulloa, O., Canfield, D.E., DeLong, E.F., Letelier, R.M., and Stewart, F.J. (2012) Microbial oceanography of anoxic oxygen minimum zones. *Proc Natl Acad Sci USA* **109**: 15996-16003.

- Urakawa, H., Martens-Habbena, and Stahl, D.A. (2011) Physiology and genomics of ammonia-oxidizing archaea. In *Nitrification*. BB Ward, M.K., DJ Arp (ed). Washington, DC: ASM Press, pp. 117-155.
- Vajrala, N., Martens-Habbena, W., Sayavedra-Soto, L.A., Schauer, A., Bottomley, P.J., Stahl, D.A., and Arp, D.J. (2013) Hydroxylamine as an intermediate in ammonia oxidation by globally abundant marine archaea. *P Natl Acad Sci USA* **110**: 1006-1011.
- Walker, C.B., de la Torre, J.R., Klotz, M.G., Urakawa, H., Pinel, N., Arp, D.J. et al. (2010) Nitrosopumilus maritimus genome reveals unique mechanisms for nitrification and autotrophy in globally distributed marine crenarchaea. *P Natl Acad Sci USA* **107**: 8818-8823.
- Wuebbles, D.J. (2009) Nitrous oxide: no laughing matter. *Science* **326**: 56-57.
- Yool, A., Martin, A.P., Fernandez, C., and Clark, D.R. (2007) The significance of nitrification for oceanic new production. *Nature* **447**: 999-1002.
- Yoshinari, T. (1976) Nitrous oxide in the sea. *Mar Chem* **4**: 189-202.
- Yuan, J.C., and Shiller, A.M. (2004) Hydrogen peroxide in deep waters of the North Pacific Ocean. *Geophys Res Lett* **31**.
- Yuan, J.C., and Shiller, A.M. (2005) Distribution of hydrogen peroxide in the northwest Pacific Ocean. *Geochem Geophys Geosy* **6**.

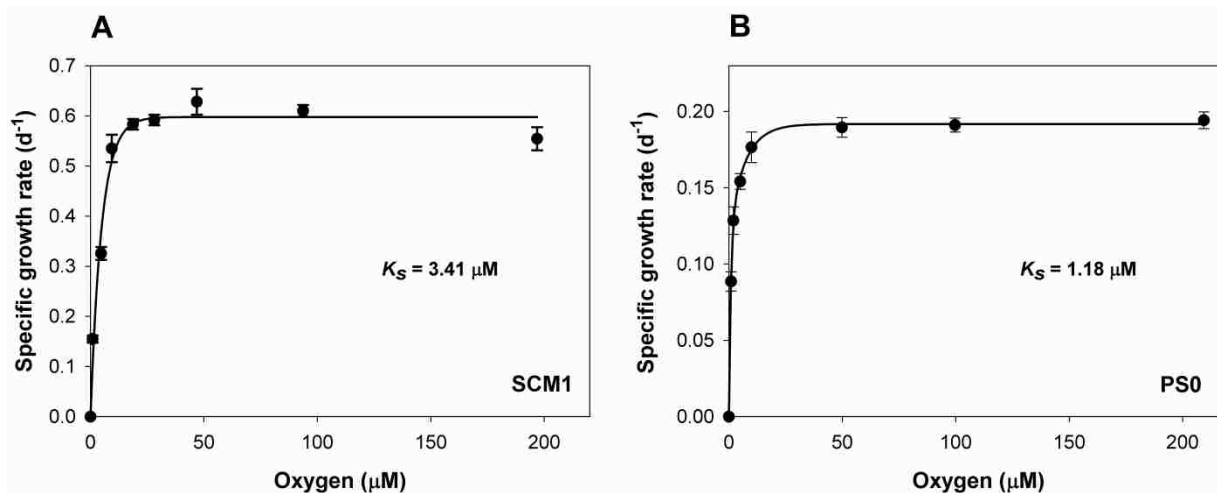


Figure 4.1. Oxygen-dependent growth kinetics of marine AOA.

Oxygen concentrations versus specific growth rates (d^{-1}) of strains SCM1 (A) and PS0 (B) fits a Monod growth model. Kinetics constants were obtained by fitting a Monod equation to O_2 concentrations and specific growth rates using the formula:

$$\mu = (\mu_{\max} \times [O_2]) \times (K_s + [O_2])^{-1}$$

Here, μ is specific growth rate (d^{-1}), μ_{\max} is the maximum specific growth rate (d^{-1}), and K_s is the half saturation constant with respect to growth. Data presented are the average of three independent biological replicates. Error bars represent the standard deviation for each sample.

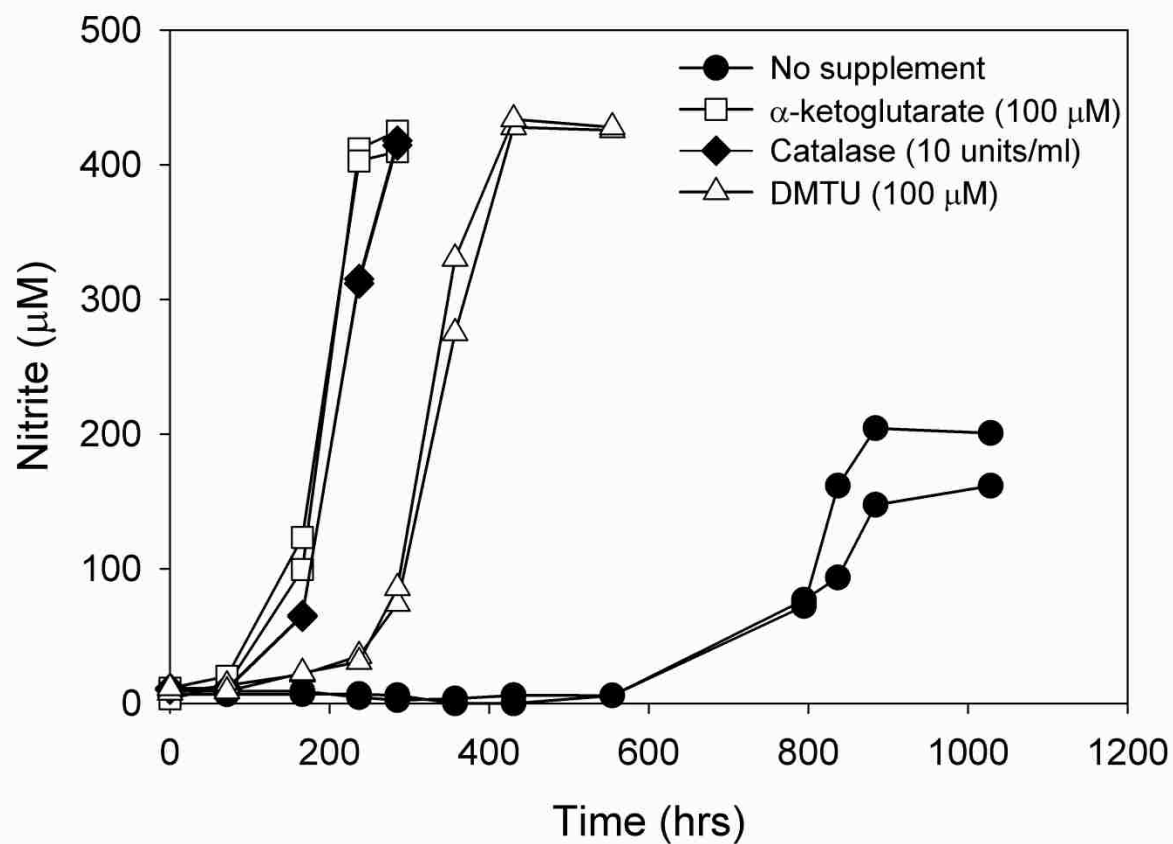


Figure 4.2. Growth curve of strain HCA1 (as measured by nitrite production) with 100 μM α -ketoglutarate, 10 units ml^{-1} catalase, or 100 μM dimethylthiourea (DMTU), relative to controls without supplements.

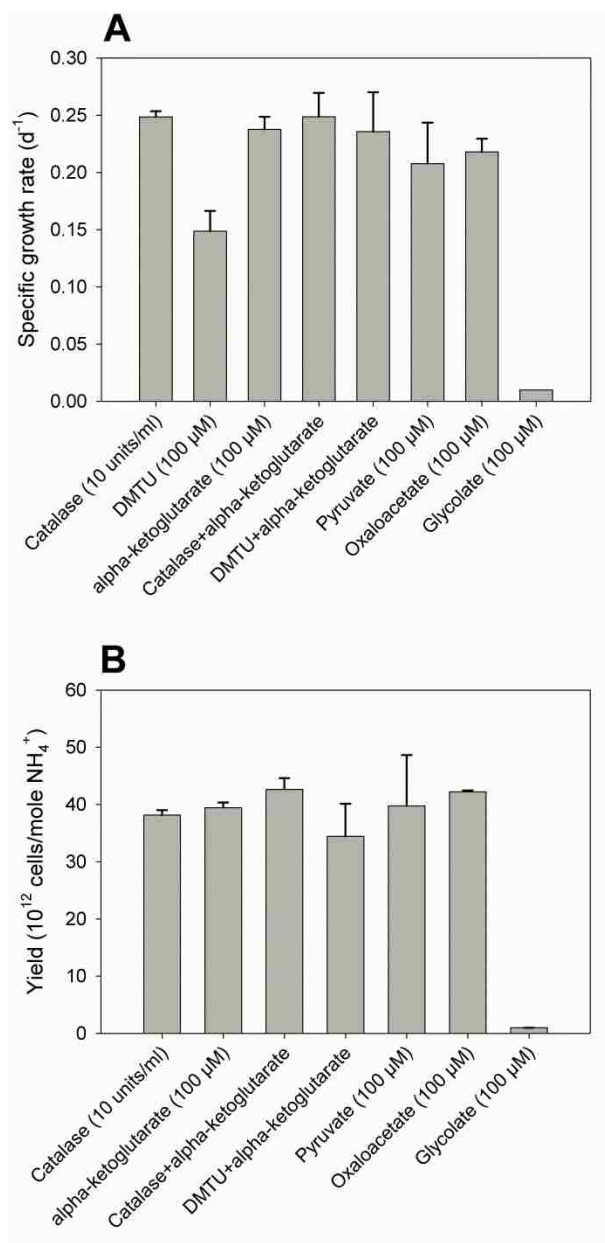


Figure 4.3. The specific growth rates (A) and specific growth yields (B) of strain PS0 cultures supplemented with H₂O₂ scavengers (10 units ml⁻¹ catalase or 100 μM dimethylthiourea (DMTU)), α-keto acids (100 μM), or a common algal exudate (glycolate, 100 μM).

No growth was observed after 23 days of incubation in medium containing glycolate. Error bars represent the standard deviation of triplicate cultures.

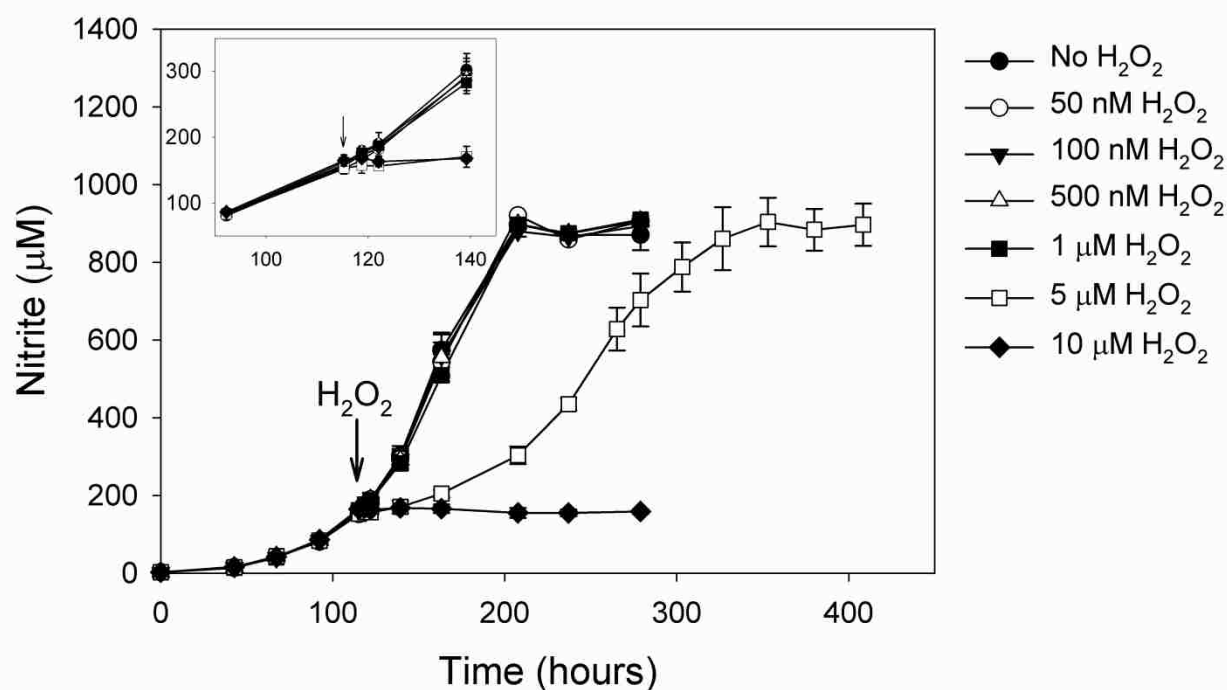


Figure 4.4. Short-term (inset panel) and long-term effects of different concentrations of H₂O₂ on the ammonia oxidation activity of exponential phase SCM1 cells.

Error bars correspond to the standard deviation of triplicate cultures. SCM1 cells were cultured in α -keto acid and H₂O₂ scavenger-free Synthetic Crenarchaeota Medium. Different concentrations of fresh H₂O₂ (Sigma-Aldrich) were added during early-exponential growth ($\sim 1.5 \times 10^7$ cells ml⁻¹). Nitrite production was determined at 3, 6 and 24 hours (short-term; inset panel) following addition of H₂O₂.

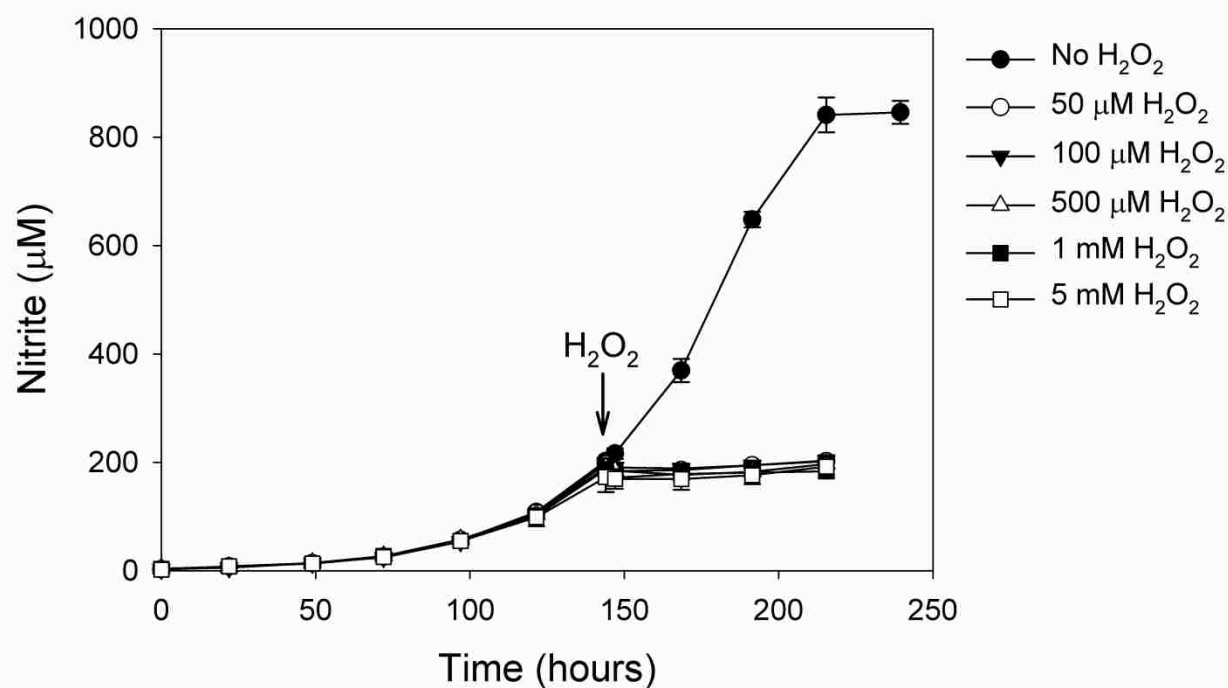


Figure 4.5. Growth curve of strain HCA1 (as measured by nitrite production) with 100 µM α -ketoglutarate, 10 units ml⁻¹ catalase, or 100 µM dimethylthiourea (DMTU), relative to controls without supplements.

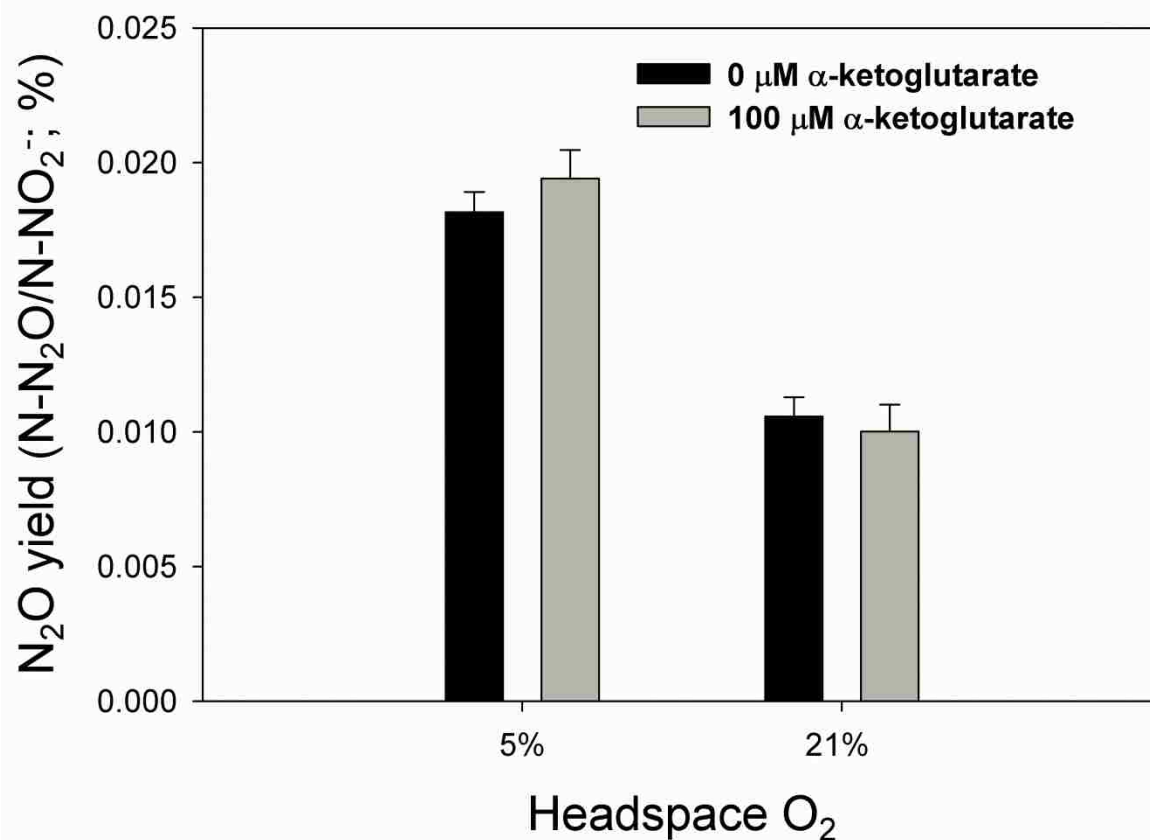


Figure 4.6. Nitrite-normalized N₂O yields of strain SCM1 with 100 μM α-ketoglutarate (grey) relative to controls without α-ketoglutarate (black).

Error bars represent the standard deviation of data from triplicate cultures.

Table 4.1. Growth^a and N₂O production^b of strains SCM1 and PS0 at different O₂ concentrations.

Strain	Initial headspace O ₂	Initial amount of O ₂ (μmol)	Residual amount of O ₂ (μmol) ^c	Initial amount of ammonia (μmol)	Residual amount of ammonia (μmol) ^d	Nitrite production (μmol)	Initial cell abundance (ml ⁻¹)	Cell abundance at early stationary phase (ml ⁻¹)	N ₂ O yield (N-N ₂ O/N-NO ₂ ⁻ ; %)	N ₂ O production (nmol N ₂ O/10 ⁹ cells)
SCM1	0.1%	6.0	0	10.0	5.6	5.1	2.83×10 ⁵	4.0×10 ⁶	0.074	6.3
	0.5%	29.8	14.8	10.0	BD	10.0	2.72×10 ⁵	6.3×10 ⁶	0.033	5.2
	1%	59.7	44.7	10.0	BD	9.8	2.78×10 ⁵	6.6×10 ⁶	0.028	4.2
	5%	298.3	283.3	10.0	BD	10.1	2.88×10 ⁵	6.8×10 ⁶	0.018	2.7
	10%	596.5	581.5	10.0	BD	10.2	2.77×10 ⁵	6.9×10 ⁶	0.014	2.0
	21%	1252.7	1237.7	10.0	BD	10.4	2.83×10 ⁵	7.9×10 ⁶	0.011	1.3
PS0	0.2%	11.9	0	10.0	ND	8.2	2.51×10 ⁵	6.7×10 ⁶	0.059	7.3
	0.5%	29.8	14.8	10.0		10.0	2.33×10 ⁵	7.0×10 ⁶	0.025	3.5
	1%	59.7	44.7	10.0		10.2	2.95×10 ⁵	7.0×10 ⁶	0.019	2.8
	5%	298.3	283.3	10.0		10.0	2.88×10 ⁵	6.8×10 ⁶	0.015	2.3
	10%	596.5	581.5	10.0		10.0	2.43×10 ⁵	6.8×10 ⁶	0.013	1.9
	21%	1252.7	1237.7	10.0		10.4	2.70×10 ⁵	6.7×10 ⁶	0.010	1.5

^a*Nitrosopumilus maritimus* strain SCM1 was maintained in HEPES-buffered Synthetic Crenarchaeota Medium supplemented with 1 mM NH₄Cl at 30 °C in the dark without shaking ((Martens-Habbena et al., 2009b) . PS0 is a recently isolated *N. maritimus*-like marine AOA strain, sharing ~98% 16S rRNA and ~94% *amoA* gene sequence identity with strain SCM1; it was isolated from beach surface sediments in Puget Sound estuary (Qin et al., 2014). Strain PS0 was maintained in HEPES-buffered Synthetic Crenarchaeota Medium supplemented with 500 μM NH₄Cl and 100 μM α-ketoglutaric acid (Qin et al., 2014). Growth experiments were carried out in 250 ml serum bottles (Wheaton, NJ, USA) that contained 100ml of HEPES-buffered Synthetic Crenarchaeota Medium supplemented with 100 μM NH₄Cl (10 micromoles NH₄Cl total; additional 100 μM α-ketoglutaric acid was added for strain PS0). The headspace of each bottle was sealed using air-tight butyl rubber septa and aluminum crimps (Wheaton). Atmospheric O₂ and N₂O were removed by flushing bottle headspace with N₂ through a sterile 0.22 μm Millex-GP syringe filter at > 50 ml/min for 10 min. The medium inside of the bottle was shaken well during the purge process. Subsequently, 0.04% (v/v) of high-purity CO₂ was injected back to exchange headspace N₂ in

bottles. The appropriate amounts of high-purity O₂ were injected back into each headspace to achieve 0.1%, 0.2%, 0.5%, 1%, 5%, 10%, and 21% O₂ (v/v) (corresponding to 1, 2, 5, 11, 53, 106, 213 μM dissolved O₂, respectively). Headspace O₂ concentration of each bottle was measured and confirmed before the experiment using an SRI 8610SC gas chromatograph with a thermal conductivity detector (SRI instruments, CA., USA). One ml of early stationary phase cultures of strains SCM1 and PS0 were inoculated into each bottle and incubated at 30 °C and 26 °C in the dark without shaking, respectively. The cell density, nitrite production, and ammonia consumption were determined as previously described. No, or only negligible, changes in pH could be detected between the beginning and end of each growth experiment.

^bTriplicate incubations were set up under each O₂ condition and uninoculated bottles served as a control for abiotic N₂O production and were analyzed in parallel with experimental bottles. Headspace N₂O concentrations were measured before incubation and after complete conversion of 100 μM ammonia to nitrite or complete consumption of O₂ by electron capture gas chromatography (GC-2014 Nitrous Oxide Analyzer, Shimadzu, Moorpark, CA).

^cThe residual amount of O₂ is calculated based on the reaction stoichiometry of 1 mol NH₃ oxidized per 1.5 mol O₂ consumed.

^dThe residual amount of ammonia was measured for strain SCM1 but not for strain PS0. BD = below detection (< 10nM); ND = not determined.

Chapter 5.

The production of nitric oxide by marine ammonia-oxidizing archaea and inhibition of archaeal ammonia oxidation by a nitric oxide scavenger

Willm Martens-Habben^{a*}, **Wei Qin^{a*}**, Rachel E. A. Horak^b, Hidetoshi Urakawa^c, Andrew J. Schauer^d, James W. Moffett^e, E. Virginia Armbrust^b, Anitra E. Ingalls^b, Allan H. Devol^b, and David A. Stahl^{a,1}

Published in *Environmental Microbiology*

2015

Volume 17, Issue 7, 2261–2274, doi: 10.1111/1462-2920.12677

^aDepartment of Civil and Environmental Engineering, University of Washington, Seattle, WA, USA; ^bSchool of Oceanography, University of Washington, Seattle, WA, USA; ^cDepartment of Marine and Ecological Sciences, Florida Gulf Coast University, Fort Myers, FL, USA;

^dDepartment of Earth and Space Sciences, University of Washington, Seattle, WA, USA;

^eDepartment of Biological Sciences, University of Southern California, Los Angeles, CA, USA

* These authors contributed equally to the present work.

¹Corresponding author E-mail: dastahl@u.washington.edu.

Abstract

Nitrification is a critical process for the balance of reduced and oxidized nitrogen pools in nature, linking mineralization to the nitrogen loss processes of denitrification and anammox. Recent studies indicate a significant contribution of ammonia-oxidizing archaea (AOA) to nitrification. However, quantification of the relative contributions of AOA and ammonia-oxidizing bacteria (AOB) to *in situ* ammonia oxidation remains challenging. We show here the production of nitric oxide (NO) by *Nitrosopumilus maritimus* SCM1. Activity of SCM1 was always associated with release of NO with quasi-steady state concentrations between 0.05 and 0.08 μM . Nitric oxide production and metabolic activity were inhibited by the nitrogen free radical scavenger 2-phenyl-4,4,5,5-tetramethylimidazoline-1-oxyl-3-oxide (PTIO). Comparison of marine and terrestrial AOB strains with SCM1 and the recently isolated marine AOA strain HCA1 demonstrated a differential sensitivity of AOB and AOA to PTIO and allylthiourea (ATU). Similar to the investigated AOA strains, bulk water column nitrification at coastal and open ocean sites with sub-micromolar ammonia/ammonium concentrations was inhibited by PTIO and insensitive to ATU. These experiments support predictions from kinetic, molecular and biogeochemical studies indicating that marine nitrification at low ammonia/ammonium concentrations is largely driven by archaea and suggest an important role of NO in the archaeal metabolism.

Introduction

Several recent discoveries of novel nitrogen cycle microorganisms have challenged our perception of the global nitrogen cycle. Particularly, the discovery of ammonia-oxidizing mesophilic and thermophilic Group I archaea (now assigned to the new archaeal phylum *Thaumarchaeota*) suggested a significant role of *Archaea* in the global nitrogen cycle (Könneke

et al., 2005; Brochier-Armanet et al., 2008; de la Torre et al., 2008; Hatzenpichler et al., 2008; Spang et al., 2010; Lehtovirta-Morley et al., 2011; Tourna et al., 2011). *Thaumarchaeota* constitute up to 40% of microbial plankton in the oceans and are abundant in soils, sediments, and geothermal hot springs (Karner et al., 2001; Pearson et al., 2004; Francis et al., 2005; Leininger et al., 2006). The majority of characterized *Thaumarchaeota* carry genes encoding a putative ammonia monooxygenase (AMO), suggesting a widespread phylogenetic distribution of ammonia oxidation within this group (Brochier-Armanet et al., 2008; Spang et al., 2010). Molecular surveys indicated that thaumarchaeal *amoA* (coding for the α -subunit of the putative AMO) gene and transcript copy numbers outnumber their ammonia-oxidizing bacterial counterparts by several orders of magnitude, particularly in oligotrophic marine systems and ammonium-depleted soils (Leininger et al., 2006; Mincer et al., 2007; Nicol et al., 2008; Santoro et al., 2010; Verhamme et al., 2011; Beman et al., 2012a; Stewart et al., 2012; Horak et al., 2013). Since ammonia oxidation is generally the rate controlling step in nitrification, these data together served to support speculation that *Thaumarchaeota* control nitrification in most low ammonia-containing environments.

Physiological characterization of the first isolated marine ammonia-oxidizing archaeon (AOA) *Nitrosopumilus maritimus* strain SCM1 (henceforth referred to as SCM1) also supported the importance of *Thaumarchaeota* in nitrification. This isolate, as well as marine ammonia-oxidizing communities dominated by AOA, exhibit an up to 200-fold higher affinity to ammonium than known ammonia-oxidizing bacteria (AOB). Thus, at least some AOA lineages are adapted to thrive under extreme nutrient limitation (Martens-Habbena et al., 2009b; Horak et al., 2013; Newell et al., 2013). AOA are also suggested to be important drivers of nitrification in

ammonium-depleted soils and have been associated with emission of nitrous oxide (N₂O) in oligotrophic open ocean waters (Leininger et al., 2006; Nicol et al., 2008; Santoro et al., 2011; Verhamme et al., 2011; Löscher et al., 2012). However, due to the metabolic similarities of AOA and AOB, direct quantifications of their nitrogen turnover in relation to gross nitrification rates and associated N₂O emissions remain challenging (Jia and Conrad, 2009; Santoro et al., 2010; Löscher et al., 2012; Taylor et al., 2012; Taylor et al., 2013; Hollibaugh et al., 2014a; Vajrala et al., 2014). Thus, significant questions remain about the contribution of AOA and AOB to *in situ* nitrification rates, particularly in terrestrial and coastal marine environments with appreciable numbers of both AOA and AOB. Furthermore, the finding in an industrial wastewater treatment plant that *amoA*-encoding and transcribing *Thaumarchaeota* may not - or at least not only - thrive by autotrophic ammonia oxidation challenges the growing perception that archaeal *amoA* gene transcription solely correlates with ammonia oxidation activity (Mussmann et al., 2011). Thus, there remains the need for selective quantification of AOA and AOB activities in the environment.

An approach to selective activity measurements was suggested by available AOA genomes and metagenomes. Sequence analysis highlighted the apparent divergence in the biochemistry of ammonia oxidation by AOA and AOB. For example, although characterized AOA produce hydroxylamine as an intermediate in ammonia oxidation pathway (Vajrala et al., 2013), they lack a homolog of the bacterial hydroxylamine dehydrogenase (HAO), previously known as hydroxylamine oxidoreductase (HAO), required for oxidizing the product of the AMO to nitrite (Hallam et al., 2006; Walker et al., 2010; Blainey et al., 2011; Kim et al., 2011; Spang et al., 2012). Another common feature of thaumarchaeal genomes is the presence of multiple genes

encoding putative copper-containing nitrite reductases (Cu-NIR), suggesting the capacity to reduce nitrite to nitric oxide (NO) (Hallam et al., 2006; Bartossek et al., 2010; Walker et al., 2010; Blainey et al., 2011; Kim et al., 2011; Spang et al., 2012).

We now show production of NO coupled to ammonia oxidation by the marine AOA SCM1 and associate NO production with energy metabolism by analyses of ammonia oxidation inhibition by an NO scavenger. Both SCM1 and a newly isolated marine AOA (strain HCA1) from the water column of Hood Canal, Washington State (Qin et al., 2014) demonstrated comparable responses to the NO scavenger. Previously reported sensitivity of AOA to chemical scavenging of NO did not associate sensitivity directly with production of NO (Shen et al., 2013; Jung et al., 2014b). In addition, both AOA isolates were shown to be relatively insensitive to chemicals commonly used to inhibit ammonia oxidation by AOB, allylthiourea (ATU) and nitrapyrin. By combining inhibitors that selectively inhibit ammonia oxidation by archaea or bacteria we show that in both coastal and open ocean waters with mixed assemblages of AOA and AOB, *in situ* nitrification is likely almost exclusively driven by members of the *Archaea*. These results could provide useful criteria to further constrain the relative contributions of AOA and AOB to nitrification in a variety of environments.

Results

Nitric oxide production by strain SCM1. Based on our previous speculation that nitrogen free radicals play a role in the nitrogen metabolism of SCM1 (Walker et al., 2010) we measured NO concentrations in SCM1 cultures using NO-selective microsensors (Fig. 5.1). We observed instantaneous NO accumulation upon addition of ammonium to resting vital cells of SCM1

harvested from late exponential phase or freshly ammonium-depleted cultures ($0.9 - 1 \text{ mM}$ nitrite, $5 - 5.2 \times 10^7 \text{ cells ml}^{-1}$; Fig. 5.1). At low total ammonia nitrogen (TAN) concentrations ($1 \text{ }\mu\text{M} - 100 \text{ }\mu\text{M}$), NO reached a quasi steady state concentration of $50 - 80 \text{ nM}$ after $6 - 10 \text{ min}$ (Fig. 5.1A). Nitric oxide was not detected in suspensions of pasteurized SCM1 cells. The NO quasi steady state concentration was tightly correlated with oxygen (O_2) consumption, which was simultaneously measured using an O_2 microsensor. As reported previously, O_2 consumption followed a stoichiometry of 1.5 O_2 consumed per ammonium oxidized and stopped when ammonium fell below 10 nM (Martens-Habbena et al., 2009b). After depletion of ammonium and cessation of O_2 consumption, the NO level quickly dropped to background levels (Fig. 5.1A). A reproducible feature was a transient increase in NO once cells had consumed most of the ammonium, and a peak when ammonium was depleted (Fig. 5.1A). Nitric oxide did not stabilize at a quasi steady state concentration with TAN concentrations greater than 2 mM . At these concentrations, NO continued to rise above $1\text{-}2 \text{ }\mu\text{M}$ accompanied by slowly declining ammonia oxidation activity (Fig. 5.1B).

The ammonium concentration further affected the rate of NO production. Figure 1C shows a representative example of a SCM1 culture sampled multiple times within a two hour period and spiked with four different concentrations of ammonium. Using the rate of NO release in the first two minutes following ammonium addition as an initial proxy for NO production rate, the NO release rose with increasing ammonium concentration from $0.2 \text{ }\mu\text{M h}^{-1}$ at $1 \text{ }\mu\text{M}$ ammonium to up to $18.8 \text{ }\mu\text{M h}^{-1}$ at 10 mM ammonium. Although we did not determine cell numbers or protein concentrations in these cultures, we could compare rates only between samples from the same original cultures, which suggest the NO production rate followed an ammonium-dependent

apparent saturation kinetic ($R^2=0.993$, $p=0.018$) with an apparent K_s of 2.1 mM ammonium (Fig. 5.1C). Further experiments will be necessary to elucidate the kinetic parameters in more detail. Although the highest rates of O_2 uptake and NO accumulation were observed at 10 mM ammonium, indicating fastest metabolism of ammonium, TAN concentrations higher than 2 mM also impaired growth (as measured by nitrite production), completely suppressing growth at 20 mM TAN (Fig. 5.2).

From these preliminary data and the reported biomass of SCM1 (Martens-Habbena et al., 2009b), we estimated a maximum initial ammonia oxidation rate of $37.7 \mu\text{mol N mg}^{-1} \text{protein h}^{-1}$ and a maximum initial NO accumulation rate of $32.9 \mu\text{mol N mg}^{-1} \text{protein h}^{-1}$ at 10 mM TAN. Thus, the NO accumulation rate reached 89.9% of the ammonia oxidation rate at 10 mM TAN, whereas it was equivalent to only 5.2% of the ammonia oxidation rate at 10 μM TAN, suggesting a nearly quantitative transformation of ammonium to NO at high ammonium levels. In contrast, neither the NO concentration nor its initial rate of accumulation increased with increasing nitrite concentrations up to 10 mM. Ammonia oxidation, O_2 uptake, and NO accumulation declined at nitrite concentrations above 1 mM.

Responses of AOA and AOB to metabolic inhibitors. The impact of known inhibitors of AOB on the activity of archaeal ammonia oxidizers was tested with two marine AOA isolates (SCM1 and HCA1). Growth of SCM1 was significantly inhibited by addition of 0.1 μM acetylene (>60% inhibition), and almost completely inhibited at 40 μM acetylene (Fig. 5.3A). Nitric oxide accumulation levels dropped immediately below the detection limit following addition of 10 μM acetylene (Fig. 5.3B). Likewise, ammonia oxidation activity of SCM1 was completely inhibited

by addition of 10 μM diethyl dithiocarbamate (DEDTC) (Fig. 5.4). These results are similar to previous studies and suggest similar mechanistic properties of AOA and AOB (Offre et al., 2009; Shen et al., 2013).

We further examined the response of the two marine AOA strains and strains belonging to all currently recognized AOB genera from marine, freshwater and soil, to the nitrogen free radical scavenger 2-phenyl-4,4,5,5-tetramethylimidazole-1-oxyl-3-oxide (PTIO). Ammonia oxidation by SCM1 was partially inhibited at low concentrations of PTIO (38% and 80% inhibition at 10 μM and 50 μM , respectively) and almost completely inhibited (>95% inhibition) at 100 μM PTIO (Fig. 5.5A). In contrast, the addition of NO-treated PTIO, yielding the scavenging inactive reduced form (PTI), showed no inhibition at 100 μM (Fig. 5.6). The response of HCA1 was similar to SCM1; it showed reduced growth rates of 17% and 60% at 10 μM and 33 μM of PTIO, respectively, and complete inhibition at 100 μM PTIO (Fig. 5.5A). Under comparable experimental conditions, 100 μM PTIO did not cause significant inhibition of any actively growing AOB strain tested (Fig. 5.5B). There was partial inhibition of *N. cryotolerans* (30% inhibition) and *N. briensis* (70% inhibition) at 330 μM PTIO. Notably, *N. briensis* and *N. cryotolerans* are known to form macroscopic aggregates or biofilms, a phenotype for which NO metabolism and signalling has been proposed to be significant (Schmidt et al., 2004b). Thus, partial inhibition of activity at a higher concentration of PTIO suggests that NO may be of physiological significance to some species of AOB.

Because AOB often encounter severe starvation in natural environments, we also investigated whether starvation influenced the sensitivity of AOB to PTIO. *N. europaea* and *N. briensis* were

starved in ammonia-free media for 20 hours and 2 weeks, respectively, and subsequently supplied with low concentrations of ammonium in the presence of 100 μM PTIO. Neither strain was inhibited by 100 μM PTIO during recovery from starvation at low ammonium concentrations (200 μM and 10 μM for *N. europaea* and *N. briensis*, respectively; Fig. 5.7). Following addition of 1 mM ammonium, nitrite production by *N. briensis* was reduced to ~ 60% of the control rate (Fig. 5.7B). However, at environmentally relevant ammonium concentrations, ammonia oxidation by the most PTIO-sensitive AOB strain tested was only partially inhibited by 100 μM PTIO following prolonged starvation. Thus, although 100 μM PTIO can lead to partial inhibition of some AOB strains during the transition from starvation to maximal growth rate at high ammonia concentrations, this effect is manifest at a significantly higher minimum inhibitory concentration than observed for AOA. Overall, these data indicated that marine AOA are between 10- and 100-time more sensitive to PTIO than AOB available in culture, suggesting that nitrogen free radicals may play different roles in AOA and AOB metabolisms.

The tested AOA and AOB strains also showed contrasting responses to allylthiourea (ATU) and nitrapyrin. SCM1 grew at its maximum growth rate in the presence of up to 10 μM ATU, was partially inhibited (~50%) at 100 μM ATU, and ~97% inhibited at 330 μM ATU (Fig. 5.5C). HCA1 was even less sensitive to high concentrations of ATU than SCM1; it showed no apparent inhibition up to 33 μM ATU, only ~14% inhibition at 100 μM ATU, and still retained nearly 40% of its maximum growth rate at 330 μM ATU (Fig. 5.5C). In contrast, all tested AOB strains were completely inhibited by less than 100 μM ATU (Fig. 5.5D). In fact, growth and activity of all tested *Nitrosomonas* and *Nitrosospira* strains from marine and terrestrial environments were completely inhibited by 3.3 μM ATU. Only *Nitrosococcus oceani*, a marine ammonia oxidizer

belonging to the *Gammaproteobacteria*, was less sensitive to ATU. *N. oceani* was partially inhibited at 33 μM ATU and fully inhibited by 100 μM ATU. Furthermore, SCM1 exhibited only partial inhibition at 10 μM nitrapyrin (Fig. 5.8A, B), whereas all AOB strains were completely inhibited at this concentration. Due to its low water solubility we could not establish a more complete inhibition kinetic curve for nitrapyrin with AOA isolates.

Differential inhibition of ammonia oxidation in natural marine communities by PTIO and ATU.

The differential response of marine AOA isolates and AOB strains to PTIO and ATU indicated these compounds could potentially serve as group-selective inhibitors of ammonia oxidation, thus serving as a tool to constrain the relative activities of these two groups of ammonia oxidizers in natural environments. To test this hypothesis, we examined the effects of these two inhibitors on ammonia oxidation rates in the coastal sampling site from which strain HCA1 was isolated (Puget Sound Regional Synthesis Model station P12, Washington State, USA) and an open ocean site (Ocean Station Papa, North Pacific Ocean). At station P12 in Hood Canal, the chlorophyll maximum was relatively shallow at approximately 10 m (Fig. 5.9). Nitrite was elevated around the chlorophyll maximum (up to 0.25 μM). Nitrate was depleted at the surface and increased with depth (Fig. 5.9). At Ocean Station Papa, the chlorophyll maximum was much deeper, peaking around 50 m (Fig. 5.10). Here, nitrite at the primary nitrite maximum (70 m) was 0.65 μM . Nitrate was elevated at the surface and increased with depth (Fig. 5.10). Ambient ammonia was below 0.1 μM at the depths of both stations used for inhibitor treatments (90 m at coastal station P12 and 70 m at Ocean Station Papa) (Figs. 4, 5).

At coastal station P12 and Ocean Station Papa archaeal *amoA* genes substantially increased from 764 (+/- 250) and 135 (+/- 57) ml⁻¹ at the surface to 3.6×10^5 (+/- 1.3×10^5) and 5.5×10^4 (+/- 1.6×10^4) ml⁻¹ around the depth of primary nitrite maximum, respectively (Figs. 4, 5). AOA *amoA* genes were found in consistently high numbers at depths below the bottom of the euphotic zones of both stations (Figs. 4, 5). The betaproteobacterial (β -AOB) *amoA* gene copy numbers were relatively uniform throughout the entire water column of coastal station P12, between 6.7×10^3 (+/- 0.9×10^3) and 2.6×10^4 (+/- 0.1×10^4) ml⁻¹, and the upper water column of Ocean Station Papa (0 – 300 m), between 2.6×10^2 (+/- 14) and 4.0×10^3 (+/- 1.4×10^2) ml⁻¹ (Figs. 4, 5). The abundance of AOA and β -AOB *amoA* genes at coastal station P12 was comparable to previous reported values (Horak et al., 2013) and higher than those at Ocean Station Papa. Assuming an average of 1 *amoA* gene copy per genome for AOA and 2 to 3 *amoA* gene copies per β -AOB genome (Norton et al., 2002; Santoro et al., 2010; Walker et al., 2010; Blainey et al., 2011), AOA outnumbered β -AOB by 34- to 132-fold and 68- to 720-fold below the base of the euphotic zones of coastal station P12 and Ocean Station Papa, respectively. In addition, AOA made up a large proportion of the total microbial population below the euphotic zone at Ocean Station Papa, contributing to 33% – 44% of the total prokaryotic population (Fig. 5.10).

In order to directly identify the primary contributors to ammonia oxidation in these natural marine systems, we combined ¹⁵N-ammonia oxidation measurements with inhibitor treatments. At coastal station P12 and Ocean Station Papa we measured ¹⁵N-ammonia oxidation with water collected from 90 m and 70 m (corresponding to the primary nitrite maximum), respectively. The addition of PTIO and ATU yielded comparable results at both stations. Similar to marine AOA isolates, both marine communities were sensitive to low concentrations of PTIO.

Ammonia oxidation was completely inhibited in the presence of 50 μM PTIO at Ocean Station Papa and 100 μM PTIO at coastal station P12 (Fig. 5.5A). In contrast, ammonia oxidation of the marine communities was relatively insensitive to ATU at the concentrations up to 10 μM , with partial inhibition (60 – 80%) at 100 μM ATU (Fig. 5.5C). The complete inhibition by ATU was only observed at 500 μM at Ocean Station Papa and 1000 μM at coastal station P12 (Fig. 5.5C). Thus, these AOA dominated natural marine communities and the marine AOA isolates were more than 100-times less sensitive to ATU than the tested *Nitrosomonas* and *Nitrosospira* strains, and 5-times less sensitive than *N. oceani*.

Discussion

Since the discovery of ammonia oxidation within the domain *Archaea*, considerable efforts have been made to elucidate details about the metabolism and the actual significance of archaeal ammonia oxidation for the global cycling of nitrogen, particularly in regard to their significance to nitrification related N_2O emission (Francis et al., 2005; Könneke et al., 2005; Leininger et al., 2006; Mincer et al., 2007; Agogué et al., 2008b; Santoro et al., 2010; Santoro et al., 2011; Löscher et al., 2012; Jung et al., 2014b; Stieglmeier et al., 2014a). The development of AOA-specific inhibitors would therefore assist in developing a more complete census of AOA impact on the nitrogen cycle (Shen et al., 2013; Taylor et al., 2013; Vajjala et al., 2014). For example, recently, Shen et al. (2013) reported that the first soil AOA isolate, *Nitrososphaera viennensis* strain EN76 was completely inhibited in the presence of 50 μM of the NO scavenger 2-(4-carboxyphenyl)-4,4,5,5-tetramethylimidazoline-1-oxyl-3-oxide (Carboxy-PTIO) and was only slightly inhibited by 80 μM ATU (Shen et al., 2013). However, those analyses did not establish a relationship between inhibition by Carboxy-PTIO (a more water soluble variant of PTIO) and

the production of NO by AOA. In addition, the interpretation of experimental results based on ‘selective inhibitors’ in pure cultures as well as in complex environments is subject to a number of potential caveats. These include the specificity of the chosen inhibitors, their potential decomposition during experimental manipulation, disruption of controlling trophic interactions, and their potential interference with analytical procedures (Oremland and Capone, 1988).

We therefore tested nitrate isotope standards of known $\delta^{15}\text{N}$ isotope composition, and showed that concentrations of PTIO or ATU up to 1 mM did not interfere with sample preparation and $\delta^{15}\text{N}$ isotope measurements, ruling out potential artifacts during nitrification rate measurements (see *Materials and Methods* for additional details). Both inhibitors are so far known to only target molecular compounds specifically associated with metabolism of NO (PTIO) and bacterial ammonia oxidation (ATU). Demonstration that NO-treated PTIO, yielding the scavenging inactive reduced form (PTI), was not inhibitory was also consistent with a specific mode of action. Although we cannot rule out nonspecific interactions, to the best of our knowledge no other enzymatic targets or metabolites that could directly influence *in situ* nitrification rates have been shown for these compounds. Thus, our studies further corroborate a direct link of inhibition by PTIO with the scavenging of NO produced by AOA during ammonia oxidation, strongly suggesting a central role of NO in AOA metabolism (Walker et al., 2010; Stieglmeier et al., 2014a).

Nitric oxide is a short-lived molecule and is rapidly turned over enzymatically or oxidized chemically (Heinrich et al., 2013). Since it rarely occurs in concentrations above the nanomolar range, the determination of its production and turnover is challenging. We thus looked at initial

rate of NO accumulation in resting cells after addition of ammonium substrate as an initial estimate for NO production. Even with the smallest ammonium concentrations tested, a near linear increase of NO in the cultures was observed over the first one to three minutes after ammonium addition. Although outside the physiological norm, ammonium concentrations of greater than 1 mM led to initial NO production rates of up to 89% of the estimated ammonia consumption, suggesting that ammonium substrate saturation leads to an almost complete conversion of ammonium into NO.

Nitric oxide is a known metabolite of several microbial energy metabolisms including denitrification, nitrifier-denitrification in AOB, and anammox. It is also a sideproduct of incomplete oxidation of hydroxylamine by AOB (Hooper, 1968; Ritchie and Nicholas, 1972; Zart et al., 2000). However, the pattern of NO accumulation and NO-scavenger sensitivity suggest different roles of NO in AOA, AOB, denitrifying, and anammox bacteria. In contrast to canonical denitrification, nitrifier-denitrification and anammox (Betlach and Tiedje, 1981; Lipschultz et al., 1981; Goretski et al., 1990; Kartal et al., 2011), NO production by SCM1 did not respond positively to increasing nitrite concentrations. In fact, nitrite concentrations above 1 mM inhibited the activity of SCM1. Only ammonium stimulated NO accumulation in SCM1. Although the bacterial HAO releases incompletely oxidized intermediates, e.g., HNO and NO at saturating turnover numbers, neither of the AOB pathways for NO production is essential for the oxidation of ammonia under aerobic conditions (Beaumont et al., 2002; Arp and Stein, 2003; Schmidt et al., 2004a; Stein, 2011a).

The relative insensitivity of AOB to PTIO in contrast to SCM1 and anammox bacteria (Kartal et al., 2011) further points to the different roles of NO in these ammonia-oxidizing organisms.

Nitric oxide serves as the oxidant of ammonia in the postulated pathway for anaerobic oxidation of ammonia (Kartal et al., 2011; Yan et al., 2012b). Notably, the ammonia-activating step of anammox is similarly sensitive to acetylene as the bacterial AMO complex, and inhibition of anaerobic ammonia oxidation by acetylene leads to a transient accumulation of NO (Kartal et al., 2011). In contrast, addition of acetylene in SCM1 cultures resulted in an instantaneous drop of NO to background levels; NO was only observed to increase following ammonium addition and to transiently increase when ammonium in culture was nearly depleted. Taken together, these results suggest that NO is mechanistically coupled directly to ammonia oxidation either as a direct free intermediate or possibly functioning as a shuttle to deliver electrons required by the AMO (Stahl and de la Torre, 2012b).

The suggestion that the AMO of AOA and AOB are mechanistically comparable is supported by their similar sensitivities to acetylene (Offre et al., 2009) and DEDTC, and the recent demonstration that hydroxylamine is an intermediate in the archaeal oxidation of ammonia (Vajrala et al., 2013). DEDTC strongly chelates copper and inhibits copper-dependent metabolisms such as nitrite reduction in denitrifying microorganisms and ammonia oxidation in AOB (Lees, 1946, 1952; Hooper and Terry, 1973; Shapleigh and Payne, 1985). The suggested importance of copper-containing enzymes in the AOA metabolism (Walker et al., 2010) is further corroborated by the inhibition of archaeal ammonia oxidation by DEDTC. Although the inhibition of bacterial ammonia oxidation by ATU is also attributed to copper chelation (Lees, 1946, 1952; Hooper and Terry, 1973; Hyman et al., 1990; McCarty, 1999), our marine AOA

pure cultures showed much lower sensitivity to ATU than marine and terrestrial AOB strains. Thus, differential response to ATU and nitrapyrin also points to basic structural or mechanistic differences between AOA and AOB. It is also possible that the accepted mechanism of inhibition by copper chelation is incorrect and that there is an alternative mechanism of ATU inhibition in AOB.

Despite the lack of direct measurements of AOA ammonia oxidation in the environment, several lines of evidence suggested their global importance to nitrification, particularly in nutrient depleted systems typical of large parts of the global oceans. AOA vastly outnumber AOB in these environments and transcripts from genes coding for the AMO are dominated by thaumarchaeal sequences, implicating AOA as significant contributors to *in situ* nitrification (Wuchter et al., 2006; Beman et al., 2012a; Löscher et al., 2012; Horak et al., 2013; Urakawa et al., 2014). These molecular inferences of AOA primacy was supported by our earlier physiological characterization of SCM1, demonstrating this organism is particularly well adapted to environments of sub-micromolar ammonium (Martens-Habbena et al., 2009b). This physiology is also consistent with ammonia oxidation kinetics and AOA abundance patterns we previously reported for one of our field sites, Hood Canal, a highly productive coastal system in the Puget Sound Estuary (Urakawa et al., 2010; Horak et al., 2013; Urakawa et al., 2014). Demonstration in this study of an *in situ* response to PTIO and ATU that is comparable to that of AOA in culture provides more direct attribution, indicating at least 95% of the bulk ammonia oxidation rate in Hood Canal and Ocean Station Papa water columns was mediated by AOA.

Assuming AOA carry a single copy of *amoA* gene, and that all populations having the gene are active nitrifiers, the bulk rate measurements translate to approximately 0.04 and 0.35 fmol ammonia oxidized cell⁻¹ day⁻¹ at 70 m water depth of Ocean Station Papa and 90 m of Hood Canal, respectively. These rates are equivalent to 0.32% and 2.8% of SCM1 activity under optimal growth conditions. Notably, it has previously been shown that NO is produced in the nitrification zones above and below oxygen minimum zones (OMZ) of the Eastern Tropical North Pacific (ETNP) (Ward and Zafiriou, 1988). If NO is indeed an intermediate in AOA metabolism, then AOA might be the primary source of NO in these zones outside the OMZ. In natural environments AOA and AOB compete for ammonia. Thus, disruption of normal trophic interactions by inhibition of archaeal ammonia oxidation by PTIO could potentially lead to an overestimation of AOB activity or vice versa. However, the K_s for ammonia oxidation in natural marine communities has been shown to be much lower than the K_s for characterized AOB (Horak et al., 2013; Newell et al., 2013). During our sampling campaign, nitrification proceeded consistently at concentrations of ammonia too low (sub-micromolar) to sustain characterized AOB (Martens-Habbena et al., 2009b). However, since AOB numbers were low at these two sampling sites, it remains to be seen how this differential inhibitor approach would work in systems with a higher relative contribution of AOB. In those cases, selective inhibition of AOB could potentially affect (i.e., stimulate) AOA activity. Nonetheless, the differential response of AOA and AOB to PTIO and ATU described here may provide a valuable tool to further elucidate the contribution of AOA and AOB to nitrification.

Materials & Methods.

Laboratory strains and culture conditions. All bacterial and archaeal ammonia oxidizers were maintained in liquid mineral medium. *Nitrosopumilus maritimus* strain SCM1, *Nitrosomonas europaea*, and *Nitrosococcus oceani* were cultured exactly as described previously (Martens-Habbena et al., 2009b). Growth experiments for these 3 strains were carried out at 30 °C. HCA1 is a newly isolated *N. maritimus*-like marine AOA strain, sharing ~99% 16S rRNA and ~95% *amoA* gene sequence identity with strain SCM1; it was isolated from a depth of 50 m water at the Puget Sound Regional Synthesis Model (PRISM) Station P10 (47.91 N, 122.62 W) in Hood Canal, Washington State, USA (Qin et al., 2014). HCA1 was cultured in HEPES-buffered synthetic crenarchaeota medium supplemented with 500 µM NH₄Cl and 100 µM α-ketoglutaric acid. Growth experiments with HCA1 were carried out at 25 °C in the dark without shaking. Strains of *Nitrosomonas oligotropha*, *Nitrosomonas ureae*, *Nitrospira multififormis*, and *Nitrospira briensis* were obtained from A. Pommerening-Röser (University of Hamburg, Germany) and cultured in artificial freshwater medium containing (per liter distilled H₂O) 0.584 g NaCl, 0.147 g CaCl₂·2H₂O, 0.074 g KCl, 0.049 g MgSO₄·7H₂O, 12.0 g HEPES, 1.0 ml cresol red solution (0.05%). The pH was adjusted to 7.8 with 10 M NaOH and the medium was autoclaved for sterilization. After cooling the medium to room temperature, the following compounds were added from sterile stock solutions (per liter freshwater medium): 2.0 ml 1 M sodium bicarbonate, 0.1 ml (2.753g/l) FeNaEDTA solution, 1.0 ml *Nitrosomonas oligotropha* trace element solution (per liter distilled H₂O: 8 ml conc. HCl, 30 mg H₃BO₃, 100 mg MnCl₂·4H₂O, 190 mg CoCl₂·6H₂O, 24 mg NiCl₂·6H₂O, 2 mg CuCl₂·2H₂O, 144 mg ZnSO₄·7H₂O, 36 mg Na₂MoO₄·2H₂O), 5.0 ml (0.4 g/l) KH₂PO₄, and 10.0 ml 1 M NH₄Cl. The marine AOB strain *Nitrosomonas cryotolerans* was obtained from ATCC and cultured in modified SCM medium (see above). The modified trace element solution was replaced with

seawater nitrosomonas trace element solution containing (per liter distilled H₂O) EDTA 2.06 g, 83.0 ml conc. HCl, 1.54 g FeSO₄ · 7H₂O, 0.2 g MnCl₂ · 4H₂O, 0.1 g Na₂MoO₄ · 2H₂O, 0.1 g ZnSO₄ · 7H₂O, 20 mg CuSO₄ · 5H₂O, 2.0 mg CoCl₂ · 6H₂O. If not otherwise indicated, all growth experiments were carried out on a rotary shaker at 25 °C and 90 rpm.

Nitric oxide production. Metabolic activities and short term response of SCM1 to metabolic inhibitors was tested by microrespirometry as described previously (Martens-Habbena and Stahl, 2011b). Briefly, simultaneous measurements of O₂ and NO were carried out in custom-built 35 ml glass vials (Uniserse AS, Denmark). Nitric oxide concentrations were measured using doped carbon fiber electrodes (amiNO-600, Innovative Instruments, Sarasota, FA) (Davies and Zhang, 2008) and signals were recorded by an Apollo 1000 Free Radical Analyzer (World Precision Instruments, Sarasota, FL). Nitric oxide sensors were calibrated using anoxic stock solutions of purified NO gas under N₂ atmosphere in SCM salts (1% NO in N₂) (Davies and Zhang, 2008). Alternatively, freshly prepared stock solutions of ProliNONOate (AG Scientific) in 10 mM ice cold NaOH were used for calibration. Both methods showed less than 10% deviation in day to day use. Nitric oxide signals were regularly confirmed by addition of NO scavengers. The detection limits of NO sensors under the given conditions was approximately 0.1 nM.

Responses of ammonia oxidizers to metabolic inhibitors. Initial tests of inhibitors with SCM1 were conducted by microrespirometry (see above). Inhibitors were further tested in growth experiments and added either before inoculation of the media or during mid-exponential growth. For comparison to inhibitor experiments of the natural marine community, inhibition in laboratory cultures were calculated by quantifying nitrite accumulation within 24 h following

addition of the inhibitors; continuous exponential increase of nitrite represented 100% activity and absence of nitrite production represented 0% activity. Whenever possible, inhibitors were added from 100-fold concentrated stock solutions in MilliQ water (for freshwater media) or basal SCM salts (for seawater media). Stock solutions of PTIO (2-phenyl-4,4,5,5-tetramethylimidazoline-1-oxyl-3-oxide, ICI America) were prepared at 5 mM concentration. Thus, samples receiving high concentrations of this inhibitor were diluted up to 20%.

Natural marine community sampling and analysis. Sampling for nutrients, ^{15}N -ammonia oxidation measurements, and molecular characterization was collected aboard RV *Clifford A. Barnes* at PRISM (Puget Sound Regional Synthesis Model) station P12 in Hood Canal (47.42 N, 123.11 W; <http://www.prism.washington.edu>), Washington, from June, 6th to 8th 2010. Sampling at Ocean Station Papa took place August 8th, 2013 at 44.98 N, 144.80 W on cruise KM-1314 aboard the R/V *Kilo Moana*. Depth profiles were recorded using a conductivity-temperature-depth (CTD)-rosette (Seabird Electronics, Bellevue, WA) equipped with Seabird SBE CTD sensor package and 12 10 l Niskin bottles (Hood Canal) or 24 10 l Niskin bottles (Ocean Station Papa). At Hood Canal, photosynthetically active radiation (PAR) was measured using a (PAR) sensor (Biospherical Instruments) mounted onto the CTD rosette. At Ocean Station Papa, PAR was measured using a Ground-based Ultraviolet/ PAR radiometer (model 511C, Biospherical Instruments), which was deployed at solar noon.

For both field sampling sites, subsamples for nutrients, ^{15}N -ammonia oxidation measurements, and molecular analyses were processed immediately after retrieval on deck. Ammonia, and nitrite were determined shipboard using published protocols (Grasshoff, 1999b; Holmes et al.,

1999). Samples for nitrate were filtered (0.22 μm) and stored frozen until laboratory analysis (UNESCO, 1994). The stock solution of ATU was 500 mM in artificial seawater, and the stock solution of PTIO was 5 mM (Hood Canal) or 25 mM (Ocean Station Papa) in artificial seawater. In order to reduce the volume of inhibitor solution and respective sample dilution a 25 mM stock solution was prepared by shaking overnight at 65°C.

Potential ammonia oxidation rate measurements. Potential ammonia oxidation measurements at coastal station P12 were conducted with water collected from 0 – 115 m in acid-washed 125 ml (175 ml capacity) polycarbonate bottles (Nalgene, USA). Bottles were rinsed twice with CTD-collected water, filled with at least one volume of overflow to maintain ambient gas concentrations, and spiked with 0.25 μM (final concentration) of $^{15}\text{NH}_4\text{Cl}$. Samples from 90 m were amended with ATU or PTIO at concentrations ranging from 0 – 1000 μM . One subsample was frozen at -20°C immediately for the initial $\delta^{15}\text{N} - \text{NO}_2^- + \text{NO}_3^-$ measurement. Samples were incubated on deck for 20 – 25 h in surface seawater-flowing incubators under simulated *in situ* light intensities using screen material. Although the temperature at 90 m was not the same as the surface temperature, previous research has shown that at this site, temperature of incubation does not alter the ammonia oxidation rate significantly during short term incubations (Horak et al., 2013). Final time point samples for $\delta^{15}\text{N} - \text{NO}_2^- + \text{NO}_3^-$ were frozen at -20°C and returned to the laboratory for further analysis.

For the metabolic inhibitors treatment at Ocean Station Papa, potential ammonia oxidation rate measurements were conducted with water collected at 70 m (primary nitrite maximum) in acid-washed and triple CTD-water rinsed 125 ml (175 ml capacity) polycarbonate bottles (Nalgene,

USA). Bottles were overflowed three times and amended with 50 nM $^{15}\text{NH}_4\text{Cl}$ (final concentration). Samples were also amended with either ATU or PTIO at concentrations ranging from 0 – 500 μM . One sample was immediately frozen for the initial $\delta^{15}\text{N} - \text{NO}_2^- + \text{NO}_3^-$ measurement. Samples were incubated shipboard in the dark at near *in situ* temperature (within 1 – 2°C) for 24 h. Final time point samples were flash frozen in a -70°C freezer and stored at -20°C until further analysis in the laboratory.

For experiments at both field sites, potential nitrification rates were determined by following accumulation of ^{15}N label in the $\text{NO}_2^- + \text{NO}_3^-$ pool with the “sodium azide method” as described previously (McIlvin and Altabet, 2005; Horak et al., 2013). Briefly, a 10 ml water sample was mixed with 100 μl 1 M imidazole buffer (final pH 8.5) and 0.4 g (Ocean Station Papa) or 1 g (coastal station P12) HCl-washed wet cadmium powder. Samples were shaken at 200 rpm on a rotary shaker for at least 12 h until NO_3^- was completely converted to NO_2^- . A 2 ml of cadmium-reduced sample was placed in septum vials and crimp sealed. Nitrite was converted to N_2O by addition of 0.6 ml of freshly prepared and N_2 -purged solution of 0.13 g ml^{-1} sodium azide in 20% acetic acid and neutralized with 0.3 ml 6 M NaOH. Headspace $^{44/45}\text{N}_2\text{O}$ ratios were subsequently analysed on a Thermo Finnigan Delta Plus continuous flow-isotope ratio mass spectrometer (Bremen, Germany). Nitrification rates were calculated from the change of $^{15}\text{N} - \text{NO}_2^- + \text{NO}_3^-$ at the beginning and end of the incubations according to the following equation (Ward et al., 1989; Horak et al., 2013):

$$r_{\text{NH}_4 - \text{ox}} = 2 \times N_{\text{N} + \text{N}} \times \frac{(n_i \text{NO}_x) - (n_o \text{NO}_x)}{\Delta T \times (N_T / N_{TA})}$$

Here, $r_{\text{NH}_4\text{-OX}}$ is the ammonia oxidation rate ($\text{nmol l}^{-1} \text{d}^{-1}$), $N_{\text{N+N}}$ is ambient $\text{NO}_2^- + \text{NO}_3^-$ concentration, $n_t\text{NO}_x$ is the atom percent (at %) of $^{15}\text{NO}_2^- + ^{15}\text{NO}_3^-$ at time t , $n_o\text{NO}_x$ is the measured initial at % of $^{15}\text{NO}_2^- + ^{15}\text{NO}_3^-$, ΔT is the change in time, N_T is concentration of $^{15}\text{NH}_4^+$ added, N_{TA} is tracer + ambient ammonia concentration. We assumed that initial ^{15}N at % of the unlabeled NH_4^+ pool was 0.3663.

In order to identify whether PTIO or ATU interfered with the sample $\delta^{15}\text{N}$ measurement, we added several concentrations of PTIO or ATU to sodium nitrate (NaNO_3) solutions of different $\delta^{15}\text{N}$ values, which were made by mixing NaNO_3 with $\text{Na}^{15}\text{NO}_3$ (98% ^{15}N , Cambridge Isotope Laboratory). Addition of PTIO and ATU did not affect the $\delta^{15}\text{N}$ of the solution (Fig. 5.11).

Molecular analyses. Water samples for rate measurements and molecular analyses were retrieved from the same sampling casts. From each depth, 2 l water sample was filtered onto a $0.2\mu\text{m}$ pore size Sterivex filter (GP-type, Millipore Inc.) and frozen at -80°C . In the laboratory, the Sterivex filters were opened with hot sterilized razor blades, filters were cut out, and DNA was isolated as described previously (Urakawa et al., 2010). Quantitative PCR targeting bacterial and archaeal *amoA* genes were performed on a Roche LightCycler using cycling conditions described previously (Urakawa et al., 2010; Horak et al., 2013). The primer sets used were amoA1F and amoA2R (Rotthauwe et al., 1997) targeting bacterial *amoA* genes, and CrenAmoAQ-F and CrenAmoAModR (Mincer et al., 2007) targeting archaeal *amoA* genes. Water samples for total prokaryotic cell counts were collected and fixed with glutardaldehyde (2% final concentration). Cell numbers were determined using Moviol-SybrGreen I staining

protocol (Lunau et al., 2005) with a Olympus BHS/BHT system microscope to count 20 random fields of view for each sample with 10 to 100 cells per field.

Acknowledgements

We thank the crew of the R/V *Clifford A. Barnes* and R/V *Kilo Moana* for their assistance with sample collection. We thank Carme Huguet, Amy Cash, Adam Gee, Sonia Tiquia, Laura Truxal, Davey French, Hantten Han, Katherine Heal, Maija Heller, Shady Amin, Willow Coyote-Maestas, Alex Nelson, Chelsea McCurry for assistance with onboard sample collection, nutrient analysis and/or sample preparation for mass spectrometry. We thank Emily Chang and Wade Jeffrey for technical assistance and José de la Torre, Florian Moeller, Paul Berube, Neeraja Vajrala, Luis Sajavedra-Soto, and Dan Arp for invaluable discussions. The excellent input of three anonymous reviewers greatly improved the quality of this manuscript. This work was funded by the United States National Science Foundation Grants MCB-0604448, OCE-0623174 and Dimensions of Biodiversity Program OCE-1046017.

The authors declare no conflict of interest.

References

- Agogué, H., Brink, M., Dinasquet, J., and Herndl, G.J. (2008b) Major gradients in putatively nitrifying and non-nitrifying Archaea in the deep North Atlantic. *Nature* **456**: 788-791.
- Arp, D.J., and Stein, L.Y. (2003) Metabolism of inorganic N compounds by ammonia-oxidizing bacteria. *Crit Rev Biochem Mol Biol* **38**: 471-495.
- Bartossek, R., Nicol, G.W., Lanzen, A., Klenk, H.P., and Schleper, C. (2010) Homologues of nitrite reductases in ammonia-oxidizing archaea: diversity and genomic context. *Environ Microbiol* **12**: 1075-1088.
- Beaumont, H.J.E., Hommes, N.G., Sayavedra-Soto, L.A., Arp, D.J., Arciero, D.M., Hooper, A.B. et al. (2002) Nitrite reductase of *Nitrosomonas europaea* is not essential for production of gaseous nitrogen oxides and confers tolerance to nitrite. *J Bacteriol* **184**: 2557-2560.

- Beman, J.M., Popp, B.N., and Alford, S.E. (2012a) Quantification of ammonia oxidation rates and ammonia-oxidizing archaea and bacteria at high resolution in the Gulf of California and eastern tropical North Pacific Ocean. *Limnol Oceanogr* **57**: 711-726.
- Betlach, M.R., and Tiedje, J.M. (1981) Kinetic explanation for accumulation of nitrite, nitric oxide, and nitrous oxide during bacterial denitrification. *Appl Environ Microbiol* **42**: 1074-1084.
- Blainey, P.C., Mosier, A.C., Potanina, A., Francis, C.A., and Quake, S.R. (2011) Genome of a low-salinity ammonia-oxidizing archaeon determined by single-cell and metagenomic analysis. *PLoS ONE* **6**: e16626.
- Brochier-Armanet, C., Boussau, B., Gribaldo, S., and Forterre, P. (2008) Mesophilic crenarchaeota: proposal for a third archaeal phylum, the Thaumarchaeota. *Nat Rev Microbiol* **6**: 245-252.
- Davies, I.R., and Zhang, X.J. (2008) Nitric oxide selective electrodes. *Methods Enzymol* **436**: 63-95.
- de la Torre, J.R., Walker, C.B., Ingalls, A.E., Könneke, M., and Stahl, D.A. (2008) Cultivation of a thermophilic ammonia oxidizing archaeon synthesizing crenarchaeol. *Environ Microbiol* **10**: 810-818.
- Francis, C.A., Roberts, K.J., Beman, J.M., Santoro, A.E., and Oakley, B.B. (2005) Ubiquity and diversity of ammonia-oxidizing archaea in water columns and sediments of the ocean. *P Natl Acad Sci USA* **102**: 14683-14688.
- Goretski, J., Zafiriou, O.C., and Hollocher, T.C. (1990) Steady-state nitric oxide concentrations during denitrification. *J Biol Chem* **265**: 11535-11538.
- Grasshoff, K., Kremling, K., Erhard, M. (1999b) *Methods of Seawater Analysis*: Wiley-VCH, Weinheim, Germany.
- Hallam, S.J., Konstantinidis, K.T., Putnam, N., Schleper, C., Watanabe, Y., Sugahara, J. et al. (2006) Genomic analysis of the uncultivated marine crenarchaeote *Cenarchaeum symbiosum*. *Proc Natl Acad Sci USA* **103**: 18296-18301.
- Hatzenpichler, R., Lebedeva, E.V., Spieck, E., Stoecker, K., Richter, A., Daims, H., and Wagner, M. (2008) A moderately thermophilic ammonia-oxidizing crenarchaeote from a hot spring. *P Natl Acad Sci USA* **105**: 2134-2139.
- Heinrich, T.A., da Silva, R.S., Miranda, K.M., Switzer, C.H., Wink, D.A., and Fukuto, J.M. (2013) Biological nitric oxide signalling: chemistry and terminology. *Br J Pharmacol* **169**: 1417-1429.
- Hollibaugh, J.T., Gifford, S.M., Moran, M.A., Ross, M.J., Sharma, S., and Tolar, B.B. (2014a) Seasonal variation in the metatranscriptomes of a Thaumarchaeota population from SE USA coastal waters. *ISME J* **8**: 685-698.
- Holmes, R.M., Aminot, A., Kerouel, R., Hooker, B.A., and Peterson, B.J. (1999) A simple and precise method for measuring ammonium in marine and freshwater ecosystems. *Can J Fish Aquat Sci* **56**: 1801-1808.
- Hooper, A.B. (1968) A nitrite-reducing enzyme from *Nitrosomonas europaea* - Preliminary characterization with hydroxylamine as electron donor. *Biochim Biophys Acta* **162**: 49-65.
- Hooper, A.B., and Terry, K.R. (1973) Specific inhibitors of ammonia oxidation in *Nitrosomonas*. *Antonie van Leeuwenhoek* **115**: 480-485.
- Horak, R.E.A., Qin, W., Schauer, A.J., Armbrust, E.V., Ingalls, A.E., Moffett, J.W. et al. (2013) Ammonia oxidation kinetics and temperature sensitivity of a natural marine community dominated by Archaea. *Isme J* **7**: 2023-2033.

- Hyman, M.R., Kim, C.Y., and Arp, D.J. (1990) Inhibition of ammonia monooxygenase in *Nitrosomonas europaea* by carbon disulfide. *J Bacteriol* **172**: 4775-4782.
- Jia, Z., and Conrad, R. (2009) Bacteria rather than Archaea dominate microbial ammonia oxidation in an agricultural soil. *Environ Microbiol* **11**: 1658-1671.
- Jung, M.Y., Well, R., Min, D., Giesemann, A., Park, S.J., Kim, J.G. et al. (2014b) Isotopic signatures of N₂O produced by ammonia-oxidizing archaea from soils. *ISME J* **8**: 1115-1125.
- Karner, M.B., DeLong, E.F., and Karl, D.M. (2001) Archaeal dominance in the mesopelagic zone of the Pacific Ocean. *Nature* **409**: 507-510.
- Kartal, B., Maalcke, W.J., de Almeida, N.M., Cirpus, I., Gloerich, J., Geerts, W. et al. (2011) Molecular mechanism of anaerobic ammonium oxidation. *Nature* **479**: 127-130.
- Kim, B.K., Jung, M.Y., Yu, D.S., Park, S.J., Oh, T.K., Rhee, S.K., and Kim, J.F. (2011) Genome Sequence of an Ammonia-Oxidizing Soil Archaeon, "*Candidatus Nitrosoarchaeum koreensis*" MY1. *J Bacteriol* **193**: 5539-5540.
- Könneke, M., Bernhard, A.E., de la Torre, J.R., Walker, C.B., Waterbury, J.B., and Stahl, D.A. (2005) Isolation of an autotrophic ammonia-oxidizing marine archaeon. *Nature* **437**: 543-546.
- Lees, H. (1946) Effect of copper-enzyme poisons on soil nitrification. *Nature* **158**: 97.
- Lees, H. (1952) The biochemistry of the nitrifying organisms. 1. The ammonia-oxidizing systems of *Nitrosomonas*. *Biochem J* **52**: 134-139.
- Lehtovirta-Morley, L.E., Stoecker, K., Vilcinskas, A., Prosser, J.I., and Nicol, G.W. (2011) Cultivation of an obligate acidophilic ammonia oxidizer from a nitrifying acid soil. *Proc Natl Acad Sci USA* **108**: 15892-15897.
- Leininger, S., Urich, T., Schloter, M., Schwark, L., Qi, J., Nicol, G.W. et al. (2006) Archaea predominate among ammonia-oxidizing prokaryotes in soils. *Nature* **442**: 806-809.
- Lipschultz, F., Zafiriou, O.C., Wofsy, S.C., Mcelroy, M.B., Valois, F.W., and Watson, S.W. (1981) Production of NO and N₂O by soil nitrifying bacteria. *Nature* **294**: 641-643.
- Löscher, C.R., Kock, A., Könneke, M., LaRoche, J., Bange, H.W., and Schmitz, R.A. (2012) Production of oceanic nitrous oxide by ammonia-oxidizing archaea. *Biogeosciences* **9**: 2419-2429.
- Lunau, M., Lemke, A., Walther, K., Martens-Habbena, W., and Simon, M. (2005) An improved method for counting bacteria from sediments and turbid environments by epifluorescence microscopy. *Environ Microbiol* **7**: 961-968.
- Martens-Habbena, W., and Stahl, D.A. (2011b) Nitrogen metabolism and kinetics of ammonia-oxidizing archaea. *Methods Enzymol* **496**: 465-487.
- Martens-Habbena, W., Berube, P.M., Urakawa, H., de la Torre, J.R., and Stahl, D.A. (2009b) Ammonia oxidation kinetics determine niche separation of nitrifying Archaea and Bacteria. *Nature* **461**: 976-U234.
- McCarty, G.W. (1999) Modes of action of nitrification inhibitors. *Biol Fertil Soils* **29**: 1-9.
- Mellvin, M.R., and Altabet, M.A. (2005) Chemical conversion of nitrate and nitrite to nitrous oxide for nitrogen and oxygen isotopic analysis in freshwater and seawater. *Anal Chem* **77**: 5589-5595.
- Mincer, T.J., Church, M.J., Taylor, L.T., Preston, C., Karl, D.M., and DeLong, E.F. (2007) Quantitative distribution of presumptive archaeal and bacterial nitrifiers in Monterey Bay and the North Pacific Subtropical Gyre. *Environ Microbiol* **9**: 1162-1175.
- Mussmann, M., Brito, I., Pitcher, A., Damsté, J.S.S., Hatzenpichler, R., Richter, A. et al. (2011) Thaumarchaeotes abundant in refinery nitrifying sludges express *amoA* but are not obligate autotrophic ammonia oxidizers. *Proc Natl Acad Sci USA* **108**: 16771-16776.

- Newell, S.E., Fawcett, S.E., and Ward, B.B. (2013) Depth distribution of ammonia oxidation rates and ammonia-oxidizer community composition in the Sargasso Sea. *Limnol Oceanogr* **58**: 1491-1500.
- Nicol, G.W., Leininger, S., Schleper, C., and Prosser, J.I. (2008) The influence of soil pH on the diversity, abundance and transcriptional activity of ammonia oxidizing archaea and bacteria. *Environ Microbiol* **10**: 2966-2978.
- Norton, J.M., Alzerreca, J.J., Suwa, Y., and Klotz, M.G. (2002) Diversity of ammonia monooxygenase operon in autotrophic ammonia-oxidizing bacteria. *Arch Microbiol* **177**: 139-149.
- Offre, P., Prosser, J.I., and Nicol, G.W. (2009) Growth of ammonia-oxidizing archaea in soil microcosms is inhibited by acetylene. *FEMS Microbiol Ecol* **70**: 99-108.
- Oremland, R.S., and Capone, D.G. (1988) Use of specific inhibitors in biogeochemistry and microbial ecology. *Adv Microb Ecol* **10**: 285-383.
- Pearson, A., Huang, Z., Ingalls, A.E., Romanek, C.S., Wiegel, J., Freeman, K.H. et al. (2004) Nonmarine crenarchaeol in Nevada hot springs. *Appl Environ Microbiol* **70**: 5229-5237.
- Qin, W., Amin, S.A., Martens-Habbena, W., Walker, C.B., Urakawa, H., Devol, A.H. et al. (2014) Marine ammonia-oxidizing archaeal isolates display obligate mixotrophy and wide ecotypic variation. *P Natl Acad Sci USA* **111**: 12504-12509.
- Ritchie, G.A.F., and Nicholas, D.J. (1972) Identification of the sources of nitrous oxide produced by oxidative and reductive processes in *Nitrosomonas europaea*. *Biochem J* **126**: 1181-1191.
- Rotthauwe, J.H., Witzel, K.P., and Liesack, W. (1997) The ammonia monooxygenase structural gene *amoA* as a functional marker: Molecular fine-scale analysis of natural ammonia-oxidizing populations. *Appl Environ Microbiol* **63**: 4704-4712.
- Santoro, A.E., Casciotti, K.L., and Francis, C.A. (2010) Activity, abundance and diversity of nitrifying archaea and bacteria in the central California Current. *Environ Microbiol* **12**: 1989-2006.
- Santoro, A.E., Buchwald, C., McIlvin, M.R., and Casciotti, K.L. (2011) Isotopic Signature of N₂O Produced by Marine Ammonia-Oxidizing Archaea. *Science* **333**: 1282-1285.
- Schmidt, I., van Spanning, R.J., and Jetten, M.S. (2004a) Denitrification and ammonia oxidation by *Nitrosomonas europaea* wild-type, and NirK- and NorB-deficient mutants. *Microbiol* **150**: 4107-4114.
- Schmidt, I., Steenbakkers, P.J.M., op den Camp, H.J.M., Schmidt, K., and Jetten, M.S.M. (2004b) Physiologic and proteomic evidence for a role of nitric oxide in biofilm formation by *Nitrosomonas europaea* and other ammonia oxidizers. *J Bacteriol* **186**: 2781-2788.
- Shapleigh, J.P., and Payne, W.J. (1985) Differentiation of *c*, *d*₁ cytochrome and copper nitrite reductase production in denitrifiers. *FEMS Microbiol Lett* **26**: 275-279.
- Shen, T.L., Stieglmeier, M., Dai, J.L., Urich, T., and Schleper, C. (2013) Responses of the terrestrial ammonia-oxidizing archaeon *Ca. Nitrososphaera viennensis* and the ammonia-oxidizing bacterium *Nitrospira multififormis* to nitrification inhibitors. *FEMS Microbiol Lett* **344**: 121-129.
- Spang, A., Hatzenpichler, R., Brochier-Armanet, C., Rattei, T., Tischler, P., Spieck, E. et al. (2010) Distinct gene set in two different lineages of ammonia-oxidizing archaea supports the phylum Thaumarchaeota. *Trends Microbiol* **18**: 331-340.
- Spang, A., Poehlein, A., Offre, P., Zumbragel, S., Haider, S., Rychlik, N. et al. (2012) The genome of the ammonia-oxidizing Candidatus *Nitrososphaera gargensis*: insights into metabolic versatility and environmental adaptations. *Environ Microbiol* **14**: 3122-3145.

- Stahl, D.A., and de la Torre, J.R. (2012b) Physiology and diversity of ammonia-oxidizing archaea. *Annu Rev Microbiol* **66**: 83-101.
- Stein, L.Y. (2011a) Surveying N₂O-producing pathways in bacteria. *Methods Enzymol* **486**: 131-152.
- Stewart, F.J., Ulloa, O., and DeLong, E.F. (2012) Microbial metatranscriptomics in a permanent marine oxygen minimum zone. *Environ Microbiol* **14**: 23-40.
- Stieglmeier, M., Mooshammer, M., Kitzler, B., Wanek, W., Zechmeister-Boltenstern, S., Richter, A., and Schleper, C. (2014a) Aerobic nitrous oxide production through N-nitrosating hybrid formation in ammonia-oxidizing archaea. *ISME J* **8**: 1135-1146.
- Taylor, A.E., Zeglin, L.H., Wanzek, T.A., Myrold, D.D., and Bottomley, P.J. (2012) Dynamics of ammonia-oxidizing archaea and bacteria populations and contributions to soil nitrification potentials. *ISME J* **6**: 2024-2032.
- Taylor, A.E., Vajrala, N., Giguere, A.T., Gitelman, A.I., Arp, D.J., Myrold, D.D. et al. (2013) Use of aliphatic n-alkynes to discriminate soil nitrification activities of ammonia-oxidizing thaumarchaea and bacteria. *Appl Environ Microbiol* **79**: 6544-6551.
- Tourna, M., Stieglmeier, M., Spang, A., Könneke, M., Schintlmeister, A., Urich, T. et al. (2011) *Nitrososphaera viennensis*, an ammonia oxidizing archaeon from soil. *Proc Natl Acad Sci USA* **108**: 8420-8425.
- UNESCO (1994) Protocols for the Joint Global Ocean Flux Study (JGOFS) Core Measurements. In *IOC Manual and Guides* 29.
- Urakawa, H., Martens-Habbena, W., and Stahl, D.A. (2010) High abundance of ammonia-oxidizing archaea in coastal waters, determined using a modified DNA extraction method. *Appl Environ Microbiol* **76**: 2129-2135.
- Urakawa, H., Martens-Habbena, W., Huguet, C., de la Torre, J.R., Ingalls, A.E., Devol, A.H., and Stahl, D.A. (2014) Ammonia availability shapes the seasonal distribution and activity of archaeal and bacterial ammonia oxidizers in the Puget Sound Estuary. *Limnol Oceanogr* (*in press*).
- Vajrala, N., Bottomley, P.J., Stahl, D.A., Arp, D.J., and Sayavedra-Soto, L.A. (2014) Cycloheximide prevents the *de novo* polypeptide synthesis required to recover from acetylene inhibition in *Nitrosopumilus maritimus*. *FEMS Microbiol Ecol* **88**: 495-502.
- Vajrala, N., Martens-Habbena, W., Sayavedra-Soto, L.A., Schauer, A., Bottomley, P.J., Stahl, D.A., and Arp, D.J. (2013) Hydroxylamine as an intermediate in ammonia oxidation by globally abundant marine archaea. *P Natl Acad Sci USA* **110**: 1006-1011.
- Verhamme, D.T., Prosser, J.I., and Nicol, G.W. (2011) Ammonia concentration determines differential growth of ammonia-oxidising archaea and bacteria in soil microcosms. *ISME J* **5**: 1067-1071.
- Walker, C.B., de la Torre, J.R., Klotz, M.G., Urakawa, H., Pinel, N., Arp, D.J. et al. (2010) *Nitrosopumilus maritimus* genome reveals unique mechanisms for nitrification and autotrophy in globally distributed marine crenarchaea. *P Natl Acad Sci USA* **107**: 8818-8823.
- Ward, B.B., and Zafiriou, O.C. (1988) Nitrification and nitric oxide in the oxygen minimum of the eastern tropical North Pacific. *Deep-Sea Res I* **35**: 1127-1142.
- Ward, B.B., Kilpatrick, K.A., Renger, E.H., and Eppley, R.W. (1989) Biological nitrogen cycling in the nitracline. *Limnol Oceanogr* **34**: 493-513.
- Wuchter, C., Abbas, B., Coolen, M.J.L., Herfort, L., van Bleijswijk, J., Timmers, P. et al. (2006) Archaeal nitrification in the ocean. *Proc Natl Acad Sci USA* **103**: 12317-12322.

Yan, J., Haaijer, S.C.M., den Camp, H.J.M.O., van Niftrik, L., Stahl, D.A., Konneke, M. et al. (2012b) Mimicking the oxygen minimum zones: stimulating interaction of aerobic archaeal and anaerobic bacterial ammonia oxidizers in a laboratory-scale model system. *Environ Microbiol* **14**: 3146-3158.

Zart, D., Schmidt, I., and Bock, E. (2000) Significance of gaseous NO for ammonia oxidation by *Nitrosomonas eutropha*. *Antonie van Leeuwenhoek* **77**: 49-55.

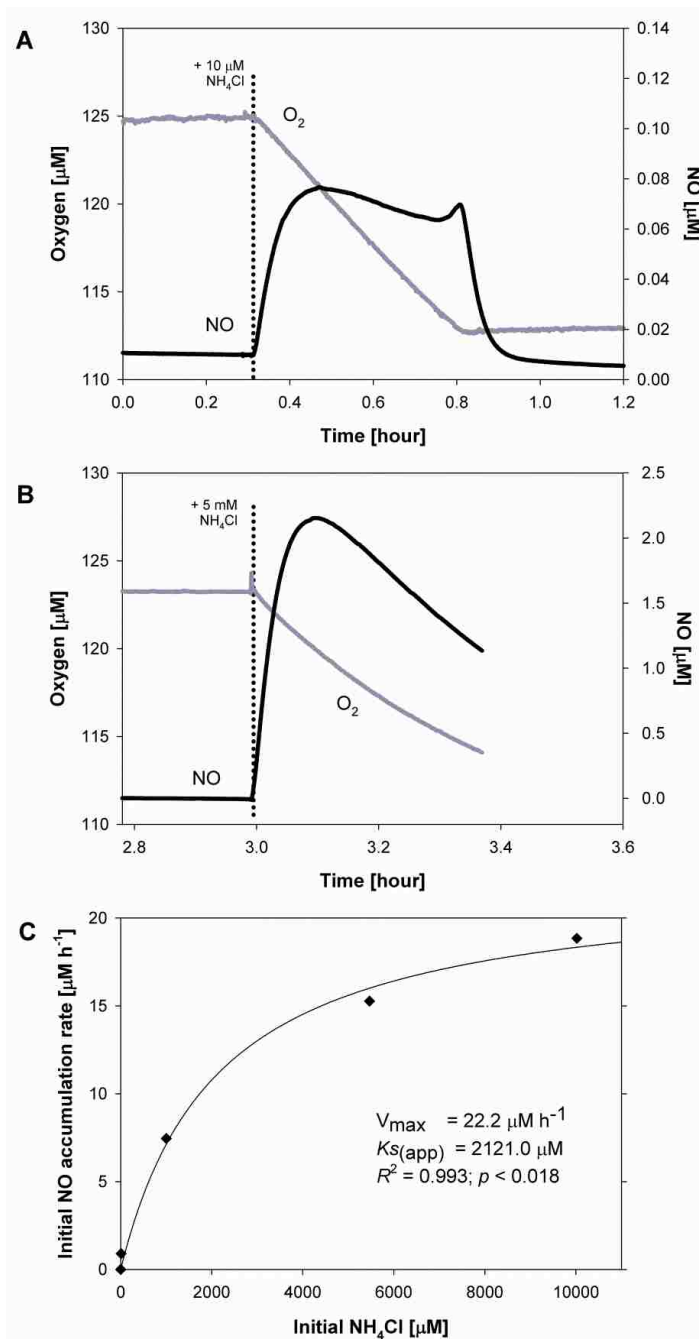


Figure 5.1. Metabolism of NO in SCM1.

(A, B) Oxygen uptake and NO accumulation following ammonium addition to ammonium-depleted cultures of SCM1. Oxygen uptake and NO accumulation at $10 \mu\text{M TAN}$ (A) and 5 mM TAN (B) are shown. (C) Ammonium-dependent kinetics of initial NO accumulation.

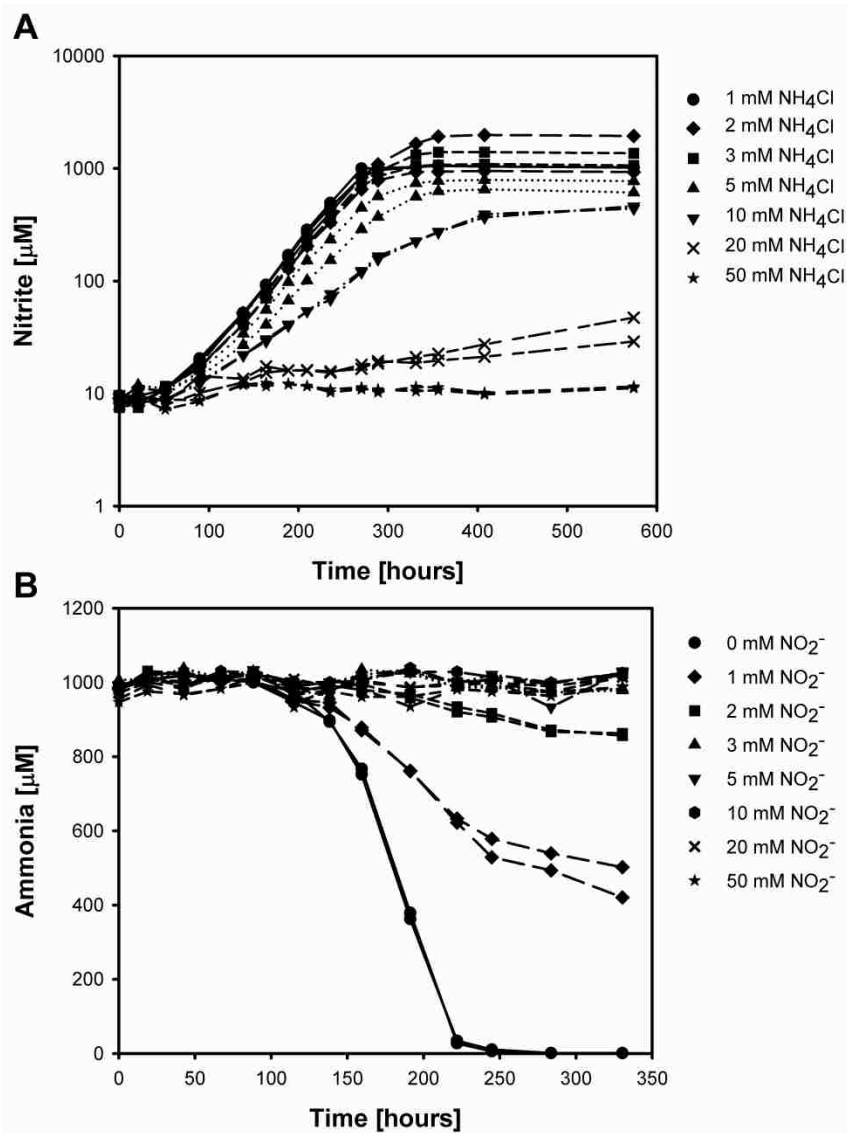


Figure 5.2. Growth of SCM1 as a function of initial ammonia (A) and nitrite concentrations (B). Cells from exponentially growing culture ($\sim 500 \mu\text{M}$ ammonia and $500 \mu\text{M}$ nitrite) were transferred to growth medium with various initial ammonia or nitrite concentrations, and nitrite accumulation (logarithmic scale) and ammonia consumption (linear scale) were monitored daily.

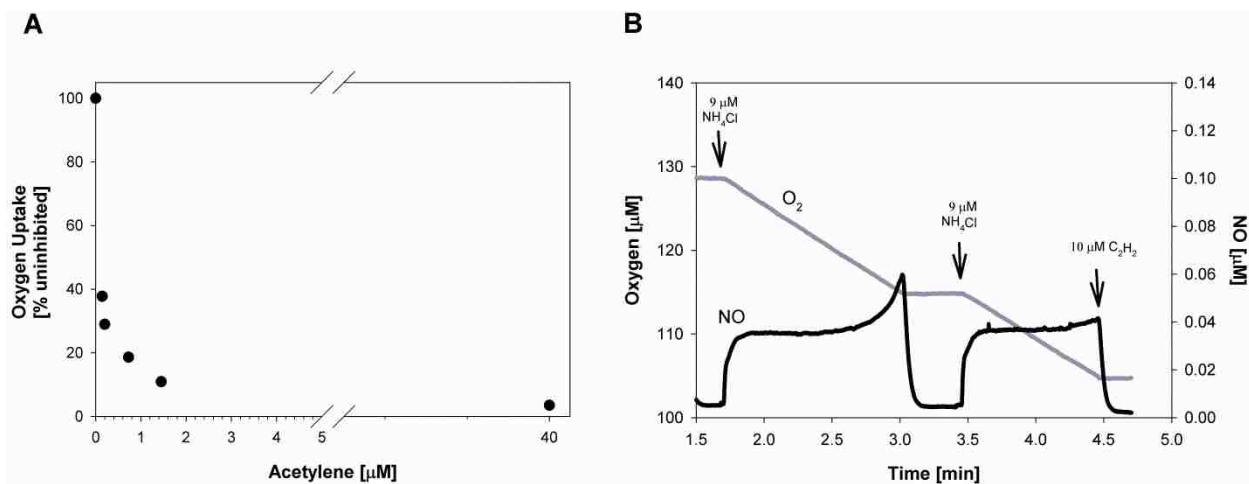


Figure 5.3. Inhibition of ammonia oxidation in SCM1 by acetylene.

(A) Kinetics of acetylene inhibition. (B) Inhibition of ammonia dependent O_2 uptake and NO accumulation by acetylene determined in microelectrode chamber experiments. Acetylene was added with $3\mu\text{M}$ ammonia remaining.

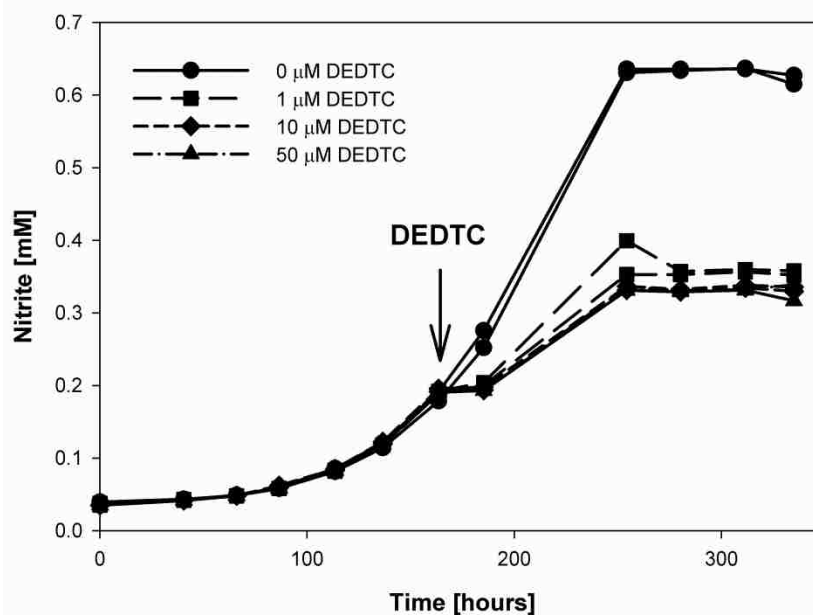


Figure 5.4. Effect of different concentrations of DEDTC on the growth of mid-exponential phase SCM1 cells as measured by nitrite production.

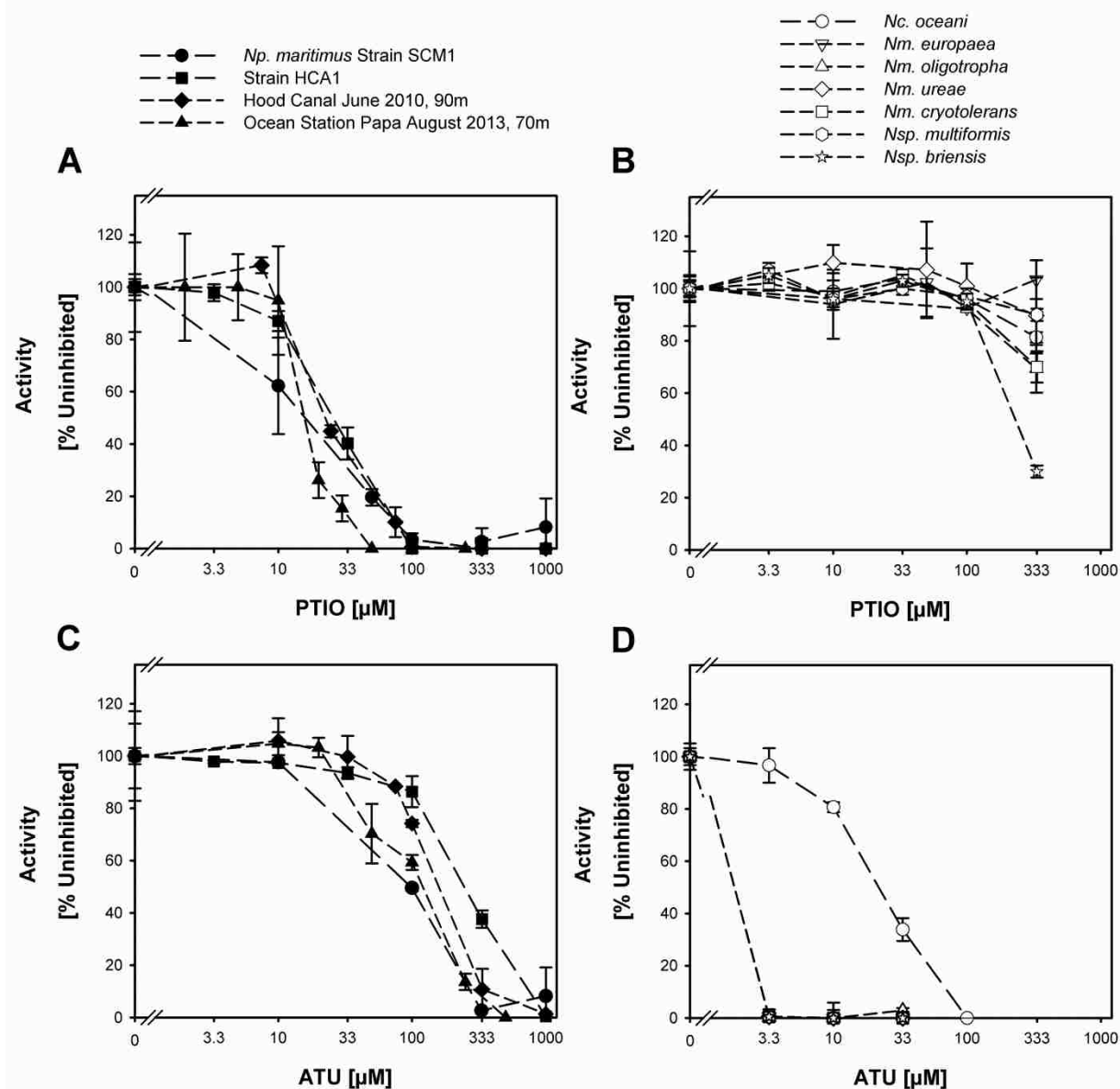


Figure 5.5. Response of marine AOA isolates, and natural communities (solid) and β -AOB and γ -AOB strains (open) to the nitrogen free radical scavenger PTIO (A, B) and ATU (C, D).

AOA and AOB strains were amended with PTIO and ATU during exponential growth phase and nitrite production was determined after a 24 h incubation.

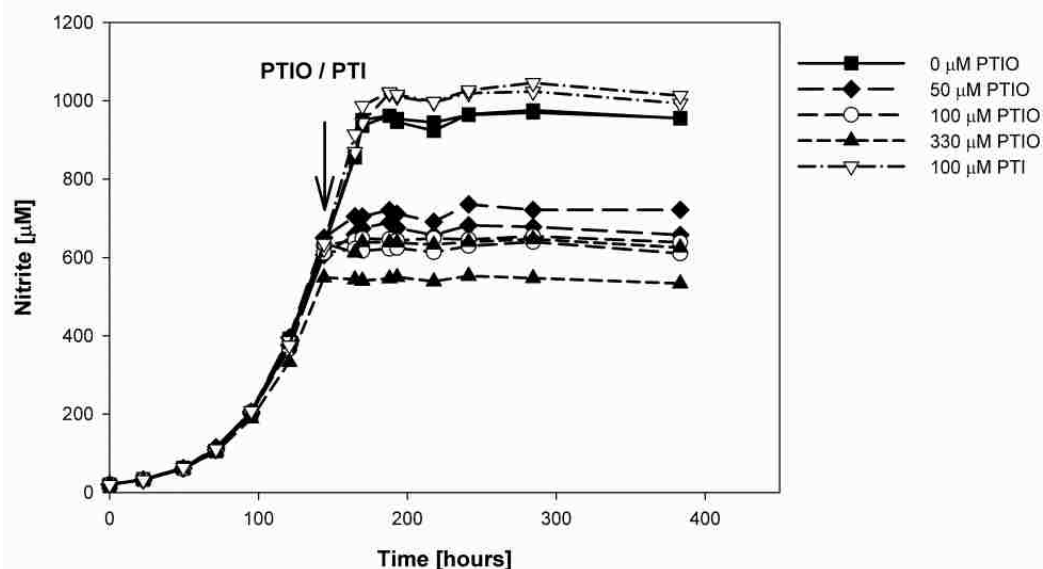


Figure 5.6. Influence of PTIO and PTI (NO-treated PTIO) on ammonia oxidation activity of mid-exponential phase SCM1 cells.

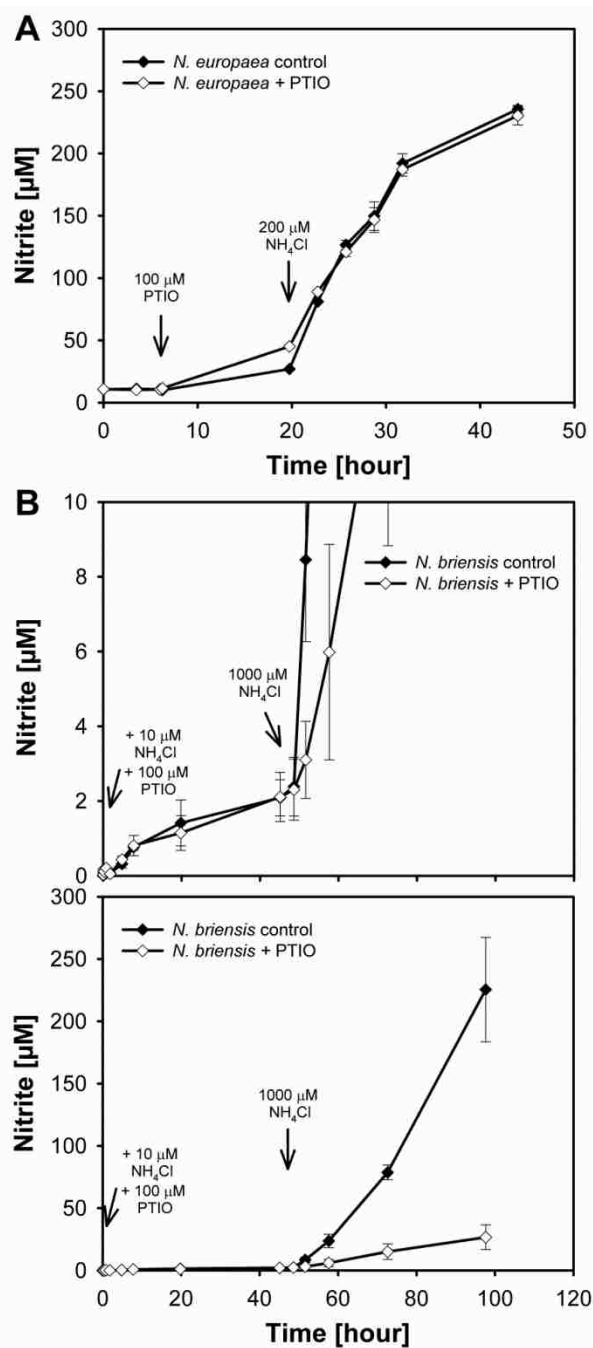


Figure 5.7. Influence of ammonia starvation on the response of *N. europaea* (A) and *N. briensis* (B) to 100 μM PTIO addition.

Cells harvested from exponential growth phase were starved for 20 h (*N. europaea*), and 200 h (*N. briensis*), and subsequently revived with ammonia in the presence or absence of PTIO. The scale used in the y axis is different to allow a proper representation of results.

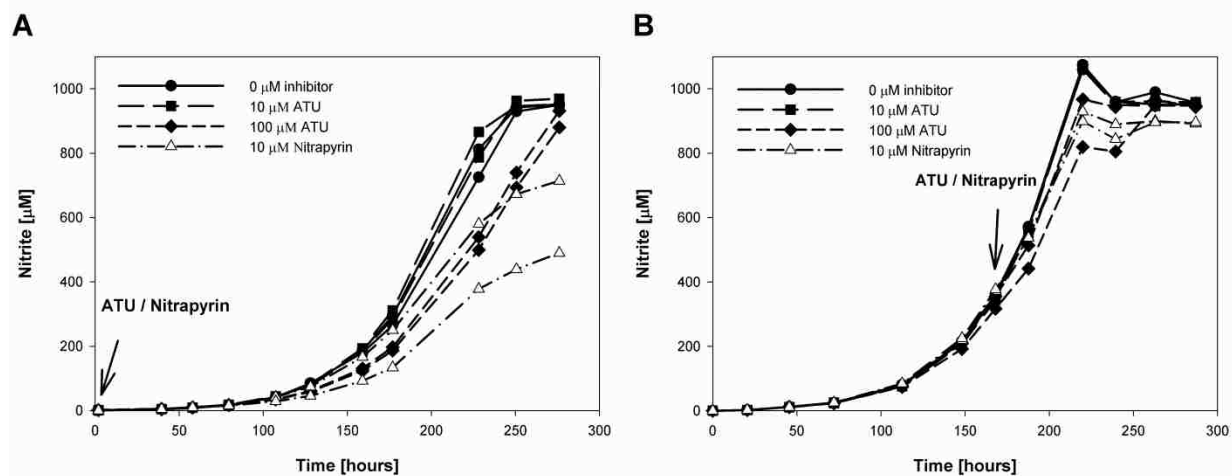


Figure 5.8. Influence of ATU and nitrapyrin on ammonia oxidation activity of SCM1. ATU and nitrapyrin were added either at $t = 0$ (A), or at mid-exponential phase (B).

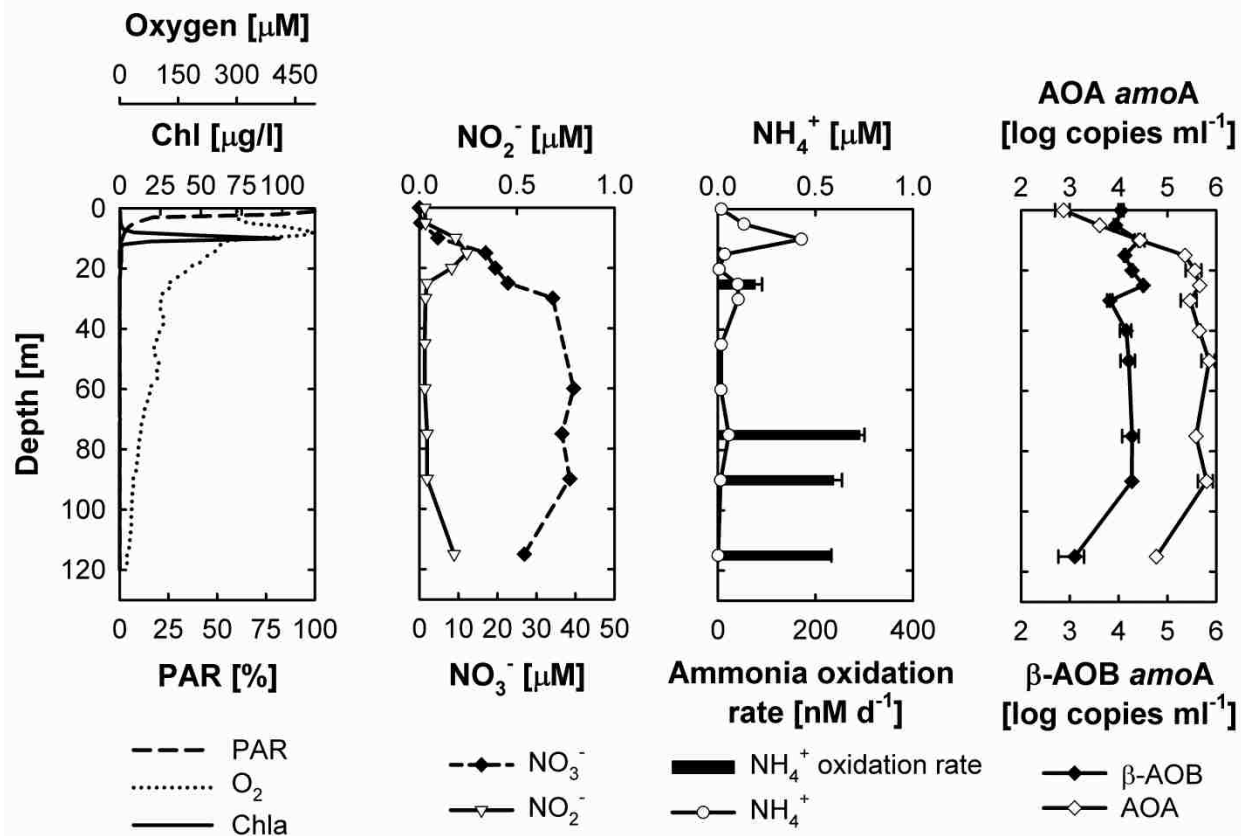


Figure 5.9. Hydrography, inorganic nitrogen nutrients, ammonia oxidation rates and AOA and β -AOB *amoA* gene copy numbers in Hood Canal, WA, on June 2010.

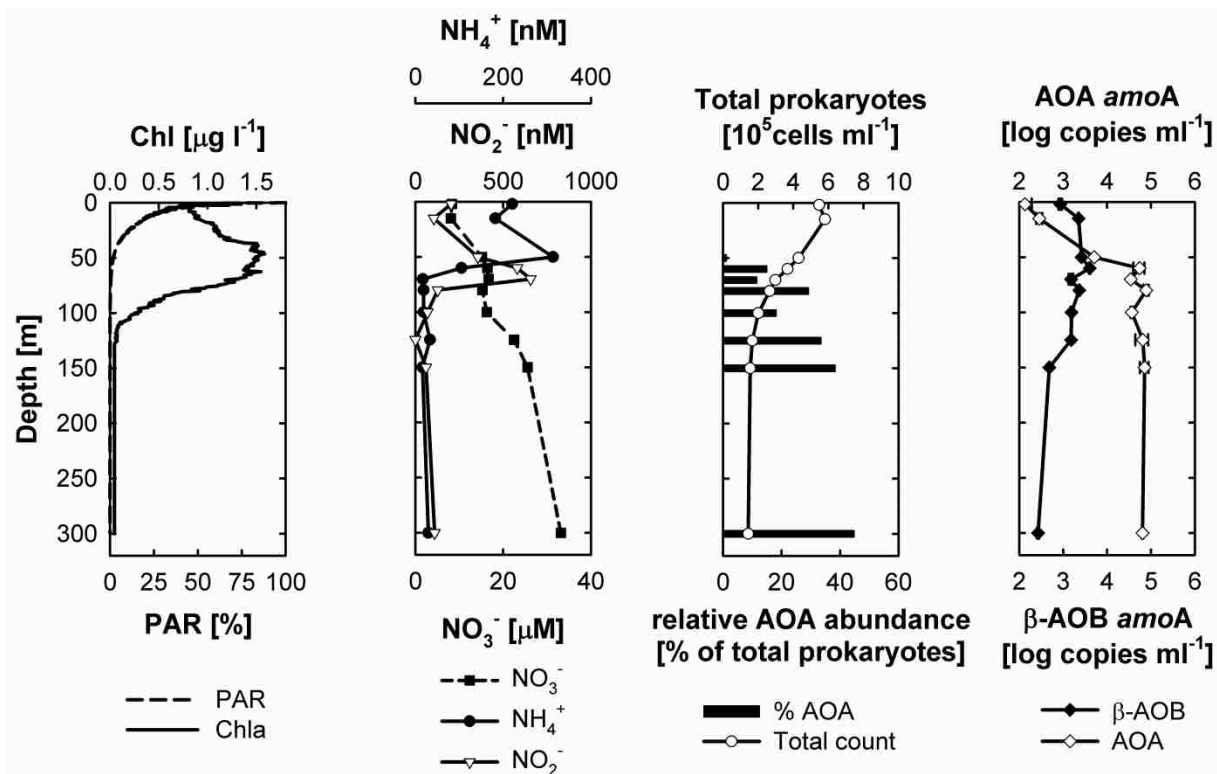


Figure 5.10. Hydrography, inorganic nitrogen nutrients, total prokaryotic cell counts, and AOA and β -AOB *amoA* gene copy numbers in Ocean Station Papa, North Pacific Ocean, on August 2013.

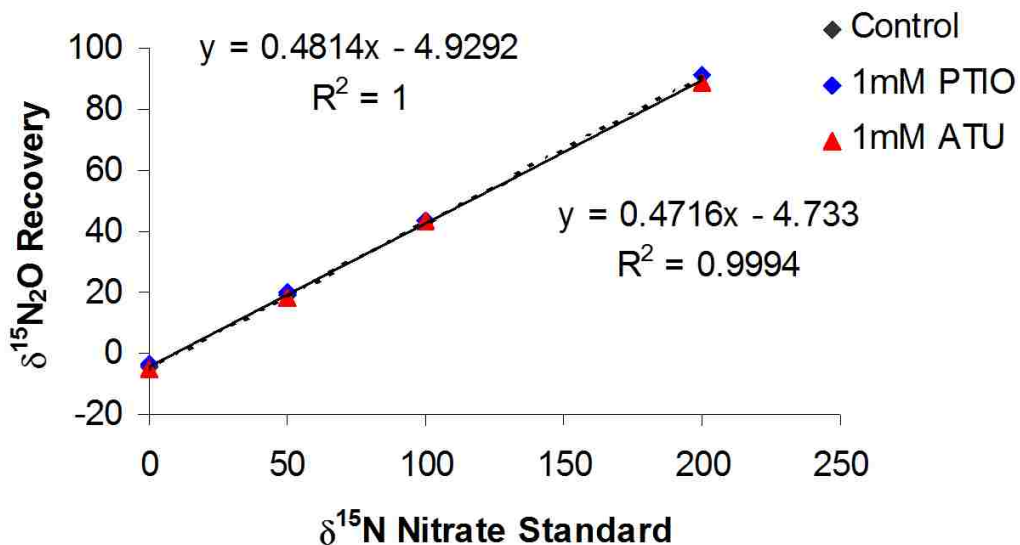


Figure 5.11. The influence of PTIO and ATU on the sample $\delta^{15}\text{N}$ measurement.

The $\delta^{15}\text{N}_2\text{O}$ recovery were plotted against NaNO_3 solutions of different $\delta^{15}\text{N}$ values with 1 mM PTIO, 1mM ATU relative to control without inhibitor addition. The linear regression lines and equations were generated and R^2 values were calculated for PTIO treatment samples (dotted line, $y = 0.4814x - 4.9292$; $R^2 = 1.0000$) and ATU treatment samples (solid line, $y = 0.4716x - 4.733$; $R^2 = 0.9994$), respectively.

Chapter 6.

Influence of ammonia and copper availabilities on the molecular physiology of the marine ammonia-oxidizing archaeon

Nitrosopumilus maritimus

Wei Qin¹, Shady A. Amin², Rachel A. Lundeen¹, Katherine R. Heal¹, Willm Martens-Habben¹, Hidetoshi Urakawa³, Kyle C. Costa⁴, Serdar Turkarslan⁵, Erik Hendrickson¹, David Beck¹, Sonia Tequia⁶, Fred Taub¹, Andrew Holmes⁷, Todd Lowe⁷, James W. Moffett⁸, Alan H. Devol¹, Nitin Baliga⁵, Daniel Arp⁹, Luis A. Sayavedra-Soto⁹, Murray Hackett¹, E. Virginia Armbrust¹, Anitra E. Ingalls¹, and David A. Stahl^{1,*}

In preparation

¹University of Washington; ²NYU Abu Dhabi; ³Florida Gulf Coast University; ⁴California Institute of Technology; ⁵Institute for Systems Biology; ⁶University of Michigan, Dearborn; ⁷University of California, Santa Cruz; ⁸University of Southern California; ⁹Oregon State University.

*Corresponding author E-mail: dastahl@u.washington.edu.

Abstract

Marine ammonia-oxidizing archaea (AOA) are among the most abundant microorganisms in the ocean. They play a key role in the marine nitrogen cycle by catalyzing the oxidation of ammonia to nitrite via a copper-centric enzymatic system, and are well-adapted to life under the extreme ammonia limitation common in oligotrophic oceans. Here we use whole-genome microarray and RNA-sequencing transcriptomics, as well as high-resolution mass spectrometry-based proteomics to study the molecular level responses of the model marine ammonia-oxidizing archaeon *Nitrosopumilus maritimus* to changing ammonia and copper availability. In exponentially growing cells, approximately 90% and 69% of protein-coding genes were detected in the transcriptome and proteome, respectively. Overall the transcriptome indicated an apparent reduction in the essential energy production and biosynthetic functions in the ammonia-starved and Cu-stressed cells, and an activation of the ammonia oxidation pathway during ammonia-recovery. We show that *N. maritimus* down-regulated the transcription of genes encoding the A and B subunits of ammonia monooxygenase (AMO) under starvation condition, yet maintained relatively high levels of the transcription of *amoC* encoding the C subunit. Thus, as is hypothesized for the bacterial ammonia oxidizers, the AmoC is most likely a starvation stress-responsive subunit facilitating recovery of an active AMO. Notably, we demonstrated that a remarkably high fraction of intracellular cobalamin (vitamin B₁₂) is in the form of nitrocobalamin, and suggest that its formation results from the reaction of cobalamin with nitric oxide (NO) produced during ammonia oxidation. The up-regulation of most genes in the pathway for cobalamin synthesis was correlated with increased fractional representation of the nitrocobalamin form, implicating an important interplay between NO flux and cobalamin synthesis in the ecophysiology of AOA. Together, this study provides new insights into the

molecular physiological basis of the adaptation of AOA to physicochemical changes in marine systems.

Introduction

The discovery of ammonia-oxidizing archaea (AOA) in marine and terrestrial environments has changed our understanding of the global nitrogen cycle (Stahl and de la Torre, 2012a). Their high abundance and activity in the pelagic ocean, comprising as 40% of the total microbial population (Karner et al., 2001; Francis et al., 2005), and their transcripts sometimes constituting a major fraction of marine metatranscriptomes (Hollibaugh et al., 2011; Baker et al., 2012; Stewart et al., 2012), suggest they play major roles in global biogeochemical cycles. Indeed, AOA play a critical role in marine nitrification by converting ammonia, a major product of nitrogen fixation and mineralization, to nitrite (Martens-Habbena et al., 2009b; Martens-Habbena et al., 2015). Nitrite is subsequently utilized by nitrite-oxidizing bacteria to generate nitrate, which constitutes the major bioavailable source of nitrogen for phytoplankton in the marine environment (Yool et al., 2007). AOA also play an important role in carbon fixation (Könneke et al., 2014) and production of greenhouse gases, such as nitrous oxide and methane (Santoro et al., 2011; Metcalf et al., 2012).

The oceans are dynamic environments with often low and patchy distribution of nutrients (Guasto et al., 2012). The high abundance and activity of AOA throughout the marine environment suggest strong adaptation and resilience to such dynamic conditions. For example, AOA possess a high affinity for ammonia that presumably helps sustain ammonia oxidation and growth despite low ammonium concentrations in large areas of the oceans (Martens-Habbena et

al., 2009b; Horak et al., 2013; Nakagawa and Stahl, 2013). In addition, some AOA isolates can use other sources of nitrogen besides ammonia, such as cyanate or urea (Qin et al., 2014; Palatinszky et al., 2015). Despite these adaptations, it is not clear how AOA respond to sporadic pulses of nitrogen over the span of hours or days, and the molecular machinery that facilitates such responses.

Similarly, a variant trace element requirement of AOA may allow them to persist throughout the marine environment. Most notably, a large fraction of proteins involved in electron transfer and ammonia oxidation in AOA are copper-dependent enzymes (Walker et al., 2010). Such a reliance on copper rather than the typical iron-dependent proteins (e.g., cytochromes) suggests AOA may be more competitive relative to other microbes in the open ocean where iron is often limiting and competition for iron is high (Amin et al., 2013). However, laboratory studies using *Nitrosopumilus maritimus* SCM1 suggest that AOA may be limited by copper concentrations prevalent in many regions in the marine environment (Amin et al., 2013; Jacquot et al., 2014).

Here we explore the molecular mechanisms possibly contributing to the success of AOA in the marine environment by examining the metabolic responses of *N. maritimus* SCM1 to ammonia and copper availabilities using transcriptional, proteomic and metabolomic analyses.

Results and Discussion

Global proteome

The global proteome of mid-exponential phase *N. maritimus* cells were analyzed by high-resolution mass spectrometry as detailed in materials and methods. Approximately 69% of the

total predicted proteins were recovered by proteomics analysis, indicating that, consistent with the oceanic species “*Candidatus Nitrosopelagicus brevis*” (Santoro et al., 2015), *N. maritimus* translated a high fraction of its genome during growth. The number of spectra detected for any given protein is dependent on many factors including protein size, how well the protein can be isolated, which is generally very poorly for membrane proteins, and how easily the component peptides can be detected by the mass spectrometer. Because of these factors, comparing total spectral counts between proteins is at best a rough estimate of protein levels within the cell. Nonetheless, the proteins with the highest number of spectral counts were consistent with expectations. The two proteins of highest abundances (Nmar_1547 and Nmar_1201) were the two predicted S-layer proteins (Fig. 6.1). S-layer proteins are expected to be present at high concentrations as they form a coat on the surface of *N. maritimus* and many other archaea and bacteria (Sara and Sleytr, 2000). Consistently, their homologous proteins (T478_1299 and T478_1300) were among the top three most abundant proteins in the proteome of early stationary phase *N. brevis* cells (Santoro et al., 2015). Likewise, of the most abundant transcripts reported in the marine metatranscriptomics study by Hollibaugh et. al., these two putative S-layer proteins (Nmar_1547 and Nmar_1201) top the list (no. 1 and 3 respectively) (Hollibaugh et al., 2011). In addition to S-layer and cell surface associated proteins, other most abundant proteins in the proteome were involved in energy production and conversion, transcription and translation, and carbon fixation (Fig. 6.1). Although the B subunit of the ammonia monooxygenase (Nmar_1503), a main component of ammonia oxidation pathway, was highly abundant (among the top 50 most abundant proteins) (Fig. 6.1), the A and C subunits (Nmar_1500 and Nmar_1502) were detected at relative low numbers of spectral counts, possibly due to poor protein recovery of these membrane-associated proteins.

Overall transcriptomic responses to changing ammonia and copper availability

The transcriptome of *N. maritimus* was measured under mid-log, ammonia starvation, and ammonia recovery conditions using microarrays. The arrays were designed using an early genome annotation (designation Nmar) (Walker et al., 2010). The arrays covered 1799 of the predicted 1997 Nmar open reading frames (Walker et al., 2010). The global gene expression patterns of the biological replicates were well clustered by different experimental conditions, indicating the good reproducibility of replicates (Fig. 6.2). Among the three conditions, the exponentially growing (mid-log) condition and recovery condition had similar transcriptomic profiles, but both were strikingly different from those of the ammonia starvation condition (Fig. 6.2A). Mid-log phase cells provided a control against cells deprived of ammonia to investigate the transcriptional response to ammonia starvation in *N. maritimus*. Using a P-value cutoff of 0.05, the ammonia-starved condition showed 480 transcripts with significantly altered abundance, 208 with reduced abundance, and 272 with increased abundance, compared to the non-starved mid-log controls. On the other hand, to better understand the transcriptional regulation of *N. maritimus* in response to ammonia resupply after ammonia deprivation, the transcriptome of cultures collected under the recovery and starvation conditions were compared. A total of 335 genes were differentially regulated, including 186 up-regulated genes and 149 down-regulated genes, in ammonia-revived cells relative to ammonia-starved cells. As expected, the transcript abundance changes in response to ammonia starvation and recovery conditions displayed an opposite global trend (Fig. 6.3A).

We also used RNA-sequencing to globally track changes in transcript abundances of *N. maritimus* cells grown under Cu-limited (5 nM total Cu) or Cu-toxic (750 nM total Cu) conditions compared to under Cu-replete condition (50 nM total Cu). Significant decrease in the nitrification production rate of *N. maritimus* were observed when copper concentrations were limiting or at an inhibitory excess. Of the 1799 transcripts detected by RNA-sequencing, 526 and 480 showed significant upregulation and downregulation ($P < 0.05$), respectively, in Cu-limited cells relative to control cells; while 460 and 344 were present at significantly increased and decreased levels, respectively, under Cu-toxic condition compared to Cu-replete condition. The hierarchical clustering analysis showed clear separation of the transcriptomic profiles of Cu-stressed cells from those of Cu-replete cells (Fig. 6.2B). Regardless of the large difference in copper concentrations, most of genes displayed similar transcriptional responses under Cu-limited and Cu-toxic conditions (Fig. 6.3B).

Ammonia oxidation and assimilation

The archaeal ammonia-oxidizing pathway has not been fully identified (Walker et al., 2010). However, it is known to be different than the bacterial pathway. One consistency between bacterial and archaeal systems is the ammonia monooxygenase (AMO) subunits. Of these, subunits A (Nmar_1500) and B (Nmar_1503) showed reduced transcript levels in ammonia-starved relative to control cells (Fig. 6.4). Notably, although, as part of the same operon, the subunit C (Nmar_1502) exhibited a different expression pattern, and its transcripts were presented at higher levels after 24 hours of ammonia deprivation (Fig. 6.4). The persistence of the AmoC message, or enhanced transcription of the *amoC*, following depletion of ammonia was previously shown in the ammonia-oxidizing bacteria, a beta-proteobacterium *Nitrosomonas*

europaea and a gamma-proteobacterium *Nitrosococcus oceani* (Sayavedra-Soto et al., 1998; Hommes et al., 2001; Stein et al., 2013).

To get additional insights into the transcriptional dynamics of *amo* operon in AOA and AOB during ammonia starvation, the transcript abundances of *amoA*, *B*, and *C* of *N. maritimus* and *N. europaea* were monitored by RT-qPCR over the starvation period of up to 200 hours (> 8days). The copy numbers of *amoA* and *amoB* transcripts per cell quickly dropped by up to 32-fold in *N. maritimus* after 9 hours of ammonia depletion and stayed at low levels for the rest of the starvation period (Fig. 6.5A). In contrast, consistent with the microarray data, *amoC* transcript abundance increased, or at least stayed relatively constant during the short-term starvation period (within 24 hours) (Fig. 6.5A). Although a marked decrease was observed after 2 days (48 hours) of starvation, the *amoC* transcript was still more abundant than the *amoA* and *amoB* transcripts in *N. maritimus* over more than 4 days (96 hours) of starvation (Fig. 6.5A). The similar expression patterns of *amoA*, *B*, and *C* was also observed in starved *N. europaea* cells. Although the *amoC* transcript was less abundant than those of *amoA* and *amoB* during exponential growth, it remained higher during ammonia starvation than the significantly reduced abundance of *amoA* transcripts (Fig. 6.5B). Taken together, these results revealed a similar differential regulation of *amo* gene transcript abundance in both *N. maritimus* and *N.europaea* in response to ammonia depletion. Thus, the retention of high levels of the *amoC* transcripts during energy starvation is a shared feature of the AOA and AOB. Previous studies with β - and γ -AOB suggested AmoC may act as a chaperone to repair and stabilize AMO holoenzyme during starvation (Berube et al., 2007; El Sheikh and Klotz, 2008; Berube and Stahl, 2012). It now appears that the AmoC

subunit of *N. maritimus* may also serve a similar role in maintaining ammonia oxidation function in response to transients of ammonia availability.

AOB has long been known to be remarkably resistant to energy source deprivation. For example, it was shown that *N. europaea* was capable of rapid resuscitation and retained more than 50% of maximum oxygen uptake activity after 17 days of starvation (Tappe et al., 1999). Yet, very little is known regarding the starvation resilience and recovery physiology of marine AOA. Therefore, parallel with the transcript abundance measurement, we also evaluated the starvation and recovery behavior of *N. maritimus* via the measurement of spontaneous oxygen update rate before and after a 100 μ M ammonia pulse following different time periods of starvation. After depletion of ammonia, the respiratory activity of *N. maritimus* immediately decreased to around background levels (Fig. 6.6). This trend was similar to that of the rapid decay of *amoA* and *amoB* transcripts in absence of ammonia (Fig. 6.5A). Notably, the abundance of *amoC* transcripts was tightly correlated with the ammonia-oxidizing potential during starvation of *N. maritimus*. When *amoC* transcripts were elevated during short-term starvation (<24 hours), the original activity was regained readily after ammonia readdition (Fig. 6.6). With significant decrease of *amoC* transcript abundance with prolonged starvation, *N. maritimus* cells lost capacity for rapid recovery (Fig. 6.6). Therefore, the combination of comparative transcriptional and physiological processes is consistent with a role of the *N. maritimus* AmoC in recovery from ammonia starvation stress, enabling cells to maintain a state of readiness for rapid recovery of ammonia-oxidizing activity after short-term starvation. Although *N. maritimus*-like AOA appear much less tolerant to extended starvation than characterized AOB, given their extremely low K_m value (24–133 nM) and substrate threshold (<

10 nM) for ammonia oxidation (Martens-Habbena et al., 2009b; Peng et al., 2016), they are expected to be infrequently experience long period of ammonia shortage in marine environments. In contrast, the growth thresholds of all characterized AOB to date are much higher than ammonia levels in most open ocean waters (Martens-Habbena et al., 2009b), suggesting that marine AOB may often face long-term energy limitation or starvation. Indeed, previous molecular surveys and field studies applying the selective inhibitors for bacterial ammonia oxidizer both indicated that, although present, AOB are not actively oxidizing ammonia and likely persist in a nearly dormant state in ammonia-depleted coastal waters and open oceans (Santoro et al., 2010; Stewart et al., 2012; Horak et al., 2013; Martens-Habbena et al., 2015). Thus, the AOB appear to have a different life history strategy, providing them adaptive advantage during long periods of low ammonia availability. For example, the generally quiescent marine AOB populations are expected to respond rapidly to the release of high concentrations of ammonia during and following a phytoplankton bloom.

Taken together, apart from substrate affinity and threshold, the starvation-recovery response also plays a critical role in niche differentiation between marine AOA and AOB. However, it still remains questionable whether the survival strategy of marine AOA is also shared with terrestrial AOA affiliated to the families *Nitrososphaeraceae* and *Nitrosotenuaceae*, which are commonly distributed in ammonia-rich environments, such as soil, hot spring, and engineered systems (Hatzenpichler et al., 2008; Lebedeva et al., 2013; Stieglmeier et al., 2014b; Li et al., 2016b). For example, a recent study by French et al. reported that a *Nitrosotenuis* species was capable of recovery even after starvation periods of nearly two months, and no significant differences in the speed of resuscitation were found during first 10 days of starvation (French and Bollmann,

2015). Notably, although most sequenced genomes of both marine and terrestrial AOA encode only one copy of *amoA* and *amoB*, in contrast to marine AOA, many characterized terrestrial AOA affiliated with the genera *Nitrososphaera*, *Nitrosocosmicus*, and *Nitrosotenuis* have more than one copy of *amoC* per genome (Spang et al., 2012; Lebedeva et al., 2013; Kerou et al., 2016; Li et al., 2016b), which may enhance their survival capacity under long-term energy starvation.

Since the abundance of AOA *amoC* transcripts have been reported to be particularly high in the oligotrophic open ocean, and orders of magnitude greater than those of *amoA* and *amoB* genes (Shi et al., 2011), the results of our study also suggest that a considerable fraction of marine AOA in oligotrophic areas frequently face short periods of energy starvation or limitation, which might due to low mineralization rates or competition with ammonia-assimilating phytoplankton and heterotrophs. It is worth noting that previous studies have indicated that bacterial AmoC was also required to cope with heat shock and other membrane stress conditions (Berube and Stahl, 2012). Although no induction of *amoC* expression was detected for *N. maritimus* under Cu-stressed conditions, we cannot exclude that archaeal AmoC may also play a broader role in responding to other unfavorable environmental conditions besides energy starvation. In addition, notably, AmoC proteins harboring a N-terminal acetylation modification were identified in our proteomic analysis. Since reversible acetylation has been known to function as part of the regulatory mechanism in response to substrate availability and redox status (Wang et al., 2010; Weinert et al., 2013), a question to be addressed in future research is whether AmoC is also subject to reversible modifications that contributes in some way to recovery from energy limitation.

In addition to AMO, the copper-containing nitrite reductase (NirK), which catalyzes the nitrite reduction to nitric oxide (NO), has also been identified in both AOA and AOB genomes (Walker et al., 2010). Recent studies have demonstrated that NO is a central intermediate required for ammonia oxidation pathway of marine (Martens-Habbena et al., 2015) and soil AOA (Kozlowski et al., 2016b), suggesting NirK plays an important role in AOA ammonia catabolism. *N. maritimus* encodes two paralogs of NirK (Nmar_1667 and Nmar_1259), which share ~91% amino acid identity with each other. A high expression of *nirK* genes were found in exponentially growing cells, both at the transcript and protein levels. In particular, the Nmar_1667 transcript was the third most abundant transcript based on microarray fluorescent intensity measurements. These results are congruent with previous field studies underscoring the high expression of *nirK*-like genes in marine metatranscriptomes and metaproteomes (Stewart et al., 2012; Hawley et al., 2014). Both *nirK* transcripts showed decreased levels under ammonia limitation and Cu stresses and increased levels during recovery (Fig. 6.4). Thus, similar to *amoA*, the elevated expression of *nirK* is also a hallmark of initial recovery of *N. maritimus* from nutrient limitation. Therefore, the expression of *nirK* may also serve as a promising molecular marker for monitoring the activity of natural marine AOA communities (Lund et al., 2012).

Previous studies observed the rapid NO cycling during NH₂OH oxidation to nitrite in a soil AOA *N. viennensis*, and thus proposed that the NO-dependent dehydrogenation of NH₂OH to nitrite is the central reaction in archaeal ammonia oxidation, although no enzyme catalyzing this reaction has been identified in AOA (Kozlowski et al., 2016b). Nitric oxide has also been suggested to function as a redox shuttle to deliver electrons to the AMO (Stahl and de la Torre, 2012a).

Notably, the recent characterization of a purified small cupredoxin (Nmar_1307) from *N. maritimus* showed that this protein contained a copper center with the conspicuously high reduction potential and an open binding site containing water (Hosseinzadeh et al., 2016). These unique features were associated with the capacity of this unusual type 1 Cu cupredoxin to directly oxidize NO to nitrite (Hosseinzadeh et al., 2016). These findings, along with the presence of active NirK in marine AOA cells, support the plausibility of the redox recycling of NO during ammonia oxidation. Although Nmar_1307 was not identified in the proteome of mid-log phase *N. maritimus* cells, given the many caveats of current proteomics technology its possible functional significance in ammonia oxidation cannot be discounted.

The characterized archaeal ammonia oxidizers lack genes for the hydroxylamine-ubiquinone redox module found in AOB (Walker et al., 2010). It has been demonstrated that *N. maritimus* produces NH_2OH as an intermediate during ammonia oxidation to nitrite (Vajrala et al., 2013), suggesting that the NH_2OH oxidation may be carried out by a novel enzyme or novel enzyme systems that possibly involve some of the periplasmic multicopper oxidases (Nmar_1131, 1136, 1354, 1663). Of these, three (Nmar_1136, 1354, 1663) were detected in the proteome and two (Nmar_1354 and 1663) were among the top 5% most abundant transcripts in the transcriptome during exponential growth. Both Nmar_1354 and Nmar_1663 transcripts showed decreased levels under stressed conditions and showed increased levels during resuscitation. Only one protein (Nmar_1663) has putative orthologues in the genomes of all orders of *Thaumarchaeota*, particularly in the streamlined genome of “*Ca. N. brevis*” (Santoro et al., 2015). Furthermore, the orthologous protein (T478_0261) was also detected in the proteome of exponential cells of “*Ca. N. brevis*” (Santoro et al., 2015). Taken together, Nmar_1663 is considered to be the most

likely candidate for a direct role in NH_2OH oxidation. However, given most orthologues of Nmar_1663 flank genes encoding metal transporters, it may also function as part of a metal homeostasis system (Walker et al., 2010). Thus, future isolation and characterization of the candidate NH_2OH dehydrogenase is likely necessary to extend our understanding of the mysterious biochemistry of ammonia oxidation in *Thaumarchaeota*.

The electrons produced from NH_2OH oxidation might then be transferred by small blue copper-containing plastocyanin-like electron carriers. *N. maritimus* encodes for 17 small blue plastocyanins (Nmar_0004, 0185, 0815, 0918, 1102, 1129, 1142, 1161, 1226, 1273, 1307, 1443, 1542, 1637, 1650, 1665, 1678) which, apart from the NO oxidation activity of the biochemically characterized Nmar_1307, have no described function. Thus, as yet, only the (meta)transcriptomics data has highlighted the potentially more biochemically significant among these 17. Hollibaugh *et. al.* observed that Nmar_1102 was the only one of the 17 that was observed at more than 50 reads mapped in metatranscriptomes of marine AOA in coastal waters (Hollibaugh et al., 2011). Notably, Nmar_1102 is one of four (Nmar_1102, 1226, 1650, 0185) that showed reduced transcript levels under ammonia starvation and Cu stresses and increased levels during recovery (Fig. 6.4), like other components of the ammonia oxidation pathway. This protein was also among the top 5% most abundant proteins in the proteome of growing *N. maritimus* cells. Therefore, our results support previous metatranscriptomic studies suggesting that Nmar_1102 is most likely a major electron carrier for electron transfer to electron transport chain or to NirK (Hollibaugh et al., 2011). In contrast to Nmar_1102, three plastocyanin transcripts (Nmar_1161, 1637, 1678) were much more abundant under Cu-limited and Cu-excess conditions. The increase in these transcripts, albeit not significant, was also observed under

ammonia starvation, suggesting they may have important role in electron transfer pathway under stresses. All available thaumarchaeotal genomes, including the notably streamlined genomes of oceanic thaumarchaeota, possess multiple copies of genes coding for plastocyanin proteins, which most probably originate from extensive and wide-spread gene duplication events within different thaumarchaeotal lineages (Walker et al., 2010). These presumably paralogous plastocyanin genes likely have adaptive significance, functioning under specific physiological and physicochemical conditions associated with the dynamic marine environment.

A proton motive force (PMF) would be generated via electron transfer through complex III and complex IV, and conversion of the PMF to energy via ATP synthase. Transcript levels for the complex III proteins (Nmar_1542-1544) showed no significant changes in response to ammonia starvation and recovery (Fig. 6.4). However, the transcript levels of these genes were significantly lower in Cu-stressed cells than in Cu-replete cells (Fig. 6.4). The complex IV is encoded by four clustered genes (Nmar_0182-0185), three of which (Nmar_0182, 0184, and 0185) were expressed to significantly lower levels under stressed conditions and to higher levels under recovery condition (Fig. 6.4). As expected, many ATP synthase subunits (Nmar_1688-1693) were among the mostly highly represented in the transcriptome and proteome of actively growing cells and showed significant reductions in the transcriptome of stressed cells (Fig. 6.4). The lack of gene encoding the NADH binding subunit of NADH dehydrogenase (NuoF) in the genomes of *N. maritimus* and other AOA necessitates complex I enzymes (Nmar_0276-0286; Nuo ABCDHIJKMLN) interact with alternative electron carriers, such as ferredoxin and flavodoxin. Reduced cofactors (NAD(P)H) required for downstream cellular activities would be generated via ferredoxin or FAD-dependent oxidoreductases. In general, complex I genes were

significantly down-regulated in more slowly metabolizing cells (Fig. 6.4). Notably, ferredoxins are among the genes showing the greatest decrease and increase in transcript levels under ammonia starvation and recovery, respectively. In addition, ferredoxins were among the most highly expressed genes in both the transcript and protein pools of our cultures and AOA natural assemblages in coastal waters with relatively high iron availability (Hollibaugh et al., 2011; Williams et al., 2012), suggesting, besides copper-containing plastocyanins, these iron-containing redox carriers also play an active role in electron transport in marine AOA. Similarly, it has been shown that some oceanic diatom species also possess more than one active redox cofactor system (Groussman et al., 2015), suggesting the potential use of alternative electron transfer strategies to reduce diatom dependence on sole redox metal in metal-deficient pelagic regions. For example, the substitution of ferredoxin for flavodoxin occurs in many diatoms under iron limitation (LaRoche et al., 1996; Whitney et al., 2011; Lommer et al., 2012).

We therefore expect that marine AOA are also able to switch between the use of plastocyanin, ferredoxin, or flavodoxin in response to changing Cu and Fe availability in the environment. However, no induction of expression of ferredoxin or flavodoxin was observed in *N. maritimus* cells under severe Cu limitation (5 nM total Cu), suggesting the requirement of Cu-containing plastocyanin in respiratory electron transport could not be replaced by other electron carriers. It is also possible that, similar to the substitution between ferredoxin and flavodoxin regulated by iron limitation in diatom species *Fragilariopsis cylindrus* (Pankowski and McMinn, 2009), the replacement of plastocyanin for other electron carriers in *N. maritimus* mainly occurs at the early stage of Cu limitation with minor growth rate depression. However, the growth rates was significantly limited by Cu (~30% decrease compared to maximum) in our Cu-limited cultures

and the decrease in the expression of non-copper-containing electron carriers might primarily reflect growth rate depression rather than be a specific response to low Cu. Thus, additional studies of the regulation of iron and copper availabilities on plastocyanin, ferredoxin, and flavodoxin expressions are needed to extend our understanding of the adaptive strategies enabling marine AOA to thrive in low iron and copper regimes.

Overall the transcriptome indicated an apparent reduction in the pathway for ammonia oxidation and respiration in ammonia-starved and Cu-stressed cells (Fig. 6.4). However, apart from being used as the energy source, ammonia is the primary nitrogen source for biosynthesis. Ammonia is usually transported into the cells via ammonium transport proteins (Amts) and further assimilated into cellular nitrogen through the activities of glutamine synthetase (GS) and glutamate synthase (GOGAT), though some organisms employ glutamate dehydrogenase (GDH) rather than GOGAT (Leigh and Dodsworth, 2007). Consistent with other free-living AOA, *N. maritimus* encodes for two types of phylogenetically and possibly functionally distinct ammonium transporters: Amt1 (Nmar_0588) and Amt2 (Nmar_1698) (Walker et al., 2010). Although Amt1 was expressed at lower levels relative to Amt2, they are both among the most abundant transcripts in the transcriptome of mid-log phase cells. However, only Amt2 proteins (Nmar_1698 and T478_1378) were highly detected in the proteomes of mid-log phase *N. maritimus* and *N. brevis* cells (Santoro et al., 2015), contrarily, Amt1 proteins (Nmar_0588 and T478_1350) were either not detected or only presented at very low levels.

A recent transcription study by Nakagawa et al. reported that the actively growing *N. maritimus* cells sustained high levels of *amt2* expression at environmentally relevant ammonium

concentrations (down to the low nanomolar range), whereas expression of *amt1* was depressed (Nakagawa and Stahl, 2013). This is consistent with our observation of no significant changes in the levels of *amt2* transcript after 24 hours of ammonium starvation relative to mid-log control, and a significant decrease and increase ($P < 0.01$) of *amt1* transcripts in response to the short-term ammonium deprivation and replenishment, respectively (Fig. 6.4). The apparent constitutive expression of *amt2* suggests that *N. maritimus* retains its high affinity ammonium uptake system that is essential for reinitiating growth under ammonia limitation.

Strain SCM1 also codes for the PII signal transduction proteins of many *Bacteria* and *Archaea* to sense the intracellular nitrogen and energy status, and thereby control various regulatory and catalytic components of the ammonia assimilation pathway (Leigh and Dodsworth, 2007). In the well-studied *Escherichia coli* systems, the PII protein GlnK remains in the cytoplasm under nitrogen starvation, but is rapidly sequestered by membrane-bound AmtB and blocks the ammonium transporter under nitrogen excess (Coutts et al., 2002). Similarly, the Amt1, but not Amt2 proteins, of Group I.1 *Thaumarchaeota* possess a C-terminal extension (Offre et al., 2014), a cytoplasmic region serving for docking with GlnK-like PII proteins in many organisms in aquatic environments (Tremblay and Hallenbeck, 2009; Huergo et al., 2013). A tight linkage between the gene coding for the PII signal transduction protein (Nmar_0587) and *amt1* (Nmar_0588) is highly conserved across all known Group I.1a genomes, suggesting that these two proteins serve a related, but likely opposite role in the AOA – presumably functioning to block *amt1* transport only under conditions of ammonia limitation.

N. maritimus contains two GS genes (Nmar_1771 and Nmar_1790), whereas *N. brevis*, with a more streamlined genome, only contain one (T478_1493) (Santoro et al., 2015), a homolog to Nmar_1790. These two GS proteins in *N. maritimus* share only ~44.1% amino acid identity and both were highly detected in the proteome during unlimited growth, suggestive of the functional redundancy or compensation between paralogs. As with all other sequenced AOA genomes, only GDH (Nmar_1312), but no GOGAT gene was identified in *N. maritimus*, indicating that ammonium is assimilated in AOA cells by GDH-GS pathway rather than GS/GOGAT cycle.

Because *N. maritimus* uses ammonia not only for cellular nitrogen but also oxidizes ammonia as an energy source, ammonia assimilation and energy production would be competing pathways. In particular, the high affinity of the characterized AOA for ammonia (Martens-Habbena et al., 2009b) would seem to put the pathways for ammonia oxidation and assimilation in conflict at the low ammonia concentrations sustaining growth of this organism. This conflict is reflected in transcriptional response of genes involved in the oxidation and assimilation of ammonia. Transcription of both pathways was reduced in the ammonia-starved sample (Fig. 6.4), presumably to ameliorate possible competition between these two essential pathways. After 24 hours of ammonia re-addition, the transcripts of the key genes for ammonia oxidation pathway, such as *amoA*, *nirK*, and plastocyanin gene (Nmar_1102), showed significantly increased levels ($P < 0.05$) compared to ammonia starvation controls. In contrast, no significant increase in the transcript levels of GS gene (Nmar_1790) was observed following 24 hours of recovery after ammonia starvation, suggesting ammonia assimilation activity is likely retarded until sufficient energy is available. Taken together, our results showed that the *N. maritimus* cells when recovering from ammonia starvation prioritizes gene expression, initially investing in

reestablishing and repairing systems for energy generation and only later transcribes genes required for anabolism, such as ammonia assimilation.

Carbon fixation

N. maritimus grows autotrophically by fixing inorganic carbon via a modified version of 3-hydroxypropionate/4-hydroxybutyrate (HP/HB) cycle, representing the most energy-efficient aerobic autotrophic pathway yet characterized (Könneke et al., 2014). All previously characterized thaumarchaeotal HP/HB cycle enzymes were identified in the proteome of exponentially growing cells and many of them were among the most abundant proteins based on their spectral counts, including acetyl-/propionyl-CoA carboxylase (Nmar_0273), malonic semialdehyde reductase (Nmar_1110), 3-hydroxypropionyl-CoA synthetase (Nmar_1309), 3-hydroxybutyryl-CoA dehydratase (Nmar_1308), 4-hydroxybutyryl-CoA dehydratase (Nmar_0207), and acetoacetyl-CoA β -ketothiolase (Nmar_1631). Their homologous proteins were also highly detected in marine metaproteomes (Williams et al., 2012; Hawley et al., 2014).

Under Cu-stressed conditions, *N. maritimus* appeared to down-regulate the transcription of the entire carbon fixation pathway, as most of the known thaumarchaeotal HP/HB cycle genes were transcribed at significantly lower levels ($P < 0.05$) under these stressed conditions compared to under optimal growth condition (Fig. 6.7). In contrast, only a few characterized HP/HB pathway gene transcripts responded to the different ammonia availabilities. Notably, the transcript levels of the gene encoding malonic semialdehyde reductase (Nmar_1110), which catalyzes the reduction of malonic semialdehyde with NAD(P)H to 3-hydroxypropionate, was among the most depressed in the absence of ammonia and most elevated upon exposure to ammonia (Fig. 6.7).

The subsequent conversion of 3-hydroxypropionate to 3-hydroxypropionyl-CoA is an ATP-consuming step of the HP/HB cycle that requires 3-hydroxypropionyl-CoA synthetase (Nmar_1309). The V_{\max} value of the recombinant 3-hydroxypropionyl-CoA synthetase ($0.59 \pm 0.03 \mu\text{mol}\cdot\text{min}^{-1}\cdot\text{mg}^{-1}$ protein) is by far the lowest among the characterized enzymes of thaumarchaeotal HP/HB cycle, and its K_m value (1.2 ± 0.2 mM) is the highest half-saturation constant obtained for any characterized HP/HB pathway enzymes to date (Könneke et al., 2014; Otte et al., 2015). Since activation 3-hydroxypropionate appears to be the major kinetic and energetic bottleneck in the thaumarchaeotal HP/HB cycle, regulation of 3-hydroxypropionate formation would serve to depress flux of carbon and energy through this pathway under conditions of energy limitation. This may involve both transcriptional (as shown in this study) and other levels of control, such as post-translational modification and allosteric modulation of malonic semialdehyde reductase activity, to coordinate the balance between major energy yielding and energy-consuming biosynthetic processes.

N. maritimus encodes two putative acetoacetyl-CoA β -ketothiolases (Nmar_0841 and Nmar_1631), which share only ~31.3% amino acid identity. Acetoacetyl-CoA β -ketothiolase catalyzes the conversion of acetoacetyl-CoA into two acetyl-CoAs. In addition to acting as the substrate for the carbon-fixing acetyl-CoA carboxylase, acetyl-CoA is the substrate and precursor metabolite in the downstream metabolic networks of AOA, including the incomplete tricarboxylic acid (TCA) cycle and pathways for amino acid and fatty acid synthesis. Of the two candidate acetoacetyl-CoA β -ketothiolases, only Nmar_1631 was detected in the proteome of *N. maritimus* under normal growth condition. As expected, Nmar_1631 was transcribed at significantly lower levels ($P < 0.01$) in the slowly metabolizing cells grown under Cu-stressed

conditions compared to Cu-replete controls (Fig. 6.7). In contrast, Nmar_0841 showed the opposite trend; it was up-regulated (~ 3 folds, $P < 0.01$) under Cu-limited and Cu-excess conditions relative to controls (Fig. 6.7). Increased expression of this acetoacetyl-CoA β -ketothiolase variant may relate to its possible regulatory function through protein acetylation, as modification known to regulate gene expression and metabolic flux in relationship to energy status (Norris et al., 2009). We speculate that under Cu-stressed conditions, increased expression of this ketothiolase variant is also coupled to altered activity or regulation through protein acetylation. Taken together, our results suggest that Nmar_1631 and Nmar_0841 likely represent two different types of acetoacetyl-CoA β -ketothiolase. Comparative phylogenetic analysis revealed that these two types of putative acetoacetyl-CoA β -ketothiolase encoded in all characterized AOA genomes and form two distinct and highly-supported lineages (Fig. 6.8). Since N-acetylation of proteins was observed in the proteome of *N. maritimus*, it will be of considerable interest to verify the two proposed activities and assess whether functional diversification of acetoacetyl-CoA β -ketothiolases is conserved across different groups of AOA.

Many key enzymes involved in the HP/HB cycle have been neither biochemically characterized nor bioinformatically identified, including malonyl-CoA reductase, acryloyl-CoA reductase, succinyl-CoA reductase, and succinic semialdehyde reductase (Könneke et al., 2014; Otte et al., 2015). We attempted to use the transcriptomic and proteomic information to predict the candidate genes encoding yet-to-be-identified components of thaumarchaeotal HP/HB cycle, which may guide further biochemical characterizations. Acryloyl-CoA reductase and succinic semialdehyde reductase have been biochemically characterized in crenarchaeon *Metallosphaera sedula* (Kockelkorn and Fuchs, 2009; Teufel et al., 2009), and they both belong to the family of

zinc (Zn)-containing alcohol dehydrogenase. *N. maritimus* contains several related genes encoding Zn-containing alcohol dehydrogenases of unknown specific function, and two of them (Nmar_1622, Nmar_0523) were highly detected in the proteome of exponentially growing cells. In particular, the corresponding protein of Nmar_1622 ranked as the 4th most abundant protein in terms of spectral counts (Fig. 6.1). Additionally, their homologous proteins were highly abundant in the proteome of *N. brevis* (T478_1333 and T478_0389) as well as in marine metaproteomes (Hawley et al., 2014; Santoro et al., 2015). An alignment of Nmar_1622, Nmar_0523 with their homologous proteins from *Thaumarchaeota* showed the presence of a conserved sequence for a NADPH/NADP⁺ binding domain and a structural Zn binding site (CXXCXXCXXXXXXXXXC). It has been reported that distinct enzymes catalyze the same HP/HB cycle reaction in *Crenarchaeota* and *Thaumarchaeota*, indicating the convergent evolution of autotrophic CO₂ fixation pathways in these two phyla. Similarly, Nmar_1622 and Nmar_0523 both show only moderate similarities with the *Metallosphaera* acryloyl-CoA reductase (Msed_1426) and succinic semialdehyde reductase (Msed_1424) (25.7% to 30.2% amino acid identities).

The reduction of malonyl-CoA and succinyl-CoA is carried out by a promiscuous enzyme (Msed_0709) in *M. sedula*, speculated to reduce the cost of protein biosynthesis (Berg et al., 2007). Marine AOA may use a similar cost-efficient way to adapt to life in nutrient-poor environments. Malonyl-CoA/succinyl-CoA reductase of *M. sedula* is a paralog of its aspartate semialdehyde dehydrogenase (Alber et al., 2006). However, only one copy of aspartate semialdehyde dehydrogenase gene (Nmar_1586) was identified in the genome of *N. maritimus* (Walker et al., 2010), suggesting that other distantly related candidate genes encode enzymes

catalyze malonyl-CoA and succinyl-CoA reduction. Among candidate genes, Nmar_1043 (annotated as an NAD(P)H/NAD(P)⁺-dependent short-chain dehydrogenase) was down-regulated under ammonia-starving and Cu-stressed conditions, and its corresponding protein was also highly represented in the proteome. Nmar_1043 shows 30% amino acid identity with the malonyl-CoA reductase involved in the 3-hydroxypropionate cycle of a phototrophic bacterium *Chloroflexus aurantiacus* and may mediate the reduction of Malonyl-CoA in *N. maritimus*. Although Nmar_1608 was earlier predicted to function as succinate semialdehyde dehydrogenase (Walker et al., 2010), this enzyme shows some similarity to the *Thermoproteus* succinyl-CoA reductase (33% amino acid identity with Tneu_0421) (Ramos-Vera et al., 2011) and may actually function as a succinyl-CoA reductase in *N. maritimus*. Thus, additional biochemical studies are needed to resolve these alternative functions.

Cobalamin biosynthesis

The putative thaumarchaeotal cobalamin (vitamin B₁₂) biosynthetic pathway has been previously identified in marine AOA genomes and metagenomes (Walker et al., 2010; Doxey et al., 2015; Santoro et al., 2015). Critical cobalamin-dependent enzymes include the different isomerases and methyltransferases activities of methylmalonyl-CoA mutase (MCM), methionine synthase (MetH), and ribonucleotide reductase (Walker et al., 2010; Doxey et al., 2015). Biosynthesis of cobalamin was recently confirmed by the direct measurement of cobalamin production in pure cultures of marine AOA (Heal, et al., 2016). Intracellular production of hydroxocobalamin (HOCbl), and two biologically active species, methylcobalamin (MeCbl) and 5'-deoxyadenosylcobalamin (AdoCbl) was evident in all characterized marine AOA isolates (Heal, et al., 2016). Those studies also revealed remarkably high carbon specific-cobalamin cell quotas (2800 –

11600 nmol B₁₂ per mol C), suggesting that marine AOA are a major source of cobalamin in seawater, particularly below the euphotic zone (Heal, et al., 2016). High cell content may in part relate to the central role of cobalamin as a cofactor of MCM in the thaumarchaeotal HB/HP cycle. However, little is known about the regulation of cobalamin synthesis in *Thaumarchaeota* or its more general functions in the biochemistry of the AOA.

Enzymes for most steps in the cobalamin biosynthetic pathway were detected in the proteome of actively growing *N. maritimus*. Surprisingly, *N. maritimus* increased the abundance of most transcripts associated with cobalamin biosynthetic pathway under ammonia-depleted and Cu-stressed conditions, while reducing these transcripts during recovery (Fig. 6.9). These observations suggest an increased need for cobalamin when *N. maritimus* is exposed to different types of nutrient stress. MCM uses AdoCbl as a cofactor, the production of which has been shown to be tightly associated with the activity of marine AOA (Qin, et al., 2016). Consistent with the transcriptional response of most anabolic genes, the transcript abundances of MCM genes (Nmar_0954 and Nmar_0958) were decreased under stressed conditions relative to controls. This suggested a lower AdoCbl demand of MCM in slowly metabolizing cells compared to control cells. Indeed, the intracellular AdoCbl concentrations in Cu-limited cells (26.0 ± 3.8 pM cells⁻¹) and the cells supplemented with inhibitory high concentrations of copper (63.5 ± 32.0 pM cells⁻¹) were generally lower than those measured for Cu-replete controls (92.9 ± 13.5 pM cells⁻¹).

Another biological active form of B₁₂ in AOA is MeCbl, which acts as an intermediate methyl group carrier in MetH (Doxey et al., 2015). This enzyme plays important roles in folate-

mediated one-carbon metabolism and S-adenosylmethionine (SAM)-dependent methylation reactions (Banerjee and Matthews, 1990). The higher levels of MetH transcripts (Nmar_1267 and Nmar_1268), albeit not always significant, were found for *N. maritimus* under stressed conditions compared to under optimal growth condition. In addition, we found that when copper concentrations were at an inhibitory excess, cells maintained significantly higher ratio of the concentration of SAM to SAH (S-adenosyl homocysteine) ($P < 0.05$) than Cu-replete controls. An increase in SAM/SAH ratio indicated the higher methylation capacity (Yi et al., 2000). It suggests that when copper was supplied at higher inhibitory levels, *N. maritimus* cells appeared to enhance MetH activity and methylation to cope with Cu-induced oxidative stress. This increase potentially resulted in higher demand of MeCbl under stressed condition. However, we found that MeCbl accounted for less than 1% of total intracellular cobalamin pool in both stressed and control cells, a demand seemingly insufficient to account for the observed up-regulation of nearly the entire cobalamin biosynthetic pathway gene expression. Taken together, these data suggest cobalamin may serve other essential but unexplored roles in the general physiological response of marine AOA to different types of environmental stress.

An alternative function of cobalamin was suggested by the earlier observation that AOA produce NO as an intermediate in the ammonia oxidation pathway (Martens-Habbena et al., 2015). NO can rapidly bind and react with the reduced forms of cobalamin to produce nitrosylcobalamin (NOCbl) (Danishpajooch et al., 2001; Kambo et al., 2005). NOCbl is extremely oxygen-sensitive and is rapidly oxidized to nitrocobalamin (NO₂Cbl) in the presence of oxygen (Wolak et al., 2006). Because the produced NOCbl has diminished ability to serve as cofactors in MCM and MetH (Brouwer et al., 1996), the increase in cellular NO synthesis can effectively inhibit the

activity of cobalamin dependent enzymes. As reported previously, at physiological ammonia concentrations, NO was released and reached relatively stable levels of 50–80 nM in *N. maritimus* cells; while at saturating ammonia concentrations, NO accumulated to levels of more than 2 μ M during ammonia oxidation (Martens-Habbena et al., 2015). We therefore speculated that endogenously produced NO could effectively react with cobalamin species in AOA cells, which may have significant physiological impact.

To evaluate the possible formation of nitrosylated cobalamin, we measured intracellular NO₂Cbl concentrations in *N. maritimus* cells using liquid-chromatography mass spectrometry (LC-MS). Notably, we provide the conclusive evidence that NO₂Cbl was formed in AOA cells (Fig. 6.10). Even more surprisingly, we found that *N. maritimus* cells contained more NO₂Cbl than the common cobalamin metabolites (AdoCbl, MeCbl, and HOcbl) under optimal growth condition (Fig. 6.10), indicating that the majority of generated cobalamin species were reacting with NO during the growth of AOA. When cells were grown under Cu-stressed conditions, we observed a significantly higher proportion of N₂OCbl in total intracellular cobalamin pool compared to that for Cu-replete controls (Fig. 6.10). Assuming that N₂OCbl is an inactive form of this essential cofactor, the loss of a significant part of the cobalamin pool to the nitrated form may explain the unusually high cellular quotas observed during normal growth and the increased transcription of the B₁₂ biosynthetic pathway under stressed conditions. In addition, besides the cobalamin species measured in this study, the precursor of cobalamin, cobinamide (Cbi) and the “base-off” form of cobalamin has even higher affinity for NO (Sharma et al., 2003). Therefore, although physiological concentrations of AdoCbl, MeCbl, and OHcbl are low in AOA cells, a variety of unique Cbls, Cbis, and corrins have higher capacity to scavenge intracellularly produced NO and

may serve an expected role in NO detoxification. Taken together, our findings reveal an unexplored, yet important, connection between ammonia oxidation and cobalamin biosynthesis metabolisms in AOA cells.

Other molecular responses to ammonia starvation, Cu limitation, and Cu excess

Archaeal transcriptional regulators and general transcription factors exert significant effect on the large-scale as well as gene-specific regulation of transcription in response to changing environmental conditions (Geiduschek and Ouhammouch, 2005; Facciotti et al., 2007). In addition to the expected transcriptional regulatory and two-component regulatory proteins *N. maritimus* is unusual in possessing 8 transcription factor B (TFB; Nmar_0013, 0020, 0517, 0624, 0979, 0987, 1340, and 1341) proteins and two TATA binding proteins (TBP; Nmar_0598 and Nmar_1519) that are thought to regulate transcription by recruitment of selected regulatory factors similar to that of bacterial sigma factors. The remarkable genome content of these factors is among the highest yet observed in archaeal genomes (Walker et al., 2010). Most of the identified transcription factors and transcriptional regulators in *N. maritimus* genome showed no significant changes or decreased levels in their transcripts under stressed conditions relative to controls. Nevertheless, 4 of the 10 most highly up-regulated genes in ammonia-starved cells were transcriptional regulators and transcription factor genes, including two AsnC-like transcriptional regulators (Nmar_0854 and Nmar_1524), one GntR-like transcription factor (Nmar_0033), and one TFB (Nmar_0013). Interestingly, the GntR-like and AsnC-like transcription factors were up-regulated only in response to ammonia starvation, not copper stress, suggesting a specific role in cellular response to ammonia availability. In contrast, the increased

expression of one of eight TFB genes (Nmar_0013) in response to both ammonia limitation and copper stress suggests a role as part of general stress response regulatory system.

N. maritimus genome contains a gene cluster (Nmar_1650–1657) annotated as functioning in Cu uptake and homeostasis, which includes a plastocyanin-like protein (Nmar_1650), a copper resistant D domain protein (Nmar_1652), an ABC-type metal transporter (Nmar_1654), and a metal-responsive transcriptional regulator (Nmar_1656) (Walker et al., 2010). However, we found divergent transcriptional responses of these genes to Cu-stresses, exhibiting both increased and decreased transcript abundance, suggesting this gene cluster may not serve as a functional unit regulating copper trafficking and resistance as previously predicted (Walker et al., 2010). In addition, we found that many genes encoding divalent metal transporters were up-regulated in response to limiting or inhibitory copper concentrations, suggesting they are bidirectional transporters involved in Cu uptake under copper limitation and export when copper is at higher inhibitory levels.

Free cytoplasmic copper is extremely toxic, as a result of its contribution to the generation of superoxide, hydroxyl radicals, and other reactive oxygen species (ROS) by Fenton reaction (Rensing and Grass, 2003). Indeed, our RNA-sequencing data showed that toxic copper concentration resulted in significantly increased expression of one putative superoxide dismutase (Nmar_0729, $P < 0.01$) and one putative alkyl hydroperoxide reductase (Nmar_1438, $P < 0.05$). The transcription of these peroxidase genes also increased under Cu-limited and ammonia-starved conditions, suggesting they may serve to protect AOA cells from ROS and reactive nitrogen species associated with either metal stress or suboptimal growth conditions. Increased

copper has also been shown to catalyze the formation of non-native disulfide bonds (Dsb) in membrane proteins and cause protein misfolding in the periplasm (Takemoto and Hansen, 1982). Correct Dsb formation is catalyzed by DsbA-type proteins that effectively compete with copper in protein folding (Hiniker et al., 2005). Notably, *N. maritimus* contains a conspicuously high numbers of putative DsbA-type proteins sharing the conserved thioredoxin-like active site FXXXXCXXC motif (Nmar_0639, 0655, 0829, 1140, 1143, 1148, 1150, 1181, 1658, and 1670) (Walker et al., 2010). Among these, Nmar_1140 and Nmar_1143 were significantly up-regulated ($P < 0.05$) under Cu-excess condition relative to controls, but showed no significant response to starvation and Cu-limitation, suggesting a specific role of these DsbA-like proteins for *N. maritimus* cells to grow and survive under oxidative copper stress conditions.

Conclusions

Overall the transcriptome indicated an apparent reduction in ammonia oxidation, ammonia assimilation, and carbon fixation in the ammonia-starved and Cu-stressed cells, and an activation of the major energy production and biosynthesis pathways during ammonia-recovery. *N. maritimus* is much less tolerant to starvation than known AOB, and AmoC is most likely a starvation stress-responsive subunit facilitating recovery of an active AMO. Notably, we show high cellular quotas of cobalamin in AOA and provide compelling evidence that a large fraction is in the NOCbl and NO₂Cbl forms. The high cellular quotas of cobalamin may therefore reflect the loss of a fraction of active cobalamin to nitrosylation by NO during normal cell growth. Similarly, the up-regulation of cobalamin biosynthesis in response to copper stress may serve to replenish cobalamin lost to excess NO produced during unbalanced growth. However, we should also consider a more direct role of the nitrosylated cobalamins in the central biochemistry

of the AOA. Thus, the interaction between NO and cobalamin must now be considered a critical component of the fundamental physiology of AOA that may play a major role in shaping their ecology in natural environment. Future studies determining the bioavailability of nitrosylated species of cobalamin and their distribution in marine waters may advance our understanding of the cobalamin-based microbial interdependencies in the ocean.

Materials and Methods

Culture maintenance and growth

All *Nitrosopumilus maritimus* SCM1 cultures were maintained at 30°C in the dark. For all experiments except Cu studies, cells were grown and maintained in synthetic seawater medium as described previously (Martens-Habbena et al., 2009b; Qin et al., 2014). All cultures were regularly monitored for bacterial contamination by checking for bacterial growth in Zobell marine broth (Zobell, 1941) and by using Sybr Green I staining followed by microscopy. Growth was measured either by measuring nitrite concentrations spectrophotometrically (Grasshoff et al., 1999) or by performing cell counts on the day of sampling using Sybr Green I staining and epi-fluorescent microscopy (Nikon Eclipse 80i) as described previously (Lunau et al., 2005).

Media composition and preparation for Cu studies were carried out as described previously (Amin et al., 2013). In brief, cells were grown in trace-metal depleted media using Chelex-100 resin in the presence of 1 μ M 1,4,8,11-tetraazacyclotetradecane-1,4,8,11-tetraacetic acid (TETA) to control metal speciation. Cultures were acclimated to either Cu-replete conditions (50 nM Cu), Cu-limited (5 nM Cu) or Cu-toxic (750 nM Cu) conditions (Amin et al., 2013). For large-

volume cultures, 500 mL of SCM1 was grown in 2 L acid-washed polycarbonate bottles to afford 6 L for Cu-replete and Cu-toxic and 10.5 L for Cu-limited conditions in the dark without shaking at 30°C. Growth was monitored by measuring nitrite concentrations. Cultures were harvested at mid-exponential growth once nitrite concentrations reached half their maximum value for each respective condition. Cultures from each respective condition were then pooled into triplicates for gene expression and metabolome sampling.

Gene expression microarrays for ammonia starvation and recovery

N. maritimus was grown in batch cultures with 1 mM NH₄Cl. The mid-log control treatment was comprised of mid-exponential phase cells after ~0.5 mM ammonia consumption. For the ammonia starvation treatment, the mid-log phase cells were harvested, resuspended in ammonia free medium, and incubated for 24 h. Ammonia-starved cells were then exposed to 1mM NH₄Cl and incubated for 24 h to investigate the induction of gene expression by recovery. Three biological replicates were measured for the mid-log and 24-hour ammonia-starved conditions and two replicates for the recovery condition from ammonia starvation.

Total RNA was isolated from all samples as described previously (Horak et al., 2013).

Ribosomal RNA and *amo* gene copy numbers were determined by qPCR on a Roche Light Cycler machine. For microarrays, total RNA from three independent cultures was pooled for each microarray incubation. Three replicate hybridizations were done for each experimental condition. All microarray incubations were conducted by NimbleGen in Iceland.

Metabolic activity measurements

In order to determine the viability and metabolic response to ammonia starvation, oxygen consumption of *N. maritimus* cells was measured in subsamples of late-exponential and ammonia-starved cultures. Briefly, subsamples were drawn from 400 mL cultures at given time points before and after ammonium depletion. Oxygen consumption was determined using oxygen microsensors as described previously (Martens-Habbena et al., 2009b; Martens-Habbena and Stahl, 2011a). After establishing the rate of oxygen uptake in starving cells, cells were supplied with 100 μM NH_4Cl and a second 'recovered' oxygen uptake rate was determined.

Gene expression and metabolome analyses for Cu cultures

For gene expression samples, each 1 L of culture was filtered onto 0.2- μm sterivex cartridges using a peristaltic pump. Cartridges were flash-frozen in liquid nitrogen and were stored in -80°C until RNA isolation and the supernatant was immediately processed for extracellular metabolome collection (below). For RNA isolation, cartridges were opened to remove the inner filter membranes and RNA was isolated using the RNeasy Qiagen kit (Qiagen). SCM1 cells were lysed using mechanical shaking (5 min) with sterile glass beads according to the manufacturer's protocol. RNA was stored at -80°C until further processing. Residual DNA was depleted from RNA samples using the RNAqueous-4PCR kit according to the manufacturer's instructions. RNA samples were depleted of ribosomal RNAs by using Illumina RiboZero rRNA removal kit (Illumina, San Diego, CA).

For intracellular metabolome samples, 200 mL of Cu-replete and Cu-toxic and 300 mL of Cu-limited triplicate cultures were filtered onto 0.1 μm PES membrane filters housed in an acid-washed PES filtration rigs (Nalgene). Filtered were immediately removed and flash frozen in

liquid nitrogen in baked borosilicate glass vials (450°C for 6 hrs). For extracellular metabolome samples, three solid-phase extraction columns were used to capture a wide variety of molecules from the supernatant: MCX (Waters) mixed-mode cation exchange, MAX (Waters) mixed-mode anion exchange and HLB (Waters) reversed-phase with hydrophilic functionalization. All columns were conditioned according to the manufacturer's instructions. 500 mL of supernatant collected after filtration with sterivex cartridges (above) were slightly acidified with 88% formic acid (J.T. Baker) to pH 6.5. MCX columns were connected to silicon tubing attached to a peristaltic pump and supernatant was passed through at 5 mL/min. The eluate was collected at the end of the column and pH adjusted to 10.0 using concentrated NH₄OH (J.T. Baker). The supernatants were then passed through the MAX columns as before. The pH of the collected eluants was further adjusted to 3.0 using formic acid and passed through the HLB columns. All columns were eluted according to the manufacturer's instructions. Extracts were dried using nitrogen gas and samples were stored at -80°C until mass spectrometric analysis.

Transcript Abundance Determination with RNA-sequencing

Samples were prepared with TrueSeq Stranded mRNA HT library preparation kit (Illumina, San Diego, CA) and sequenced by using Illumina HiSeq 2000 sequencing machine with approximately 10-15 million reads per sample. Paired-end 50 bp long reads were checked for technical artifacts by using FastQC software (Andrews, 2010) following Illumina default quality filtering steps. Reads were further trimmed based on base quality scores and cleaned up for adapter contamination by using Trimmomatic (Bolger et al., 2014). Alignment of reads to reference *Nitrosopumilus maritimus* SCM1 (Genome Assembly ASM18465 v1.25) transcriptome was performed by using STAR RNA-seq aligner software (Dobin et al., 2013)

with modification of recommended parameters where appropriate. Read counts were collected by using HTSeq package (Anders et al., 2015) followed by normalization and analysis by using DESeq2 R package (Love et al., 2014). All fastq files used in this study will be deposited into SRA.

Quantification of cobalamin

To analyze cobalamins, SAM, and SAH, filtered cells were subjected to a two-phase extraction based on previous work (Bligh and Dyer, 1959; Canelas et al., 2009) paired with mechanical lysing using glass beads. Each filter was split between 2 bead-beating tubes, and 750 μL of dichloromethane (DCM) and 1:1 methanol: water was added. Samples were kept on ice and solvents stored at -20°C . The samples were then bead beaten three times over 30 minutes and kept at -20°C between bead-beating sessions. After centrifuging for 90 seconds at 5000 RPM, the two solvent layers separated and the top aqueous layer was transferred to a glass centrifuge tube. The remaining DCM was rinsed three times with fresh 1:1 methanol:water as before and the aqueous layer was removed each time. The aqueous aliquot (containing analytes of interest) was then rinsed with 2 mL DCM, centrifuged, transferred to a new glass vial, and dried under clean N_2 with low heat ($<35^{\circ}\text{C}$). Samples were reconstituted with internal standards and analyzed by liquid chromatography mass spectrometry as previously described (Heal et al., 2014a), while additionally monitoring for SAH. To measure SAH, we used a cone voltage of 10 with collision energies of 20 and 18 V to monitor the transitions from 385.1 to 88.1 and 385.1 to 136.1 m/z, which were tuned using a standard of SAH. For cobalamins, quantification was performed using standard addition as previously described (Heal et al., 2014a). For SAM and

SAH, relative amounts between samples were calculated by normalizing each compounds peak area to the cell density of each biological replicate.

Protein extraction and proteomic analysis

SCM1 cells were grown in SCM1 media (Martens-Habbena et al., 2009b; Qin et al., 2014; Martens-Habbena et al., 2015) supplemented with 1 mM NH₄Cl. Cell biomass was collected by filtering 200 mL of a late-exponential phase (approximately 8×10^7 cells/mL) culture onto 0.2 μ m Durapore filters. Filters were stored at -80°C until extraction. Filters were thawed, cut with sterile scissors and one-quarter of the filter (estimated 4×10^9 cells or approx. 20.4 μ g protein) was resuspended in 1 mL of 50 mM NH₄HCO₃ (AMBIC) with 5 mM EDTA disodium salt dihydrate buffer (pH 8) in a microcentrifuge tube containing glass beads. Control samples containing only 1 mL of AMBIC/EDTA were processed alongside culture samples. Each filter suspension was subjected to bead-beating for 30 seconds at 6 m/s, frozen at -20 °C for 45 minutes, and thawed. The bead-beating and freeze-thaw cycles were repeated twice followed by a third bead-beating cycle and an overnight freeze at -20°C. Subsequently, filter resuspensions were thawed and lysed cells with beads were vortexed and then centrifuged at 8,000 rpm for 3 minutes. A 500 μ L aliquot was transferred to a 2 mL protein LoBind Eppendorf tube for proteomic processing (see below).

Estimated bulk protein concentration for lysed cell extracts were measured using the Lowry assay (DC protein assay, Bio-Rad). Lowry assay samples were prepared according to the manufacturer's instructions adapted for analysis using a microcuvette (requiring only 5 μ L of sample). Protein concentrations were analyzed using a spectrophotometer (Beckman-Coulter

DU800) and determined by comparing sample absorbance units to a bovine serum albumin (BSA) protein concentration calibration curve (prepared in 50 mM AMBIC, 5 mM EDTA). In our downstream processing, we have assumed *a*) the Lowry assay overestimated the concentration of protein by a conservative factor of 2.5 (most likely due to matrix effects not accounted for in the BSA calibration; unpublished results) and *b*) an 80% extraction efficiency to lyse cells by bead-beating. Thus from *a*) and *b*), we estimated that approximately 13 μg of protein from 1.6×10^9 cells were used for downstream proteomics processing.

Lysed cells (500 μL) were subjected to in-solution proteolytic digestion. First, RapiGest SF (Waters), an acid labile surfactant, was added to help facilitate protein solubilization (0.06% w/v). Next, disulfide bonds were reduced with tris(2-carboxyethyl)phosphine (TCEP; to a final concentration of 10 mM) for 1 hr at room temperature in the dark. Reduced samples were then alkylated with iodoacetamide (to a final concentration of 30 mM) for 1 hr at room temperature in the dark. Excess iodoacetamide was quenched by the addition of dithiothreitol to a final concentration of 5 mM) for 1 hr at room temperature in the dark. Protein extracts were proteolytically digested with sequencing-grade trypsin (Promega) at an estimated substrate-to-enzyme ratio of 25:1 for 12 hours at 37°C containing a final concentration of 0.05% w/v RapiGest, 50 mM AMBIC and 5 mM EDTA (pH 8). Subsequently, RapiGest was hydrolyzed by the addition of trifluoroacetic acid (0.5% final v/v, pH < 2; concurrently terminating trypsin activity), heated for 30 minutes at 37°C and centrifuged at 14,000 rpm at 4°C for 15 minutes to precipitate the water immiscible decomposition product, dodeca-2-one. The supernatant was removed, transferred to a new protein LoBind eppendorf tube and samples were dried to near-dryness using a centrivap concentrator (Thermo Savant SPD2010 SpeedVac). Digested samples

were desalted using a MacroSpin C18 column (NestGroup) following the manufacturer instructions. Samples were eluted from the MacroSpin columns using 2x 200 μL of 80% LCMS-grade acetonitrile with 20% LCMS-grade water containing 0.1% LCMS-grade formic acid. Desalted samples were concentrated using the centrivap to near dryness and were immediately resuspended in 95% LCMS-grade water with 5% LCMS-grade acetonitrile containing 0.1% LCMS-grade formic acid. The resuspension solution also contained an internal standard of synthetic peptides (Hi3 *Escherichia coli* Standard, Waters) at 50 fmol/ μL . All resuspensions were to an approximate 0.5 $\mu\text{g}/\mu\text{L}$ protein concentration (see above) and control samples processed alongside were resuspended with an averaged resuspension volume. Samples were immediately analyzed by LCMS (see below) or stored at -80°C .

Samples were injected onto the column of a Waters ACQUITY M-class UPLC; a 2 μL injection volume corresponded to an estimated 1 μg protein on-column. Peptide separation was performed by reversed-phase chromatography using a nanoACQUITY HSS T3 C18 column (1.8 μm , 75 μm x 250 mm; 45 $^{\circ}\text{C}$) with an ACQUITY UPLC M-class Symmetry C18 trapping column (180 μm x 20 mm). The peptides were trapped at a flow rate of 5 $\mu\text{L}/\text{min}$ at 99% A for 3 minutes. A flow rate of 0.3 $\mu\text{L}/\text{min}$ was used over a gradient between LCMS-grade water (A) and LCMS-grade acetonitrile (B), both supplemented with 0.1% LCMS-grade formic acid. The total 145-minute gradient method for the separation of the peptides started at 95% A and ramped to 60% A over the course of 120 minutes. The gradient then switched to 15% A at 122-127 minutes followed by a ramp back to starting conditions 95% A at 128-145 minutes.

The ACQUITY M-class was coupled to a Thermo QExactive HF Orbitrap high-resolution mass spectrometer (HRMS) equipped with a nano-electrospray (NSI) source made in-house following the University of Washington Proteomic Resource (UWPR) design. Using a MicroTee (PEEK, 0.025" OD), the commercial analytical column was connected to a commercial emitter (PicoTip, Waters) and the liquid path was applied a high voltage through a platinum wire (adapted from UWPR design). All analyses were carried out in positive mode and a NSI spray voltage of 2.0 kV. Data was collected using data dependent acquisition (DDA) using Xcalibur 4.0 data acquisition software (Thermo Fisher). The MS scan range was 400-2000 m/z at 60,000 resolution with a maximum injection time of 30 ms and automated gain control of $1e6$ (Nesvizhskii et al., 2007). Following each MS scan (Nesvizhskii et al., 2007), data-dependent MS (dd-MS) (Eng et al., 2013) was set to perform on the top 10 ions in a data-dependent manner at 15,000 resolution with a normalized collision energy of 27 eV. Additional selection criteria for dd-MS (Eng et al., 2013) were as follows: maximum injection time of 50 ms with an automated gain control of $5e4$, the isolation window was 1.5 Da and dynamic exclusion was set at 20 sec.

Data Analysis and Protein Identification

Data processing was conducted using the software from the trans-proteomic pipeline (TPP v.4.8.1) (Nesvizhskii et al., 2007). Briefly, raw data was converted to mzML and searched using COMET (Eng et al., 2013; Eng et al., 2015) against a FASTA protein database consisting of *N. maritimus* (Uniprot NITMS 1,795 proteins accessed August 2015; KEGG estimated protein-coding genes 1,795), *E.coli* chaperone protein (Hi3 standard; P63284), and concatenated with two sets of randomized sequences. Additional COMET parameters included trypsin enzyme

specificity, one allowed non-tryptic termini, up to two missed cleavage sites, carbamidomethylation of cysteine residues as a fixed modification (+57.021464 Da), and oxidation of methionine residues (+15.9949 Da) as a variable modification. The COMET pep.xml files from each technical triplicate were then grouped and searched in PeptideProphet followed by iProphet (Shteynberg et al., 2011) and ProteinProphet (Nesvizhskii et al., 2003) within the TPP. A second search was conducted using these same parameters but with the addition of protein N-terminal acetylation (+42.010565 Da) and N-terminal methionine clipping as a variable modifications. When the difference in spectral counts was greater than 10 between the two sets of searches, the peptides corresponding to a protein N-terminal acetylation were manually validated. If N-terminal acetylation was observed in *both* b- and y-ions of the modified peptide MS/MS spectrum, then spectral counts containing protein N-terminal acetylation were used. If peptides did not have the observed N-terminal acetylation modification, then only spectral counts from the original search were used. The two sets of randomized sequences were decoy peptides used for the purpose of calculating peptide and protein false discovery rates (FDR). The list of protein identifications was filtered using a 95% or greater protein probability as calculated from ProteinProphet corresponding to a FDR of 0.1% (protein level 2/1320; peptide level 60/79658) and further to a minimum of two unique peptides in the combined analysis.

References

- Alber, B., Olinger, M., Rieder, A., Kockelkorn, D., Jobst, B., Hugler, M., and Fuchs, G. (2006) Malonyl-coenzyme A reductase in the modified 3-hydroxypropionate cycle for autotrophic carbon fixation in archaeal Metallosphaera and Sulfolobus spp. *J Bacteriol* **188**: 8551-8559.
- Amin, S.A., Moffett, J.W., Martens-Habbena, W., Jacquot, J.E., Han, Y., Devol, A. et al. (2013) Copper requirements of the ammonia-oxidizing archaeon Nitrosopumilus maritimus SCM1 and implications for nitrification in the marine environment. *Limnol Oceanogr* **58**: 2037-2045.
- Anders, S., Pyl, P.T., and Huber, W. (2015) HTSeq-a Python framework to work with high-throughput sequencing data. *Bioinformatics* **31**: 166-169.

- Andrews, S. (2010) FastQC: A quality control tool for high throughput sequence data.
- Baker, B.J., Lesniewski, R.A., and Dick, G.J. (2012) Genome-enabled transcriptomics reveals archaeal populations that drive nitrification in a deep-sea hydrothermal plume. *Isme J* **6**: 2269-2279.
- Banerjee, R.V., and Matthews, R.G. (1990) Cobalamin-Dependent Methionine Synthase. *Faseb J* **4**: 1450-1459.
- Berg, I.A., Kockelkorn, D., Buckel, W., and Fuchs, G. (2007) A 3-hydroxypropionate/4-hydroxybutyrate autotrophic carbon dioxide assimilation pathway in archaea. *Science* **318**: 1782-1786.
- Berube, P.M., and Stahl, D.A. (2012) The Divergent AmoC(3) Subunit of Ammonia Monooxygenase Functions as Part of a Stress Response System in *Nitrosomonas europaea*. *J Bacteriol* **194**: 3448-3456.
- Berube, P.M., Samudrala, R., and Stahl, D.A. (2007) Transcription of all amoC copies is associated with recovery of *Nitrosomonas europaea* from ammonia starvation. *J Bacteriol* **189**: 3935-3944.
- Bligh, E.G., and Dyer, W.J. (1959) A Rapid Method of Total Lipid Extraction and Purification. *Can J Biochem Phys* **37**: 911-917.
- Bolger, A.M., Lohse, M., and Usadel, B. (2014) Trimmomatic: a flexible trimmer for Illumina sequence data. *Bioinformatics* **30**: 2114-2120.
- Brouwer, M., Chamulitrat, W., Ferruzzi, G., Sauls, D.L., and Weinberg, J.B. (1996) Nitric oxide interactions with cobalamins: Biochemical and functional consequences. *Blood* **88**: 1857-1864.
- Canelas, A.B., ten Pierick, A., Ras, C., Seifar, R.M., van Dam, J.C., van Gulik, W.M., and Heijnen, J.J. (2009) Quantitative Evaluation of Intracellular Metabolite Extraction Techniques for Yeast Metabolomics. *Anal Chem* **81**: 7379-7389.
- Coutts, G., Thomas, G., Blakey, D., and Merrick, M. (2002) Membrane sequestration of the signal transduction protein GlnK by the ammonium transporter AmtB. *Embo J* **21**: 536-545.
- Danishpajoo, I.O., Gudi, T., Chen, Y.C., Kharitonov, V.G., Sharma, V.S., and Boss, G.R. (2001) Nitric oxide inhibits methionine synthase activity in vivo and disrupts carbon flow through the folate pathway. *J Biol Chem* **276**: 27296-27303.
- Dobin, A., Davis, C.A., Schlesinger, F., Drenkow, J., Zaleski, C., Jha, S. et al. (2013) STAR: ultrafast universal RNA-seq aligner. *Bioinformatics* **29**: 15-21.
- Doxey, A.C., Kurtz, D.A., Lynch, M.D.J., Sauder, L.A., and Neufeld, J.D. (2015) Aquatic metagenomes implicate Thaumarchaeota in global cobalamin production. *Isme J* **9**: 461-471.
- El Sheikh, A.F., and Klotz, M.G. (2008) Ammonia-dependent differential regulation of the gene cluster that encodes ammonia monooxygenase in *Nitrosococcus oceanus* ATCC 19707. *Environ Microbiol* **10**: 3026-3035.
- Eng, J.K., Jahan, T.A., and Hoopmann, M.R. (2013) Comet: An open-source MS/MS sequence database search tool. *Proteomics* **13**: 22-24.
- Eng, J.K., Hoopmann, M.R., Jahan, T.A., Egertson, J.D., Noble, W.S., and MacCoss, M.J. (2015) A Deeper Look into Comet-Implementation and Features. *J Am Soc Mass Spectr* **26**: 1865-1874.
- Facciotti, M.T., Reiss, D.J., Pan, M., Kaur, A., Vuthoori, M., Bonneau, R. et al. (2007) General transcription factor specified global gene regulation in archaea. *P Natl Acad Sci USA* **104**: 4630-4635.

- Francis, C.A., Roberts, K.J., Beman, J.M., Santoro, A.E., and Oakley, B.B. (2005) Ubiquity and diversity of ammonia-oxidizing archaea in water columns and sediments of the ocean. *P Natl Acad Sci USA* **102**: 14683-14688.
- French, E., and Bollmann, A. (2015) Freshwater Ammonia-Oxidizing Archaea Retain amoA mRNA and 16S rRNA during Ammonia Starvation. *Life (Basel)* **5**: 1396-1404.
- Geiduschek, E.P., and Ouhammouch, M. (2005) Archaeal transcription and its regulators. *Mol Microbiol* **56**: 1397-1407.
- Grasshoff, K., Kremling, K., and Erhard, M. (1999) *Methods of Seawater Analysis, 3rd edn.* : Wiley-VCH.
- Groussman, R.D., Parker, M.S., and Armbrust, E.V. (2015) Diversity and Evolutionary History of Iron Metabolism Genes in Diatoms. *Plos One* **10**.
- Guasto, J.S., Rusconi, R., and Stocker, R. (2012) Fluid Mechanics of Planktonic Microorganisms. *Annu Rev Fluid Mech* **44**: 373-400.
- Hatzenpichler, R., Lebedeva, E.V., Spieck, E., Stoecker, K., Richter, A., Daims, H., and Wagner, M. (2008) A moderately thermophilic ammonia-oxidizing crenarchaeote from a hot spring. *P Natl Acad Sci USA* **105**: 2134-2139.
- Hawley, A.K., Brewer, H.M., Norbeck, A.D., Pasa-Tolic, L., and Hallam, S.J. (2014) Metaproteomics reveals differential modes of metabolic coupling among ubiquitous oxygen minimum zone microbes. *P Natl Acad Sci USA* **111**: 11395-11400.
- Heal, K.R., Carlson, L.T., Devol, A.H., Armbrust, E.V., Moffett, J.W., Stahl, D.A., and Ingalls, A.E. (2014a) Determination of four forms of vitamin B-12 and other B vitamins in seawater by liquid chromatography/tandem mass spectrometry. *Rapid Commun Mass Sp* **28**: 2398-2404.
- Hiniker, A., Collet, J.F., and Bardwell, J.C.A. (2005) Copper stress causes an in vivo requirement for the Escherichia coli disulfide isomerase DsbC. *J Biol Chem* **280**: 33785-33791.
- Hollibaugh, J.T., Gifford, S., Sharma, S., Bano, N., and Moran, M.A. (2011) Metatranscriptomic analysis of ammonia-oxidizing organisms in an estuarine bacterioplankton assemblage. *Isme J* **5**: 866-878.
- Hommes, N.G., Sayavedra-Soto, L.A., and Arp, D.J. (2001) Transcript analysis of multiple copies of amo (encoding ammonia monooxygenase) and hao (encoding hydroxylamine oxidoreductase) in Nitrosomonas europaea. *J Bacteriol* **183**: 1096-1100.
- Horak, R.E.A., Qin, W., Schauer, A.J., Armbrust, E.V., Ingalls, A.E., Moffett, J.W. et al. (2013) Ammonia oxidation kinetics and temperature sensitivity of a natural marine community dominated by Archaea. *Isme J* **7**: 2023-2033.
- Hosseinzadeh, P., Tian, S.L., Marshall, N.M., Hemp, J., Mullen, T., Nilges, M.J. et al. (2016) A Purple Cupredoxin from Nitrosopumilus maritimus Containing a Mononuclear Type 1 Copper Center with an Open Binding Site. *J Am Chem Soc* **138**: 6324-6327.
- Huergo, L.F., Chandra, G., and Merrick, M. (2013) PII signal transduction proteins: nitrogen regulation and beyond. *Fems Microbiol Rev* **37**: 251-283.
- Jacquot, J.E., Horak, R.E.A., Amin, S.A., Devol, A.H., Ingalls, A.E., Armbrust, E.V. et al. (2014) Assessment of the potential for copper limitation of ammonia oxidation by Archaea in a dynamic estuary. *Mar Chem* **162**: 37-49.
- Kambo, A., Sharma, V.S., Casteel, D.E., Woods, V.L., Pilz, R.B., and Boss, G.R. (2005) Nitric oxide inhibits mammalian methylmalonyl-CoA mutase. *J Biol Chem* **280**: 10073-10082.
- Karner, M.B., DeLong, E.F., and Karl, D.M. (2001) Archaeal dominance in the mesopelagic zone of the Pacific Ocean. *Nature* **409**: 507-510.

- Kerou, M., Offre, P., Valledor, L., Abby, S.S., Melcher, M., Nagler, M. et al. (2016) Proteomics and comparative genomics of *Nitrososphaera viennensis* reveal the core genome and adaptations of archaeal ammonia oxidizers. *Proc Natl Acad Sci U S A*.
- Kockelkorn, D., and Fuchs, G. (2009) Malonic Semialdehyde Reductase, Succinic Semialdehyde Reductase, and Succinyl-Coenzyme A Reductase from *Metallosphaera sedula*: Enzymes of the Autotrophic 3-Hydroxypropionate/4-Hydroxybutyrate Cycle in Sulfolobales. *J Bacteriol* **191**: 6352-6362.
- Könneke, M., Schubert, D.M., Brown, P.C., Hugler, M., Standfest, S., Schwander, T. et al. (2014) Ammonia-oxidizing archaea use the most energy-efficient aerobic pathway for CO₂ fixation. *P Natl Acad Sci USA* **111**: 8239-8244.
- Kozlowski, J.A., Stieglmeier, M., Schleper, C., Klotz, M.G., and Stein, L.Y. (2016b) Pathways and key intermediates required for obligate aerobic ammonia-dependent chemolithotrophy in bacteria and Thaumarchaeota. *Isme J* **10**: 1836-1845.
- LaRoche, J., Boyd, P.W., McKay, R.M.L., and Geider, R.J. (1996) Flavodoxin as an in situ marker for iron stress in phytoplankton. *Nature* **382**: 802-805.
- Lebedeva, E.V., Hatzenpichler, R., Pelletier, E., Schuster, N., Hauzmayer, S., Bulaev, A. et al. (2013) Enrichment and Genome Sequence of the Group I. 1a Ammonia-Oxidizing Archaeon "Ca. Nitrosotenuis uzonensis" Representing a Clade Globally Distributed in Thermal Habitats. *Plos One* **8**.
- Leigh, J.A., and Dodsworth, J.A. (2007) Nitrogen regulation in bacteria and archaea. *Annual Review of Microbiology* **61**: 349-377.
- Li, Y.Y., Ding, K., Wen, X.H., Zhang, B., Shen, B., and Yang, Y.F. (2016b) A novel ammonia-oxidizing archaeon from wastewater treatment plant: Its enrichment, physiological and genomic characteristics. *Sci Rep-Uk* **6**.
- Lommer, M., Specht, M., Roy, A.S., Kraemer, L., Andreson, R., Gutowska, M.A. et al. (2012) Genome and low-iron response of an oceanic diatom adapted to chronic iron limitation. *Genome Biol* **13**.
- Love, M.I., Huber, W., and Anders, S. (2014) Moderated estimation of fold change and dispersion for RNA-seq data with DESeq2. *Genome Biol* **15**.
- Lunau, M., Lemke, A., Walther, K., Martens-Habbena, W., and Simon, M. (2005) An improved method for counting bacteria from sediments and turbid environments by epifluorescence microscopy. *Environ Microbiol* **7**: 961-968.
- Lund, M.B., Smith, J.M., and Francis, C.A. (2012) Diversity, abundance and expression of nitrite reductase (*nirK*)-like genes in marine thaumarchaea. *Isme J* **6**: 1966-1977.
- Martens-Habbena, W., and Stahl, D.A. (2011a) Nitrogen Metabolism and Kinetics of Ammonia-Oxidizing Archaea. *Method Enzymol* **496**: 465-487.
- Martens-Habbena, W., Berube, P.M., Urakawa, H., de la Torre, J.R., and Stahl, D.A. (2009b) Ammonia oxidation kinetics determine niche separation of nitrifying Archaea and Bacteria. *Nature* **461**: 976-U234.
- Martens-Habbena, W., Qin, W., Horak, R.E.A., Urakawa, H., Schauer, A.J., Moffett, J.W. et al. (2015) The production of nitric oxide by marine ammonia-oxidizing archaea and inhibition of archaeal ammonia oxidation by a nitric oxide scavenger. *Environ Microbiol* **17**: 2261-2274.
- Metcalf, W.W., Griffin, B.M., Cicchillo, R.M., Gao, J.T., Janga, S.C., Cooke, H.A. et al. (2012) Synthesis of Methylphosphonic Acid by Marine Microbes: A Source for Methane in the Aerobic Ocean. *Science* **337**: 1104-1107.

- Nakagawa, T., and Stahl, D.A. (2013) Transcriptional Response of the Archaeal Ammonia Oxidizer *Nitrosopumilus maritimus* to Low and Environmentally Relevant Ammonia Concentrations. *Appl Environ Microb* **79**: 6911-6916.
- Nesvizhskii, A.I., Vitek, O., and Aebersold, R. (2007) Analysis and validation of proteomic data generated by tandem mass spectrometry. *Nat Methods* **4**: 787-797.
- Nesvizhskii, A.I., Keller, A., Kolker, E., and Aebersold, R. (2003) A statistical model for identifying proteins by tandem mass spectrometry. *Anal Chem* **75**: 4646-4658.
- Norris, K.L., Lee, J.Y., and Yao, T.P. (2009) Acetylation Goes Global: The Emergence of Acetylation Biology. *Sci Signal* **2**.
- Offre, P., Kerou, M., Spang, A., and Schleper, C. (2014) Variability of the transporter gene complement in ammonia-oxidizing archaea. *Trends Microbiol* **22**: 665-675.
- Otte, J., Mall, A., Schubert, D.M., Konneke, M., and Berg, I.A. (2015) Malonic Semialdehyde Reductase from the Archaeon *Nitrosopumilus maritimus* Is Involved in the Autotrophic 3-Hydroxypropionate/4-Hydroxybutyrate Cycle. *Appl Environ Microb* **81**: 1700-1707.
- Palatinszky, M., Herbold, C., Jehmlich, N., Pogoda, M., Han, P., von Bergen, M. et al. (2015) Cyanate as an energy source for nitrifiers. *Nature* **524**: 105-+.
- Pankowski, A., and McMinn, A. (2009) Development of Immunoassays for the Iron-Regulated Proteins Ferredoxin and Flavodoxin in Polar Microalgae. *J Phycol* **45**: 771-783.
- Peng, X.F., Fuchsman, C.A., Jayakumar, A., Warner, M.J., Devol, A.H., and Ward, B.B. (2016) Revisiting nitrification in the Eastern Tropical South Pacific: A focus on controls. *J Geophys Res Oceans* **121**: 1667-1684.
- Qin, W., Amin, S.A., Martens-Habbena, W., Walker, C.B., Urakawa, H., Devol, A.H. et al. (2014) Marine ammonia-oxidizing archaeal isolates display obligate mixotrophy and wide ecotypic variation. *P Natl Acad Sci USA* **111**: 12504-12509.
- Ramos-Vera, W.H., Weiss, M., Strittmatter, E., Kockelkorn, D., and Fuchs, G. (2011) Identification of Missing Genes and Enzymes for Autotrophic Carbon Fixation in Crenarchaeota. *J Bacteriol* **193**: 1201-1211.
- Rensing, C., and Grass, G. (2003) *Escherichia coli* mechanisms of copper homeostasis in a changing environment. *Fems Microbiol Rev* **27**: 197-213.
- Santoro, A.E., Casciotti, K.L., and Francis, C.A. (2010) Activity, abundance and diversity of nitrifying archaea and bacteria in the central California Current. *Environ Microbiol* **12**: 1989-2006.
- Santoro, A.E., Buchwald, C., McIlvin, M.R., and Casciotti, K.L. (2011) Isotopic Signature of N₂O Produced by Marine Ammonia-Oxidizing Archaea. *Science* **333**: 1282-1285.
- Santoro, A.E., Dupont, C.L., Richter, R.A., Craig, M.T., Carini, P., McIlvin, M.R. et al. (2015) Genomic and proteomic characterization of "Candidatus *Nitrosopelagicus brevis*": An ammonia-oxidizing archaeon from the open ocean. *P Natl Acad Sci USA* **112**: 1173-1178.
- Sara, M., and Sleytr, U.B. (2000) S-layer proteins. *J Bacteriol* **182**: 859-868.
- Sayavedra-Soto, L.A., Hommes, N.G., Alzerreca, J.J., Arp, D.J., Norton, J.M., and Klotz, M.G. (1998) Transcription of the *amoC*, *amoA* and *amoB* genes in *Nitrosomonas europaea* and *Nitrospira* sp, NpAV. *Fems Microbiol Lett* **167**: 81-88.
- Sharma, V.S., Pilz, R.B., Boss, G.R., and Magde, D. (2003) Reactions of nitric oxide with vitamin B-12 and its precursor, cobinamide. *Biochemistry-Us* **42**: 8900-8908.
- Shi, Y.M., Tyson, G.W., Eppley, J.M., and DeLong, E.F. (2011) Integrated metatranscriptomic and metagenomic analyses of stratified microbial assemblages in the open ocean. *Isme J* **5**: 999-1013.

- Shteynberg, D., Deutsch, E.W., Lam, H., Eng, J.K., Sun, Z., Tasman, N. et al. (2011) iProphet: Multi-level Integrative Analysis of Shotgun Proteomic Data Improves Peptide and Protein Identification Rates and Error Estimates. *Mol Cell Proteomics* **10**.
- Spang, A., Poehlein, A., Offre, P., Zumbragel, S., Haider, S., Rychlik, N. et al. (2012) The genome of the ammonia-oxidizing Candidatus Nitrososphaera gargensis: insights into metabolic versatility and environmental adaptations. *Environ Microbiol* **14**: 3122-3145.
- Stahl, D.A., and de la Torre, J.R. (2012a) Physiology and Diversity of Ammonia-Oxidizing Archaea. *Annu Rev Microbiol* **66**: 83-101.
- Stein, L.Y., Campbell, M.A., and Klotz, M.G. (2013) Energy-mediated vs. ammonium-regulated gene expression in the obligate ammonia-oxidizing bacterium, Nitrosococcus oceani. *Front Microbiol* **4**.
- Stewart, F.J., Ulloa, O., and DeLong, E.F. (2012) Microbial metatranscriptomics in a permanent marine oxygen minimum zone. *Environ Microbiol* **14**: 23-40.
- Stieglmeier, M., Klingl, A., Alves, R.J.E., Rittmann, S.K.M.R., Melcher, M., Leisch, N., and Schleper, C. (2014b) Nitrososphaera viennensis gen. nov., sp nov., an aerobic and mesophilic, ammonia-oxidizing archaeon from soil and a member of the archaeal phylum Thaumarchaeota. *Int J Syst Evol Micr* **64**: 2738-2752.
- Takemoto, L.J., and Hansen, J.S. (1982) Intermolecular Disulfide Bonding of Lens Membrane-Proteins during Human Cataractogenesis. *Invest Opth Vis Sci* **22**: 336-342.
- Tappe, W., Laverman, A., Bohland, M., Braster, M., Rittershaus, S., Groeneweg, J., and van Verseveld, H.W. (1999) Maintenance energy demand and starvation recovery dynamics of Nitrosomonas europaea and Nitrobacter winogradskyi cultivated in a retentostat with complete biomass retention. *Appl Environ Microb* **65**: 2471-2477.
- Teufel, R., Kung, J.W., Kockelkorn, D., Alber, B.E., and Fuchs, G. (2009) Hydroxypropionyl-Coenzyme A Dehydratase and Acryloyl-Coenzyme A Reductase, Enzymes of the Autotrophic 3-Hydroxypropionate/4-Hydroxybutyrate Cycle in the Sulfolobales. *J Bacteriol* **191**: 4572-4581.
- Tremblay, P.L., and Hallenbeck, P.C. (2009) Of blood, brains and bacteria, the Amt/Rh transporter family: emerging role of Amt as a unique microbial sensor. *Mol Microbiol* **71**: 12-22.
- Vajjala, N., Martens-Habbena, W., Sayavedra-Soto, L.A., Schauer, A., Bottomley, P.J., Stahl, D.A., and Arp, D.J. (2013) Hydroxylamine as an intermediate in ammonia oxidation by globally abundant marine archaea. *P Natl Acad Sci USA* **110**: 1006-1011.
- Walker, C.B., de la Torre, J.R., Klotz, M.G., Urakawa, H., Pinel, N., Arp, D.J. et al. (2010) Nitrosopumilus maritimus genome reveals unique mechanisms for nitrification and autotrophy in globally distributed marine crenarchaea. *P Natl Acad Sci USA* **107**: 8818-8823.
- Wang, Q.J., Zhang, Y.K., Yang, C., Xiong, H., Lin, Y., Yao, J. et al. (2010) Acetylation of Metabolic Enzymes Coordinates Carbon Source Utilization and Metabolic Flux. *Science* **327**: 1004-1007.
- Weinert, B.T., Iesmantavicius, V., Wagner, S.A., Scholz, C., Gummesson, B., Beli, P. et al. (2013) Acetyl-Phosphate Is a Critical Determinant of Lysine Acetylation in E. coli. *Mol Cell* **51**: 265-272.
- Whitney, L.P., Lins, J.J., Hughes, M.P., Wells, M.L., Chappell, P.D., and Jenkins, B.D. (2011) Characterization of putative iron responsive genes as species-specific indicators of iron stress in Thalassiosiroid diatoms. *Front Microbiol* **2**.
- Williams, T.J., Long, E., Evans, F., DeMaere, M.Z., Lauro, F.M., Raftery, M.J. et al. (2012) A metaproteomic assessment of winter and summer bacterioplankton from Antarctic Peninsula coastal surface waters. *Isme J* **6**: 1883-1900.

Wolak, M., Stochel, G., and van Eldik, R. (2006) Reactivity of aquacobalamin and reduced cobalamin toward S-nitrosoglutathione and S-nitroso-N-acetylpenicillamine. *Inorg Chem* **45**: 1367-1379.

Yi, P., Melnyk, S., Pogribna, M., Pogribny, I.P., Hines, R.J., and James, S.J. (2000) Increase in plasma homocysteine associated with parallel increases in plasma S-adenosylhomocysteine and lymphocyte DNA hypomethylation. *J Biol Chem* **275**: 29318-29323.

Yool, A., Martin, A.P., Fernandez, C., and Clark, D.R. (2007) The significance of nitrification for oceanic new production. *Nature* **447**: 999-1002.

Zobell, C.E. (1941) Studies on marine bacteria I The cultural requirements of heterotrophic aerobes. *J Mar Res* **4**: 42-75.

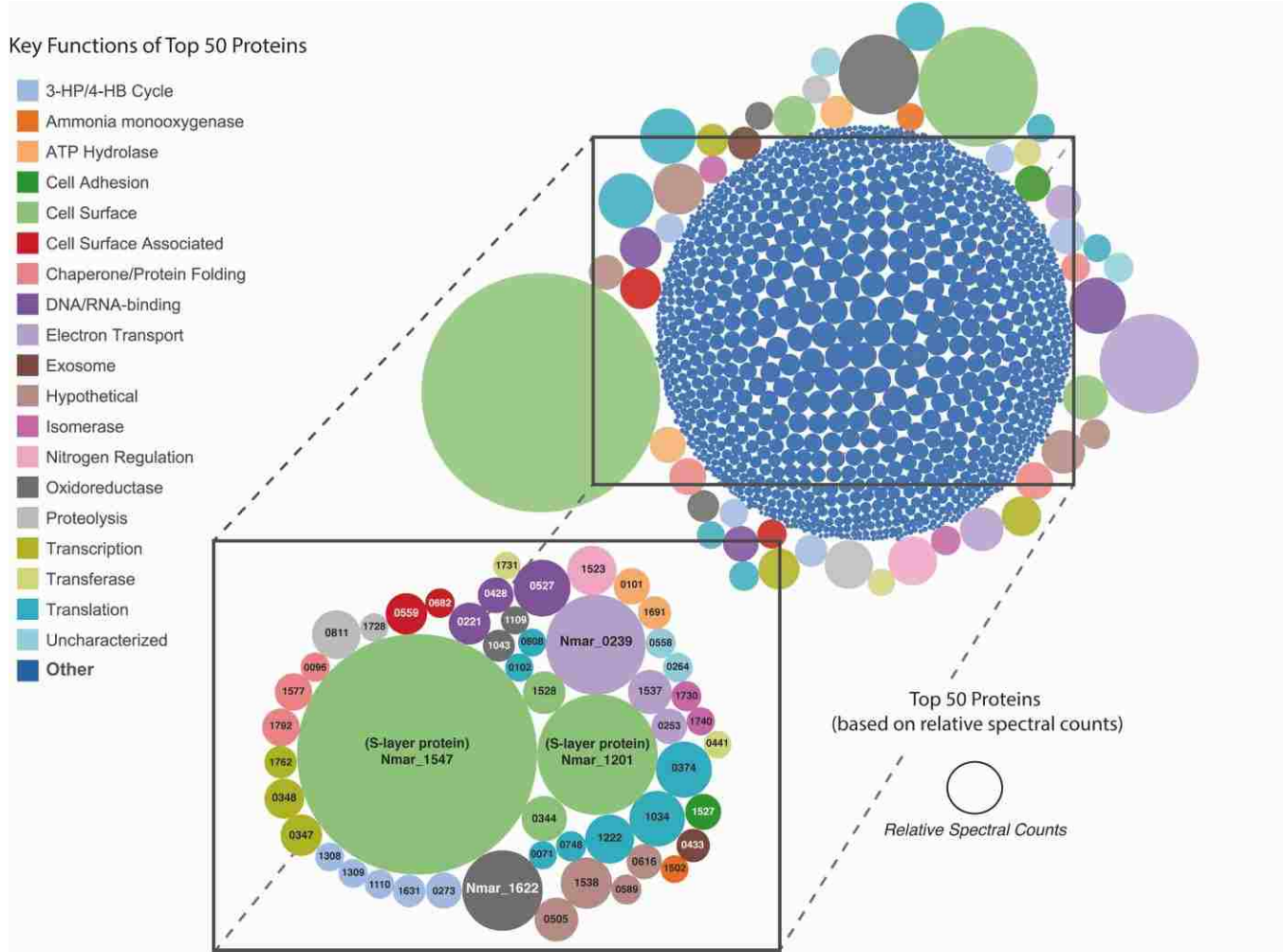


Figure 6.1. Proteome of *N. maritimus*.

Area of bubbles corresponds to protein abundance; bubble color corresponds to functional classification according to the annotation of the genome.

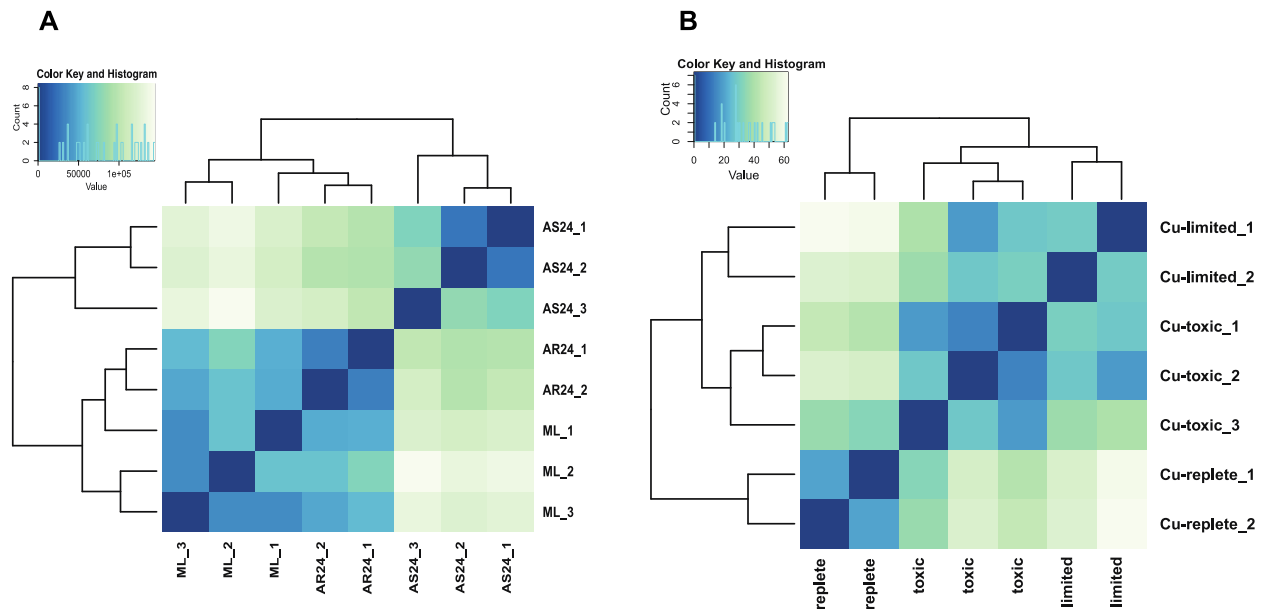


Figure 6.2. Unsupervised hierarchical clustering of *N. maritimus* cultures grown with different ammonia (A) and copper (B) availabilities based on global gene expression profiles as assessed using microarray and RNA-sequencing, respectively.

ML: mid-log phase cells, three biological replicates; AS24: 24 hrs ammonia-starved cells, three replicates; AR24: 24 hrs ammonia-recovered cells after starvation, two replicates. Cu-replete: Cu-replete (50 nM Cu) cells, two replicates; Cu-limited: Cu-limited (5 nM Cu) cells, two replicates; Cu-toxic: cells grown under Cu-toxic (750 nM Cu) condition, three replicates.

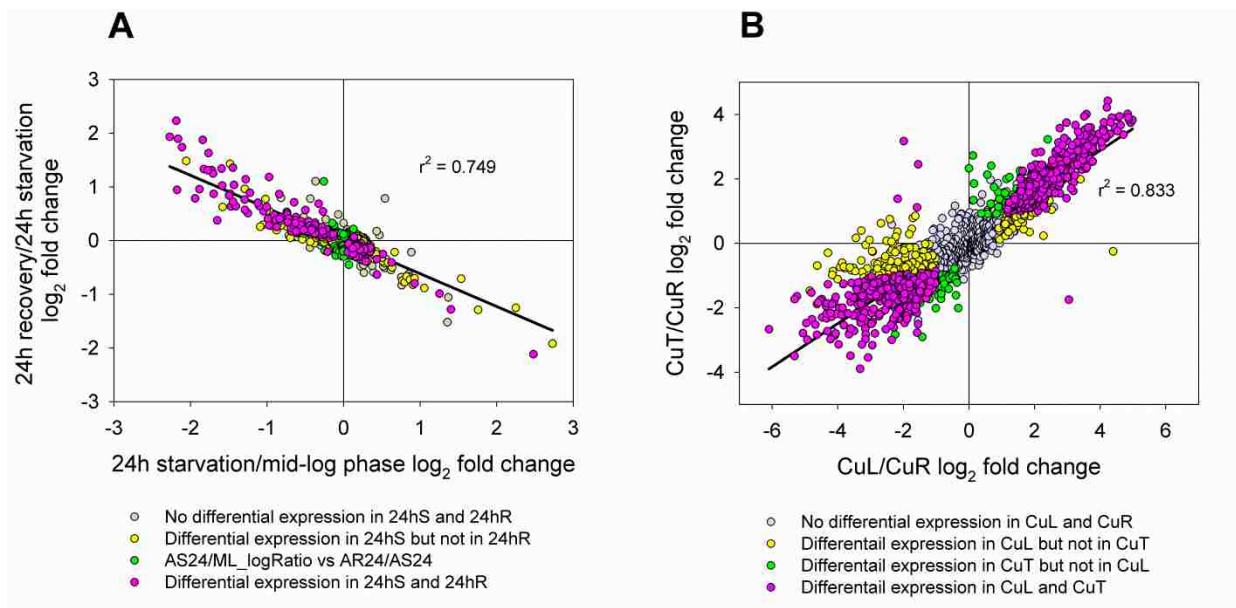


Figure 6.3. Comparative transcriptome responses of *N. maritimus* cultures to ammonia starvation vs. recovery after ammonia readdition (A) and Cu limitation vs. Cu toxicity (B).

The \log_2 fold changes for the transcript abundance of ammonia-starved cultures compared to mid-log phase cultures (A) and Cu-limited cultures compared to Cu-replete cultures (B) are shown on x axis, and the \log_2 fold changes for the transcript abundance of ammonia-recovery cultures relative to starved cultures (A) and the cultures with inhibitory high Cu concentration relative Cu-replete cultures (B) are shown on y axis. Each point represents the average of 2 to 3 replicates.

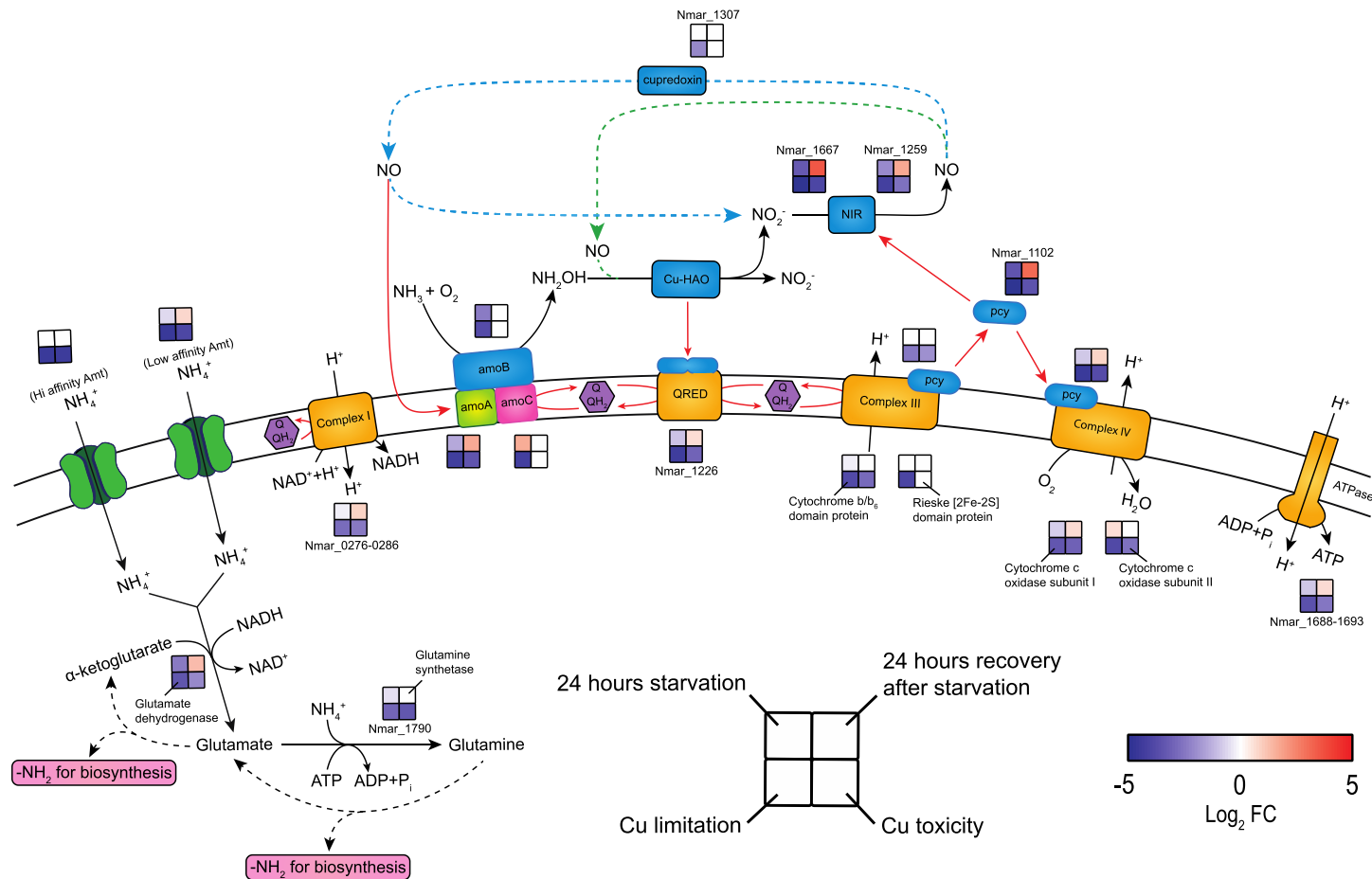


Figure 6.4. Transcriptional changes for the proposed ammonia oxidation, electron transfer and ammonia assimilation pathways in response to ammonia starvation, recovery, Cu limitation, and Cu excess conditions.

Log₂ fold changes in expression ranging from -5 to 5 are shown for the 24 hours starvation vs. exponential growth, 24 hours recovery after ammonia readdition vs. 24 hours starvation, Cu limitation vs. Cu replete, and Cu excess vs. Cu replete with up-regulation represented in red, down-regulation represented by blue, and no significantly differential expression represented in white.

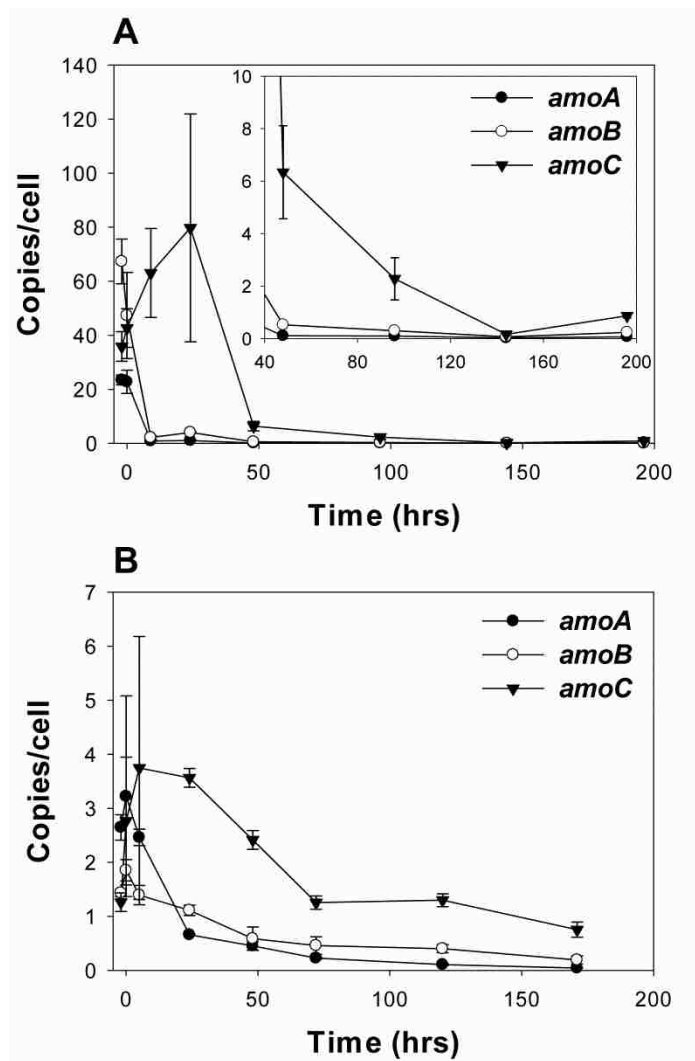


Figure 6.5. Transcript copies of *amoA*, *B* and *C* per cell during late exponential growth (before time 0) and stationary phase (from time 0) of *Nitrosopumilus maritimus* (A) and *Nitrosomonas europaea* (B). Error bars are the SD among average from triplicate cultures. Transcript pre cell values of *N. maritimus* from 40 hours of starvation to 200 hours are shown in inset box.

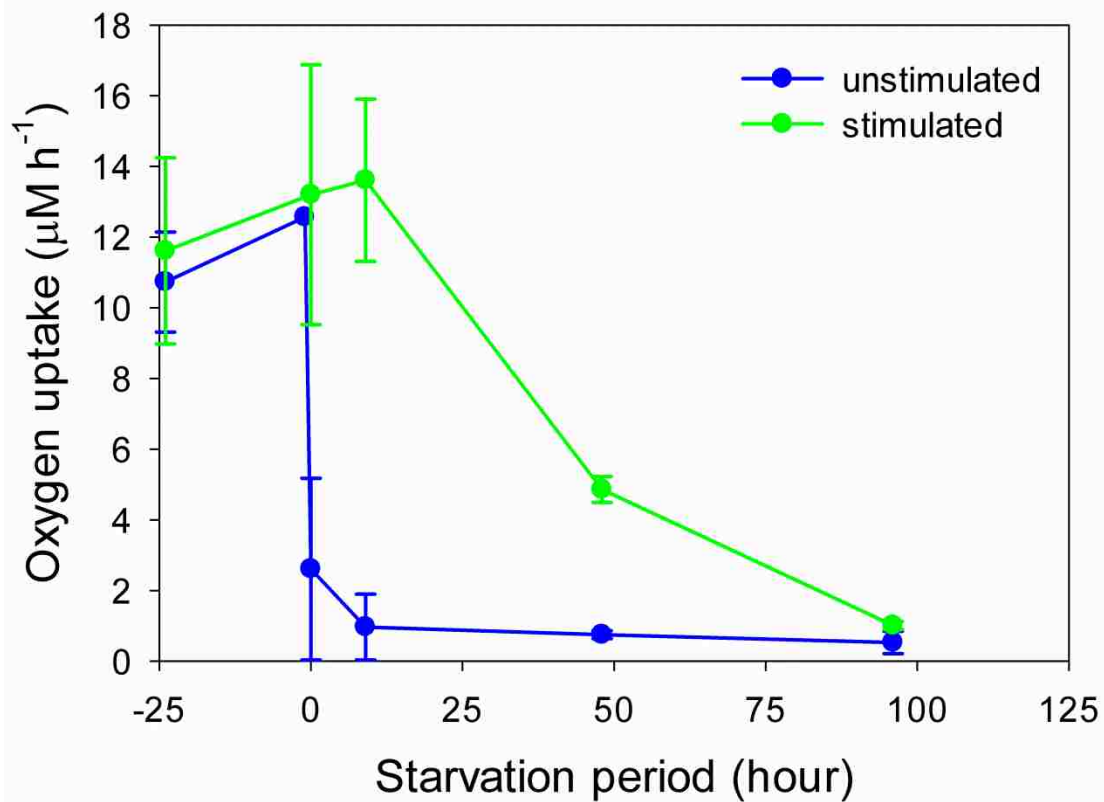


Figure 6.6. Spontaneous oxygen uptake rate of *N. maritimus* cells during late exponential growth (before time 0) and before (blue) and after (green) ammonia spike following time periods of ammonia-starvation (after time 0).

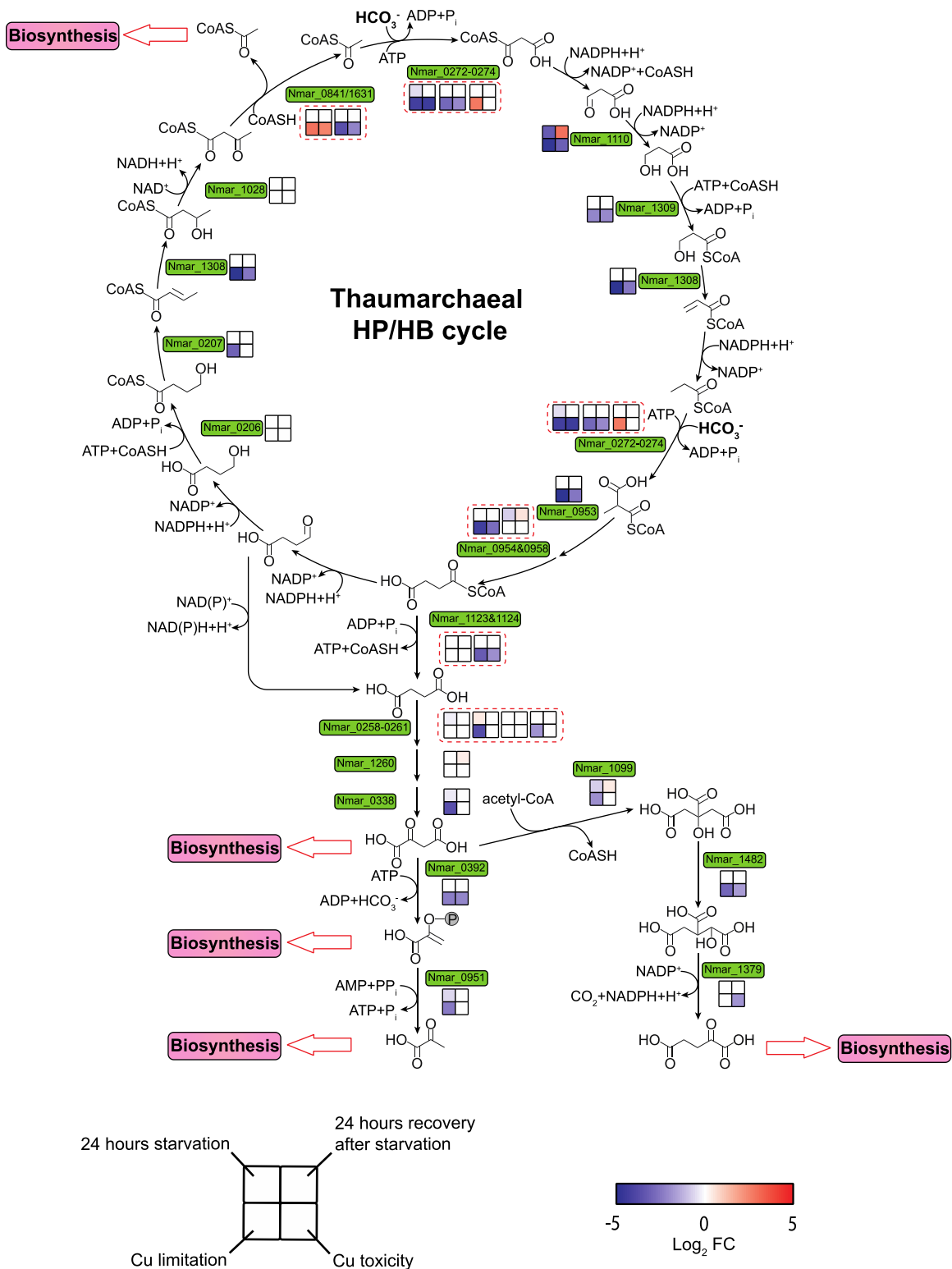
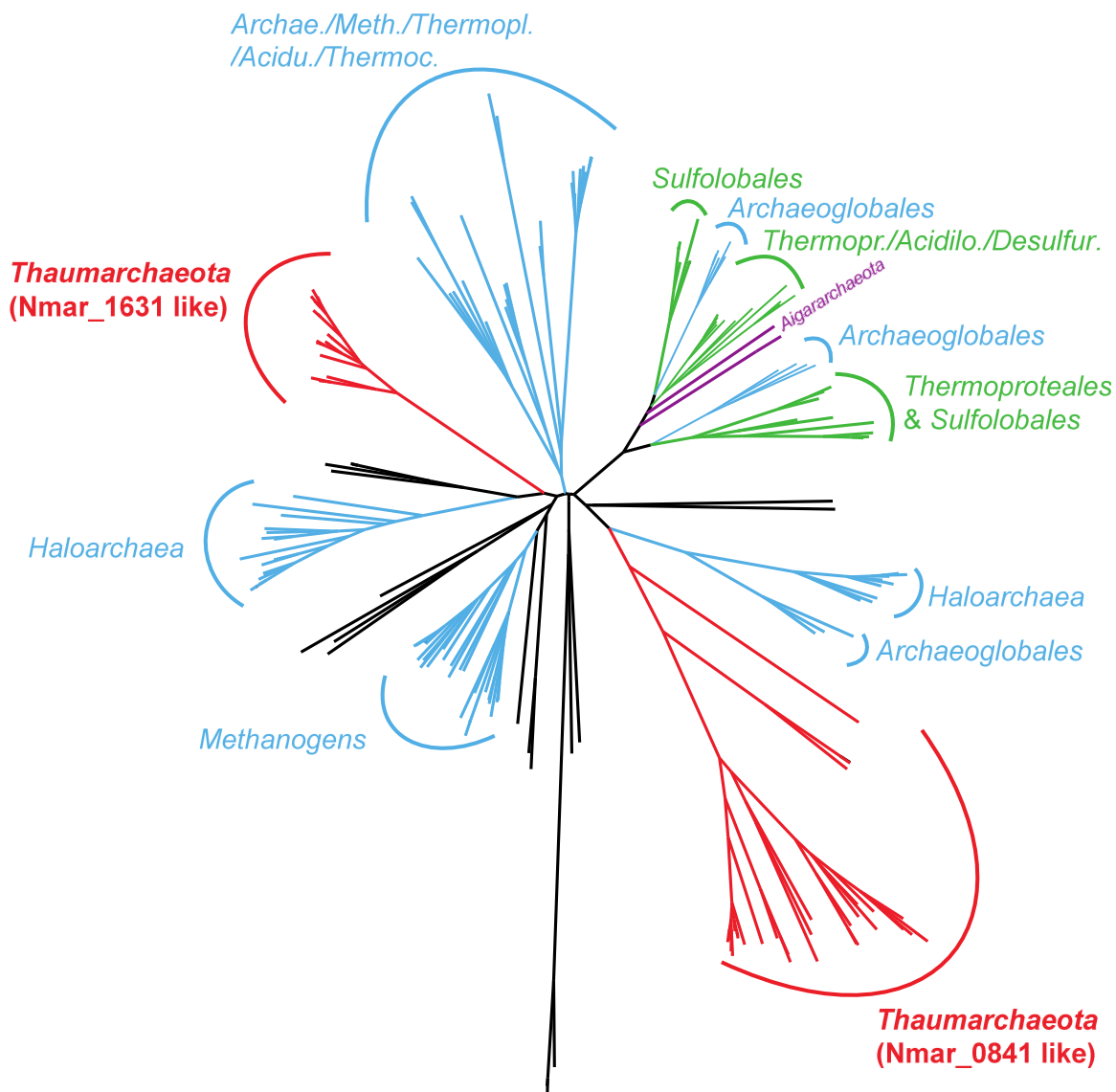


Figure 6.7. Transcriptional changes for the thaumarchaeotal 3-HP/4-HB carbon fixation pathway in response to ammonia starvation, recovery, Cu limitation, and Cu excess conditions.

Red represents up-regulation, blue represents down-regulations, and white represents genes whose expression levels are not significantly different from controls. P-value cutoff of 0.05 was taken as the threshold of the significant alteration in expression relative to controls.



0.1

Figure 6.8. Phylogenetic trees of gene encoding acetoacetyl-CoA beta-ketothiolase.

Thaumarchaeotal sequences are shown in red, Crenarchaeotal sequences are shown in green, Euryarchaeotal sequences are shown in blue, and bacterial sequences are shown in black. The tree is based on nucleotide sequence analysis.

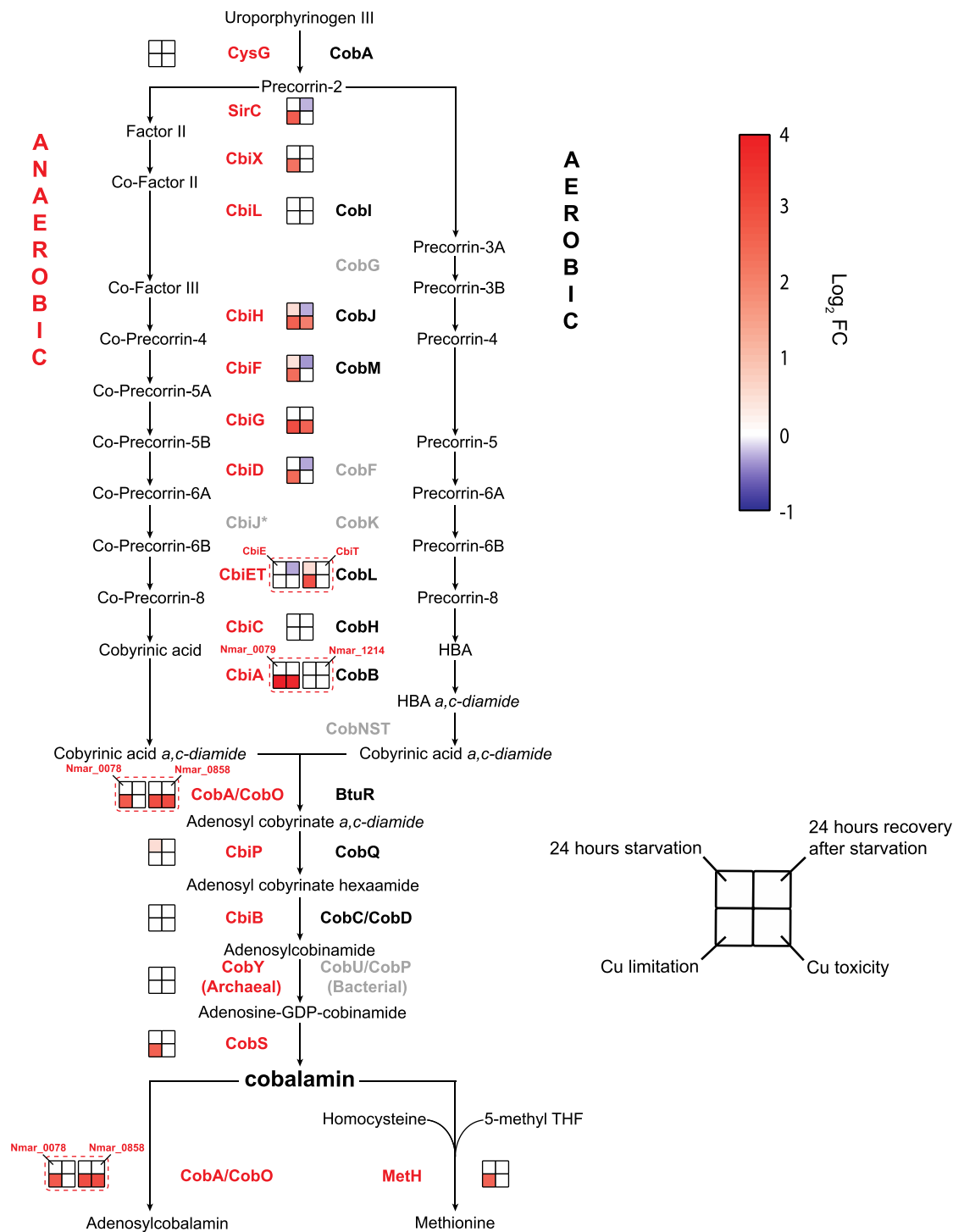


Figure 6.9. Transcriptional changes for the thaumarchaeotal cobalamin synthesis pathway in response to ammonia starvation, recovery, Cu limitation, and Cu excess conditions. Genes and gene clusters are shown as up-regulated (red), down-regulated (blue), or not differentially regulated (white) in stressed or recovery cultures relative to controls.

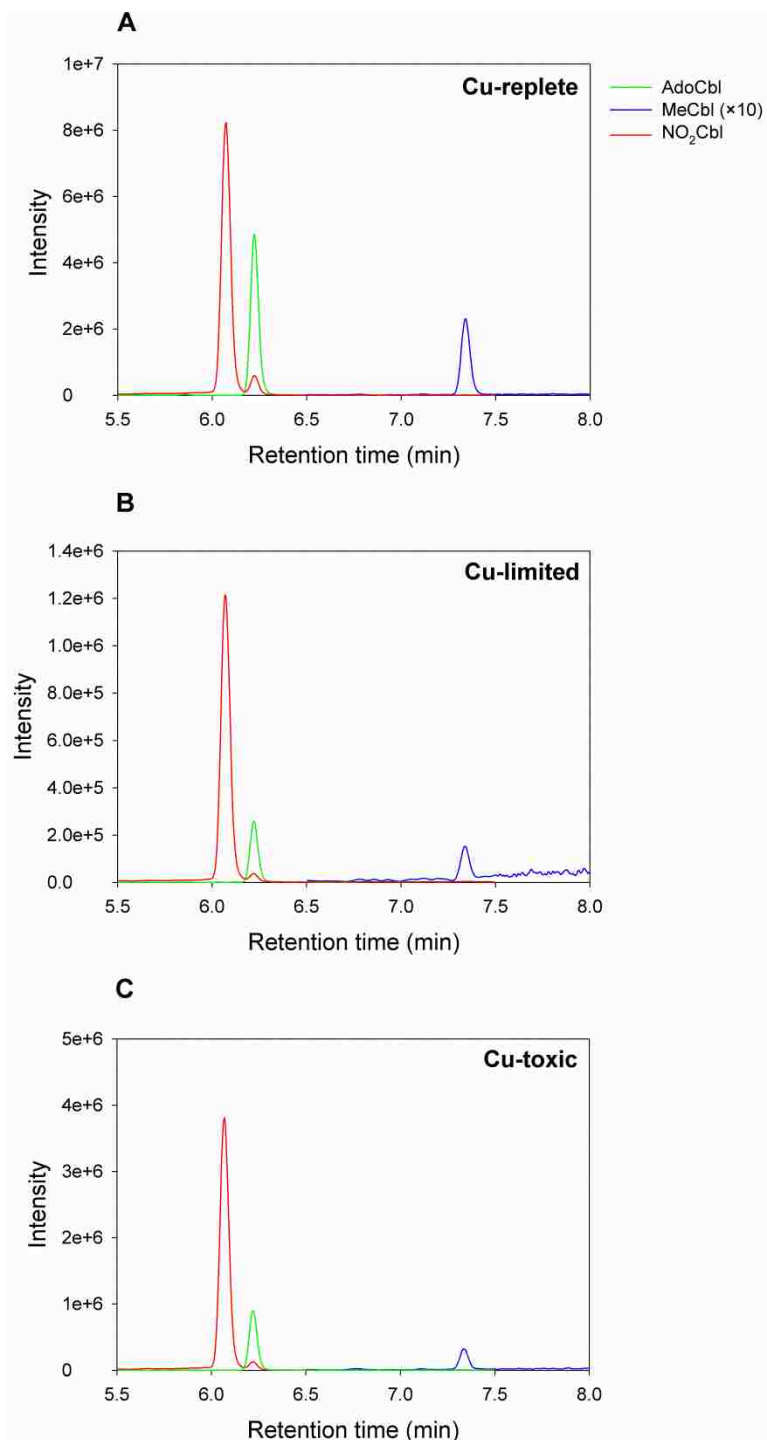


Figure 6.10. Chromatograms showing the distribution of AdoCbl, MeCbl (10 folds of the measured ion intensity), and NO₂Cbl in *N. maritimus* cells grown under Cu-replete (A), Cu-limited (B), and Cu-toxic (C) conditions.

Chapter 7.

Confounding effects of oxygen and temperature on the TEX₈₆ signature of marine thaumarchaeota

Wei Qin^a, Laura T. Carlson^b, E. Virginia Armbrust^b, Allan H. Devol^b, James W. Moffett^c,
David A. Stahl^{a,1} and Anitra E. Ingalls^{b,1}

Published in *Proceedings of the National Academy of Sciences of the United States of America*
2015

vol. 113, no. 35, 10979–10984, doi: 10.1073/pnas.1501568112

^aDepartment of Civil and Environmental Engineering, University of Washington, Seattle, WA 98195; ^bSchool of Oceanography, University of Washington, Seattle, WA 98195; ^cDepartment of Biological Sciences, University of Southern California, Los Angeles, CA 90089

¹Corresponding author E-mail: dastahl@u.washington.edu or aingalls@uw.edu.

Abstract

Marine ammonia-oxidizing archaea (AOA) are among the most abundant of marine microorganisms, spanning nearly the entire water column of diverse oceanic provinces. Historical patterns of abundance are preserved in sediments in the form of their distinctive glycerol dibiphytanyl glycerol tetraether (GDGT) membrane lipids. The correlation between the composition of GDGTs in surface sediment and the overlying annual average sea surface temperature forms the basis for a paleotemperature proxy (TEX_{86}) that is used to reconstruct surface ocean temperature as far back as the Middle Jurassic. However, mounting evidence suggests that factors other than temperature could also play an important role in determining GDGT distributions. We here use a study set of four marine AOA isolates to demonstrate that these closely related strains generate different TEX_{86} -temperature relationships and that oxygen (O_2) concentration is at least as important as temperature in controlling TEX_{86} values in culture. All of the four strains characterized showed a unique membrane compositional response to temperature, with TEX_{86} -inferred temperatures varying as much as 12°C from the incubation temperatures. In addition, both linear and non-linear TEX_{86} -temperature relationships were characteristic of individual strains. Increasing relative abundance of GDGT-2 and GDGT-3 with increasing O_2 limitation, at the expense of GDGT-1, lead to significant elevations in TEX_{86} -derived temperature. Although the adaptive significance of GDGT compositional changes in response to both temperature and O_2 is unclear, this observation necessitates a reassessment of archaeal lipid-based paleotemperature proxies, particularly in records that span low oxygen events or underlie oxygen minimum zones.

Significance statement

Ammonia-oxidizing archaea (AOA) are among the most abundant microorganisms in the ocean. Apart from having a major influence on the nitrogen cycle, the glycerol dibiphytanyl glycerol tetraether (GDGT) membrane lipids of AOA are widely used to reconstruct past sea surface temperatures. We here provide compelling evidence that the composition of membrane lipids of marine AOA show strain-specific dependence on temperature. We also show that oxygen (O_2) concentration greatly influences membrane lipid composition, leading to significant increases in TEX_{86} -derived temperatures with increasing O_2 limitation. This finding challenges the convention that GDGT composition correlates solely with ocean temperature and necessitates a reassessment of archaeal lipid-based paleoclimate proxies, particularly when applied to environments where O_2 is depleted.

Introduction

Marine ammonia-oxidizing archaea (AOA) (now assigned to the phylum *Thaumarchaeota*) are among the most ubiquitous and abundant organisms in the ocean, constituting up to 40% of microbial plankton in the meso- and bathypelagic zones (Karner et al., 2001; Francis et al., 2005; Könneke et al., 2005; Brochier-Armanet et al., 2008). They are generally recognized as the main drivers of oceanic nitrification (Beman et al., 2012a; Horak et al., 2013; Martens-Habbena et al., 2014), are closely coupled with anammox organisms in oxygen minimum zones (OMZ) (Lam et al., 2009; Yan et al., 2012a; Hawley et al., 2014), and have been implicated as a source of the greater part of oceanic emissions of the ozone-depleting greenhouse gas nitrous oxide (Santoro et al., 2011). Their wide habitat range suggests both high ecotypic diversity and adaptive capacity (Martens-Habbena et al., 2009b; Qin et al., 2014).

The adaptive basis for their dominant role in the nitrogen cycle has in part been attributed to highly efficient systems of ammonia oxidation and carbon fixation, and a primarily copper-based respiratory system that reduces reliance on iron availability in the often iron depleted marine environment (Martens-Habbena et al., 2009b; Walker et al., 2010; Amin et al., 2013; Könneke et al., 2014). In addition, compositional regulation of their distinctive glycerol dibiphytanyl glycerol tetraether (GDGT) lipid membrane (Fig. 7.1) is implicated in adaptation and acclimation to energy-limited environments (Elling et al., 2014). Relative to the bacterial membrane bilayer, the membrane-spanning lipids of archaea are less permeable to ions and protons (van de Vossenberg et al., 1998; Valentine, 2007). Lower permeability is suggested to reduce maintenance energy costs, an important adaptive feature of extreme oligophiles such as the AOA. Thus, growth temperature-dependent modulation of membrane composition is likely associated with maintenance of appropriate permeability, as well as other membrane functions (van de Vossenberg et al., 1998).

The influence of temperature on membrane composition has been the major focus of studies of the environmental distribution of archaeal membrane lipids in the present and for interpreting lipids preserved in the sedimentary record (Pearson and Ingalls, 2013). In particular, the correlation between sea surface temperature (SST) and the cyclopentane ring distribution of GDGTs in a sample set of globally distributed core top sediments is the basis for a widely applied paleotemperature proxy, TEX₈₆ (TetraEther indeX of lipids with 86 carbon atoms). The TEX₈₆ proxy has been used to reconstruct surface ocean temperature as far back as the Middle Jurassic (Schouten et al., 2002; Jenkyns et al., 2012). However, the extent to which temperature is the causative agent behind the correlation has not fully been examined. Moreover, it is not

evident how a group of organisms that live at depths below the upper-photoc zone and are the dominant prokaryote of the abyss can record SST via a physiological response.

Interpretation of TEX_{86} records that deviate from expectation are usually interpreted from the point of view that temperature is still the main underlying influence on TEX_{86} . That is, disagreement with other proxy records, unreasonably large swings in TEX_{86} over short time periods or warm biases in semi-enclosed basins (Mediterranean and Red Seas) have been attributed to changes in circulation, seasonal timing of production, selective export to sediments or to autochthonous archaeal populations having slightly different temperature responses (Trommer et al., 2009; Shevenell et al., 2011; Pearson and Ingalls, 2013; Kim et al., 2015).

Large discrepancies between *in situ* and TEX_{86} -derived temperatures from suspended particulate matter (SPM) samples, particularly from low oxygen (O_2) environments, have been observed in many regions (Ingalls et al., 2006; Basse et al., 2014; Xie et al., 2014; Kim et al., 2015), but O_2 has not explicitly been suggested as a cause of these discrepancies. Instead, it is thought that some local environments select for ecotypes having slightly different TEX_{86} -temperature relationships.

TEX_{86} reconstructions of the distant past, when oceanic conditions could be quite different from today, present the greatest challenge to interpretation. For example, inferred Cretaceous SSTs are higher than physically plausible for the ocean (Schouten et al., 2003). Thus, considerable efforts have been made to develop and apply new TEX_{86} equations suitable for high temperature environments (TEX_{86}^H), low temperature environments (TEX_{86}^L), local systems (TEX_{86}'), the

marine water column, and mesocosms (Wuchter et al., 2004; Wuchter et al., 2005; Sluijs et al., 2006; Kim et al., 2010; Shevenell et al., 2011).

The availability of a number of pure cultures of marine AOA (Qin et al., 2014) now serves to test strain-specific response to temperature, as well as the influence of ecophysiological factors other than temperature, on lipid composition. Here we grew pure cultures of four marine AOA strains to evaluate the influence of growth conditions on core lipid composition. Despite relatively close phylogenetic relationships, these isolates are physiologically distinct ecotypes recovered from dimly lit deep waters, the nitrite maximum near the euphotic zone, and near-surface sediment (Qin et al., 2014). The influence of temperature and dissolved O₂ (DO) on GDGT composition and TEX₈₆ values was examined by independently varying these two important environmental variables. These experiments revealed significant strain-specific variation in temperature-associated GDGT distribution. More striking was the observation that in addition to temperature, the DO concentration had a profound impact on membrane composition, skewing TEX₈₆-derived temperatures by more than 20°C at a single growth temperature. These findings necessitate reinterpretation and possible reformulation of this important paleo-climate proxy.

Results

Early stationary phase cultures were used to investigate total GDGT content and the distribution of GDGTs in different AOA strains (strains are described in detail in Qin et al., 2014) (Qin et al., 2014). Cell pellet hydrolysis ensured the complete recovery of all cellular lipids and removed polar head groups from intact GDGTs so they could be analyzed as core GDGTs (Hopmans et al., 2000). Different strains of marine AOA contained variable amounts of total GDGTs per cell

(calculated based on cell counts and lipid abundance) and each strain contained a similar amount of total lipids per cell regardless of the growth temperature. Strain HCE1 contained 1.47 ± 0.096 fg GDGTs cell⁻¹ (at 15–20°C, n=6), which was less than half of the total GDGTs recovered from PS0 cells (3.01 ± 0.065 fg cell⁻¹ at 25°C, n=3) (Table 7.1). Cells of strains HCA1 and SCM1 contained similar lipid content (2.04 ± 0.21 fg cell⁻¹ at 15–30°C for HCA1, n=12 and 2.08 ± 0.12 fg cell⁻¹ at 20–30°C for SCM1, n=9; SI Appendix, Table 7.1). These values were within the range reported for the cellular lipid contents of SCM1 and natural marine communities dominated by AOA (0.1–8.5 fg cell⁻¹) (Huguet et al., 2010c; Elling et al., 2014). GDGTs of SCM1 accounted for approximately 10% of dry cell weight (20 fg cell⁻¹) (Martens-Habbena et al., 2009b). This value is at the higher end of previous estimates for methanogenic and thermoacidophilic archaea that contain 2.5–10% total lipids on a dry weight basis (Langwort.Ta et al., 1974; Ferrante et al., 1988; Hedrick et al., 1991).

All isolates showed substantially different TEX₈₆ values when grown at 25°C (0.56 ± 0.02 for HCA1, 0.51 ± 0.01 for SCM1, 0.42 ± 0.01 for HCE1 and 0.38 ± 0.01 for PS0) (SI Appendix, Table 7.1). TEX₈₆ values calculated using the calibration curve of Kim et al. (2008) correspond to TEX₈₆-derived temperatures ranging from 10.5 to 20.7°C; all below their actual growth temperature of 25°C (Fig. 7.2) (Kim et al., 2008). To further test the strain specific relationship between TEX₈₆ values and growth temperatures, SCM1 (optimum growth temperature at 32°C), HCA1 and HCE1 (optimum growth temperatures at 25°C) were incubated at temperatures ranging from 15 to 35°C, 10 to 30°C and 10 to 25°C, respectively (see SI Appendix, Fig. 7.3 and Table 7.1 for experimental details and results at the different growth temperatures). The relationship between TEX₈₆ values and growth temperatures of SCM1 was a linear function,

showing a general pattern of increased TEX_{86} values with increasing temperature (Fig. 7.4A; see SI Appendix, Fig. 7.5A and Table 7.2 for additional details of relative abundance of GDGTs):

$$TEX_{86} = 0.015T + 0.21 \quad (r^2 = 0.85) \quad (1)$$

A linear relationship was also found between the TEX_{86} -derived temperature reconstructed using the Kim et al., (2008) calibration equation and actual growth temperature of SCM1 (Fig. 7.6A) (Kim et al., 2008). These calculated TEX_{86} temperatures were 0.13–7.28°C lower than incubation temperatures, explaining the difference between the global calibration line ($T = -10.78 + 56.2 \times TEX_{86}$) and the culture correlation line ($T = -14 + 66.7 \times TEX_{86}$). In contrast, there was no linear dependence of growth temperature on the TEX_{86} value of strains HCA1 and HCE1. Instead, the data of HCA1 (equation 2) and HCE1 (equation 3) fitted best to polynomial curves, reaching the maximum TEX_{86} values at 20°C (Fig. 7.4B and C; see SI Appendix, Fig. 7.5B and C and Table 7.2 for additional details of relative abundance of GDGTs):

$$TEX_{86} = -0.0006T^2 + 0.023T + 0.33 \quad (r^2 = 0.94) \quad (2)$$

$$TEX_{86} = -0.0017T^2 + 0.054T + 0.11 \quad (r^2 = 0.89) \quad (3)$$

Similarly, second-order polynomials resulted in good fits to TEX_{86} -derived temperature of HCA1 and HCE1 versus incubation temperature (Fig. 7.6B and C). The temperatures derived from TEX_{86} values of HCA1 and HCE1 reflected the *in situ* temperatures, within calibration error, at 20°C (TEX_{86} temperatures of HCA1 and HCE1 were 21.1°C and 19.3°C, respectively). However, large discrepancies between TEX_{86} -derived temperatures and actual growth temperatures (up to 12°C) were observed at low- and high-growth temperatures of HCA1 and HCE1. All isolates had different ring index values (a common metric of GDGT cyclization) when grown at 25 °C (Table 7.2) (Pearson et al., 2004). The ring index values of strains SCM1,

HCA1 and HCE1 all showed a linear increase in cyclization of total GDGTs with increasing temperature (Fig. 7.7).

In addition to the expected adaptation to changes in temperature, the observation of abundant and transcriptionally active AOA populations near the oxic-anoxic boundary of OMZs also suggested a capacity to grow in highly O₂ depleted waters (Lam et al., 2009; Stewart et al., 2012). Both SCM1 and PS0 were shown to be capable of growing at very low O₂ (0.1% to 21% of initial headspace O₂ in sealed culture bottles; see SI Appendix, Fig. 7.8 and Table 7.3 for experimental details and results at different % O₂). All ammonia (10 micromoles) was completely oxidized to nitrite when O₂ was in stoichiometric excess (0.5% to 21% initial headspace O₂). In accordance with the established reaction stoichiometry of 1 mole NH₃ oxidized per 1.5 moles O₂ consumed (Martens-Habbena et al., 2009b), approximately 15 to 1238 micromoles of O₂ remained at the end of the incubation (Fig. 7.8 and Table 7.3). In contrast, all headspace O₂ was consumed at 0.1% and 0.2% initial O₂, resulting in residual ammonia and a lower level of nitrite production (~5.1 and ~8.2 micromoles nitrite, respectively) also consistent with predicted reaction stoichiometry (~4.0 and ~7.8 micromoles nitrite for 0.1% and 0.2% O₂, respectively) (Fig. 7.8 and Table 7.3). Ammonia oxidation was coupled to growth at all O₂ concentrations. The cell densities of early stationary phase cultures of SCM1 and PS0 were 13-27 times and 25-29 times higher than initial cell densities, respectively (Table 7.3).

Since marine AOA demonstrate the ability to grow at very low O₂ in the lab and the environment, we next asked whether changes in membrane composition might also be associated with the growth of AOA at low O₂ concentrations. The relative abundances of GDGT-2 and

GDGT-3 (Fig. 7.1 and 7.9) increased as initial headspace O₂ concentration decreased (Fig. 7.10 and Table 7.4). Notably, the abundance of GDGT-2 in SCM1 and PS0 showed a significant and continuous increase from 12.4% and 7.7% at 21% O₂ to 16.6% and 27.0% at 0.1% O₂, respectively. In contrast, a 5.2% and 5.7% decrease in the relative abundance of GDGT-1 was observed between 21% O₂ and 0.1% O₂ treatments for SCM1 and PS0, respectively (Fig. 7.10 and Table 7.4). These changes along with changes in GDGT-0 and crenarchaeol abundance were reflected in the increase in ring index values as the O₂ concentration decreased with the exception of the lowest O₂ treatments (Table 7.4). Crenarchaeol regioisomer (cren') (Fig. 7.1) was detected in low abundance (<1.3%) in all samples. The relative decrease in GDGT-1, and increase in GDGT-2 and GDGT-3, at low O₂ concentrations resulted in higher calculated TEX₈₆ temperatures in O₂-deficient cultures. Nearly 12°C of TEX₈₆-derived temperature elevation reconstructed using the Kim et al., (2008) calibration equation was observed for strain SCM1 from 21% O₂ to 0.1% O₂ (Fig. 7.11A) (Kim et al., 2008). Likewise, the TEX₈₆-derived temperatures of PS0 were 11.4°C below incubation temperature (26°C) at 21% O₂, but changed to 9.9°C above incubation temperature at 0.1% O₂ (Fig. 7.11B). Although some change in DO is expected with growth, the comparable growth kinetics observed at the higher, but non-limiting, O₂ concentrations suggest that O₂ concentration primarily influences lipid composition (Fig. 7.8).

Discussion

Although the TEX₈₆ paleothermometer has been applied in diverse depositional settings across more than 100 million years of geological history, the TEX₈₆-SST relationship is strictly a correlation among environmental data. The precise cause of the global correlation and observed deviations within this correlation dataset remain poorly understood (Pearson and Ingalls, 2013).

Sedimentary GDGTs likely originate from a variety of GDGT-producing organisms all of which are members of the archaeal domain. Planktonic *Thaumarchaeota* are considered to be a major source of sedimentary GDGTs, but their populations are often most abundant in subsurface waters, near the base of the photic zone, leaving unknown the causative factor driving the correlations between sedimentary GDGT composition and growth temperature (likely subsurface) (Pearson and Ingalls, 2013). Likewise, there is also some contribution from pelagic *Euryarchaeota* and sediment dwelling *Archaea* (Lipp et al., 2008; Lincoln et al., 2014a).

Prior to the availability of pure cultures, mesocosms for North Sea water pre-incubated at high (27°C) and low (13°C) temperatures were used to test the validity of the TEX₈₆ proxy (Wuchter et al., 2004). The lipid composition was determined following shifts in incubation temperature. Incubations of the high temperature mesocosm (pre-incubated at 27°C) between 10°C and 35°C generated TEX₈₆ values having the same slope, but different intercepts from the global calibration. Even more surprisingly, no linear dependence of growth temperature versus TEX₈₆ values could be found for the low temperature mesocosm (pre-incubated at 13°C) when incubated at the other temperatures (5–35°C). Instead, a plot of TEX₈₆ vs temperature had a concave down shape (Wuchter et al., 2004). However, when all data were combined, the non-linearity was less apparent (Wuchter et al., 2004).

Our use of pure cultures of marine AOA allowed us to independently examine the influence of growth temperature and O₂ on TEX₈₆, and variation in response among different AOA strains. Notably, despite the close phylogenetic relationships, all four marine AOA isolates differed markedly in their TEX₈₆ values at the same growth temperature, and strains SCM1, HCA1 and

HCE1 exhibited distinctly different temperature-TEX₈₆ relationships. The tropical (strain SCM1) and temperate (strains HCA1 and HCE1) marine AOA isolates were initially enriched at 28°C and 15°C, respectively (Könneke et al., 2005; Qin et al., 2014), temperatures comparable to those (27°C and 13°C) applied in the mesocosm study (Wuchter et al., 2004). Interestingly, the linear and curved temperature-TEX₈₆ trends for strains SCM1, HCA1 and HCE1 are very similar to those observed in the high and low temperature mesocosms, respectively (Wuchter et al., 2004). The large offsets between TEX₈₆-inferred temperatures and growth temperatures of these isolates (up to 12°C) are consistent with the mesocosm experiments. The TEX₈₆ variation among strains at the same growth temperature suggests this index is reporting both variation in SST and variation in biosynthetic response of distinct AOA ecotypes. In addition, the different temperature optima of our AOA isolates suggests that temperature may select for ecotypes having significantly different temperature-TEX₈₆ relationships.

Significant increase in the relative abundance of crenarchaeol with increasing growth temperature was observed with all examined AOA isolates (strains SCM1, HCA1 and HCE1). This suggests the preferential synthesis of crenarchaeol relative to GDGT-1–3 and cren' could be a common feature for marine AOA in warmer environments as suggested by the 40°C temperature optimum of crenarchaeol synthesis (Zhang et al., 2006; Pearson and Ingalls, 2013). Therefore, the ring index equation may be a more suitable proxy for temperature than the TEX₈₆ equation. Indeed, although no linear dependence of growth temperature and TEX₈₆ values was found for some isolates, there was a linear relationship between ring index values and growth temperatures for all the marine AOA examined in this study. Notably, the temperate isolates (HCA1 and HCE1), having a growth optimum near 25°C, displayed a similar degree of

cyclization of total GDGTs at a given temperature. In contrast, strain SCM1 produced a membrane with a higher ring index than temperate isolates at all temperatures, possibly related to its adaptation to higher temperature environments. However, further studies are needed to more fully evaluate the utility of ring index values as a complementary temperature proxy.

Alternative factors known to influence membrane composition of archaea include pH and salinity. The GDGT composition of cultured thermophilic AOA *Nitrosocaldus yellowstonii* and members of *Crenarchaeota* vary with pH (de la Torre et al., 2008; Pearson et al., 2008; Boyd et al., 2011; Pearson and Ingalls, 2013). However, for the highly buffered ocean, pH variability is relatively small, and thus would not be expected to significantly bias reconstructed SST. In addition, although salinity has been shown to exert substantial control on the lipid composition of halophilic archaea (Dawson et al., 2012), no significant variation of GDGT distributions was found in a marine mesocosm study where salinity was varied (Wuchter et al., 2004). In contrast, the influence of O₂ concentration on lipid composition is relatively unexplored. Thus, the striking response of the marine AOA isolates to reduced O₂ was surprising, demonstrating an increase in TEX₈₆-derived temperatures of up to 21°C by varying O₂ concentration alone.

O₂ concentrations are known to span a wide range of values with depth in the ocean and in sediment. Suboxia and anoxia prevail in some modern enclosed basins and in restricted waterways present early in Earth history such as the Atlantic Ocean during the Oceanic Anoxic Events (OAE) of the Cretaceous and Jurassic periods (Meyer and Kump, 2008). Presently, the ocean is also home to several large OMZs where subsurface waters experience varying degrees of suboxia and anoxia. Thus, our observation of a major controlling influence of O₂ on TEX₈₆

values is important for interpretation of environments and sedimentary records influenced by low O_2 or anoxia. Notably, anomalously warm TEX_{86} patterns of SPM samples have been reported over a wide range of suboxic settings, such as in the permanent OMZ of the Arabian Sea and the Eastern Tropical North Pacific Ocean, and seasonally O_2 deficient regions in coastal upwelling areas (Schouten et al., 2012; Basse et al., 2014; Xie et al., 2014). In addition, TEX_{86} values of sediment recovered from the summit of the Murray Ridge seamount that extends into the OMZ of the Arabian Sea were higher than those of sediment recovered from below the OMZ, and the reconstructed TEX_{86} temperatures from sediment cores within the OMZ were more than $5^\circ C$ higher than the mean annual SST (Lengger et al., 2012).

While surface waters are not O_2 deficient in these areas, the AOA are of higher abundance in the oxycline and upper OMZ where waters can be oxygen deficient (Lam et al., 2009; Hawley et al., 2014). The AOA living under O_2 limitation would likely be the major contributor to the sedimentary GDGTs collected within the Arabian Sea OMZ (Lengger et al., 2012). Elevated TEX_{86} values were mainly the result of the relative increase in GDGT-2 that we have now shown to increase under low O_2 concentrations with pure cultures of marine AOA (Basse et al., 2014; Xie et al., 2014; Kim et al., 2015). Thus, our study clearly implicates high TEX_{86} values produced in the waters of the OMZ with the lipid biosynthetic response of AOA to reduced O_2 concentrations. In addition, if reduced O_2 concentrations select for a different marine archaeal community, then an altered species composition could also influence the composition of GDGTs preserved in the sediments. However, resolving the relative importance of adaptation versus selection on the TEX_{86} record in response to 'greenhouse' climates will require a more complete understanding of thaumarchaeal ecophysiology.

Our laboratory findings may also provide an explanation for some unexpected TEX_{86} sedimentary records. The Jurassic and Cretaceous Periods are known as relatively warm intervals in Earth history. One consequence of warmer water is lower DO, since O_2 is less soluble in warm water than cold water. TEX_{86} -derived temperature records of this time period routinely exceed modern temperatures at equivalent latitudes (Schouten et al., 2003; Damsté et al., 2010; Littler et al., 2011; Jenkyns et al., 2012; van Bentum et al., 2012). Our results suggest decreased DO concentrations of warm ancient seawater would raise reconstructed temperatures to values somewhat higher than the actual SST. During particular intervals of Earth history, such as the many OAEs and Paleocene/Eocene thermal maximum (PETM), widespread dysoxic or even anoxic conditions impinged on the photic zone as indicated by a sedimentary biomarker (isorenieratane) for photic zone anoxia (Sluijs et al., 2006; Meyer and Kump, 2008; van Bentum et al., 2012; Schoon et al., 2014; Sluijs et al., 2014). Although some increase in temperature during OAEs and the PETM is consistent with paleoclimate model simulations and planktonic foraminiferal $\delta^{18}\text{O}$ based SST reconstructions, TEX_{86} values (as high as 0.95) and TEX_{86} -derived temperatures (up to 43°C) observed during these low oxygen events appear anomalously high (Sluijs et al., 2006; Zachos et al., 2006; Damsté et al., 2010; van Bentum et al., 2012; Schoon et al., 2014; Sluijs et al., 2014; van Helmond et al., 2014). However, since $\delta^{18}\text{O}$ -based temperature estimates are not available throughout the black shales of an OAE, there is no independent validation of the exceptionally warm TEX_{86} -inferred temperatures for these climate periods (Erbacher et al., 2001; Sluijs et al., 2006; Wagner et al., 2008).

Excursions in O₂ concentration are also associated with short historic periods of pronounced cooling (Forster et al., 2007; Damsté et al., 2010; van Bentum et al., 2012). For example, the TEX₈₆ paleotemperature proxy suggests a cooling of up to 12°C during the Plenus Cold Event (PCE) of OAE-2 (Damsté et al., 2010). However, the PCE is also marked by a drop in isorenieratane concentrations in the sedimentary record, indicative of re-oxygenation of a previously anoxic photic zone (van Bentum et al., 2012). Since the steep decrease in TEX₈₆ values within OAEs is difficult to explain with a drastic drop of SSTs only, re-oxygenation would offer an explanation for large swings in TEX₈₆ values observed during these events. Thus, together our data now implicate DO as an additional causative factor of anomalously high or low TEX₈₆ values and inferred temperatures.

We recognize that more experiments with AOA strains representing a broader range of ecotypes are necessary to further explore environmental influences on GDGT composition and how these factors relate to physiology. There also remains the question of the biophysical significance of thaumarchaeal membrane compositional changes associated with reduced O₂ concentration. It has been suggested that an increase in cyclopentane rings reduces proton permeability as a result of denser membrane packing (Gabriel and Chong, 2000; Valentine, 2007). This adaptive response may allow AOA to cope with the energy stress of low O₂ environments, such as the boundary of the OMZs in today's oceans and during past periods of low O₂ availability, such as the OAE of the mid-Cretaceous. However, apart from the questions of physiological significance highlighted by these studies, the available data do offer an argument in favor of viewing the global calibration datasets of TEX₈₆ index as a compilation of local calibrations (Pearson and Ingalls, 2013) and point to the need to reevaluate inferences of paleoclimate from

geologic records where conditions differ significantly from the modern and from unique local environments such as those underlying OMZs.

Finally, in addition to the significance of our observations for reinterpreting past climates and oceanic conditions, the adaptive response of these AOA may have relevance to predicting the response of oceanic populations impacted by climate change. Predicted warming, deoxygenation and acidification of the global ocean will certainly have an impact on major biogeochemical systems (Matear and Hirst, 2003; Meehl et al., 2005; Orr et al., 2005). Thus, better resolving the physiological response of marine AOA to these changes is of global significance. Phenotypic plasticity that enhances the adaptive capacity of AOA may mitigate some of these responses with important implications for both adaptation to and reconstruction of change in present and past marine environments, respectively.

Methods

Culture maintenance and experimental setup. All materials and methods for marine AOA pure culture maintenance and temperature and O₂ growth experiments are described in detail in *SI Appendix, Materials and Methods*.

Lipid extraction and analysis. Lipids were extracted from 0.22 µm Durapore membrane filters (Millipore Co., MA, U.S.) containing early stationary phase cells and analyzed using atmospheric pressure chemical ionization (APCI) on an Agilent 1100 Series liquid chromatograph coupled to an Agilent ion trap (XCT) mass spectrometer (LC-MS). For details, see *SI Appendix, Materials and Methods*.

Calculation of TEX₈₆ index, TEX₈₆-derived temperature and ring index. The TEX₈₆ values were calculated based on the relative abundances of GDGT-1, GDGT-2, GDGT-3 and Cren' using the respective peak areas (Schouten et al., 2002):

$$TEX_{86} = \frac{[GDGT-2] + [GDGT-3] + [Cren']}{[GDGT-1] + [GDGT-2] + [GDGT-3] + [Cren']} \quad (4)$$

The reconstructed TEX₈₆ temperatures were calculated on the basis of the core-top linear calibration of Kim et al. (2008) (Kim et al., 2008):

$$SST = -10.78 + 56.2 \times TEX_{86} \quad (r^2 = 0.94) \quad (5)$$

The ring index was calculated according to Pearson et al. (2004) (Pearson et al., 2004):

$$Ring\ index = \frac{[GDGT-1] + 2 \times [GDGT-2] + 3 \times [GDGT-3] + 5 \times [Cren + Cren']}{[GDGT-0] + [GDGT-1] + [GDGT-2] + [GDGT-3] + [Cren + Cren']} \quad (6)$$

SI Appendix

Materials and Methods

Culture maintenance and experimental setup. All four strains of marine AOA were maintained in artificial seawater medium in the dark without shaking. *Nitrosopumilus maritimus* strain SCM1 was grown in HEPES-buffered Synthetic Crenarchaeota Medium (SCM) containing 1 mM NH₄Cl as described previously (Könneke et al., 2005; Martens-Habbenha et al., 2009b). Strains HCA1, HCE1 and PS0 are three newly isolated *N. maritimus*-like marine AOA strains; they were isolated from a depth of 50 m water at the Puget Sound Regional Synthesis Model (PRISM) Station P10, a depth of 17 m water (nitrite maximum) at the PRISM Station P12, and Puget Sound surface sediment collected from a Seattle beach, respectively (Qin et al., 2014).

These new isolates were defined as obligate mixotrophs and cultured in HEPES-buffered SCM supplemented with 500 μM NH_4Cl and 100 μM α -ketoglutaric acid (Qin et al., 2014). To investigate the influence of growth temperature on the membrane compositional regulation of marine AOA, early stationary phase cultures of strains SCM1, HCA1, HCE1 and PS0 (1ml) were inoculated into 100 ml growth medium and incubated in triplicate at temperatures ranging from 15 to 35°C, 10 to 30°C, 10 to 25 °C, and 25°C, respectively. To assess the impact of O_2 concentration on membrane composition, strains SCM1 and PS0 were grown in triplicate at nine different O_2 concentrations, from 0.1% to 21% in the headspace. Briefly, experiments were carried out in 246 ml capacity serum bottles (Wheaton, NJ, USA) that contained 100ml of HEPES-buffered SCM supplemented with 100 μM NH_4Cl (10 micromoles NH_4Cl total). An organic supplement (100 μM α -ketoglutaric acid) was additionally added to medium used to culture strain PS0. The headspace of each bottle was sealed using air-tight butyl rubber septa and aluminum crimps (Wheaton). Atmospheric O_2 was removed by flushing bottle headspace with N_2 through a sterile 0.22 μm Millex-GP syringe filter at > 50 ml/min for 10 min. The medium inside of the bottle was shaken well during the purge process. Subsequently, 0.04% (v/v) of high-purity CO_2 was injected back to exchange headspace N_2 in bottles. The appropriate amounts of high-purity O_2 were also injected back into each headspace to achieve 0.1%, 0.2%, 0.5%, 1%, 2%, 3%, 5%, 10%, and 21% O_2 (v/v). Initial O_2 concentration in the aqueous phase were calculated according to Henry`s law, approximately achieving 1, 2, 5, 11, 21, 32, 53, 106, 213 μM in the aqueous phase under equilibrium conditions. Headspace O_2 concentration of each bottle was measured and confirmed before each experiment using an SRI 8610SC gas chromatograph equipped with a thermal conductivity detector (SRI instruments, CA., USA). The initial amounts of O_2 present in the serum bottles varied from ~6 to ~1253 micromoles

(corresponding to 0.1% to 21% of initial headspace O₂). Early stationary phase cultures of strains SCM1 and PS0 (1ml) were inoculated into each bottle and incubated at 30°C and 26°C, respectively. Growth was routinely monitored by sampling and measuring nitrite production as described previously (Qin et al., 2014). All experiments were conducted in SCM buffered with 10mM HEPES, which is sufficient to maintain culture pH with as much as 2.5mM nitrite production. Since no more than 1mM nitrite was produced in any of the growth experiments, there was no appreciable change in pH among culture treatments and between the beginning and end of each growth experiment. The final cell densities were determined by microscopic counts of SybrGreen-stained cells (Invitrogen, Carlsbad, USA) as previously described (Qin et al., 2014). Early stationary phase cells were harvested on 0.22 µm Durapore membrane filters (Millipore Co., MA, U.S.) and stored at -20°C until acid hydrolysis.

Lipid extraction and analysis. Durapore membrane filters containing the cultured cells were handled according to Huguet et al., (2010) (Huguet et al., 2010a). Briefly, filters were placed in Teflon vials, flushed with N₂, and hydrolyzed with 5% HCl in methanol (v/v) for 4 hours at 70°C. After heating, the methanol was transferred to a combusted glass vial and equal parts dichloromethane (DCM) and MilliQ were added to separate the phases. The DCM fraction, containing GDGTs with polar head groups removed during the hydrolysis step, was collected and transferred to a second combusted glass vial. The remaining acid solution was extracted 3 additional times with DCM, and the DCM extracts were combined. The DCM extract was rinsed at least six times with water to remove any remaining acid. The extracts were dried under N₂ before analysis using HPLC/MS. A known amount of the internal quantification standard, C₄₆ GDGT, was added to all dried extracts (Huguet et al., 2006). The samples with internal standard

were re-dissolved in 1% isopropanol in hexane (v/v) before injection on the HPLC/MS. Lipid analysis was done using atmospheric pressure chemical ionization (APCI) on an Agilent 1100 Series liquid chromatograph coupled to an Agilent ion trap (XCT) mass spectrometer (LC-MS) according to Hopmans et al., (2000) (Hopmans et al., 2000). Separation of the core GDGTs was achieved on an Alltech Prevail Cyano column (2.1×150 mm, $3 \mu\text{m}$) maintained at 30°C . The column was fitted with a Prevail Cyano guard column (7.5×4.6 mm, $5 \mu\text{m}$). Core GDGTs were eluted with 99:1 hexane to isopropanol (solvent A) and 90:10 hexane to isopropanol (solvent B) at a flow rate of 0.2 ml min^{-1} . Solvent A was run isocratically from 0 to 5 min, followed by a linear gradient of 0 to 8.2% solvent B over the next 40 min. The column was cleaned by back flushing with 100% solvent B for 8 min and then equilibrated back to 100% solvent A for 10 min. Detection was achieved using APCI in positive mode with the following conditions: nebulizer pressure of 60 psi, vaporizer temperature of 400°C , nitrogen drying gas flow of 6 l min^{-1} at 200°C , capillary voltage of -3.5 kV, and corona of $4 \mu\text{A}$. The scanning mass range was 730–1350 m/z. Triplicate filters from the same culture treatment were analyzed and each filter sample was injected onto the LC-MS at least 2 times. Lipid concentrations were calculated by comparison of the peak area of the C_{46} internal standard to the peak area of each GDGT.

Acknowledgements

We thank Kelley Meinhardt, Julia Kobelt, Frederick Von Netzer, Angie Boysen and David French for technical assistant and Willm Martens-Habbena, Shady Amin, Birte Meyer and Katherine Heal for invaluable discussions. This work was funded by National Science Foundation Grants MCB-0604448 to DAS, MCB-0920741 to DAS, Dimensions of Biodiversity

Program OCE-1046017 to DAS, EVA, AHD, JWM, and AEI, and OCE-1029281 and OCE-1205232 to AEI.

References

- Amin, S.A., Moffett, J.W., Martens-Habbena, W., Jacquot, J.E., Han, Y., Devol, A. et al. (2013) Copper requirements of the ammonia-oxidizing archaeon *Nitrosopumilus maritimus* SCM1 and implications for nitrification in the marine environment. *Limnol Oceanogr* **58**: 2037-2045.
- Basse, A., Zhu, C., Versteegh, G.J.M., Fischer, G., Hinrichs, K.U., and Mollenhauer, G. (2014) Distribution of intact and core tetraether lipids in water column profiles of suspended particulate matter off Cape Blanc, NW Africa. *Org Geochem* **72**: 1-13.
- Beman, J.M., Popp, B.N., and Alford, S.E. (2012a) Quantification of ammonia oxidation rates and ammonia-oxidizing archaea and bacteria at high resolution in the Gulf of California and eastern tropical North Pacific Ocean. *Limnol Oceanogr* **57**: 711-726.
- Boyd, E.S., Pearson, A., Pi, Y.D., Li, W.J., Zhang, Y.G., He, L. et al. (2011) Temperature and pH controls on glycerol dibiphytanyl glycerol tetraether lipid composition in the hyperthermophilic crenarchaeon *Acidilobus sulfurireducens*. *Extremophiles* **15**: 59-65.
- Brochier-Armanet, C., Boussau, B., Gribaldo, S., and Forterre, P. (2008) Mesophilic crenarchaeota: proposal for a third archaeal phylum, the Thaumarchaeota. *Nat Rev Microbiol* **6**: 245-252.
- Damsté, J.S.S., van Bentum, E.C., Reichart, G.J., Pross, J., and Schouten, S. (2010) A CO₂ decrease-driven cooling and increased latitudinal temperature gradient during the mid-Cretaceous Oceanic Anoxic Event 2. *Earth Planet Sci Lett* **293**: 97-103.
- Dawson, K.S., Freeman, K.H., and Macalady, J.L. (2012) Molecular characterization of core lipids from halophilic archaea grown under different salinity conditions. *Org Geochem* **48**: 1-8.
- de la Torre, J.R., Walker, C.B., Ingalls, A.E., Könneke, M., and Stahl, D.A. (2008) Cultivation of a thermophilic ammonia oxidizing archaeon synthesizing crenarchaeol. *Environ Microbiol* **10**: 810-818.
- Elling, F.J., Könneke, M., Lipp, J.S., Becker, K.W., Gagen, E.J., and Hinrichs, K.U. (2014) Effects of growth phase on the membrane lipid composition of the thaumarchaeon *Nitrosopumilus maritimus* and their implications for archaeal lipid distributions in the marine environment. *Geochim Cosmochim Acta* **141**: 579-597.
- Erbacher, J., Huber, B.T., Norris, R.D., and Markey, M. (2001) Increased thermohaline stratification as a possible cause for an ocean anoxic event in the Cretaceous period. *Nature* **409**: 325-327.
- Ferrante, G., Ekiel, I., Patel, G.B., and Sprott, G.D. (1988) Structure of the major polar lipids isolated from the acetoclastic methanogen, *Methanotherx concilii* Gp6. *Biochim Biophys Acta* **963**: 162-172.
- Forster, A., Schouten, S., Moriya, K., Wilson, P.A., and Damsté, J.S.S. (2007) Tropical warming and intermittent cooling during the Cenomanian/Turonian oceanic anoxic event 2: Sea surface temperature records from the equatorial Atlantic. *Paleoceanography* **22**.

- Francis, C.A., Roberts, K.J., Beman, J.M., Santoro, A.E., and Oakley, B.B. (2005) Ubiquity and diversity of ammonia-oxidizing archaea in water columns and sediments of the ocean. *P Natl Acad Sci USA* **102**: 14683-14688.
- Gabriel, J.L., and Chong, P.L.G. (2000) Molecular modeling of archaeobacterial bipolar tetraether lipid membranes. *Chem Phys Lipids* **105**: 193-200.
- Hawley, A.K., Brewer, H.M., Norbeck, A.D., Pasa-Tolic, L., and Hallam, S.J. (2014) Metaproteomics reveals differential modes of metabolic coupling among ubiquitous oxygen minimum zone microbes. *P Natl Acad Sci USA* **111**: 11395-11400.
- Hedrick, D.B., Guckert, J.B., and White, D.C. (1991) Archaeobacterial ether lipid diversity analyzed by supercritical fluid chromatography - integration with a bacterial lipid protocol. *J Lipid Res* **32**: 659-666.
- Hopmans, E.C., Schouten, S., Pancost, R.D., van der Meer, M.T.J., and Damsté, J.S.S. (2000) Analysis of intact tetraether lipids in archaeal cell material and sediments by high performance liquid chromatography/atmospheric pressure chemical ionization mass spectrometry. *Rapid Commun Mass Spectrom* **14**: 585-589.
- Horak, R.E.A., Qin, W., Schauer, A.J., Armbrust, E.V., Ingalls, A.E., Moffett, J.W. et al. (2013) Ammonia oxidation kinetics and temperature sensitivity of a natural marine community dominated by Archaea. *Isme J* **7**: 2023-2033.
- Huguet, C., Martens-Habbena, W., Urakawa, H., Stahl, D.A., and Ingalls, A.E. (2010a) Comparison of extraction methods for quantitative analysis of core and intact polar glycerol dialkyl glycerol tetraethers (GDGTs) in environmental samples. *Limnol Oceanogr Methods* **8**: 127-145.
- Huguet, C., Hopmans, E.C., Febo-Ayala, W., Thompson, D.H., Damsté, J.S.S., and Schouten, S. (2006) An improved method to determine the absolute abundance of glycerol dibiphytanyl glycerol tetraether lipids. *Org Geochem* **37**: 1036-1041.
- Huguet, C., Urakawa, H., Martens-Habbena, W., Truxal, L., Stahl, D.A., and Ingalls, A.E. (2010c) Changes in intact membrane lipid content of archaeal cells as an indication of metabolic status. *Org Geochem* **41**: 930-934.
- Ingalls, A.E., Shah, S.R., Hansman, R.L., Aluwihare, L.I., Santos, G.M., Druffel, E.R.M., and Pearson, A. (2006) Quantifying archaeal community autotrophy in the mesopelagic ocean using natural radiocarbon. *Proc Natl Acad Sci USA* **103**: 6442-6447.
- Jenkyns, H.C., Schouten-Huibers, L., Schouten, S., and Damsté, J.S.S. (2012) Warm Middle Jurassic-Early Cretaceous high-latitude sea-surface temperatures from the Southern Ocean. *Clim Past* **8**: 215-226.
- Karner, M.B., DeLong, E.F., and Karl, D.M. (2001) Archaeal dominance in the mesopelagic zone of the Pacific Ocean. *Nature* **409**: 507-510.
- Kim, J.-H., Schouten, S., Rodrigo-Gámiz, M., Rampen, S., Marino, G., Huguet, C. et al. (2015) Influence of deep-water derived isoprenoid tetraether lipids on the TEX₈₆ paleothermometer in the Mediterranean Sea. *Geochim Cosmochim Acta* **150**: 125-141.
- Kim, J.H., Schouten, S., Hopmans, E.C., Donner, B., and Damsté, J.S.S. (2008) Global sediment core-top calibration of the TEX₈₆ paleothermometer in the ocean. *Geochim Cosmochim Acta* **72**: 1154-1173.
- Kim, J.H., van der Meer, J., Schouten, S., Helmke, P., Willmott, V., Sangiorgi, F. et al. (2010) New indices and calibrations derived from the distribution of crenarchaeal isoprenoid tetraether lipids: Implications for past sea surface temperature reconstructions. *Geochim Cosmochim Acta* **74**: 4639-4654.

- Könneke, M., Bernhard, A.E., de la Torre, J.R., Walker, C.B., Waterbury, J.B., and Stahl, D.A. (2005) Isolation of an autotrophic ammonia-oxidizing marine archaeon. *Nature* **437**: 543-546.
- Könneke, M., Schubert, D.M., Brown, P.C., Hugler, M., Standfest, S., Schwander, T. et al. (2014) Ammonia-oxidizing archaea use the most energy-efficient aerobic pathway for CO₂ fixation. *Proc Natl Acad Sci USA* **111**: 8239-8244.
- Lam, P., Lavik, G., Jensen, M.M., van de Vossenberg, J., Schmid, M., Wobken, D. et al. (2009) Revising the nitrogen cycle in the Peruvian oxygen minimum zone. *Proc Natl Acad Sci USA* **106**: 4752-4757.
- Langwort.Ta, Mayberry, W.R., and Smith, P.F. (1974) Long-chain glycerol diether and polyol dialkyl glycerol triether lipids of *Sulfolobus acidocaldarius*. *J Bacteriol* **119**: 106-116.
- Lengger, S.K., Hopmans, E.C., Reichart, G.J., Nierop, K.G.J., Damsté, J.S.S., and Schouten, S. (2012) Intact polar and core glycerol dibiphytanyl glycerol tetraether lipids in the Arabian Sea oxygen minimum zone. Part II: Selective preservation and degradation in sediments and consequences for the TEX₈₆. *Geochim Cosmochim Acta* **98**: 244-258.
- Lincoln, S.A., Wai, B., Eppley, J.M., Church, M.J., Summons, R.E., and DeLong, E.F. (2014a) Planktonic Euryarchaeota are a significant source of archaeal tetraether lipids in the ocean. *Proc Natl Acad Sci USA* **111**: 9858-9863.
- Lipp, J.S., Morono, Y., Inagaki, F., and Hinrichs, K.U. (2008) Significant contribution of Archaea to extant biomass in marine subsurface sediments. *Nature* **454**: 991-994.
- Littler, K., Robinson, S.A., Bown, P.R., Nederbragt, A.J., and Pancost, R.D. (2011) High sea-surface temperatures during the Early Cretaceous Epoch. *Nat Geosci* **4**: 169-172.
- Martens-Habbena, W., Berube, P.M., Urakawa, H., de la Torre, J.R., and Stahl, D.A. (2009b) Ammonia oxidation kinetics determine niche separation of nitrifying Archaea and Bacteria. *Nature* **461**: 976-U234.
- Martens-Habbena, W., Qin, W., Horak, R.E., Urakawa, H., Schauer, A.J., Moffett, J.W. et al. (2014) The production of nitric oxide by marine ammonia-oxidizing archaea and inhibition of archaeal ammonia oxidation by a nitric oxide scavenger. *Environ Microbiol*.
- Matear, R.J., and Hirst, A.C. (2003) Long-term changes in dissolved oxygen concentrations in the ocean caused by protracted global warming. *Glob Biogeochem Cycles* **17**.
- Meehl, G.A., Washington, W.M., Collins, W.D., Arblaster, J.M., Hu, A.X., Buja, L.E. et al. (2005) How much more global warming and sea level rise? *Science* **307**: 1769-1772.
- Meyer, K.M., and Kump, L.R. (2008) Oceanic euxinia in Earth history: Causes and consequences. *Annu Rev Earth Planet Sci* **36**: 251-288.
- Orr, J.C., Fabry, V.J., Aumont, O., Bopp, L., Doney, S.C., Feely, R.A. et al. (2005) Anthropogenic ocean acidification over the twenty-first century and its impact on calcifying organisms. *Nature* **437**: 681-686.
- Pearson, A., and Ingalls, A.E. (2013) Assessing the use of archaeal lipids as marine environmental proxies. *Annu Rev Earth Planet Sci* **41**: 359-384.
- Pearson, A., Huang, Z., Ingalls, A.E., Romanek, C.S., Wiegel, J., Freeman, K.H. et al. (2004) Nonmarine crenarchaeol in Nevada hot springs. *Appl Environ Microbiol* **70**: 5229-5237.
- Pearson, A., Pi, Y.D., Zhao, W.D., Li, W.J., Li, Y.L., Inskeep, W. et al. (2008) Factors controlling the distribution of archaeal tetraethers in terrestrial hot springs. *Appl Environ Microbiol* **74**: 3523-3532.
- Qin, W., Amin, S.A., Martens-Habbena, W., Walker, C.B., Urakawa, H., Devol, A.H. et al. (2014) Marine ammonia-oxidizing archaeal isolates display obligate mixotrophy and wide ecotypic variation. *Proc Natl Acad Sci USA* **111**: 12504-12509.

- Santoro, A.E., Buchwald, C., McIlvin, M.R., and Casciotti, K.L. (2011) Isotopic Signature of N₂O Produced by Marine Ammonia-Oxidizing Archaea. *Science* **333**: 1282-1285.
- Schoon, P.L., Heilmann-Clausen, C., Schultz, B.P., Sinninghe Damsté, J.S., and Schouten, S. (2014) Warming and environmental changes in the eastern North Sea Basin during the Palaeocene-Eocene Thermal Maximum as revealed by biomarker lipids. *Org Geochem* **78**: 79-88.
- Schouten, S., Hopmans, E.C., Schefuß, E., and Damsté, J.S.S. (2002) Distributional variations in marine crenarchaeotal membrane lipids: a new tool for reconstructing ancient sea water temperatures? *Earth Planet Sci Lett* **204**: 265-274.
- Schouten, S., Hopmans, E.C., Forster, A., van Breugel, Y., Kuypers, M.M.M., and Damsté, J.S.S. (2003) Extremely high sea-surface temperatures at low latitudes during the middle Cretaceous as revealed by archaeal membrane lipids. *Geology* **31**: 1069-1072.
- Schouten, S., Pitcher, A., Hopmans, E.C., Villanueva, L., van Bleijswijk, J., and Damsté, J.S.S. (2012) Intact polar and core glycerol dibiphytanyl glycerol tetraether lipids in the Arabian Sea oxygen minimum zone: I. Selective preservation and degradation in the water column and consequences for the TEX₈₆. *Geochim Cosmochim Acta* **98**: 228-243.
- Shevenell, A.E., Ingalls, A.E., Domack, E.W., and Kelly, C. (2011) Holocene Southern Ocean surface temperature variability west of the Antarctic Peninsula. *Nature* **470**: 250-254.
- Sluijs, A., van Roij, L., Harrington, G.J., Schouten, S., Sessa, J.A., Levay, L.J. et al. (2014) Warming, euxinia and sea level rise during the Paleocene-Eocene Thermal Maximum on the Gulf Coastal Plain: implications for ocean oxygenation and nutrient cycling. *Clim Past* **10**: 1421-1439.
- Sluijs, A., Schouten, S., Pagani, M., Woltering, M., Brinkhuis, H., Damsté, J.S.S. et al. (2006) Subtropical arctic ocean temperatures during the Palaeocene/Eocene thermal maximum. *Nature* **441**: 610-613.
- Stewart, F.J., Ulloa, O., and DeLong, E.F. (2012) Microbial metatranscriptomics in a permanent marine oxygen minimum zone. *Environ Microbiol* **14**: 23-40.
- Trommer, G., Siccha, M., van der Meer, M.T.J., Schouten, S., Damsté, J.S.S., Schulz, H. et al. (2009) Distribution of Crenarchaeota tetraether membrane lipids in surface sediments from the Red Sea. *Org Geochem* **40**: 724-731.
- Valentine, D.L. (2007) Adaptations to energy stress dictate the ecology and evolution of the Archaea. *Nature Rev Microbiol* **5**: 316-323.
- van Bentum, E.C., Reichart, G.J., Forster, A., and Damsté, J.S.S. (2012) Latitudinal differences in the amplitude of the OAE-2 carbon isotopic excursion: pCO₂ and paleo productivity. *Biogeosciences* **9**: 717-731.
- van de Vossenberg, J.L.C.M., Driessen, A.J.M., and Konings, W.N. (1998) The essence of being extremophilic: the role of the unique archaeal membrane lipids. *Extremophiles* **2**: 163-170.
- van Helmond, N.A.G.M., Sluijs, A., Reichart, G.J., Damsté, J.S.S., Slomp, C.P., and Brinkhuis, H. (2014) A perturbed hydrological cycle during Oceanic Anoxic Event 2. *Geology* **42**: 123-126.
- Wagner, T., Herrle, J.O., Damsté, J.S.S., Schouten, S., Stüsser, I., and Hofmann, P. (2008) Rapid warming and salinity changes of Cretaceous surface waters in the subtropical North Atlantic. *Geology* **36**: 203-206.
- Walker, C.B., de la Torre, J.R., Klotz, M.G., Urakawa, H., Pinel, N., Arp, D.J. et al. (2010) Nitrosopumilus maritimus genome reveals unique mechanisms for nitrification and autotrophy in globally distributed marine crenarchaea. *P Natl Acad Sci USA* **107**: 8818-8823.

- Wuchter, C., Schouten, S., Coolen, M.J.L., and Damsté, J.S.S. (2004) Temperature-dependent variation in the distribution of tetraether membrane lipids of marine Crenarchaeota: Implications for TEX₈₆ paleothermometry. *Paleoceanography* **19**.
- Wuchter, C., Schouten, S., Wakeham, S.G., and Damsté, J.S.S. (2005) Temporal and spatial variation in tetraether membrane lipids of marine Crenarchaeota in particulate organic matter: Implications for TEX₈₆ paleothermometry. *Paleoceanography* **20**.
- Xie, S.T., Liu, X.L., Schubotz, F., Wakeham, S.G., and Hinrichs, K.U. (2014) Distribution of glycerol ether lipids in the oxygen minimum zone of the Eastern Tropical North Pacific Ocean. *Org Geochem* **71**: 60-71.
- Yan, J., Haaijer, S.C.M., den Camp, H.J.M.O., van Niftrik, L., Stahl, D.A., Könneke, M. et al. (2012a) Mimicking the oxygen minimum zones: stimulating interaction of aerobic archaeal and anaerobic bacterial ammonia oxidizers in a laboratory-scale model system. *Environ Microbiol* **14**: 3146-3158.
- Zachos, J.C., Schouten, S., Bohaty, S., Quattlebaum, T., Sluijs, A., Brinkhuis, H. et al. (2006) Extreme warming of mid-latitude coastal ocean during the Paleocene-Eocene Thermal Maximum: Inferences from TEX₈₆ and isotope data. *Geology* **34**: 737-740.
- Zhang, C.L., Pearson, A., Li, Y.L., Mills, G., and Wiegel, J. (2006) Thermophilic temperature optimum for crenarchaeol synthesis and its implication for archaeal evolution. *Appl Environ Microbiol* **72**: 4419-4422.

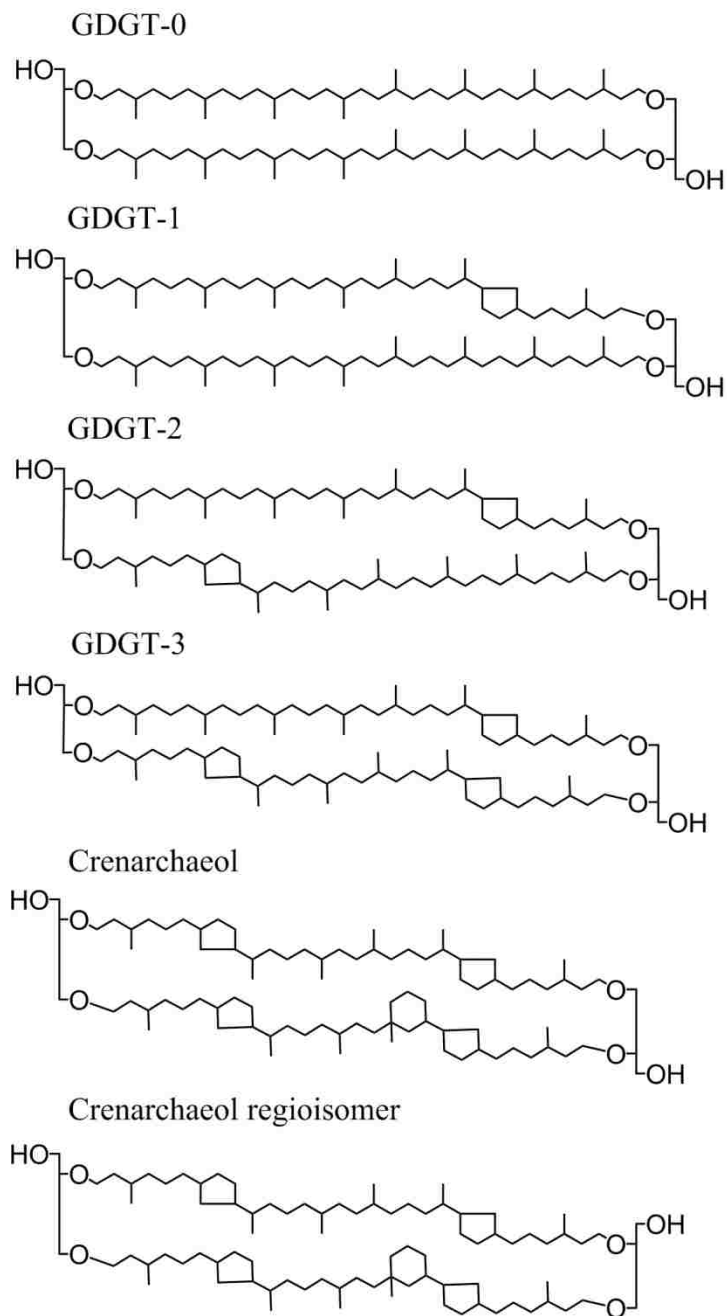


Figure 7.1. Structures of the glycerol dibiphytanyl glycerol tetraethers (GDGTs) core lipids of marine AOA.

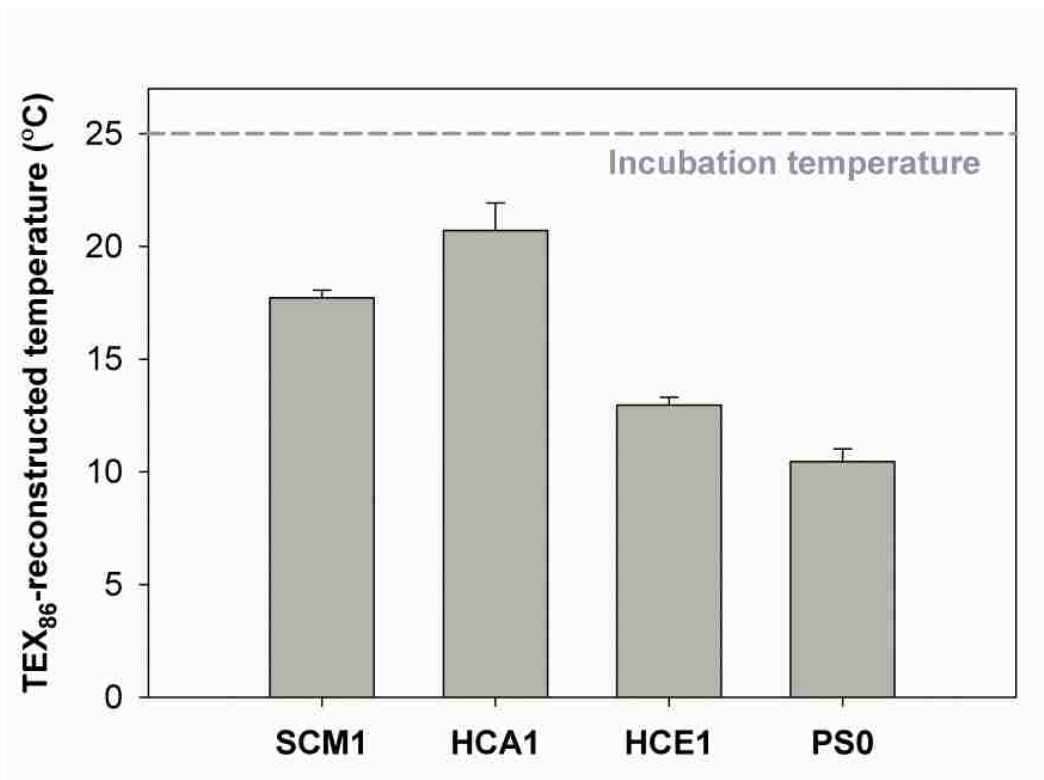


Figure 7.2. Reconstructed TEX_{86} -derived temperatures of four marine AOA isolates incubated at 25°C (dashed line).

Each bar represents the average of measurements from triplicate incubations and at least duplicate injections. Error bars are the standard deviation among average values of triplicate incubations.

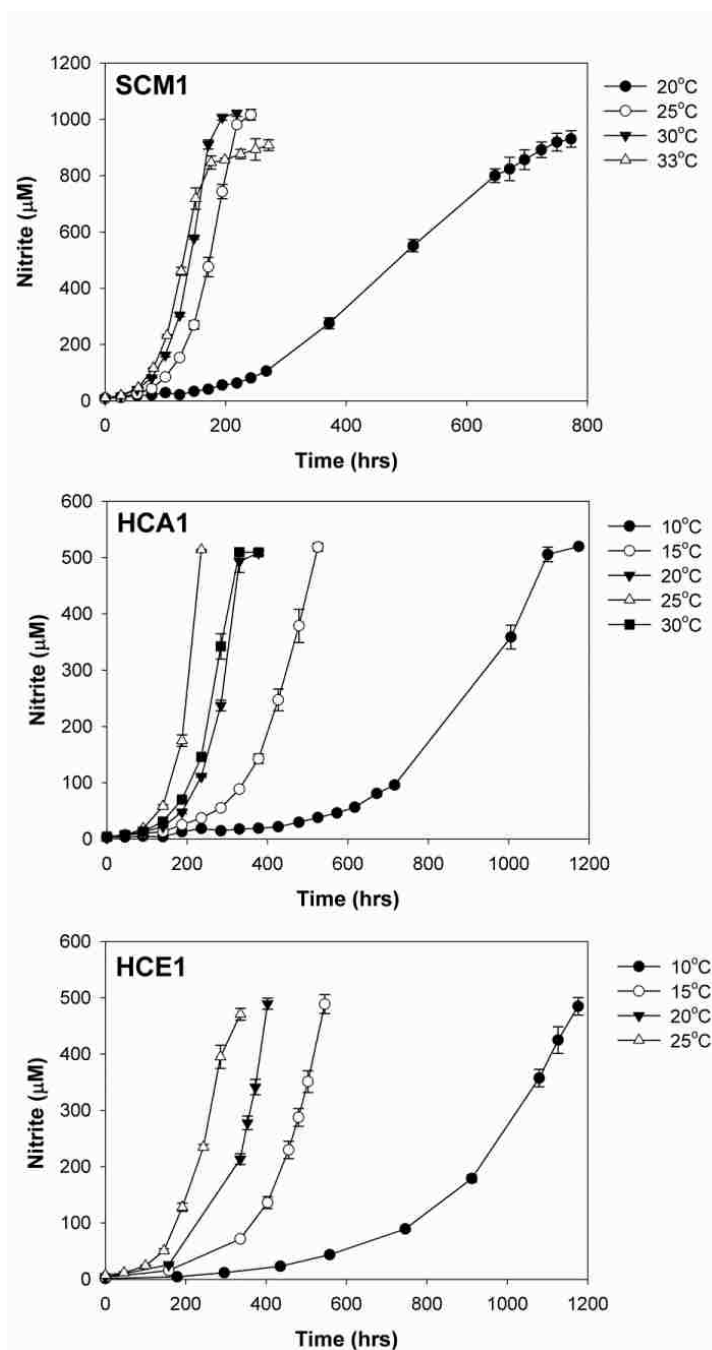


Figure 7.3. Effects of temperature on the ammonia oxidation activities of strains SCM1, HCA1 and HCE1.

Early stationary phase cultures (1% inoculum) were transferred to the growth medium supplemented with 1mM NH_4Cl (strain SCM1) or 500 μM NH_4Cl (strains HCA1 and HCE1). Ammonia oxidation activity was indicated by nitrite accumulation over time. Early stationary phase cells were harvested for the lipid analysis. Error bars represent the SD of data from triplicate cultures.

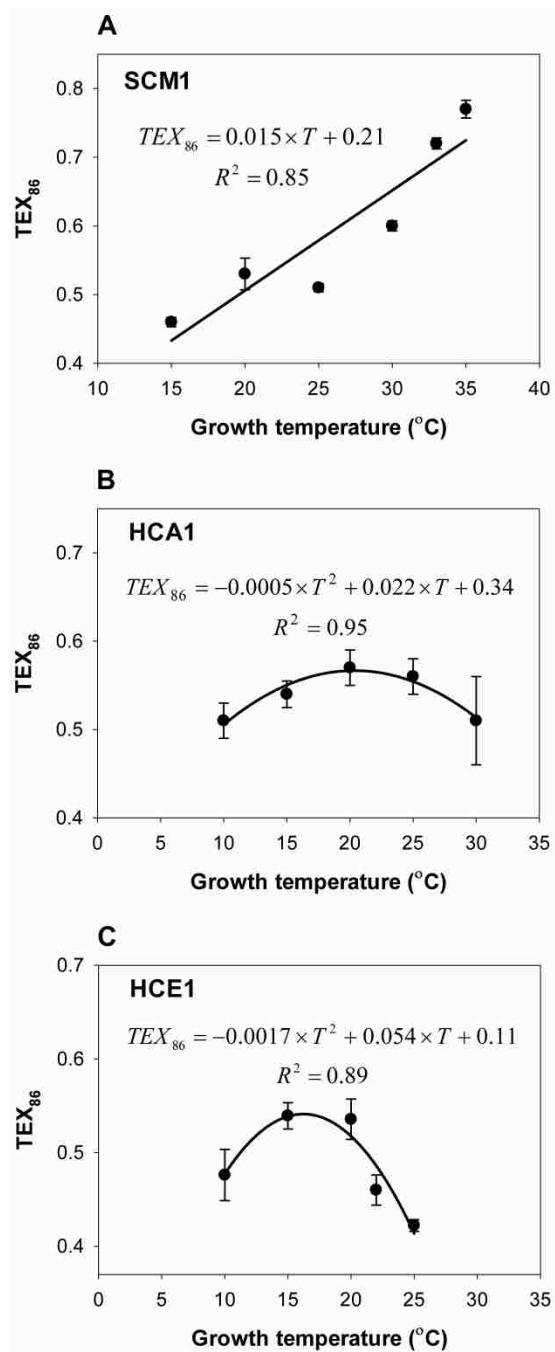


Figure 7.4. Correlations of TEX_{86} values with growth temperatures of strains SCM1 (A), HCA1 (B) and HCE1 (C).

Error bars represent the SD of data from triplicate cultures.

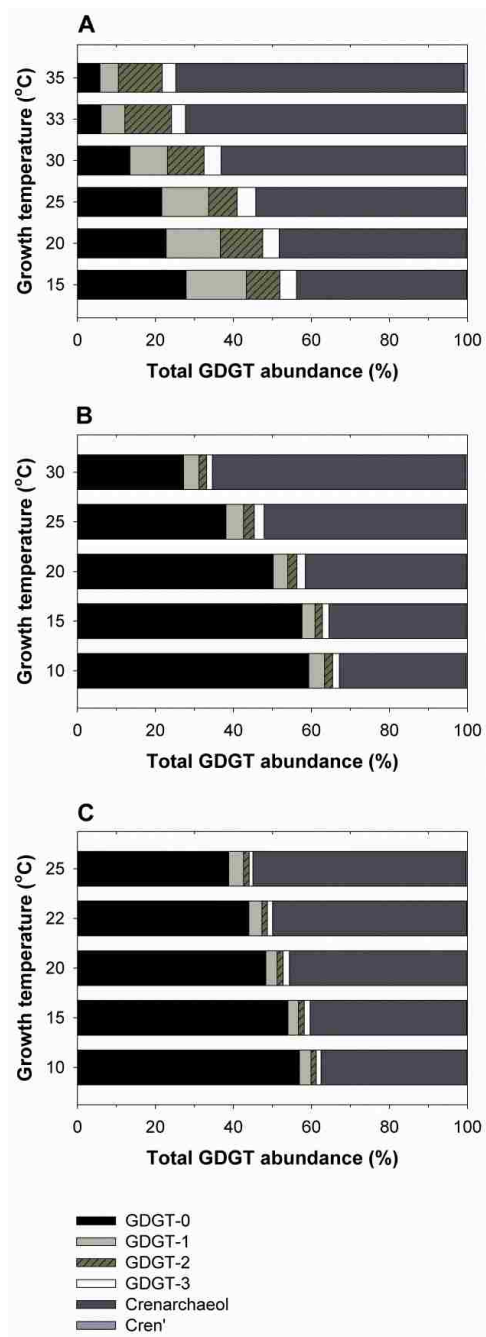


Figure 7.5. Relative abundances of GDGTs in total cellular lipids of marine AOA strains SCM1 (A), HCA1 (B) and HCE1 (C) at different temperatures.

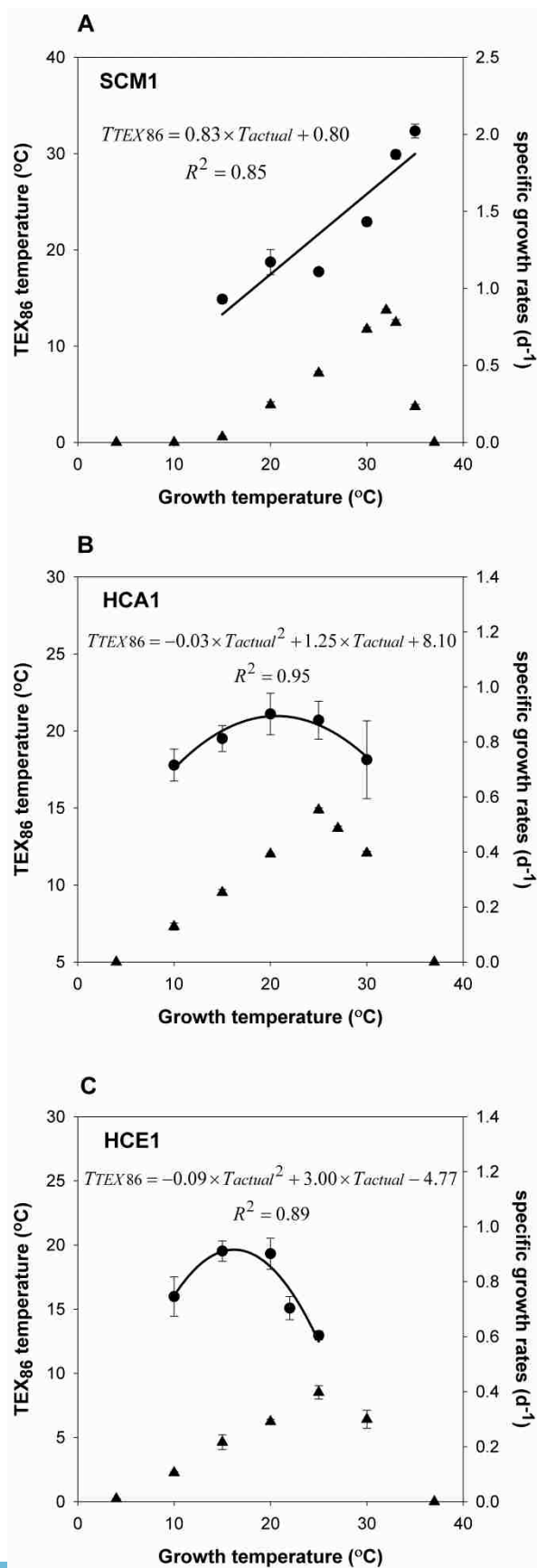


Figure 7.6. Correlation of TEX_{86} -derived temperature (filled circles) with growth temperature of strains SCM1 (A), HCA1 (B) and HCE1 (C).

Filled triangles represent the temperature dependence of the growth of strains SCM1 (A), HCA1 (B) and HCE1 (C) (in terms of specific growth rates (d^{-1})). All plotted data represent the average of measurements from triplicate incubations. Error bars represent the SD of triplicates.

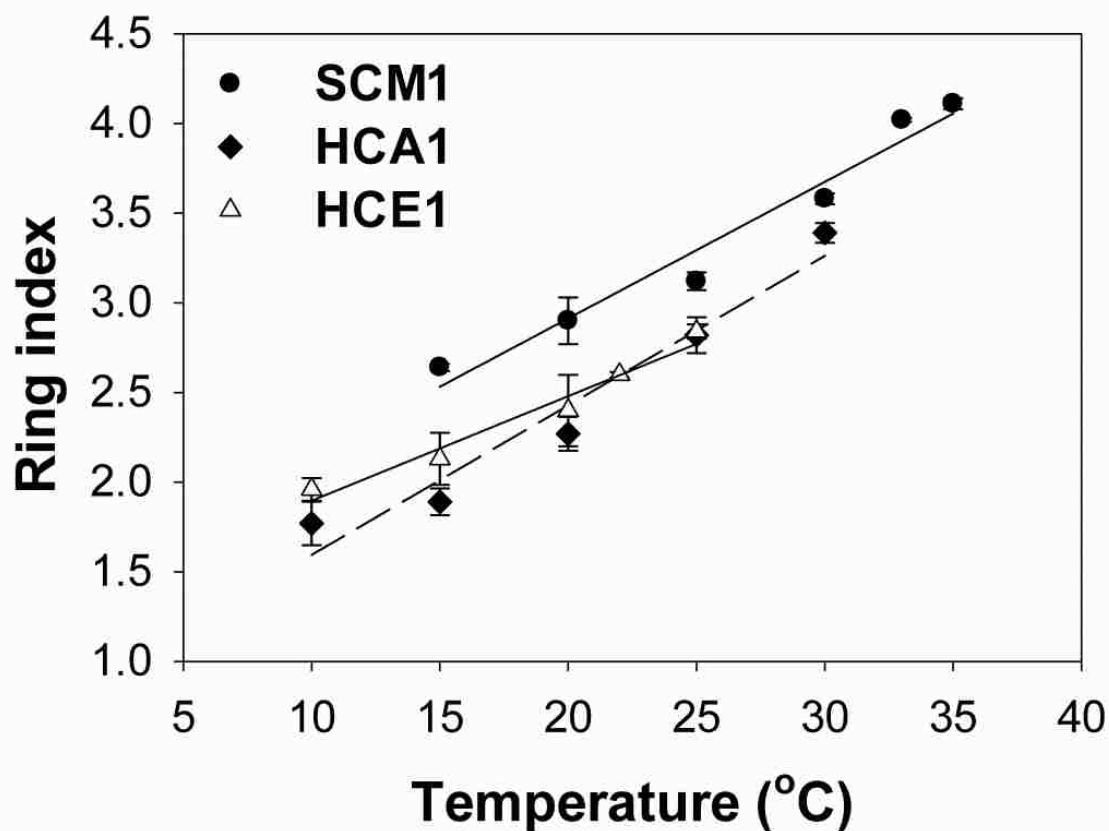


Figure 7.7. Correlations of ring index values with growth temperatures of strains SCM1 (15–35°C), HCA1 (10–30°C) and HCE1 (10–25°C).

The linear regression lines of SCM1 (solid line), HCA1 (dashed line) and HCE1 (solid line) are

$$y = 0.076x + 1.40 \quad (r^2 = 0.96), \quad y = 0.082x + 0.77 \quad (r^2 = 0.94) \quad \text{and} \quad y = 0.058x + 1.31 \quad (r^2 = 0.95),$$

respectively. Error bars represent the SD of data from triplicate cultures (some error bars are too small to be visible in the figure).

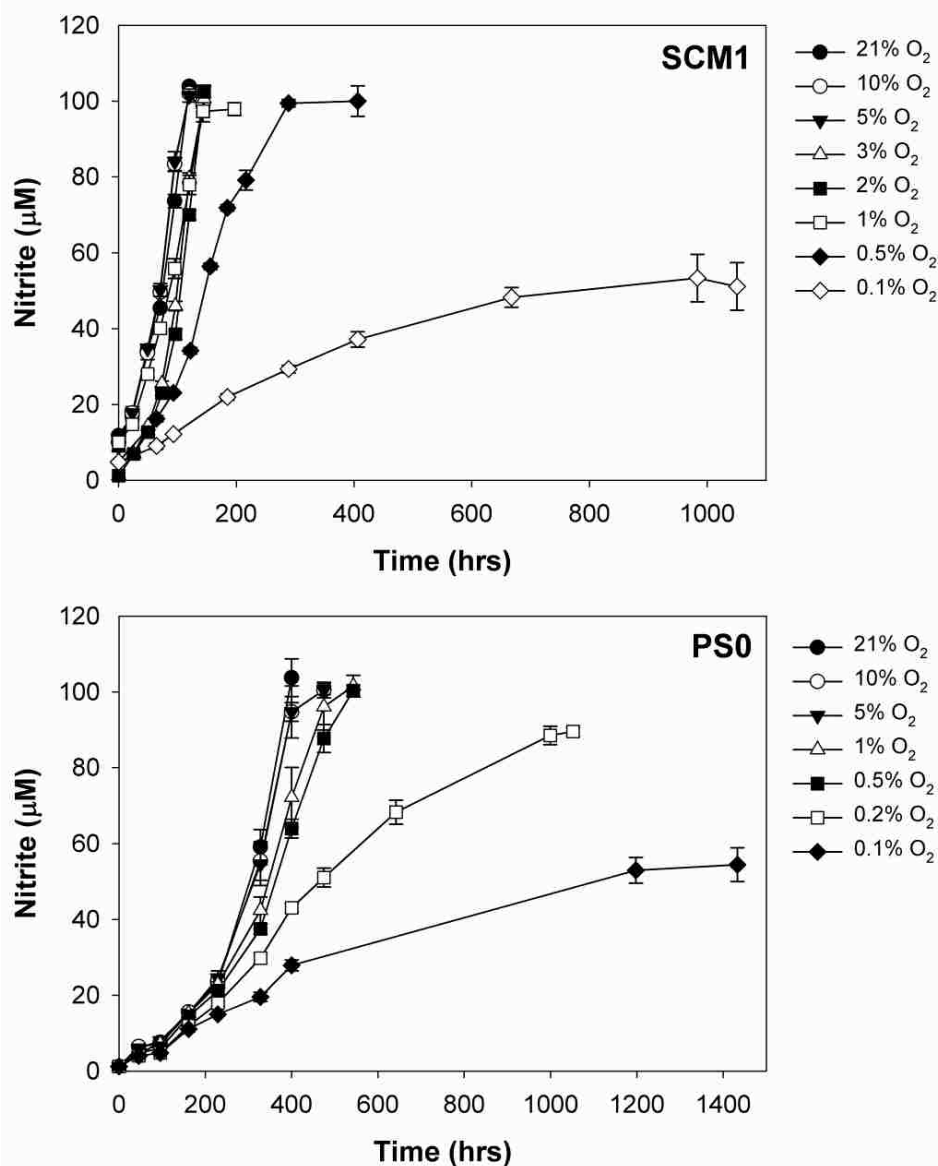


Figure 7.8. Effects of O₂ concentration on the ammonia oxidation activities of strains SCM1 and PS0.

Early stationary phase cultures (1% inoculum) were transferred to the growth medium supplemented with 100 µM NH₄Cl for both strains SCM1 and PS0. Early stationary phase cells were harvested for the lipid analysis. Error bars represent the SD of data from triplicate cultures.

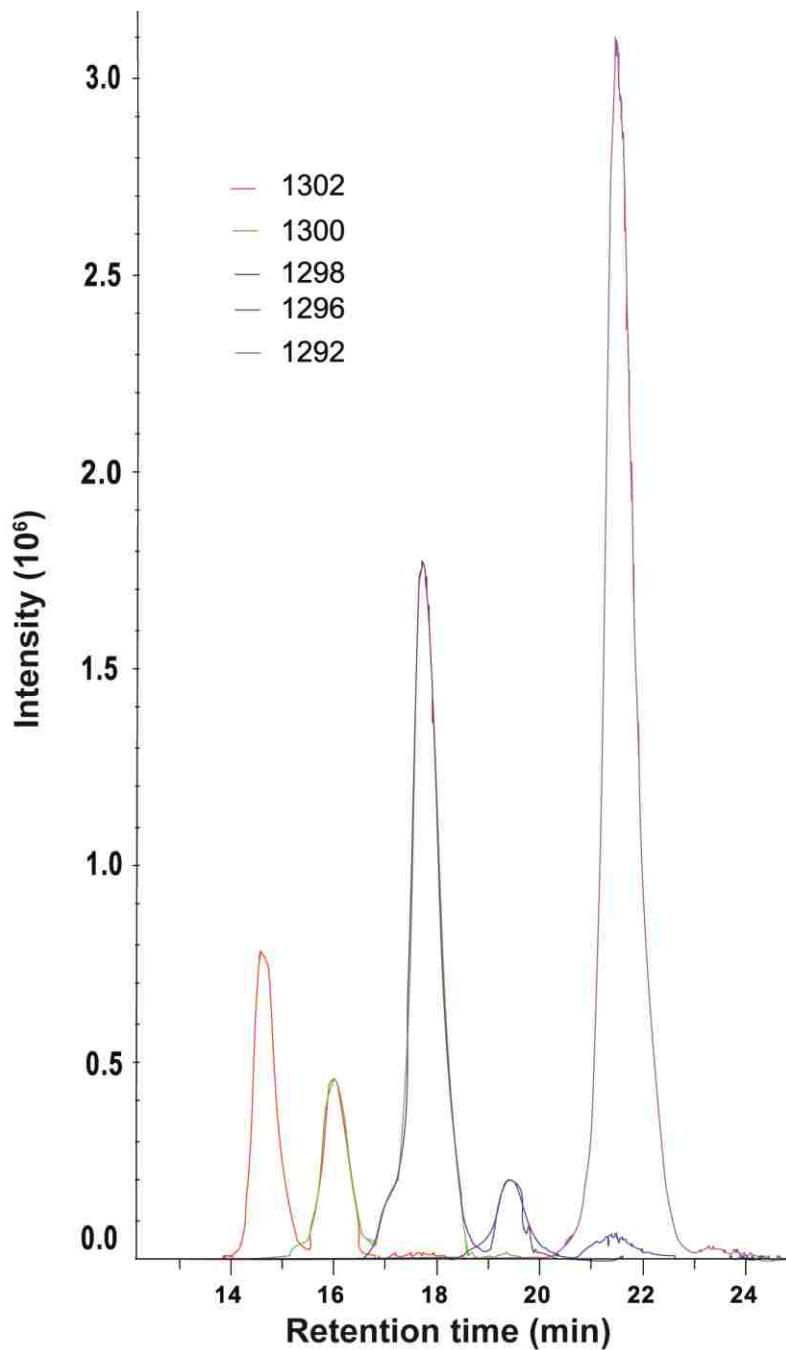


Figure 7.9. HPLC/MS base peak chromatogram showing the distribution of GDGT-0 (m/z 1302), GDGT-1 (m/z 1300), GDGT-2 (m/z 1298), GDGT-3 (m/z 1296), crenarchaeol and crenarchaeol regioisomer (m/z 1292) of marine AOA grown at 0.1% initial headspace O_2 .

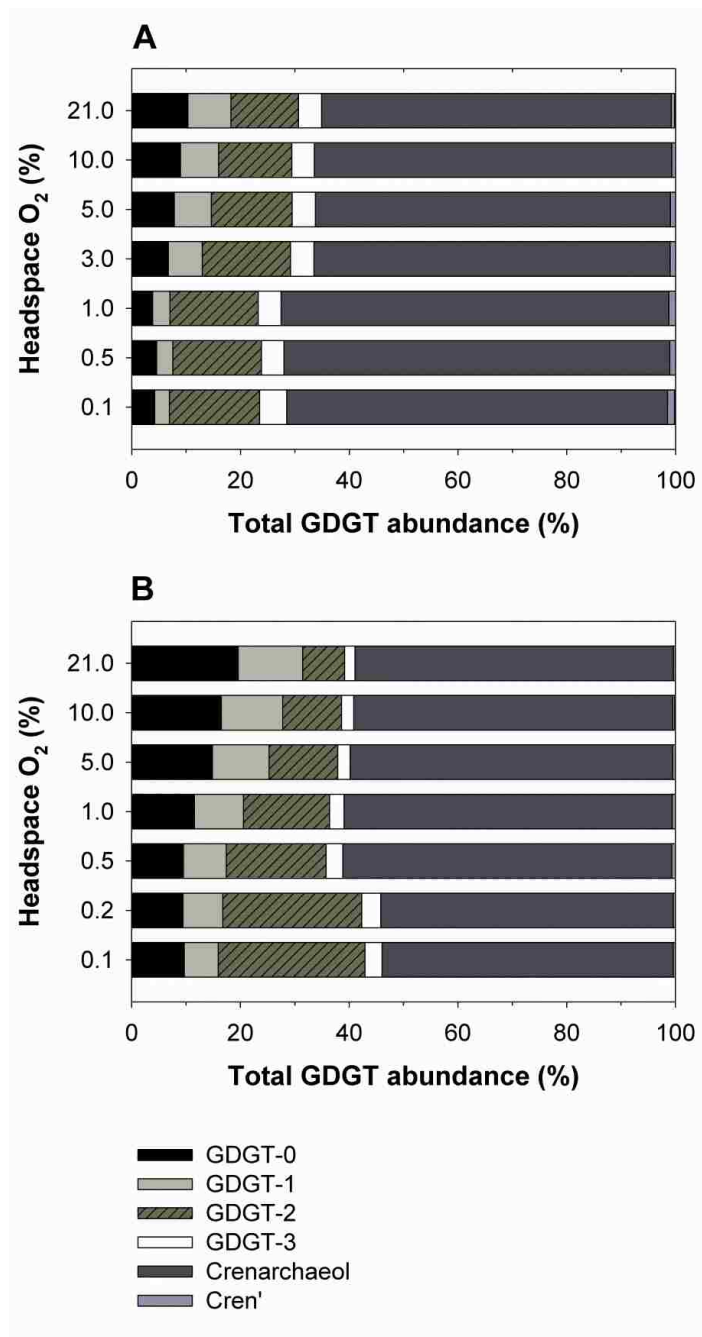


Figure 7.10. Relative abundances of GDGTs in total cellular lipids of marine AOA strains SCM1 (A) and PS0 (B) with different initial headspace O₂ concentrations.

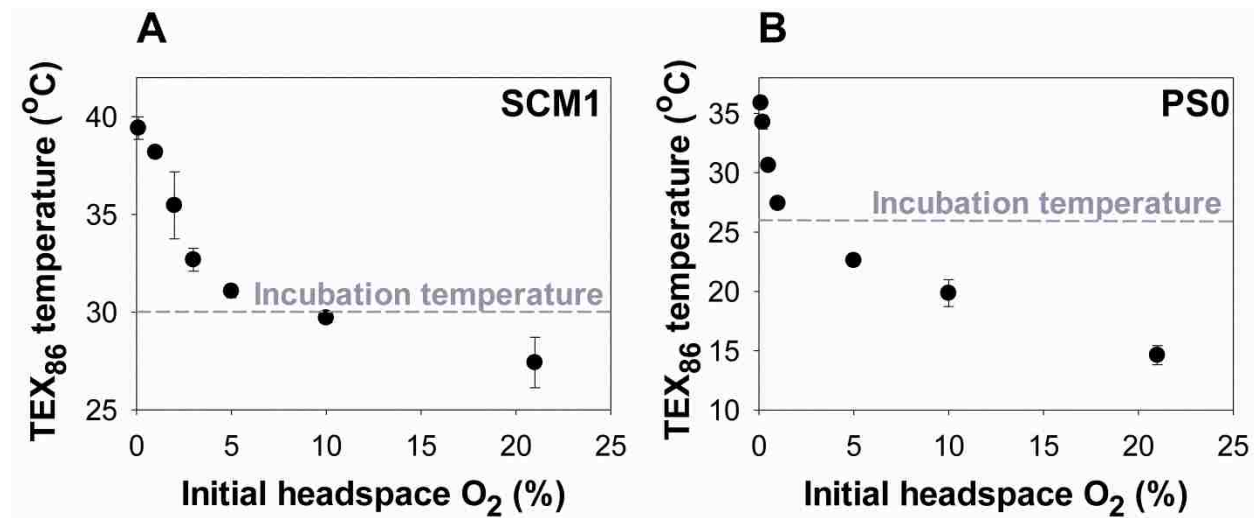


Figure 7.11. Reconstructed TEX₈₆ temperatures for the total cellular lipids of strains SCM1 (A) and PS0 (B) showing the exponential TEX₈₆-derived temperature increase from 21% O₂ to 0.1% O₂.

Dashed lines represent the constant incubation temperature of strains SCM1 (A) and PS0 (B) at 30°C and 26°C, respectively. Error bars represent the SD of the mean of triplicate cultures.

Table 7.1. Cell densities, lipid contents and TEX₈₆ values of different marine AOA strains grown at selected temperatures

Strain	Growth temperature (°C)	Cell density at early stationary phase (ml ⁻¹)	Total GDGTs (fg cell ⁻¹)	TEX ₈₆
SCM1	15	–	–	0.46
	20	7.27×10 ⁷	2.00	0.53
	25	8.10×10 ⁷	2.22	0.51
	30	8.35×10 ⁷	2.02	0.60
	35	–	–	0.77
HCA1	10	–	–	0.51
	15	3.82×10 ⁷	2.05	0.54
	20	3.87×10 ⁷	2.09	0.57
	25	3.49×10 ⁷	1.76	0.56
	30	3.65×10 ⁷	2.27	0.51
HCE1	15	3.69×10 ⁷	1.53	0.54
	20	3.70×10 ⁷	1.41	0.54
	25	–	–	0.42
PS0	25	3.59×10 ⁷	3.01	0.38

Table 7.2. Relative abundances of GDGTs in total cellular lipids and ring index values of marine AOA isolates grown at selected temperatures

Strain	Growth temperature (°C)	Relative abundance of GDGTs (%)						Ring index
		0	1	2	3	Cren	Cren'	
SCM1	15	27.86	15.47	8.57	4.28	43.67	0.15	2.65
	20	22.76	13.91	10.84	4.26	47.99	0.24	2.90
	25	21.62	12.02	7.32	4.76	53.91	0.37	3.12
	30	13.47	9.63	9.37	4.37	62.58	0.58	3.57
	33	6.04	6.14	11.97	3.56	71.73	0.56	4.02
	35	5.78	4.71	11.26	3.49	73.91	0.84	4.11
HCA1	10	59.34	4.04	2.09	1.71	32.51	0.31	1.77
	15	57.60	3.34	1.88	1.71	35.17	0.30	1.90
	20	50.22	3.73	2.37	2.15	41.27	0.26	2.23
	25	38.09	4.52	2.71	2.54	51.78	0.36	2.78
	30	27.23	3.95	1.97	1.45	64.90	0.50	3.39
HCE1	10	56.92	2.98	1.34	1.25	37.39	0.12	1.97
	15	53.99	2.71	1.46	1.50	40.14	0.20	2.12
	20	48.33	2.90	1.53	1.58	45.42	0.23	2.39
	22	43.96	3.36	1.41	1.32	49.78	0.17	2.60
	25	38.81	3.78	1.46	0.96	54.65	0.34	2.85
PS0	25	25.33	12.59	5.53	1.83	54.41	0.31	3.03

Table 7.3. Cell densities, O₂ utilization and TEX₈₆ values of marine AOA strains grown at selected initial headspace O₂ concentrations

Strain	Initial headspace O ₂	Initial amount of O ₂ (micromole)	Residual amount of O ₂ (micromole)	Initial Cell density (ml ⁻¹)	Cell density at early stationary phase (ml ⁻¹)	TEX ₈₆
SCM1	0.1%	6.0	0	2.83×10 ⁵	4.0×10 ⁶	0.89
	0.5%	29.8	14.8	2.72×10 ⁵	6.3×10 ⁶	0.88
	1%	59.7	44.7	2.78×10 ⁵	6.6×10 ⁶	0.87
	5%	298.3	283.3	2.88×10 ⁵	6.8×10 ⁶	0.74
	10%	596.5	581.5	2.77×10 ⁵	6.9×10 ⁶	0.72
	21%	1252.7	1237.7	2.83×10 ⁵	7.9×10 ⁶	0.68
PS0	0.2%	11.9	0	2.51×10 ⁵	6.7×10 ⁶ *	0.80
	0.5%	29.8	14.8	2.33×10 ⁵	7.0×10 ⁶	0.74
	1%	59.7	44.7	2.95×10 ⁵	7.0×10 ⁶	0.68
	5%	298.3	283.3	2.88.×10 ⁵	6.8×10 ⁶	0.59
	10%	596.5	581.5	2.43.×10 ⁵	6.8×10 ⁶	0.55
	21%	1252.7	1237.7	2.70.×10 ⁵	6.7×10 ⁶	0.45

*The slightly higher cell densities than predicted from ammonia oxidation may reflect some variation in the incorporation of α-ketoglutarate into cellular biomass under low O₂.

Table 7.4. Relative abundances of GDGTs in total cellular lipids and ring index values of strains SCM1 and PS0 grown at selected initial headspace O₂ concentrations

Strain	Initial headspace O ₂	Relative abundance of GDGTs (%)						Ring index
		0	1	2	3	Cren	Cren'	
SCM1	0.1%	4.21	2.70	16.60	4.99	70.03	1.28	4.08
	1%	3.84	3.17	16.26	4.19	71.35	1.18	4.11
	5%	7.81	6.84	14.84	4.3	65.28	0.89	3.80
	10%	8.95	7.04	13.43	4.16	65.72	0.62	3.78
	21%	10.32	7.93	12.42	4.26	64.28	0.61	3.71
PS0	0.1%	9.69	6.24	27.00	3.14	53.53	0.37	3.39
	0.2%	9.44	7.31	25.58	3.48	53.78	0.36	3.40
	0.5%	9.50	7.90	18.37	3.06	60.49	0.64	3.60
	1%	11.57	9.00	15.82	2.69	60.33	0.55	3.53
	5%	14.84	10.45	12.62	2.26	59.34	0.43	3.42
	10%	16.49	11.30	10.81	2.22	58.70	0.39	3.35
	21%	19.58	11.89	7.69	1.94	58.53	0.29	3.27

Chapter 8.

Summary and Perspectives

Marine AOA are well adapted to life in low energy (Könneke et al., 2014), oligotrophic marine environments (Martens-Habbena et al., 2009b) and tend to evolve streamlined genomes with low metabolic versatility (Walker et al., 2010; Santoro et al., 2015). Our proteomics analysis showed that marine AOA cells translated a high fraction of their genomes for growth on ammonia, its sole energy and reductant source. Although marine AOA favor active maintenance under low energy flux, they are much less tolerant to nutrient starvation than characterized AOB. Marine AOA cells decrease their overall gene expression of essential energy production and biosynthetic pathways in response to energy starvation and Cu-stressed conditions. When marine AOA cells are nutrient limited, they appear to up-regulate genes to a lesser extent than many heterotrophs. Therefore, marine AOA may also undergo additional physiological changes to enhance their chances for survival under stressed conditions. The regulation of the composition of the GDGT lipid membrane of marine AOA is implicated in adaptation and acclimation to changing environments (Qin et al., 2015d). One key finding of the studies presented in this thesis was that, apart from temperature, O₂ concentration greatly influenced the membrane lipid composition of marine AOA (Qin et al., 2015d). Interestingly, marine AOA isolates preferentially adjust the relative abundance of GDGT-2 with varying O₂ concentrations; while they mainly modulate the relative abundance of crenarchaeol with changing growth temperature (Qin et al., 2015d). These marked differences suggest that different GDGT species

may provide specific adaptive advantages to marine AOA survival under a range of stress conditions. However, because the biosynthetic pathway of GDGTs remains partially unknown, and the specific role of the unique cyclohexane ring in membrane physiology is still unclear, there are plenty of unsolved mysteries regarding the mechanisms of regulation of marine AOA membrane lipid composition and the associated biophysical significance. In addition, because the AOA cell membrane hosts a large number of key enzymes involved in ammonia oxidation and electron transfer systems, it is possible that the changes in membrane lipid composition have a direct influence on the conformation of the active site of the membrane-associated enzymes, which may lead to changes in the activity of energy production and respiration. The studies in this dissertation are only preliminary, more experiments with AOA strains representing a broader range of ecotypes are necessary to further explore environmental influences on GDGT composition and how these factors relate to physiology.

Although the overall stoichiometry of ammonia oxidation to nitrite by AOA is identical to that of AOB, the underlying biochemical pathways appear to be vastly different. So far, the archaeal ammonia-oxidizing pathway has not been fully identified. Although AOA lack genes for the hydroxylamine-ubiquinone redox module found in AOB, hydroxylamine has been observed as an intermediate during archaeal ammonia oxidation, suggesting that this pathway is mediated by a novel enzyme or novel enzyme systems that possibly involve some of the periplasmic multicopper oxidases (Vajrala et al., 2013). The transcriptomic and proteomic information presented in this dissertation serve to predict the most likely candidates for a direct role in hydroxylamine oxidation. Future isolation and characterization of the candidate hydroxylamine dehydrogenase will be required to extend our understanding of the mysterious biochemistry of

archaeal ammonia oxidation. In addition, the studies presented herein demonstrate that nitric oxide is a central intermediate required for archaeal ammonia oxidation pathway (Martens-Habbena et al., 2015). This important finding has laid the groundwork for the development of selective inhibitors to distinguish the relative contributions of AOA and AOB to *in situ* ammonia oxidation (Martens-Habbena et al., 2015). Although the production and consumption of nitric oxide was shown to be tightly controlled during normal growth of marine AOA species, unbalanced growth was observed at saturating ammonia concentrations with the accumulation of high concentrations of nitric oxide (Martens-Habbena et al., 2015). Nitric oxide can rapidly bind and react with the reduced forms of cobalamin to produce nitrosylcobalamin (Danishpajooch et al., 2001; Kambo et al., 2005), which is rapidly oxidized to nitrocobalamin in the presence of oxygen (Wolak et al., 2006). Notably, it was found that the most of the cellular cobalamin pool had reacted with nitric oxide to form nitrosylated and nitrated cobalamin during the growth of AOA. In addition, gene expression studies showed that the entire cobalamin biosynthesis pathway is regulated by the level of nitrosative stress, suggesting that the interplay between nitric oxide production and cobalamin synthesis is a critical component for the fundamental physiology of AOA that may play a major role in shaping their ecology in natural environments. Future studies determining the bioavailability of nitrosylated species of cobalamin and their distribution in marine waters may advance our understanding of the cobalamin-based microbial interdependencies in the ocean.

The comparative physiological studies presented in this dissertation highlighted the remarkable physiological diversity within a genetically closely circumscribed set of AOA (Qin et al., 2014). In particular, it was demonstrated that phylogenetically closely related AOA strains were

associated with significant variation in their sensitivities to reactive oxygen species, suggesting the requirement for further studies to better constrain the environmental significance of this sensitivity. However, as yet, the characterization of AOA in culture has not informed environmental data indicating that a significant fraction of cellular carbon is derived from organic carbon (Ingalls et al., 2006). Given the restricted origins of existing marine AOA isolates so far, the capture of a greater representation of AOA environmental diversity in pure culture should therefore serve to expand understanding of physiological diversity and metabolic capacity of this globally significant assemblage of microorganisms.

In conclusion, the studies presented in this dissertation have led to new insights into the ecophysiology of marine ammonia-oxidizing archaea and their response to the ongoing changes in the world's oceans. Overall, these studies underscored the importance of an expanded pure culture collection and systematic physiological characterization of biogeochemically significant organisms for developing fundamental understanding of their adaptive capacity to the predicted warming, deoxygenation, and acidification of the global ocean. In addition, the studies in this dissertation highlight the important role of the cell envelope in physiological adaptation and how a physiological understanding can inform the use of the membrane lipid as a tracer of past environmental conditions on Earth. In particular, the finding of the significant effects of O₂ on TEX₈₆ values necessitates a re-evaluation of inferences of past climate made from TEX₈₆-based historical records (Qin et al., 2015d). Finally, the different responses of AOA and AOB isolates to metabolic inhibitors PTIO and ATU observed in the laboratory informed the development of an approach of selective activity measurements of these groups in natural marine systems (Martens-Habbena et al., 2015). These results are expected to provide useful tools to further

constrain the relative contributions of AOA and AOB to nitrification and associated greenhouse gas emissions in a variety of environments. Therefore, these studies offered a good example of how to combine laboratory studies and field work to establish relationships between microbial biology and system level processes. It is the hope that further characterization of the ecology, physiology, and underlying biochemistry of marine AOA will lead to new exciting discoveries of Archaea and nitrogen cycle research.

References

- Danishpajoo, I.O., Gudi, T., Chen, Y.C., Kharitonov, V.G., Sharma, V.S., and Boss, G.R. (2001) Nitric oxide inhibits methionine synthase activity in vivo and disrupts carbon flow through the folate pathway. *J Biol Chem* **276**: 27296-27303.
- Ingalls, A.E., Shah, S.R., Hansman, R.L., Aluwihare, L.I., Santos, G.M., Druffel, E.R.M., and Pearson, A. (2006) Quantifying archaeal community autotrophy in the mesopelagic ocean using natural radiocarbon. *Proc Natl Acad Sci USA* **103**: 6442-6447.
- Kambo, A., Sharma, V.S., Casteel, D.E., Woods, V.L., Pilz, R.B., and Boss, G.R. (2005) Nitric oxide inhibits mammalian methylmalonyl-CoA mutase. *J Biol Chem* **280**: 10073-10082.
- Könneke, M., Schubert, D.M., Brown, P.C., Hugler, M., Standfest, S., Schwander, T. et al. (2014) Ammonia-oxidizing archaea use the most energy-efficient aerobic pathway for CO₂ fixation. *P Natl Acad Sci USA* **111**: 8239-8244.
- Martens-Habbena, W., Berube, P.M., Urakawa, H., de la Torre, J.R., and Stahl, D.A. (2009b) Ammonia oxidation kinetics determine niche separation of nitrifying Archaea and Bacteria. *Nature* **461**: 976-U234.
- Martens-Habbena, W., Qin, W., Horak, R.E.A., Urakawa, H., Schauer, A.J., Moffett, J.W. et al. (2015) The production of nitric oxide by marine ammonia-oxidizing archaea and inhibition of archaeal ammonia oxidation by a nitric oxide scavenger. *Environ Microbiol* **17**: 2261-2274.
- Qin, W., Carlson, L.T., Armbrust, E.V., Devol, A.H., Moffett, J.W., Stahl, D.A., and Ingalls, A.E. (2015d) Confounding effects of oxygen and temperature on the TEX₈₆ signature of marine Thaumarchaeota. *P Natl Acad Sci USA* **112**: 10979-10984.
- Qin, W., Amin, S.A., Martens-Habbena, W., Walker, C.B., Urakawa, H., Devol, A.H. et al. (2014) Marine ammonia-oxidizing archaeal isolates display obligate mixotrophy and wide ecotypic variation. *P Natl Acad Sci USA* **111**: 12504-12509.
- Santoro, A.E., Dupont, C.L., Richter, R.A., Craig, M.T., Carini, P., McIlvin, M.R. et al. (2015) Genomic and proteomic characterization of "Candidatus Nitrosopelagicus brevis": An ammonia-oxidizing archaeon from the open ocean. *P Natl Acad Sci USA* **112**: 1173-1178.
- Vajjala, N., Martens-Habbena, W., Sayavedra-Soto, L.A., Schauer, A., Bottomley, P.J., Stahl, D.A., and Arp, D.J. (2013) Hydroxylamine as an intermediate in ammonia oxidation by globally abundant marine archaea. *P Natl Acad Sci USA* **110**: 1006-1011.

- Walker, C.B., de la Torre, J.R., Klotz, M.G., Urakawa, H., Pinel, N., Arp, D.J. et al. (2010) Nitrosopumilus maritimus genome reveals unique mechanisms for nitrification and autotrophy in globally distributed marine crenarchaea. *P Natl Acad Sci USA* **107**: 8818-8823.
- Wolak, M., Stochel, G., and van Eldik, R. (2006) Reactivity of aquacobalamin and reduced cobalamin toward S-nitrosoglutathione and S-nitroso-N-acetylpenicillamine. *Inorg Chem* **45**: 1367-1379.

Chapter 9.

Other Scientific Contributions

9.1 Order *Nitropumilales*, Family *Nitrosopumilaceae*, Genus *Nitrosopumilus*

Wei Qin¹, Willm Martens-Habbena^{1,2}, Julia N. Kobelt³, and David A. Stahl¹

Published in *Bergey's Manual of Systematics of Archaea and Bacteria*, 3rd Edition
2016

DOI: 10.1002/9781118960608.obm00122

¹Department of Civil and Environmental Engineering, University of Washington, Seattle, WA, USA; ²Molecular Epidemiology Inc., Lake Forest Park, WA, USA; ³Department of Biology, University of Washington, Seattle, WA, USA.

Abstract. Mesophilic to moderately thermophilic, neutrophilic, motile or nonmotile, slender rods or irregular cocci. Obligately aerobic ammonia-oxidizing archaea; many members, but not all, are capable of using urea as substrate. Autotrophic, using a modified version of 3-hydroxypropionate/4-hydroxybutyrate pathway for CO₂ fixation, although some organic material may be needed to support growth. Cells are free-living or symbiotic. Outer cell wall structure is composed of a hexagonally arrayed single S-layer. Cell membrane is composed of glycerol dibiphytanyl glycerol tetraether lipids, including large amounts of crenarchaeol. Cells are light-

sensitive. Organisms are widely distributed in marine, terrestrial, and geothermal environments. *Nitrosopumilales* can be phylogenetically differentiated from other orders within the phylum *Thaumarchaeota*, by comparison of the 16S rRNA and *amoA* (encoding the α -subunit of ammonia monooxygenase) sequences. Unlike *Nitrosopumilales*, no rod-shaped cell forms have so far been observed among the members of the orders *Nitrososphaerales* and *Nitrosocaldales*. Cultivated representatives of this order are neutrophilic. In contrast, most members of the order *Nitrosotaleales* are acidophilic. The order contains two families, *Nitrosopumilaceae* and *Nitrosotenuaceae*. The type genus is *Nitrosopumilus*.

Corresponding author E-mail: dastahl@u.washington.edu.

9.2 Order *Nitrosocaldales*, Family *Nitrosocaldaceae*, Genus *Nitrosocaldus*

Wei Qin¹, Talia N. M. Jewell^{2,3}, Virginia V. Russell³, Brian P. Hedlund⁴, José R. de la Torre³,
and David A. Stahl¹

Submitted to *Bergey's Manual of Systematics of Archaea and Bacteria*, 3rd Edition

2016

(Accepted)

¹Department of Civil and Environmental Engineering, University of Washington, Seattle, WA, USA; ²Earth and Environmental Sciences, Lawrence Berkeley National Laboratory, Berkeley, CA, USA; ³Department of Biology, San Francisco State University, San Francisco, CA, USA; ⁴School of Life Sciences, University of Nevada, Las Vegas, Las Vegas, Nevada, USA.

Abstract. Coccoid cells reproduce by binary fission. Thermophilic and neutrophilic.

Obligately aerobic. Chemolithoautotrophic growth by ammonia oxidation to nitrite using CO₂ as carbon source. Some members can also use urea as an alternative source of energy for growth.

Cell membrane is composed of isoprenoid tetraether lipids, including large amounts of acyclic and cyclized glycerol trialkyl glycerol tetraethers (GTGTs) and crenarchaeol (a unique glycerol dibiphytanyl glycerol tetraether (GDGT) containing one cyclohexane ring and four cyclopentane rings). Fully saturated and monounsaturated menaquinones with 6 isoprenoid units are present.

They are globally distributed in various geothermal environments. Phylogenetic analyses of 16S rRNA and *amoA* gene sequences place the monophyletic order *Nitrosocaldales* as a basal lineage within the phylum *Thaumarchaeota*. This order can be distinguished from the closest order *Nitrososphaerales* by a lower mol% G+C content, a higher growth temperature (> 60°C), and a

higher relative abundance of GTGT. The order *Nitrosocaldales* is currently represented by a single family *Nitrosocaldaceae*. The type genus is *Nitrosocaldus*.

Corresponding author E-mail: dastahl@u.washington.edu.

9.3 Two distinct pools of B₁₂ analogs reveal community interdependencies in the ocean

Katherine R. Heal^a, **Wei Qin**^b, Francois Ribalet^a, Anthony D. Bertagnoli^{b,c}, Willow Coyote-Maestas^{a,d}, Laura R. Hmelo^a, James W. Moffett^c, Allan H. Devol^a, E. Virginia Armbrust^a, David A. Stahl^b, Anitra E. Ingalls^{a,1}

Submitted to *Proceedings of the National Academy of Sciences of the United States of America*

2016

(Accepted)

^aSchool of Oceanography, University of Washington, Seattle, WA 98195; ^bDepartment of Civil and Environmental Engineering, University of Washington, Seattle, WA 98195; ^ccurrent affiliation: The Millennial Institute of Oceanography at Universidad de Concepcion, P.O. Box 160 C. Concepción, Chile; ^dcurrent affiliation: Department of Biochemistry, Biophysics and Molecular Biology, University of Minnesota, Minneapolis, MN, 55455; ^eDepartments of Biological Sciences and Earth Sciences and Civil and Environmental Engineering, University of Southern California, Los Angeles, CA, 90089-0894

Abstract. Organisms within all domains of life require the cofactor cobalamin (vitamin B₁₂), which is produced only by a subset of bacteria and archaea. Based on genomic analyses, cobalamin biosynthesis in marine systems has been inferred in three main groups: select heterotrophic Proteobacteria, chemoautotrophic Thaumarchaeota, and photoautotrophic Cyanobacteria. Culture work demonstrates that many Cyanobacteria do not synthesize cobalamin, but rather produce pseudocobalamin, challenging the connection between the occurrence of cobalamin biosynthesis genes and production of the compound in marine ecosystems. Here we show that cobalamin and pseudocobalamin coexist in the surface ocean,

have distinct microbial sources, and support different enzymatic demands. Even in the presence of cobalamin, Cyanobacteria synthesize pseudocobalamin – likely reflecting their retention of an oxygen-independent pathway to produce pseudocobalamin, which is used in as a cofactor in their specialized methionine synthase (MetH). This contrasts a model diatom, *Thalassiosira pseudonana*, which transported pseudocobalamin into the cell but was unable to use pseudocobalamin in their homolog of MetH. Our genomic and culture analyses showed that marine Thaumarchaeota and select heterotrophic bacteria produce cobalamin. This indicates that cobalamin in the surface ocean is a result of *de novo* synthesis by heterotrophic bacteria or via modification of closely related compounds like cyanobacterially-produced pseudocobalamin. Deeper in the water column, our study implicates Thaumarchaeota as the major producers of cobalamin based on genomic potential, cobalamin cell quotas, and abundance. Together, these findings establish the distinctive roles played by abundant prokaryotes in cobalamin-based microbial interdependencies that sustain community structure and function in the ocean.

¹Corresponding author E-mail: aingalls@uw.edu.

9.4 Ammonia oxidation kinetics and temperature sensitivity of a natural marine community dominated by Archaea

Rachel E. A. Horak¹, Wei Qin², E. Virginia Armbrust¹, Anitra E. Ingalls¹, James W. Moffett³, David A. Stahl², and Allan H. Devol¹

Published in *ISME Journal*

2013

Vol. 7, pages 2023–2033; doi:10.1038/ismej.2013.75

¹School of Oceanography, University of Washington, Seattle, WA 98195; ²Civil and Environmental Engineering, University of Washington, Seattle, WA 98195; ³Department of Biological Sciences, University of Southern California, Los Angeles, CA 90089

Abstract. Archaeal ammonia oxidizers (AOA) are increasingly recognized as prominent members of natural microbial assemblages. Evidence that links the presence of AOA with *in situ* ammonia oxidation activity is limited, and the factors that regulate the distribution of AOA natural assemblages are not well defined. We used quantitative PCR of the *amoA* gene (encodes α -subunit of ammonia monooxygenase) and *amoA* transcript copies to show that AOA greatly outnumber ammonia-oxidizing Bacteria (AOB) and *amoA* transcripts are derived primarily from AOA throughout the water column of Hood Canal, Puget Sound, WA. We generated a Michaelis-Menten kinetics curve for ammonia oxidation by the natural community and found that the measured K_m of $98 \pm 14 \text{ nmol l}^{-1}$ was close to that for cultivated AOA representative *Nitrosopumilus maritimus* SCM1. Temperature did not have a significant effect upon ammonia oxidation rates for incubation temperatures ranging from 8 – 20 °C, which is the typical

temperature range for the site. The K_m and Q_{10} measurements presented in this study will help better constrain ammonia oxidation rates with the commonly used $^{15}\text{NH}_4^+$ dilution technique. This study provides substantial evidence through both *amoA* gene copies and transcript abundances and the kinetics response that AOA are the dominant active ammonia oxidizers in this marine environment.

Corresponding author E-mail: rahorak@gmail.com.

9.5 Variable influence of light and temperature upon ammonia oxidation activity in marine *Thaumarchaeota*

Rachel E. A. Horak^a, **Wei Qin**^b, Anthony Bertagnoli^{b,1}, Alexandra Nelson^a, Katherine Heal^a, Andrew Schauer^c, Wade Jeffrey^d, E. Virginia Armbrust^a, James W. Moffett^c, Anitra E. Ingalls^a, David A. Stahl^b, Allan H. Devol^a

In preparation

^aSchool of Oceanography, University of Washington, Seattle, WA 98195; ^bDepartment of Civil and Environmental Engineering, University of Washington, Seattle, WA 98195; ^cDepartment of Earth and Space Sciences, University of Washington, Seattle, WA 98195; ^dCenter for Environmental Diagnostics and Bioremediation, University of West Florida, Pensacola, FL 32514; ^eDepartment of Biological Sciences, University of Southern California, Los Angeles, CA 90089; ¹Currently at: School of Biology, Georgia Institute of Technology, Atlanta, GA 30332

Abstract. Although many studies implicate *Thaumarchaeota* as the major ammonia oxidizers in the oceans, the abiotic factors that determine their distribution and activity are largely unexplored. A few studies with laboratory cultures and isolates have suggested differential sensitivity to sunlight, but a recent study of natural marine communities of AOA indicated no such sensitivity to sunlight (Smith et al. 2014). In this study, we examined the influence of light and temperature on ammonia oxidation rates for communities at the nitrite maximum across two transects in the North Pacific Ocean. At four stations, representing different biogeochemical regimes, we measured the change in ammonia oxidation rate under different sunlight intensities and temperatures by incubating $^{15}\text{NH}_4^+$ -spiked whole seawater collected from the nitrite maximum at five different sunlight intensities on a free floating in situ array. Most activity could

be attributed to the AOA, as inferred from quantification of ammonia monooxygenase subunit A (*amoA*) genes and transcripts. Temperature affected ammonia oxidation rates at only two of four stations. Ammonia oxidation was usually, but not always, completely inhibited by PAR at the surface. Latitudinal and longitudinal variation in light sensitivity (21 – 45% inhibited at 1% surface PAR) was correlated with shifts in major AOA phylotypes, also showing that closely related populations have different responses to light and temperature. This study highlights differences in basic physiological responses in natural marine communities of *Thaumarchaeota*.

Curriculum Vitae

Wei Qin

University of Washington
Department of Civil and Environmental Engineering
Box 355014
616 NE. Northlake PL
Seattle, WA, USA
+1-206-351-0549
ericqin@uw.edu

Education

Ph.D., (2014 – present), Civil and Environmental Engineering
University of Washington, Seattle, WA, USA
Thesis Advisor: David A. Stahl

M.A., (2010 – 2014), Civil and Environmental Engineering
University of Washington, Seattle, WA, USA
Thesis Advisor: David A. Stahl

B.Sc., (2006 – 2010), Environmental Science
Beijing Normal University, Beijing, China

Professional Experience

2010 – present	Graduate Research Assistant, David A. Stahl laboratory, University of Washington, Seattle, WA. USA.
2008 – 2010	Undergraduate Research Assistant, State Key laboratory of Water Environment Simulation, Beijing Normal University, Beijing, China.

Awards

2015	Outstanding Poster Presentation Award, 4 th International Conference on Nitrification
------	--

2009 The 1st class Professional Scholarship
2009 Merit Student in Beijing Normal University

Publications

- 1) Qin, W., Amin, S.A., Lundeen, R.A., Heal, K.R., Martens-Habbena, W., et al. Influence of ammonia and copper availabilities on the molecular physiology of the marine ammonia-oxidizing archaeon *Nitrosopumilus maritimus*. (in prep)
- 2) Horak, R.E.A., Qin, W., Bertagnolli, A.D., Nelson, A., Heal, K.R., Schauer, A., et al. Variable influence of light and temperature upon ammonia oxidation activity in marine Thaumarchaeota. (in prep)
- 3) Heal, K.R., Qin, W., Ribalet, F., Bertagnolli, A.D., Coyote-Maestas, W., Hmelo, L.R., et al. (2016) Two distinct pools of B₁₂ analogs reveal community interdependencies in the ocean. **Proc. Natl. Acad. Sci. USA.** (accepted)
- 4) Qin, W., Heal, K.R., Ramdasi, R., Kobelt, J.N., Martens-Habbena, W., Bertagnolli, A.D., Amin, S.A., et al. (2016) *Nitrosopumilus maritimus* gen. nov., sp. nov., *Nitrosopumilus cobalaminogenes* gen. nov., sp. nov., *Nitrosopumilus oxycliniae* gen. nov., sp. nov., and *Nitrosopumilus ureaphilus* gen. nov., sp. nov., four marine ammonia-oxidizing archaea of the phylum *Thaumarchaeota*. **Int. J. Syst. Evol. Microbiol.** (under review)
- 5) Qin, W., Meinhardt, K.A., Moffett, J.W., Devol, A.H., Armbrust, E.V., Ingalls, A.E., and Stahl, D.A. (2016) Influence of oxygen availability on the activities of ammonia-oxidizing archaea. **Environ. Microbiol. Rep.** (minor revision)
- 6) Qin, W., Jewell, T.N., Russell, V.V., Hedlund, B.P., de la Torre, J.R., Stahl, D.A. (2016) Order *Nitrosocaudales*, Family *Nitrosocaudaceae*, Genus *Nitrosocaudus*. In **Bergey's Manual of Systematics of Archaea and Bacteria**, 3rd Edition: John Wiley & Sons, Ltd. (accepted)
- 7) Qin, W., Martens-Habbena, W., Kobelt, J.N., Stahl, D.A. (2016) Order *Nitrosopumilales*, Family *Nitrosopumilaceae*, Genus *Nitrosopumilus*. In **Bergey's Manual of Systematics of Archaea and Bacteria**, 3rd Edition: John Wiley & Sons, Ltd.
- 8) Qin, W., Carlson, L.T., Armbrust, E.V., Devol, A.H., Moffett, J.W., Stahl, D.A., and Ingalls, A.E. (2015) Confounding effects of oxygen and temperature on the TEX₈₆ signature of marine Thaumarchaeota. **Proc. Natl. Acad. Sci. USA.** 112: 10979-10984.
- 9) Martens-Habbena, W.*, Qin, W.*, Horak, R.E.A., Urakawa, H., Schauer, A.J., Moffett, J.W., Armbrust, E.V., Ingalls, A.E., Devol, A.H., Stahl, D.A. (2015) The production of nitric oxide by marine ammonia-oxidizing archaea and inhibition of archaeal ammonia oxidation by a nitric oxide scavenger. **Environ. Microbiol.** 17: 2261-2274. *Joint first author
- 10) Qin, W., Amin, S.A., Martens-Habbena, W., Walker, C.B., Urakawa, H., Devol, A.H., Ingalls, A.E., Moffett, J.W., Armbrust, E.V., Stahl, D.A. (2014) Marine ammonia-oxidizing archaeal isolates display obligate mixotrophy and wide ecotypic variation. **Proc. Natl. Acad. Sci. USA.** 111: 12504-12509.

- 11) Qin, W. Adaptive radiation of marine ammonia-oxidizing archaea. **Master Thesis**, University of Washington (2014).
- 12) Horak, R.E.A., Qin, W., Schauer, A.J., Armbrust, E.V., Ingalls, A.E., Moffett, J.W. Devol, A.H., Stahl, D.A. (2013) Ammonia oxidation kinetics and temperature sensitivity of a natural marine community dominated by Archaea. **ISME J** 7: 2023-2033.
- 13) Tian, T., Liu, R.M., Wang, X.J., Kuang, L., Qin, W. (2011) Risk assessment of nitrogen and phosphorus export in Daning River of Three Gorges Reservoir Area. **Environ. Sci. Technol.** 34(6):185–190.
- 14) Kuang, L., Qin, W., Dong, S.K., Liu, S.L., Zhan, J.Y., Zhao, Y., Tian, T., Qian, Q.Q., Zeng, S.Y. (2010) Impact of road construction on roadside vegetations in Wuling Mountain Nature Reserve. **Chinese J. Ecol.** 29(1):146–151.

Presentations

- 2016
- Wei Qin, Shady A. Amin, Rachel A. Lundeen, et al. (Poster) The transcriptome and proteome of the ammonia-oxidizing archaeon *Nitrosopumilus maritimus* reflect marine processes. ISME Meeting, Montreal, CA, Aug 21-26.
- Anitra E. Ingalls, Wei Qin, Laura Carlson, et al. (Oral) Response of ammonia oxidizing archaea to environmental change and implications for the TEX₈₆ proxy. Ocean Sciences Meeting, New Orleans, LA, Feb 21–26.
- Katherine Heal, Wei Qin, Willow Coyote, et al. (Oral) Cobalamin and Cobalamin-like Compounds in the Sunlit Ocean: Inter-Phyla Mutualism or Competition? Ocean Sciences Meeting, New Orleans, LA, Feb 21–26.
- Rachel A Lundeen, Wei Qin, James Moffett, et al. (Poster) Proteomics as a tool to understand the distribution and activity of ammonia-oxidizing archaea. Ocean Sciences Meeting, New Orleans, LA, Feb 21–26.
- Rachel Horak, Wei Qin, Anthony Bertagnolli, et al. (Poster) Variable Influence of Light on the Activity of Ammonia-Oxidizing Thaumarchaeota in the North Pacific Ocean. Ocean Sciences Meeting, New Orleans, LA, Feb 21–26.
- 2015
- Rachel Lundeen, Wei Qin, Rachel Horak, et al. (Poster) Proteomic insights into marine ammonia-oxidizing archaea photoinhibition. Chemical Oceanography Gordon Research Conference, Holderness, NH, July 26–31.
- Wei Qin, Laura T. Carlson, E. Virginia Armbrust, et al. (Poster) Influence of oxygen concentration and temperature on marine thaumarchaeal lipid composition confounds the TEX₈₆ paleotemperature proxy. International Conference on Nitrification, Alberta, CA, June 28–July 1.

- 2015 Rachel Horak, Alex Nelson, **Wei Qin**, et al. (Poster) Light effects on ammonia oxidation in Thaumarchaeota is not uniform in the North Pacific Ocean. General Meeting of the American Society for Microbiology, New Orleans, LA, May 30–June 2.
- 2014 **Wei Qin**, Shady A. Amin, Willm Martens-Habben, et al. (Poster) High ecophysiological diversity among closely related marine ammonia-oxidizing archaea. Joint Aquatic Sciences Meeting, Portland, OR, May 18–23.
- Rachel Horak, **Wei Qin**, David Stahl, et al. (Oral) Archaeal ammonia oxidation across oceanic biomes. General Meeting of the American Society for Microbiology, Boston, MA, May 17–20.
- Katherine R. Heal, Laura Truxal Carlson, Willow Coyote-Maestas, David A. Stahl, **Wei Qin**, et al. Microbial Contribution to the Dissolved Vitamin B₁₂ Pool in Coastal Washington. Hawaii, HI, Feb 23–28.
- 2013 Rachel Horak, **Wei Qin**, E. Virginia Armbrust, et al. (Oral) Archaeal ammonia oxidation in a Puget Sound fjord: vertical distribution, kinetics, and temperature dependency. Association for the Sciences of Limnology and Oceanography Conference, New Orleans, LA, February 17–22.
- 2012 Rachel Horak, Allen Devol, **Wei Qin**, et al. (Poster) Ammonium oxidation kinetics of a natural microbial population dominated by Archaea. International Society for Microbial Ecology Conference, Copenhagen, DK, August 19–24.

Collaboration network

University of Washington	Prof. Dr. David A. Stahl (Advisor)
Civil and Environmental Engineering	Prof. Dr. H. David Stensel (Committee member)
School of Oceanography	Prof. Dr. Anitra E. Ingalls (Committee member)
	Prof. Dr. Robert M. Morris (Committee member)
	Prof. Dr. E. Virginia Armbrust (Project co-PI)
	Prof. Dr. Allen H. Devol (Project co-PI)
Department of Genome Sciences	Prof. Dr. Christine Queitsch (Committee member)
University of Southern California	Prof. Dr. James W. Moffett (Project co-PI)
California Institute of Technology	Prof. Dr. Grant J. Jensen (Project co-PI)
San Francisco State University	Prof. Dr. José R. de la Torre (co-author)
Florida Gulf Coast University	Prof. Dr. Hidetoshi Urakawa (co-author)
New York University Abu Dhabi (United Arab Emirates)	Prof. Dr. Shady A. Amin (co-author)

University of Florida
University of Nevada, Las Vegas
University of Bremen (Germany)

Prof. Dr. Willm Martens-Habbena (co-author)
Prof. Dr. Brian P. Hedlund (co-author)
Dr. Martin Könneke (co-author)

Research Cruises

- 2012–2013 Oceanographic research cruises on R/V Clifford Barnes to Puget Sound (5 cruises; 28 days in total). NSF funded project: Significance of nitrification in shaping planktonic biodiversity in the ocean.
- 2013 Oceanographic research cruise on R/V Kilo Moana to the North Pacific Ocean (30 days). NSF funded project: Significance of nitrification in shaping planktonic biodiversity in the ocean.

Mentoring and supervisory experience

Jessie Zou, Impact of organic substrates on growth and activity of marine ammonia-oxidizing archaea, University of Washington, USA, June 2013–June 2014.

Julia N. Kobelt, Isolation and ecophysiological characterization of soil and marine ammonia-oxidizing archaea, University of Washington, USA, May 2014–June 2016.

Professional Affiliations

American Society of Limnology and Oceanography (ASLO)

American Society of Microbiology (ASM)